THE UNIVERSITY
of EDINBURGH

Rewiring Central Sulphur Metabolism in *Saccharomyces cerevisiae*

Daniel Sachs

THE UNIVERSITY *of* EDINBURGH

Thesis submitted in fulfilment of
the requirements for the degree of
Doctor of Philosophy
to the
Institute of Quantitative Biology, Biochemistry and Biotechnology
University of Edinburgh
September 2019

Declaration

I declare that this thesis has been composed solely by myself and that it has not been submitted, either in whole or in part, in any previous application for a degree. Except where otherwise acknowledged, the work presented is entirely my own.

Daniel Sachs
September 2019

Abstract

Of the 20 proteinogenic amino acids used by life, only two contain a sulphur atom: methionine and cysteine. While most bacteria, fungi and plants possess the ability to synthesise sulphur amino acids from simple carbon, nitrogen and sulphur sources, methionine and cysteine are essential to all animals, including humans, and need to be taken up with their diet. Since most common feedstock crops are relatively low in sulphur amino acid content, methionine becomes the first growth limiting for many farm animals, especially young piglets, poultry and a variety of farmed fish and crustaceans, and needs to be added externally to animal feeds. Annually, more than one million tonnes of DL-methionine are produced, mostly by chemical synthesis, but chemical synthesis of methionine uses non-renewable resources and toxic intermediates, and produces a racemic mixture of methionine. The D-enantiomer has to be converted into the L-form either in the body of farm animals, reducing its nutritional value, or by enzymatic conversion, increasing the costs of pure L-methionine.

These hurdles in methionine synthesis call for a more sustainable production method of L-methionine. Several studies investigated the fermentative production of L-methionine in *Escherichia coli* or *Corynebacterium glutamicum*, but no commercial process has been established to date. Other approaches aimed at improving the nutritional value of plants by increasing the methionine production and/or overexpressing a methionine storage protein, but most studies increased the total sulphur amino acid content only slightly. This thesis aims to develop *Saccharomyces cerevisiae* strains with high amounts of sulphur amino acids that could be added directly to animal feeds. *S. cerevisiae* (baker's yeast) is a generally recognised as safe (GRAS) organism, which is genetically tractable, has a well described sulphur metabolism and is widely used in food production and animal feedstocks.

Chapter 3 describes a Design of Experiments (DOE) approach to identify key genetic and environmental factors influencing methionine production in *S. cerevisiae*. Despite the inability to generate all designed strains, the approach was able to increase the methionine titre more than 5-fold by deleting *SAM2*, *MET30* & *MET32* and inserting a strong promoter in front of the open reading frame of *MET6* and *STR3*. Furthermore, the precursor homoserine was recognised as a possible bottleneck in the biosynthesis of methionine.

In chapter 4, the native sequence encoding the *S. cerevisiae* aspartate kinase

(Hom3p) was mutated to remove its feedback inhibition by threonine. The mutation drastically increased the amounts of homoserine inside and outside the cells and induced the accumulation of cysteine in the growth medium, but failed to increase methionine titres. In order to investigate additional bottlenecks in the pathway, two bacterial O-acetylhomoserine sulfhydrylases (OAH-SHLases) with reduced feedback inhibition by methionine were expressed in homoserine accumulating strains. The expression of one of the OAH-SHLases, *RsMetZ*, did not increase methionine titres but caused the accumulation of large amounts of cystathionine, which is a precursor for the biosynthesis of cysteine. However, the co-expression of *RsMetZ* and the gene encoding the cysteine synthase, *CYS3*, did not elevate the amount of cysteine.

Finally, in chapter 5, three methionine storage proteins from plant seeds were overexpressed in *S. cerevisiae*, but only the 10-kDa δ-zein was able to be detected. However, the expression of 10-kDa δ-zein in methionine overproducing strains did not differ from the wild-type.

In summary, this work achieved to rewire central sulphur metabolism and increase the accumulation of sulphur amino acids in *S. cerevisiae*. These results represent first steps towards engineering yeast as a sulphur rich food and animal feed additive.

Lay summary

Methionine and cysteine are two essential and sulphur containing amino acids, that most bacteria, fungi and plants can synthesise, but all animals need to take up through their diet. Methionine plays a major role in animal farming, where it is routinely added to animal feeds to promote the growth of young piglets and poultry. However, almost all methionine is produced by chemical synthesis, which relies on non-renewable resources and toxic chemicals. It is therefore highly desirable to develop a new sustainable production method.

One possible method is to produce methionine in microorganisms such as baker's yeast. Baker's yeast is a safe organism that is already being used in the production of food or being added to animal feeds. Baker's yeast produce methionine naturally, albeit the amounts are kept low. Since baker's yeast can be more easily genetically manipulated than plants, increasing the amount of methionine by genetic engineering could generate nutritionally valuable yeasts that could be added directly to animal feeds instead of chemically produced methionine.

This work approaches the challenges for the production of methionine in baker's yeast in several different ways. Genetic changes aimed at abolishing the tight regulation of methionine on several levels. Enzymes from bacteria were introduced to increase the efficiency of a key reaction. Furthermore, the possibility to produce another essential amino acid in baker's yeast, cysteine, was explored. Finally, a methionine rich storage protein from maize was produced in baker's yeast in order to increase the total methionine content.

Acknowledgements

I'd like to thank Susan Rosser, who gave me the opportunity to pursue a PhD in her lab and supported me throughout my PhD. Thanks also to my PhD thesis committee members, Peter Swain and Louise Horsefall, for giving valuable feedback.

I'd like to thank Rebecca Holmes, Emily Johnston, Matt Dale and Mai-Britt Jensen for helping me out with finding my way around yeast, lab work, and providing feedback on my PhD thesis. Thanks also to everybody in the Rosser lab, who made my PhD a thoroughly enjoyable experience.

Thanks to Alan Taylor and everybody at the SIRCAMS facility at the University of Edinburgh, who supported me in running the GC-MS and analysing the data. Thanks to Jane Paget, Scott Neilson and the Edinburgh Genome Foundry for helping me with the construction of plasmids and running the instruments used for growth assays. Thanks to Julian Pietsch and Ivan Clark for helping me with a project that ultimately didn't make it into this thesis.

Finally, I'd like to thank my family and especially my parents for always supporting me during the whole period of my academic career. I'd like to thank especially Tessa Moses, who not only provided invaluable scientific advice, but always encouraged me to believe in myself.

Contents

List of Tables

List of Figures

Abbreviations

Acetyl-CoA	Acetyl coenzyme A
ALE	Adaptive Laboratory Evolution
API	Active pharmaceutical ingredient
APS	Adenylyl-sulphate
(DL-)ATC	DL-2-amino-Δ^2-thiazoline-4-carboxylic Acid
ATP	Adenosine triphosphate
ADP	Adenosine diphosphate
Cas9	CRISPR associated protein 9
CD	Circular dischroism spectroscopy
CGS	Cystathionine γ-synthase
CRISPR	Clustered regularly interspaced short palindromic repeats
DBTL	Design-Build-Test-Learn
DOE	Design of Experiments
DSB	Double stranded breaks
GC-MS	Gas chromatography mass spectrometry
HR	Homologous recombination
LC-MS	Liquid chromatography mass spectrometry
NADH	Nicotinamide adenine dinucleotide
NADPH	Nicotinamide adenine dinucleotide phosphate
(L-)NCC	*N*-carbamoyl-L-cysteine
OAH-SHLase	O-acetylhomoserine-sulfhydrylase
OAS-SHLase	O-acetylserine-sulfhydrylase
OD	Optical density
OFAT	One-factor-at-a-time
PAM	Protospacer adjacent motif
PAPS	Phosphoadenylyl-sulphate
PCA	Principal component analysis
RT-qPCR	Reverse transcription quantitative PCR
SAH	S-adenosyl homocysteine
SAM	S-adenosyl methionine
SATase	Serine O-acetyltransferase
SDS-PAGE	sodium dodecyl sulphate polyacrylamide gel electrophoresis
UAA	Unnatural amino acid

Chapter 1

Introduction

Of the naturally occuring 20 proteinogenic amino acids, only two carry a sulphur atom: methionine and cysteine (Figure 1.1). Methionine and cysteine can have two enantiomeric conformations (L- and D-), but cells synthesise and use only the L-forms. Most plants, fungi and bacteria can synthesise methionine from carbohydrates, nitrogen, and sulphur sources such as sugars, ammonium, and sulphate, whereas animals rely on externally provided sources of sulphur amino acids in the form of other plant or animal protein. While high amounts of methionine are found in many albumins, especially egg albumins, cysteine is found mainly in structural proteins such as keratin or collagen due to its ability to form stabilising disulphide bonds. Both amino acids and their derivatives have been used in various industries, including in food supplements (Henchion et al., 2017), animal feed additives (Jankowski et al., 2014), pharmaceuticals (Oz et al., 2008; Kurihara et al., 2007), and cosmetics (Humphries et al., 1972).

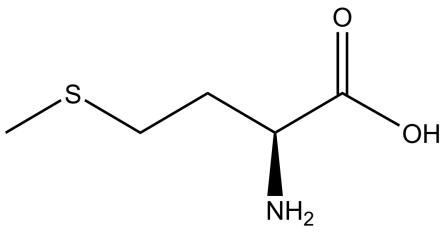

L-methionine
Chemical Formula: $C_5H_{11}NO_2S$
Molecular Weight: 149.21

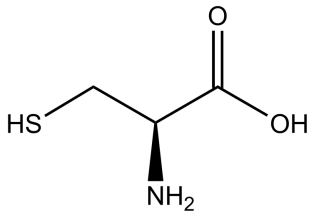

L-cysteine
Chemical Formula: $C_3H_7NO_2S$
Molecular Weight: 121.15

Figure 1.1: Chemical structure, formula, and molecular weight of L-methionine and L-cysteine.

Protein-energy malnutrition is still a major global concern, especially in rural areas of developing countries (Muller, 2005). The low amounts of lysine and methionine in cereal and legume crops severely limit their nutritional value as human food and animal feeds, and several approaches aimed at increasing the

lysine and methionine content of food and animal feed crops (Galili et al., 2005; Galili and Höfgen, 2002; Galili and Amir, 2013).

However, the majority of methionine and cysteine is currently produced by chemical synthesis (Willke, 2014) or extraction of natural sources such as human hair or feathers in the case of cysteine (Wada and Takagi, 2006). Those processes use fossil resources and produce toxic side products (Lussling et al., 1981; Sano and Mitsugi, 1978), which renders developing a process for the production of sulphur amino acids from microbial fermentation highly desirable.

In this chapter, the following will be discussed: the industrial importance and current applications of sulphur amino acids; the biosynthesis of methionine and cysteine in *Saccharomyces cerevisiae*; the biotechnological production of sulphur amino acids and their derivatives; metabolic engineering approaches in *S. cerevisiae*; the application of the Design of Experiments (DOE) methodology for biotechnological applications.

1.1 Importance and applications of methionine and cysteine

The global production of amino acids is expected to grow between 2017 and 2022 with the annual growth rate of amino acids used as feed additives of 6.9%. DL-methionine represents the third largest share of the market with an annual production of 1.1 million tonnes per year (Wendisch, 2019) and a much smaller share of the market uses L-methionine for food and pharmaceutical applications, which is produced through enzymatic conversion (Hummel et al., 2007).

About 3000 tonnes of L-cysteine are produced annually (Wendisch, 2019), with uses in the pharmaceutical, food, and cosmetic industries as preventive medicine for pulmonary diseases (Millea, 2009), as a dough conditioner (Lambert and Kokini, 2001), in nail care (Iorizzo et al., 2007), and as a hair perm agent (Humphries et al., 1972).

1.1.1 Applications of methionine in animal feeds

Most of the chemically synthesised DL-methionine is added to animal feeds to improve animal growth and immune system; especially, young piglets and poultry require a methionine rich diet (Jankowski et al., 2014). However, state regulations limit or prohibit the use of DL-methionine in organic animal farming (Willke, 2014). Adding large amounts of plant protein to aquaculture feeds can depress nutrient uptake and digestion (Tan et al., 2013; Hua et al., 2015). Similarly, the insufficient nutritional value of plant protein as an aquaculture feed can be partially overcome by the addition of methionine (Oliva-Teles, 2012), thus reducing the use of fish meal, which is produced from mostly food-grade catch (Cashion et al., 2017).

Several studies have investigated the influence of the methionine form on the utilisation of the amino acid in animals. Since D-methionine needs to be racemised into L-methionine by a D-amino acid oxidase and L-specific transaminase prior to protein biosynthesis (Koga et al., 2017), L-methionine has a 25% higher nutritional potency. Nevertheless, Sveier et al. (2001) showed that supplementing D-methionine to a soya concentrate based diet increased the growth of Atlantic salmon (*Salmon salar* L.) more than the addition of L-methionine. Niu et al. (2018) increased the bioavailability of methionine in white shrimp (*Litopenaeus vannamei*) by supplementing the feed with a commercial methionine dimer (Met-Met) instead of DL-methionine. Similarly, Tan et al. (2018) were able to replace fish meal partially with vegetable protein by adding methionine to the diet of juvenile red swamp crayfish (*Procambarus clarkii*) and thereby avoiding the growth depressing effects of plant protein.

1.2 Conventional processes for the production of methionine and cysteine

1.2.1 Chemical synthesis and enzymatic production of L-methionine

DL-methionine is chemically synthesised from methyl mercaptan, acrolein, and hydrogen cyanide (Lussling et al., 1981). The process is the major contributor to DL-methionine production and has been used for 50 years by Evonik Degussa, Germany, but uses fossil resources and produces toxic intermediates and waste (Willke, 2014).

An industrially common process for the production of pharmaceutical and food grade L-methionine involves the acetylation of DL-methionine in a first step. The resulting *N*-acetyl DL-methionine racemic mixture is subsequently treated by a membrane immobilised L-amino acylase to yield L-methionine in a continuous process (Wöltinger et al., 2005).

Other approaches enzymatically synthesise L-methionine from O-acetylhomoserine and methanethiol using a O-acetylhomoserine sulfhydrylase (OAH-SHLase, Figure 1.5) (Kim et al., 2011; Hong et al., 2017).

1.2.2 Extraction of L-cysteine and bioconversion of DL-2-amino-Δ^2-thiazoline-4-carboxylic Acid

L-cysteine can be obtained through extraction from human hair and animal feathers. During the process keratin, which is highly abundant in those sources, is treated with activated charcoal and hydrochloric acid. However, the process has major drawbacks, such as hydrochloric-acid containing waste liquid, unpleasant

odours and possible contamination with animal toxins (Wada and Takagi, 2006; Takagi and Ohtsu, 2016).

Another industrial process utilises the bioconversion of DL-2-amino-Δ^2-thiazoline-4-carboxylic Acid (DL-ATC). The enzymatic conversion of DL-ATC is performed in a continuous manner in three steps: (i) racemisation of D-ATC to L-ATC; (ii) opening of the L-ATC ring to yield *N*-carbamoyl-L-cysteine (L-NCC) as an intermediate; (iii) hydrolysing L-NCC to form L-cysteine (Sano and Mitsugi, 1978; Ryu et al., 1997).

1.3 Methionine and cysteine biosynthesis in *S. cerevisiae*

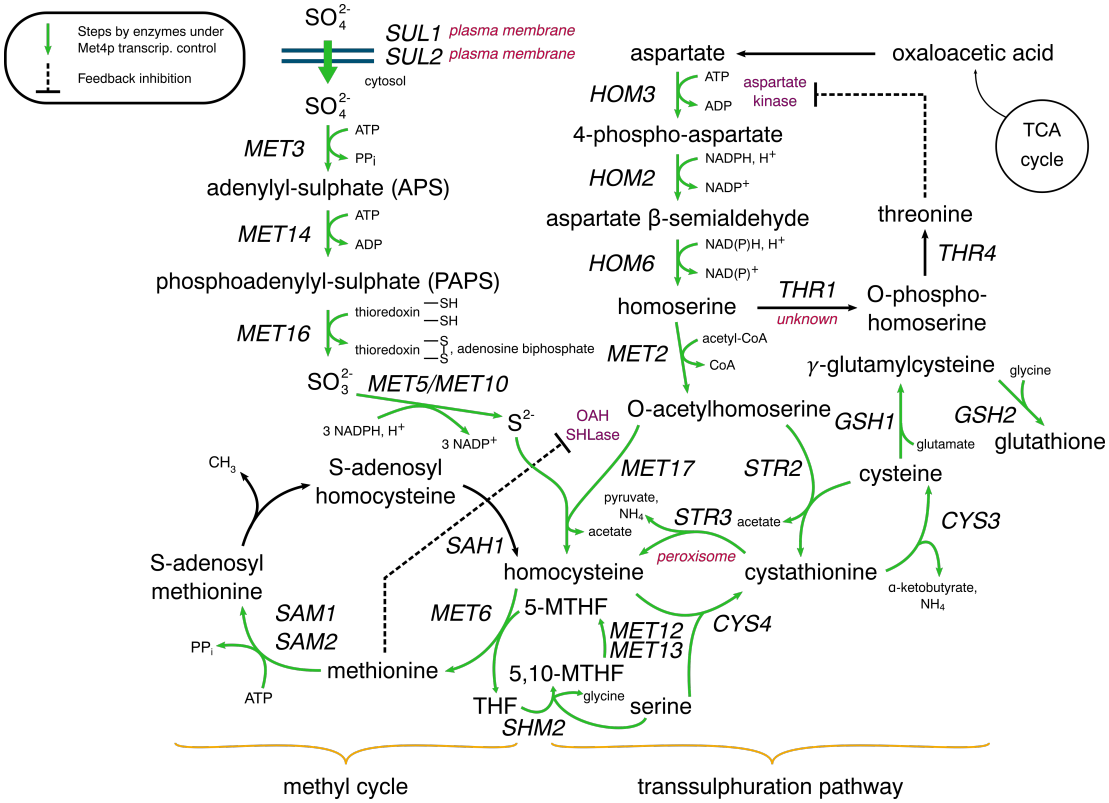

Figure 1.2: Superpathway of methionine and cysteine biosynthesis in S. cerevisiae. Names of genes encoding enzymes catalysing reactions in italic. Green arrows indicate pathway steps that are catalysed by enzymes under transcriptional control of Met4p and/or are induced under methionine restricted conditions. Inhibitions of enzymes (purple) are indicated by dotted lines. Unless otherwise stated (red), all enzymes are localised to the cytosol. OAH-SHLase: O-acetylhomoserine sulfhydrylase.

S. cerevisiae is rich in protein and as a generally recognised as safe (GRAS)

organism, it has a long history as a food additive (Anupama and Ravindra, 2000; Bekatorou et al., 2006). The metabolism of sulphur amino acids in *S. cerevisiae* has been reviewed extensively before (Thomas and Surdin-Kerjan, 1997; Ljungdahl and Daignan-Fornier, 2012).

In general, the biosynthesis of methionine and cysteine can be separated into three separate but connected parts (Figure 1.2): (i) the sulphur assimilation pathway (Figure 1.3), (ii) the synthesis and acetylation of homoserine (Figure 1.4), and (iii) the synthesis of methionine or cysteine (via cystathionine) from homocysteine (Figure 1.7 & 1.8). The three parts as well as the transcriptional regulation of the pathway are discussed in more detail below.

1.3.1 Sulphur assimilation

In order to utilise inorganic sulphur for amino acid biosynthesis, the sulphur atom in sulphate (SO_4^{2-}), oxidation state +6, needs to be reduced to form sulphide, which has an oxidation state of -2 (Figure 1.3). Extracellular sulphate is transported by two high-affinity transporters, Sul1p or Sul2p, across the plasma membrane into the cytosol (Cherest et al., 1997).

Sulphate is then activated in two steps, using two molecules of ATP in the process: The transfer of an adenosyl-phosphoryl moiety from ATP to sulphate to yield adenylyl-sulphate (APS), which is then phosphorylated, generating phosphoadenylyl-sulphate (PAPS). The first step is catalysed by the *S. cerevisiae* ATP sulphurylase, encoded by *MET3*, which is formed from six subunits arranged in two rings (Gierest et al., 1985; Ullrich et al., 2001). The subsequent phosphorylation and formation of PAPS is catalysed by the adenylylsulphate kinase, Met14p (Masselot and de Robichon-Szulmajster, 1975).

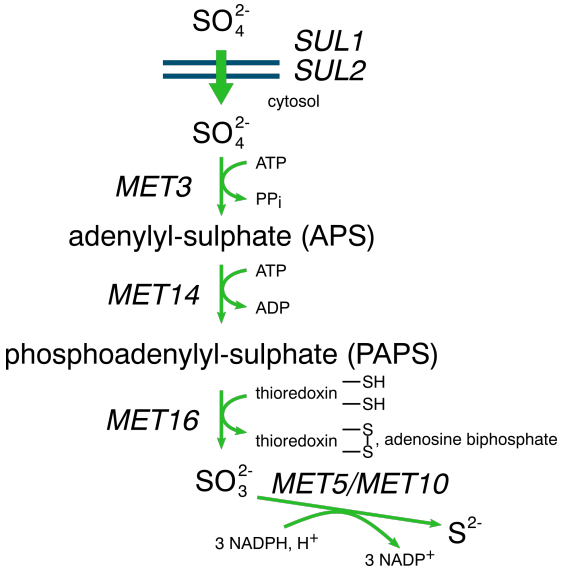

Figure 1.3: Sulphur assimilation in S. cerevisiae.

Finally, the activated sulphate is reduced to sulphide in two reactions, oxidising one molecule of thioredoxin and three molecules of NADPH in the process. The PAPS reductase, encoded by *MET16*, catalyses the formation of sulphite ($SO_3{}^{2-}$) with a reduced thioredoxin as a co-substrate (Schwenn et al., 1988; Thomas et al., 1990). Sulphite reduction to yield sulphide (S^{2-}) is catalysed by the *S. cerevisiae* sulphite reductase and oxidises three molecules of NADPH during the reaction. The sulphite reductase consists of 4 subunits that are arranged in an $\alpha_2\beta_2$ oligomeric structure with the subunits being encoded by *MET10* (α) and *MET5* (β) (Mountain et al., 1991; Hansen et al., 1994). The siroheme needed for an active sulphite reductase is synthesised by Met1p & Met8p (Hansen et al., 1997).

S. cerevisiae is also able to grow on thiosulphate ($S_2O_3{}^{2-}$) as a sole sulphur source. The utilisation pathway involves the import of thiosulphate by Sul1p or Sul2p and the subsequent conversion of thiosulphate into sulphite and sulphide by one of two endogenous rhodanese like enzymes, Rdl1p or Rdl2p (Chen et al., 2018). Yeast growing on thiosulphate (instead of sulphate) as a sulphur source accumulated more NADPH and exhibited elevated ethanol production rates (Funahashi et al., 2015).

1.3.2 Homoserine and O-acetylhomoserine biosynthesis

Homoserine is synthesised in *S. cerevisiae* in three steps from aspartic acid (Figure 1.4). The *S. cerevisiae* aspartate kinase, encoded by *HOM3*, consumes a single ATP molecule to phosphorylate aspartic acid and yield 4-phospho-aspartate (Rafalski and Falco, 1988). The next reaction, catalysed by Hom2p, converts 4-phospho-aspartate to aspartate β-semialdehyde, which in turn is converted to homoserine by Hom6p (Thomas and Surdin-Kerjan, 1989; Yumoto et al., 1991). The aspartate β-semialdehyde dehydrogenase (Hom2p) as well as the homoserine dehydrogenase (Hom6p) oxidise each a single molecule of NADPH during the reaction.

Homoserine is the substrate for two separate intracellular reactions: Homoserine kinase (Thr1p) catalyses the first step in threonine biosynthesis and homoserine-O-acetyltransferase (Met2p) catalyses the acetylation of homoserine using acetyl-CoA as a co-substrate (Mannhaupt et al., 1990; Masselot and de Robichon-Szulmajster, 1975).

1.3.3 Sulfhydrylation

Sulfhydrylation describes in *S. cerevisiae* the replacement of the homoserine side chain hydroxyl group with a thiol group after homoserine has been activated through acetylation (Figure 1.5). O-acetylhomoserine sulfhydrylases (OAHSHLases, EC 4.2.99.10) are pyridoxal 5'-phosphate (PLP) dependent enzymes catalysing the sulfhydrylation in various bacteria and fungi (Yamagata, 1989). *S. cerevisiae* uses exclusively O-acetylhomoserine as a substrate to synthesise

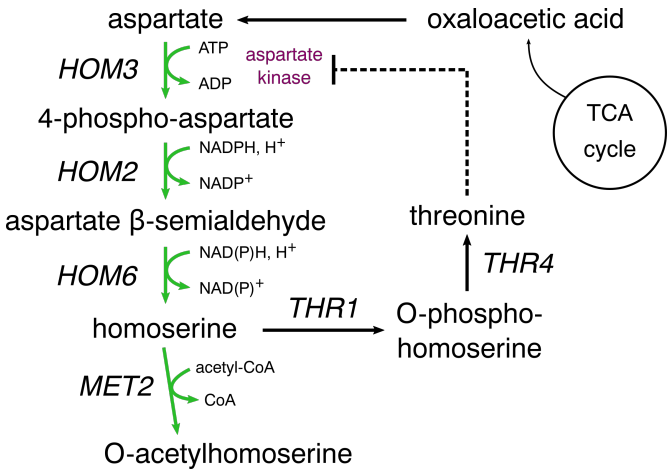

Figure 1.4: Homoserine and O-acetylhomoserine biosynthesis in S. cerevisiae.

either homocysteine from sulphide (by Met17p) or cystathionine from cysteine (by Str2p) (Masselot and de Robichon-Szulmajster, 1975; Yamagata et al., 1994; Hansen and Johannesen, 2000).

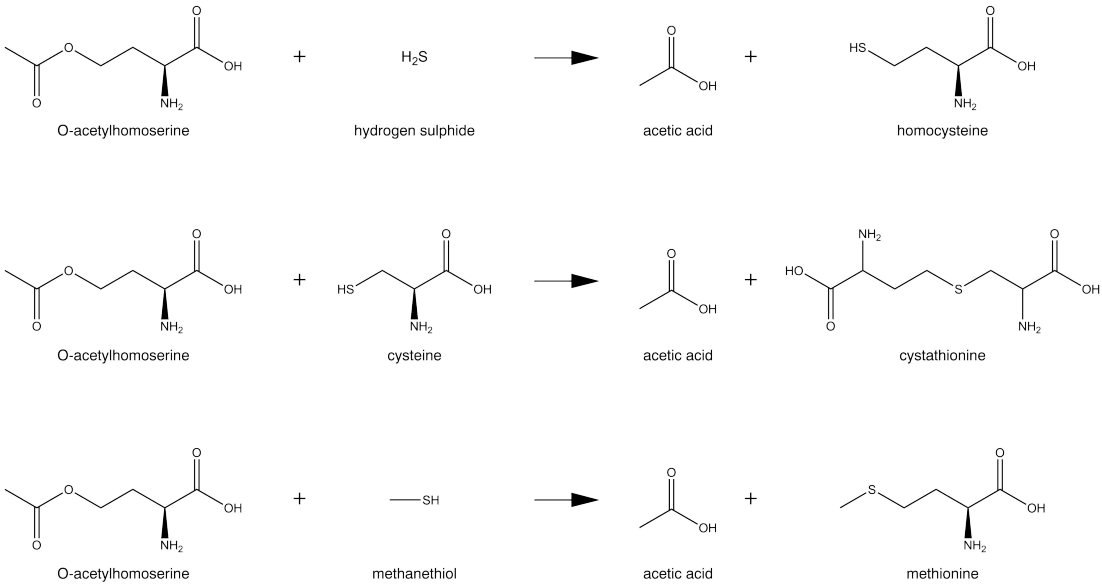

Figure 1.5: Suflhydrylation reactions.

Bacteria use a variety of substrates for sulfhydrylation and subsequent methionine biosynthesis (Figure 1.6) (Ferla and Patrick, 2014). Similar to yeast, both *Corynebacterium glutamicum* and *Pseudomonas aeruginosa* synthesise methionine through direct sulfhydrylation of activated homoserine. But unlike *S. cerevisiae* and *C. glutamicum*, which utilise O-acetylhomoserine as a substrate, the *P. aeruginosa* O-succinylhomoserine sulfhydrylase (OSH-SHLase) is specific

for O-succinylhomoserine (Hwang et al., 2002; Foglino et al., 1995). *Escherichia coli* synthesises O-acetylserine, one carbon atom fewer than O-acetylhomoserine, which is in turn used as a substrate with sulphide for the biosynthesis of cysteine by the *E. coli* O-acetylserine sulfhydrylase (OAS-SHLase) (Rabeh and Cook, 2004).

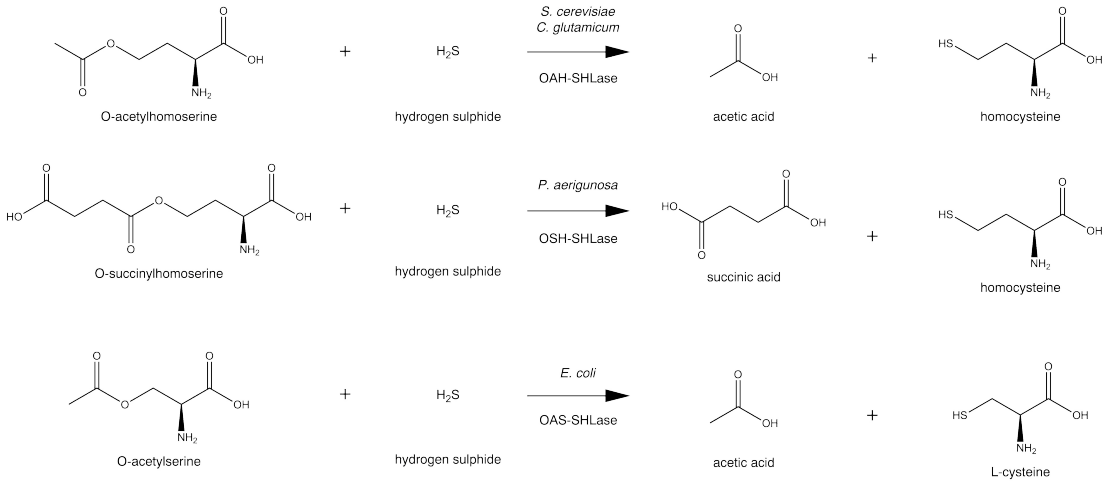

Figure 1.6: Suflhydrylation in different organisms.

Met17p has both OAH-SHLase as well as OAS-SHLase activity (Yamagata, 1981) and some *S. cerevisiae* strains have a detectable activity of a serine O-acetyltransferase (SATase), but their role *in vivo* is thought to be minimal, indicating that cysteine biosynthesis occurs exclusively through homocysteine and the transsulphuration pathway (Takagi et al., 2003).

1.3.4 Biosynthesis of methionine and S-adenosyl methionine through the methyl cycle

Methionine is synthesised from homocysteine and the methyl donor 5-methyltetrahydrofolate in a single step, which is catalysed by the *S. cerevisiae* cobalamin-independent methionine synthase, encoded by *MET6* (Masselot and de Robichon-Szulmajster, 1975; Suliman et al., 2005). Tetrahydrofolate is recycled to form 5-methylhydrofolate by a serine hydroxymethyltransferase, Shm2p (Saint-Marc et al., 2015). *S. cerevisiae* encodes two methylenetetrahydrofolate reductases (MTHFR), *MET12* & *MET13*, which catalyse the reduction to 5-methyltetrahydrofolate, but only Met13p is active *in vivo* (Raymond et al., 1999).

S-adenosylmethionine (SAM) is the main methyl donor in the transmethylation of proteins, nucleic acids, polysaccharides, phospholipids, and fatty acids (Tabor and Tabor, 1984). In *S. cerevisiae*, SAM synthesis from methionine is catalysed by two SAM synthetases, which are encoded by one of two paralogue genes (*SAM1* and *SAM2*) that arose from a whole genome duplication and are regulated by two different trancriptional mechanisms (Cherest et al., 1978; Thomas

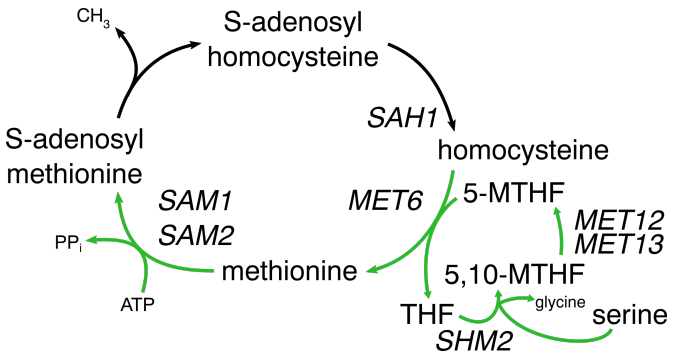

Figure 1.7: Methyl cycle in S. cerevisiae.

and Surdin-Kerjan, 1991; Kodaki et al., 2003). The possible clinical applications of SAM in treating depression or liver disease (Williams et al., 2005; Anstee and Day, 2012) sparked huge interest in *S. cerevisiae* as a production platform. Especially, the expression an ethionine resistance gene (*ERC1*) (Shiomi and Fukuda, 1990; Shiomi et al., 1995), the overexpression of *MET6* and *SAM2* (Cao et al., 2012; Chen, Wang, Wang, Dou and Zhou, 2016), the deletion of *ADO1*, encoding an adenosine kinase (Kanai et al., 2013; Oomuro et al., 2018), and increased ATP levels when using ethanol as a carbon source (Hayakawa et al., 2016, 2018) increased the SAM productivity significantly. More recently, a new approach for SAM production introduced genes encoding enzymes converting D-methionine to L-methionine intracellularly and fed DL-methionine to achieve the effective production of SAM (Liu, Tang, Shi, Lian, Huang, Cai and Xu, 2019).

After SAM donated a methyl group, S-adenosylhomocysteine (SAH) is formed. SAH is then converted to homocysteine by the SAH hydrolase (Sah1p), thus closing the methyl cycle (Tehlivets et al., 2004; Malanovic et al., 2008). *SAH1* is essential for effective growth under aerobic conditions, since SAH accumulation is toxic to yeast (Christopher et al., 2002; Giaever et al., 2002).

1.3.5 Biosynthesis of cysteine from homocysteine through the transsulphuration pathway

S. cerevisiae synthesises cysteine exclusively through the transsulphuration pathway (Cherest et al., 1993). The first enzyme, the cystathionine β-synthase Cys4p, catalyses the reaction of homocysteine and serine to yield cystathionine, which subsequently is converted to cysteine by the cystathionine γ-lyase, Cys3p (Ono et al., 1994; Cherest and Surdin-Kerjan, 1992; Ono et al., 1992). Disruption of either *CYS4* or *CYS3* confers a cysteine auxotrophy in *S. cerevisiae* (Figure 1.8).

Cysteine is the substrate in the first step of glutathione biosynthesis (by Gsh1p) to yield γ-glutamylcysteine, which is converted to glutathionine by Gsh2p (Kistler et al., 1990; Ohtake and Yabuuchi, 1991; Inoue et al., 1998). Glutathione is one of the most abundant thiol compounds in *S. cerevisiae*, playing an important

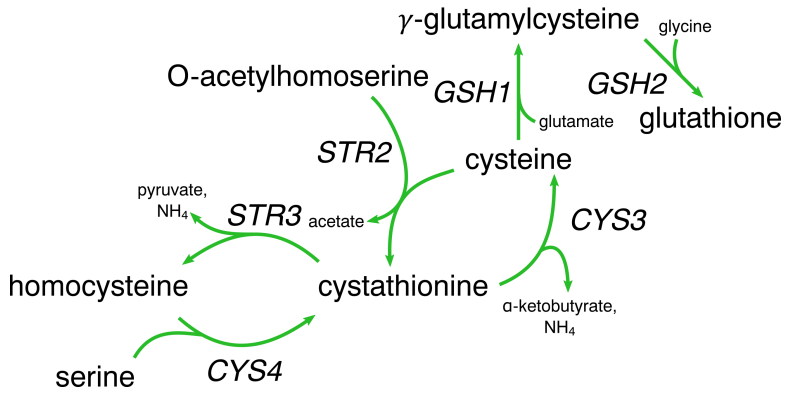

Figure 1.8: Transsulphuration pathway in S. cerevisiae.

role in resistance to oxidative stress and maintenance of redox homeostasis. Glutathione has clinical applications and glutathione overproducing yeast strains were shown to be more resistant to toxic compounds in pretreated lignocellulosic materials (Forman et al., 2009; Ask et al., 2013).

The reverse transsulphuration pathway, synthesising homocysteine from cysteine is also present in *S. cerevisiae*, although the enzymes are less well described. Strains with a disrupted *STR2* lack cystathionine γ-synthase activity and are unable to utilise cysteine as a sulphur source, indicating the synthesis of cystathionine from cysteine by Str2p (Cherest and Surdin-Kerjan, 1992; Hansen and Johannesen, 2000). The strong homology to Met17p suggests that Str2p is a sulfhydrylase using O-acetylhomoserine as a co-substrate (Hansen and Johannesen, 2000; Ljungdahl and Daignan-Fornier, 2012). Cystathionine is then converted into homocysteine by the cystathionine β-lyase Str3p (Cherest and Surdin-Kerjan, 1992; Ljungdahl and Daignan-Fornier, 2012).

1.4 Regulation of sulphur amino acid biosynthesis in *S. cerevisiae*

1.4.1 Transcriptional regulation

Transcription of most genes involved in *S. cerevisiae* sulphur amino acid metabolism requires the transcriptional activator Met4p (Lee et al., 2010). Met4p alone does not possess any DNA binding capability, it rather interacts with DNA-binding co-factors Met31p, Met32p, Cbf1p and the stabilising co-factor Met28p to form an active trancriptional complex (Blaiseau and Thomas, 1998). Met4p activity is repressed under high sulphur conditions by the Skp1p/Cdcd53p/F-box protein Met30p (SCF^{Met30}) (Kaiser et al., 2000; Rouillon et al., 2000; Kuras et al., 2002; Flick et al., 2004; Menant et al., 2006; Ouni et al., 2010). Notably, ubiquitination of Met4p by SCF^{Met30} does not induce its degradation, but Met4p-SCF^{Met30}

associated cofactors Cbf1p & Met31p or Met32p are poly-ubiquitinated and targeted for degradation in the proteasome (Figure 1.9), thus repressing Met4p activity (Kaiser et al., 2000; Flick et al., 2004; Ouni et al., 2010). Under limited intracellular levels of sulphur amino acids or heavy metal stress, Met4p and its co-factors are not ubiquitinated, inducing Met4p mediated transcription. Active Met4p causes the transcription of genes involved in sulphur assimilation, sulphur amino acid biosynthesis, and induction of cell cycle arrest in response to heavy metal stress (Kuras et al., 2002; Kaiser et al., 2006; Ouni et al., 2011). The lethality of Met4p hyperactivation in *met30*Δ strains can be overcome by the deletion of *MET32* (Patton et al., 2000; Su et al., 2005).

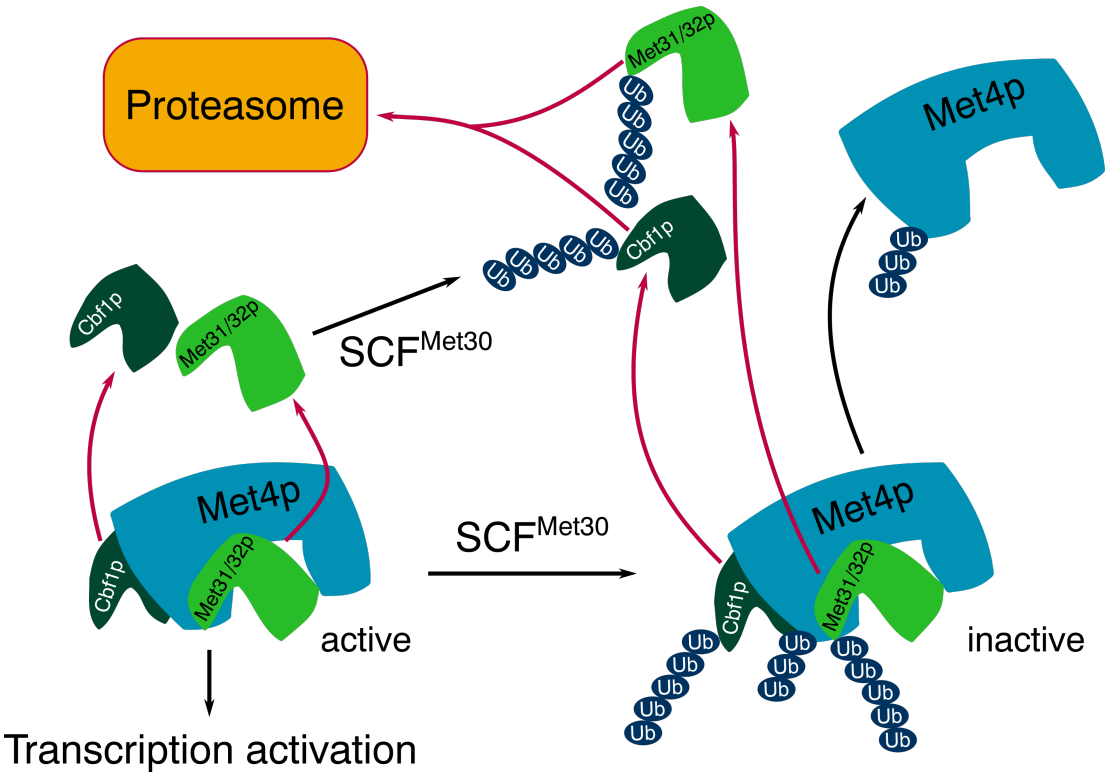

Figure 1.9: Regulation of the transcriptional activator Met4p. Active Met4p and its DNA binding co-factors Cbf1p and Met31p or Met32p induce transcription under low sulphur or heavy metal stress. Under high sulphur conditions, Met4p and its co-factors are poly-ubiquitinated by SCF^{Met30}, which inactivates the transcriptional complex. Cbf1p & Met31/32p are poly-ubiquitinated either before or after they dissociate from Met4p and are targeted for degradation to the proteasome, while dormant pools of poly-ubiquitinated Met4p are retained. Figure adapted from Ouni et al. (2011). Ub: Ubiquitin.

Several studies investigated the targets of Met4p mediated transcriptional activation (Figure 1.2, green arrows). Lee et al. (2010) identified a core regulon of 45 genes, that are targeted by Met4p and repressed in *met31*Δ/*met32*Δ

strains. While Met31p and Met32p are redundant for growth under methionine restriction, Met32p activates a larger share of transcripts, with *met30*Δ/*met32*Δ strains having decreased expression of sulphur assimilation genes compared to the wild-type or *met30*Δ/*met31*Δ strains (Carrillo et al., 2012). Of the homoserine biosynthesis genes, only *HOM3* and *HOM6* were shown to be regulated by Met4p (Carrillo et al., 2012), but high-throughput studies found *HOM2* & *HOM3* to be under General Amino Acid Control (GAAC)/Gcn4p control (Natarajan et al., 2001) and to be upregulated under methionine restricted conditions (Zou et al., 2017).

1.4.2 Inhibition of biosynthetic enzymes

While the most important regulation of sulphur amino acid biosynthesis occurs on the transcriptional level, several key enzymes are inhibited by downstream products in the pathway.

Homoserine biosynthesis is tightly regulated by a feedback inhibition of the aspartate kinase Hom3p by threonine (Ramos et al., 1991). Intracellular amounts of homoserine need to be controlled, since homoserine itself, possibly through misincorporation into proteins, as well as the precursor aspartate β-semialdehyde are growth inhibitory (Arevalo-Rodriguez et al., 2004; Kingsbury and McCusker, 2010). Interaction of Hom3p with the prolyl-isomerase FKBP12 (FK506 binding protein) is needed for the inhibition of the aspartate kinase by threonine and mutations in Hom3p that reduce the feedback inhibition of the enzyme likely influence the binding of FKBP12 to Hom3p (Alarcón and Heitman, 1997; Arevalo-Rodriguez et al., 2004; Velasco et al., 2005). Strains expressing feedback resistant Hom3p accumulate greatly increased levels of homoserine and have been applied for the production of threonine, of which homoserine is a precursor, in *S. cerevisiae* (Farfán et al., 1999; Farfán and Calderón, 2000; Velasco et al., 2005).

The *S. cerevisiae* OAH-SHLase (Met17p) is strongly inhibited by methionine and somewhat less by homoserine (Yamagata, 1971). Other OAH-SHLases with reduced feedback inhibition, such as the *Leptospira meyeri* OAH-SHLase or a mutated OAH-SHLase from *Rhodobacter sphaeroides*, were described previously and give rise to the possibility of producing methionine directly from O-acetylhomoserine and methanethiol (Belfaiza et al., 1998; Kim et al., 2011).

The homoserine O-acetyltransferase (Met2p) is inhibited by high levels (10 - 40 mM) of O-acetylhomoserine and lower levels of homocysteine, but not methionine (Yamagata, 1987). Forlani et al. (1991) reported a post-transcriptional inhibition of highly transcribed *MET2* resulting in low production of the protein, although the underlying mechanism remained unclear.

1.5 Transport of sulphur amino acids and their precursors across the plasma membrane in *S. cerevisiae*

Yeast cells measure extracellular amounts of amino acids via the Ssy1p, Ptr3p, Ssy5p (SPS) transmembrane complex and induce the transcription of amino acid uptake genes in response to low levels of amino acids (Ljungdahl, 2009). Several broad spectrum amino acid permeases, many regulated by the SPS sensor pathway, have also a substrate specificity for methionine and cysteine: Gap1p, Agp1p, Agp3p, Bap2p, Bap3p & Gnp1p (Regenberg et al., 1999; Ljungdahl and Daignan-Fornier, 2012).

Methionine uptake also occurs through two dedicated methionine permeases, Mup1p & Mup3p, which form a distinct class of amino acid permeases (Isnard et al., 1996). The two permeases have different affinities for methionine, with the high affinity permease, Mup1p, also transporting cysteine across the plasma membrane (Kosugi et al., 2001). In constrast to broad specificity permeases regulated by the SPS sensor pathway regulated, methionine uptake via Mup1p and Mup3p is diminished in high extracellular methionine concentrations by repressing the expression of *MUP1* and *MUP3* as well as inducing the ubiquitin-mediated degradation of Mup1p (Menant et al., 2006).

A high-affinity cysteine permease, Yct1p, is the major contributor to cysteine uptake at low extracellular concentrations. It belongs to the Dal5p family of transporters and its transcription is repressed by sulphur compounds in a Met4p mediated way (Kaur and Bachhawat, 2007).

Unlike in enteric bacteria, *S. cerevisiae* is able to take up SAM. The transport is mediated by a high-affinity transporter, Sam3p, and a yet unidentified low affinity transporter. A structurally similar protein, Mmp1, cannot import SAM, but S-methylmethionine instead (Rouillon et al., 1999).

Aqr1p is a plasma membrane protein belonging to the major facilitator superfamily (MFS) transporter family and confers resistance to short-chain monocarboxylic acids and quinidine (Tenreiro et al., 2002). Intriguingly, it is also to date the only described exporter of excess amino acids from the cytosol. Velasco et al. (2004) showed that Aqr1p is responsible for the secretion of threonine and homoserine in *S. cerevisiae* strains overproducing either amino acid, as well as alanine, aspartic acid and glutamic acid, which are highly abundant in the cytosol (Mülleder et al., 2016). *AQR1* has a paralogue, *QDR1*, that arose from whole genome duplication and is involved in quinidine resistance (Nunes et al., 2001).

1.6 Production of L-methionine and L-cysteine by fermentation

Production of amino acids by fermentation has a long history and many amino acids are being produced industrially by fermentation. The current status and outlook of amino acid production generally and methionine and cysteine production specifically has been review extensively (Willke, 2014; Kinoshita, 2017; Wendisch, 2019), and the following section focuses on the parts that are relevant for this work.

1.6.1 Production of L-methionine by fermentation

Metabolic engineering efforts for the production of methionine by fermentation focused mainly on *E. coli* and *C. glutamicum*. Metabolic pathway analysis of both organisms predicted the maximum theoretical carbon yields to be 52% (*E. coli*) and 49.3% (*C. glutamicum*), respectively (Krömer et al., 2006).

L-methionine production in *E. coli*

Nakamori et al. (1999) increased methionine production by mutating the *E. coli* repressor MetJ to derepress the expression of methionine biosynthetic genes. Bestel-Corre et al. (2014) mutated two other enzymes, the homoserine O-succinyltransferase MetA and the SAM synthetase MetK, in order to increase the availability of the precursor O-succinylhomoserine by diminishing the feedback inhibition of MetA and decrease methionine consumption by reducing MetK activity. Furthermore, yjeH was identified as a novel methionine exporter that increased methionine accumulation in the medium when being overexpressed (Liu et al., 2015).

Huang, Liu, Jin, Tang, Shen, Yin and Zheng (2017) combined the approaches described above, while also deleting genes of competing threonine and lysine biosynthesis pathways as well as methionine importer, to reach methionine titres of 9.75 g/l. The company Metabolic Explorer filed a patent (Dischert and Figge, 2013) for an *E. coli* strain reaching a methionine yield of 0.24 (g/g glucose) and a titre of 35 g/l, which is the highest methionine titre reported to date (Metabolic Explorer reported a methionine yield of 0.29 g/g and a methionine titre of 63 g/l, which is the solubility limit of methionine, at the Metabolic Engineering 12 conference in 2018).

L-methionine production in *C. glutamicum*

Metabolic engineering approaches for increased methionine production in *C. glutamicum* resembled the strategies chosen for *E. coli*. Several studies deleted the gene encoding the competing threonine biosynthesis pathway. Additionally, either one or a combination of the following approaches were taken: (i) overexpression of

a feedback resistant homoserine dehydrogenase (hom^m), (ii) deletion of the gene encoding the repressor (*mcbR*) of the methionine biosynthesis gene cluster, (iii) overexpression of the gene cluster (*brnF* & *brnE*) encoding the methionine export complex, (iv) overexpression of a feedback resistant aspartate kinase ($lysC^m$), and (v) deletion of the gene (*metD*) encoding the methionine uptake system (Park et al., 2007; Qin et al., 2015; Li et al., 2016). The most successful approach by Li et al. (2016) reached a titre of 6.85 g/l methionine by removing methionine uptake, reducing the feedback inhibition of enzymes by end-products, down-regulating competing pathways, and increasing the supply of precursors and NADPH.

L-methionine production in *S. cerevisiae*

Yeasts were not explored extensively as a host for the production of methionine. Brigidi et al. (1988) subjected a *Saccharomyces uvarum* strain to chemical mutagenesis and then isolated mutants that exhibited resistance to DL-ethionine, which is toxic and structurally similar to methionine. The best *S. uvarum* methionine producer was merged with an *S. cerevisiae* strain via protoplast fusion, and some of the resulting hybrids were able to accumulate up to 21 mg/l of methionine in the medium (which is lower than the 33 mg/l reached by the parent *S. uvarum* strain).

Similarly, Martinez-Force and Benitez (1992) continuously cultured a *S. cerevisiae* strain in a chemostat with increasing concentrations of DL-ethionine. One of the mutants the authors isolated had an intracellular methionine concentration of 32.6 mM (compared to 0.2 mM in the wild-type), but amino acid concentrations in the growth medium were not measured.

1.6.2 Production of L-cysteine by fermentation

The biosynthesis pathway of cysteine is closely related to the biosynthesis of methionine in *E. coli* and *C. glutamicum* (Takagi and Ohtsu, 2016).

Several recent studies successfully applied a variety of metabolic engineering strategies to improve cysteine titres in *C. glutamicum*: (i) overexpression of a mutated SATase (*cysE*) with reduced feedback inhibition, (ii) overexpression of the native OAS-SHLase (*cysK*), (iii) overexpression of *cysR*, the gene encoding the *C. glutamicum* transcription factor regulating the expression of sulphur metabolism genes, (iv) decreasing cysteine degradation by deleting the gene encoding the native cysteine dehydrogenase, (v) expression of a cysteine exporter, (vi) identifying and deleting the gene encoding the *C. glutamicum* importer of cystine (the oxidised cysteine dimer), and (vii) increasing the supply of serine (Joo et al., 2017; Kondoh and Hirasawa, 2019; Wei, Wang, Xu, Zhou, Ju, Liu and Ma, 2019). The highest titre was reached by Wei, Wang, Xu, Zhou, Ju, Liu and Ma (2019), who produced 1 g/l cysteine with thiosulphate as a sulphur source.

Similar metabolic engineering approaches were utilised in other organisms to

reach higher titres. Takumi et al. (2017) reached a titre of 2.2 g/l cysteine in *Pantoea ananatis* and Liu et al. (2018) produced 5.1 g/l cysteine in *E. coli*.

1.7 Improving the nutritional value of feedstock crops by expressing methionine storage proteins

Levels of free methionine in *Arabidopsis thaliana* (Kim et al., 2002) and potato (Di et al., 2003) leaves as well as tobacco plants (Hacham et al., 2006) were increased by overexpressing the Arabidopsis cystathionine γ-synthase (AtCGS) or its variant resistant to feedback inhibition by methionine. Co-expressing a bacterial feedback-insensitive aspartate kinase and a feedback-insensitive AtCGS in tobacco plants increased the free methionine levels 173-fold compared to wild-type plants (Hacham et al., 2008). Similar to approaches in bacteria, down-regulating the expression of the threonine synthase, which competes with methionine biosynthesis for the precursor O-phosphohomoserine, increased the soluble amounts of methionine in potato leaves (Zeh et al., 2001) and Arabidopsis plants (Bartlem et al., 2000; Avraham and Amir, 2005).

Other studies aimed at increasing the total amount of methionine by expressing a transgenic methionine storage protein. A common strategy involved the expression of 2S storage albumins. Expression of the Brazil nut 2S albumin successfully elevated the total methionine content in canola (Altenbach et al., 1992), tobacco (Altenbach et al., 1989), and *Vicia narbonensis* (Saalbach et al., 1995). Other 2S albumins expressed were the sesame 2S albumin in rice plants (Lee et al., 2003) and the sunflower 2S albumin in lupin plants (Molvig et al., 1997). However, many 2S albumins are allergens and, with the Brazil nut 2S albumin being a particularly potent allergen, their application in plant fortification might not be suitable (Bansal et al., 2007; Moreno and Clemente, 2008).

Zeins, a class of insoluble maize storage proteins (Lawton, 2002), have been utilised previously to improve plant nutritional values through transgenic gene expression. Several research groups expressed either β-zeins, γ-zeins and/or δ-zeins in a variety of plants such as tobacco, alfalfa, lotus, and soybean seeds (Bagga et al., 1995, 1997; Bellucci et al., 2002; Dinkins et al., 2001). However, the elevated levels of methionine in storage protein expressing plants can be at the expense of other sulphur containing proteins and therefore not increase the total sulphur amino acid content (Molvig et al., 1997; Tabe and Droux, 2002; Hagan et al., 2003; Chiaiese et al., 2004).

Overexpressing the feedback insensitive AtCGS elevated the expression of β-zein in alfalfa, but not tobacco (Bagga et al., 2005; Golan et al., 2005), demonstrating the influence plant post-transcriptional regulation can have on the expression of a plant protein. Furthermore, the expression of feedback insensitive AtCGS can cause oxidative stress (Matityahu et al., 2013). Similarly, the co-

expression of feedback insensitive AtCGS and β-zein in potato increased the total methionine content, but resulted in severe growth retardation and reduced anthocyanin content, thus not improving the nutritional value (Dancs et al., 2008).

1.8 Metabolic engineering and synthetic biology approaches in *S. cerevisiae*

In general, metabolic engineering describes the field of producing proteins or chemicals in microbial cell factories by altering existing metabolic pathways and/or introducing new enzymes and pathways (Bailey, 1991).

Defining the field of Synthetic Biology is particularly challenging, since it draws from many diverse disciplines such as molecular biology, genetic engineering, systems biology as well as electrical engineering. Broadly, it can be defined as the science of engineering biological systems with the aim of creating novel ("unnatural") products or applications (Endy, 2005; Serrano, 2007; Calvert, 2010).

Metabolic engineering and synthetic biology are closely related fields and sometimes not distinguishable from each other. In the following section, mainly metabolic engineering challenges and approaches as well as related synthetic biology applications in *S. cerevisiae* are discussed.

1.8.1 Metabolic engineering challenges in *S. cerevisiae*

The so called "bow-tie structure" of metabolism describes the character of cellular metabolism to convert a large number carbon, nitrogen and energy resources into a small set of central metabolites, which are involved in the synthesis of most cellular components and natural products (Csete and Doyle, 2004; Kitano, 2004). In yeast, the synthesis of metabolic enzymes is regulated by a highly interconnected transcriptional regulatory network where transcription factors regulate each other in a circular fashion, thus complicating the redirection of flux (Österlund et al., 2015).

Rewiring central metabolism for the effective production of either natural products or products traditionally produced by chemical synthesis from fossil fuels poses a variety of challenges (Yu et al., 2019). Several approaches are discussed below.

1.8.2 Design-Build-Test-Learn cycle

Given the complexity of and the frequent lack of knowledge about biological systems, a very common approach in metabolic engineering is the Design-Build-Test-Learn (DBTL) cycle. As described by Nielsen and Keasling (2016), DBTL involves four steps: (i) designing of a metabolic pathway and its genetic components for the production of a desired molecule; (ii) building the biological system from DNA parts and a microbial chassis; (iii) testing of the biological

system for the production of the desired molecule and other relevant phenotypes using various omics approaches; and (iv) learning from the gathered data to inform decisions in the design, build and/or test phase in the next iteration of the cycle.

Design

Current pathway design often suffers from a lack of standardisation and descriptive data of metabolic enzymes in common databases, therefore heavily relying on the experimental expertise of the researcher when introducing a heterologous pathways. Furthermore, the network nature of central metabolism complicates the prediction of phenotypes. Recently, genome scale models (GEM) were developed and refined to aid the design of novel metabolic pathways in *S. cerevisiae* and other organisms (OBrien et al., 2015; Sánchez et al., 2017).

Efficient design calls for the availability of a broad range well-characterised genetic parts. Most efforts in *S. cerevisiae* focused on describing promoter and terminator sequences to tune gene-expression or tags to influence the localisation of proteins (Lee et al., 2015; Reider Apel et al., 2017; Morse et al., 2017). However, the parts were characterised mainly in standard genetic backgrounds, using a single carbon source, and at a single timepoint, making it harder to predict the output of genetic circuits.

Build

Costs for the large-scale synthesis of DNA and building of metabolic pathways have fallen drastically in recent years and the establishment of biofoundries worldwide is set to accelerate this process (Kosuri and Church, 2014; Hillson et al., 2019).

The establishment of a yeast Modular Cloning (MoClo) toolkit (Lee et al., 2015) allowed the rapid protoyping of metabolic pathways in *S. cerevisiae* (Rajakumar et al., 2018) and the assembly of gRNA arrays (McCarty et al., 2019) with relative ease.

The advent of CRISPR (see section 1.8.3 for more about CRISPR applications in yeast metabolic engineering) enabled the effective engineering of the *S. cerevisiae* genome in a multiplexed way. Several studies utilised the high efficiency of homologous recombination in yeast to assemble metabolic pathways *in vivo* and integrate them into several genomic sites (Horwitz et al., 2015; Jakočiunas et al., 2015). Combining CRISPR/Cas9 genome engineering with automation enabled Si et al. (2017) to generate strains with overexpression or knockdown mutations covering more than 90% of the yeast genome. Remarkably, even in diploid or triploid industrial strains multiple genes can be knocked out with high efficiency using CRISPR/Cas9 (Lian et al., 2018).

Test

Testing the constructed strains involves the analysis of growth characteristics, protein and metabolite levels as well as the amounts of the desired product. High throughput transcriptomics, proteomics and metabolomics assays allow to describe strains on a global level (Regenberg et al., 2006; Redding-Johanson et al., 2011; Boer et al., 2010). Unfortunately, these methods are costly and time-consuming, enabling only a small subset of strains to be tested.

Several strategies have been applied to limit the number of strains to be tested or increase the screening throughput. Chen, Zhu and Liu (2016) split the 10 genes encoding the biosynthesis of fumarate into three modules, with each module consisting of 3-4 biosynthesis genes. The authors then tuned the expression and localisation of the modules to significantly increase fumarate titres in *S. cerevisiae*. Adaptive Laboratory Evolution (ALE) designs couple the formation of a desired product to cell growth. During ALE, strains are grown for many generations under a selective pressure (e. g. high/low temperature, pH or limitation of a nutrient) and fast-growing strains are isolated and sequenced. ALE has been applied to engineer thermotolerant yeast strains (Caspeta et al., 2014) and increase the production of free fatty acids in *S. cerevisiae* (Yu et al., 2018). Genetic analyisis of evolved strains enabled the identification of the mutations responsible for the phenotype. Leavitt et al. (2017) combined ALE with a fluorescent biosensor to isolate aromatic amino acid overproducers and increase the production of muconic acid in *S. cerevisiae* using flow cytometry.

Learn

The learning step relied in the past mostly on nonsystematic approaches. Comparisons with literature data and the experience of the experimenter informed the decisions in the next round of DTBL. Recently, more rigorous statistical approaches have been applied to gain more valuable insights from experimental data. Nevertheless, the growing ability to gather large datasets using genomics, transcriptomics, proteomics and metabolomics and the deposition of those datasets into databases leads to the application of machine learning for dealing with large datasets (Presnell and Alper, 2019).

The application of principal component analysis (PCA) on proteomics data enabled the identification of pathway enzymes that needed an adjustment in their expression level to improve the production of terpenes in *E. coli* (Alonso-Gutierrez et al., 2015). Costello and Martin (2018) used large proteomics and metabolomics datasets to train a machine-learning algorithm and predict pathway dynamics and guide metabolic engineering decisions. In *S. cerevisiae*, small subsets of a combinatorial library encoding heterologous pathways have been characterised to build a linear regression model (Lee et al., 2013) or a machine-learning algorithm of an artificial neural network (Zhou et al., 2018).

In addition, Design of Experiments (DOE) approaches have been successfully

applied in the past as well (Xu et al., 2017; Brown et al., 2018). The DOE methodology as a whole is discussed in section 1.9.

1.8.3 Use of CRISPR technology for metabolic engineering

Since the first description of bacterial Clustered regularly interspaced short palindromic repeats (CRISPR) and CRISPR-associated (Cas) immune systems and its capability for targeted DNA cleavage (Jinek et al., 2012), it initiated a plethora of applications in gene therapy (Karimian et al., 2019), crop engineering (Bao et al., 2019), synthetic biology (Scheller and Fussenegger, 2019), and beyond (Wu et al., 2019; Pickar-Oliver and Gersbach, 2019).

The applications of CRISPR tools for metabolic engineering and synthetic biology have been reviewed recently (Mitsui et al., 2019; Liu, Zhang and Nielsen, 2019) as well as approaches for the rewiring of cellular metabolism (Nielsen and Keasling, 2016; Yu et al., 2019). The following discussion will focus on CRISPR applications for metabolic engineering in *S. cerevisiae* (for non-conventional yeasts, see the review by Cai et al. (2019)), which are important in the context of this work.

Since *S. cerevisiae* possesses a highly efficient system for repairing double stranded breaks (DSB) by homologous recombination (HR), CRISPR induced DSB can be utilised for efficient gene editing (Storici et al., 2003). The advantage of CRISPR/Cas9 compared classical HR is the absence of a selection marker and the high efficiency when targeting several loci. The first successful application of CRISPR/Cas9 has been demonstrated by DiCarlo et al. (2013) and since then a variety of different approaches demonstrated efficient knock-outs of several genes in haploid and diploid strains (Ryan et al., 2014; Jakočiūnas et al., 2015; Lian et al., 2018). Similarly, several studies exploited the yeast HR ability to assemble and integrate single or multi-gene cassettes into one or several different loci (Horwitz et al., 2015; Jakočiunas et al., 2015; Reider Apel et al., 2017). Shi et al. (2016) integrated up to 18 copies of large DNA fragments (up to 24 kbp) encoding the xylose utilisation pathway in the Ty retrotransposon δ sites with high efficiency using CRISPR/Cas9.

Cpf1 is a CRISPR RNA guided DNA nuclease analogous to Cas9. Cpf1 has unique features that might be advantageous for gene editing: the protospacer adjacent motif (PAM) is TTTN, which enables the targeting of AT rich regions, and the RNaseIII activity of Cpf1 can be used to process precrRNA arrays for multiplexed genome editing (Zetsche et al., 2015). CRISPR/Cpf1 mediated gene disruptions have also been achieved in *S. cerevisiae* (Lian et al., 2017; Verwaal et al., 2018).

Cas9 can be turned catalytically inactive by introducing two point mutations in the catalytic domains, but, crucially, dead Cas9 (dCas9) still retains its gRNA mediated DNA binding capability. This feature has been used to down- or

up-regulate genes in a targeted manner (as opposed to a deletion or promoter swap). Down-regulation via CRISPR interference (CRISPRi) was achieved by either targeting dCas9 to the promoter sequence, blocking transcription, or fusing dCas9 to a transcription repression domain such as Mxi1. CRISPR activation (CRISPRa) is mediated by fusing dCas9 to transcription activation domains such as VP64 or VPR, that recruit transcription factors and/or RNA pol II (Gilbert et al., 2013; Farzadfard et al., 2013; Zalatan et al., 2015). Ni et al. (2019) successfully applied CRISPRi to down-regulate competing pathways in order to increase β-amyrin production in *S. cerevisiae*.

1.9 Design of Experiments for metabolic engineering

Typically, processes are optimised one-factor-at-a-time (OFAT), where only one factor is changed while all other factors remain constant. However, OFAT is unable to discern the effects of factor interactions and can lead the experimenter to find quasi optimal conditions instead of the actual optimal conditions of the system (Figure 1.10 A). OFAT is especially vulnerable to misleading conclusions when optimising biological systems, that very often involve many different and highly interdependent factors (Österlund et al., 2015).

Design of Experiments (DOE) is a multifactorial statistical methodology that applies to both the design as well as the analysis of experiments for process optimisation. In DOE, several factors (e. g. media components, temperature or expression of a gene) are varied at the same time and the system responses (e. g. product titres or growth rates) are measured (Figure 1.10 B). Several common screening designs such as Plackett-Burman (Plackett and Burman, 1946), Box-Behnken (Box and Behnken, 1960), or constrained optimal designs (Lee, 1988; de Aguiar et al., 1995) aim to reduce the variance of estimates with a minimal number of experiments performed. The availability of DOE software such as JMP (JMP and Proust, 2018) simplified the process of designing experiments and visualising the analysis of the gathered data. DOE has been applied successfully in bioprocess engineering (Mandenius and Brundin, 2008; Kumar et al., 2014), but only the recent advances in DNA synthesis and assembly made it possible to use DOE for the optimisation of metabolic pathways.

The growth media and expression levels of genes involved in the 6-aminocaproic acid pathway were co-optimised in *E. coli* using DOE. The authors insulated the transcriptional units to avoid transcriptional readthrough that could affect more than one gene when changing promoter strengths. They concluded that optimising the gene expression levels first would have lead them to a different and suboptimal combination of promoter strengths (Zhou et al., 2015). When optimising expression levels of biosynthetic enzymes, an extensive characterisation of promoter strengths and the transformation of discrete gene expression levels

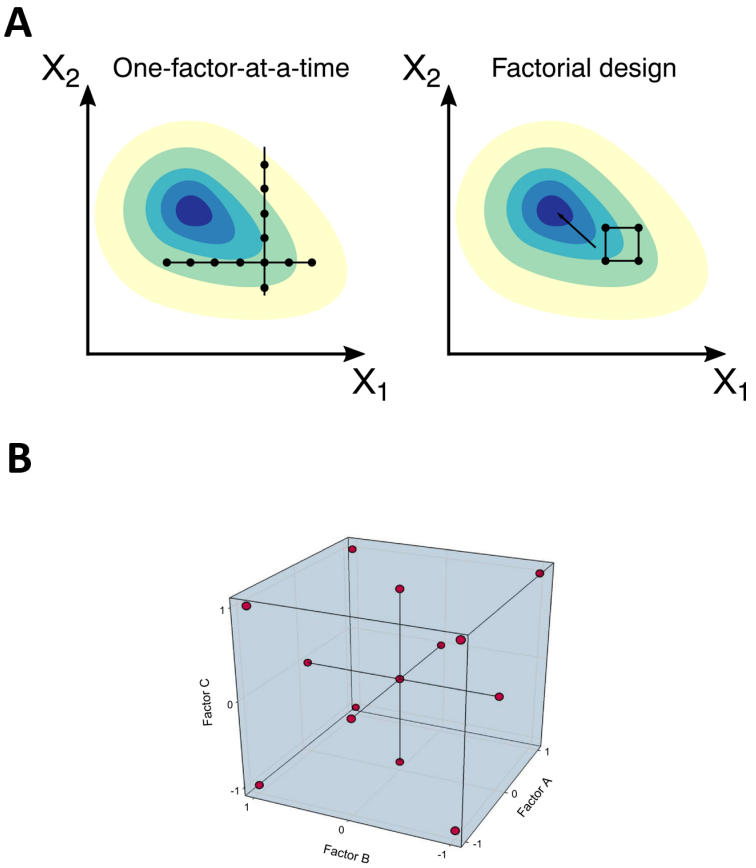

Figure 1.10: Design of Experiments. (A) The left figure shows how a true optimum can be missed in an OFAT approach. Keeping factor X_2 constant, several experiments are performed, before factor X_1 is kept constant and, starting from the optimum, more experiments are performed. Since there is an interaction between X_1 and X_2, the true optimum is never reached. By simultaneously changing both factors and analysing the results using DOE software, the direction of the true optimum can be discerned. Every black dot represents a single experiment/measurement, darker shades represent more optimal conditions. The figure is adapted from Mandenius and Brundin (2008). **(B)** A central composite design in a case with three factors. Every red dot represents a single combination of factor levels. The lowest (-1), centre (0) and highest levels of each factor are represented on the corresponding axis.

into logarithmic variables (linlog transformation) proved to be essential for a successful application of DOE (Xu et al., 2017). Young et al. (2018) used a DOE guided iterative approach to improve the production of itaconic acid in *S. cerevisiae* by first comparing alternative pathways to the product before optimising the expression levels in the pathway and overcoming bottlenecks. Another DOE approach was used to screen a subset of a combinatorial deletion library alcohol dehydrogenase isozymes in different fermentation conditions. The model was able to describe known behaviour and novel interactions of the alcohol dehydrogenase isozymes (Brown et al., 2018).

The establishment of standardisation and deposition of well characterised genetic parts, the automation of modular cloning and application of DOE methodology enables streamlining the DTBL cycle. Several recent studies demonstrated the efficient application of automated pipelines for the construction and optimisation of synthetic metabolic pathways the production of chemicals in microbial cell factories (Rajakumar et al., 2018; Carbonell et al., 2018; Exley et al., 2019).

1.10 Aim and scope of this thesis

L-methionine is a sulphur containing amino acid essential for all animals that is routinely added to animal feeds to increase growth (Willke, 2014). The fermentative production of L-methionine was achieved with high titres in *C. glutamicum* and *E. coli* (Li et al., 2016; Huang, Liu, Jin, Tang, Shen, Yin and Zheng, 2017; Dischert and Figge, 2013), while the attempts to overproduce methionine in yeast were limited (Brigidi et al., 1988). Similarly, intensive research was conducted into improving the methionine content of common crop plants by changing plant metabolism and overexpress methionine storage proteins (Galili et al., 2005; Galili and Amir, 2013; Wang et al., 2017). *S. cerevisiae*, a generally recognised as safe (GRAS) organism, has the potential to be an affordable animal feed that can be added directly to animal feeds.

The aim of this thesis is to engineer *S. cerevisiae* to overproduce methionine and increase the total sulphur amino acid content by overexpressing a methionine storage protein. The work mainly focuses on (i) identifying key factors in the pathway by applying a DOE approach, (ii) increasing sulphur amino acid supply by removing pathway bottlenecks, and (iii) overexpressing methionine storage proteins in engineered strains.

In chapter 3, a DOE approach is chosen to identify key factors influencing the production of methionine in *S. cerevisiae*. The gathered data is used to build a linear regression model, which subsequently informs the construction of a methionine overproducing strain.

In chapter 4, the supply of a methionine precursor, homoserine, is increased by rendering the key enzyme in the pathway, aspartate kinase, feedback insensitive. The resulting strain is compared to the wild-type and previously constructed

strain for methionine production. Furthermore, two OAH-SHLases from different organisms are expressed to increase the supply of homocysteine and it is investigated, whether *S. cerevisiae* can be used as production platform for another sulphur amino acid, cysteine.

Finally, three different methionine storage proteins are expressed in chapter 5. A truncated 10 kDa δ-zein from maize is expressed in the wild-type and two methionine overproducing strains. The truncated and full 10 kDa δ-zein are compared by homology modelling.

Chapter 2

Materials and Methods

2.1 Materials

2.1.1 *S. cerevisiae* growth

All OD_{600} measurements were performed using a WPA biowave CO8000 cell density meter, unless otherwise stated. All media were autoclaved prior to use.

YPD: 10 g/l yeast extract, 20 g/l peptone, 20 g/l D-glucose

SC-URA + 2 % D-Glc: 6.9 g/l yeast nitrogen base (Sigma Y0626), 0.77 g/l CSM-URA (Formedium DCS0169), 20 g/l D-glucose

SC-LEU + 2 % D-Glc: 6.9 g/l yeast nitrogen base (Sigma Y0626), 0.77 g/l CSM-LEU (Formedium DCS0091), 20 g/l D-glucose

SC-HIS + 2 % D-Glc: 6.9 g/l yeast nitrogen base (Sigma Y0626), 0.77 g/l CSM-HIS (Formedium DCS0071), 20 g/l D-glucose

SC-MET + 2 % D-Glc: 6.9 g/l yeast nitrogen base (Sigma Y0626), 0.77 g/l CSM-MET (Formedium DCS0111), 20 g/l D-glucose

SC-MET + 4 % D-Glc: 6.9 g/l yeast nitrogen base (Sigma Y0626), 0.77 g/l CSM-MET (Formedium DCS0111), 40 g/l D-glucose

SC-MET-URA + 2 % D-Glc: 6.9 g/l yeast nitrogen base (Sigma Y0626), 0.77 g/l CSM-MET-URA (Formedium DCS0651), 20 g/l D-glucose

SC-MET-URA + 4 % D-Gal: 6.9 g/l yeast nitrogen base (Sigma Y0626), 0.77 g/l CSM-MET-URA (Formedium DCS0651), 40 g/l D-galactose

SC-URA + 2 % D-Gal: 6.9 g/l yeast nitrogen base (Sigma Y0626), 0.77

g/l CSM-URA (Formedium DCS0169), 20 g/l D-galactose

YPD agar: 10 g/l yeast extract, 20 g/l peptone, 20 g/l D-glucose (Fisher Scientific, G/0500/60), 20 g/l agar (Oxoid LP0011)

SC-URA + 2 % D-Glc agar: 6.9 g/l yeast nitrogen base (Sigma Y0626), 0.77 g/l CSM-URA (Formedium DCS0169), 20 g/l D-glucose (Fisher Scientific, G/0500/60), 20 g/l agar (Oxoid LP0011)

2.1.2 *E. coli* growth

All OD_{600} measurements were performed using a WPA biowave CO8000 cell density meter, unless otherwise stated. All media were autoclaved prior to use.

LB: 10 g/l tryptone, 5 g/l yeast extract, 10 g/l NaCl

LB agar: 10 g/l tryptone, 5 g/l yeast extract, 10 g/l NaCl. 20 g/l agar

2.1.3 Antibiotics

Ampicillin: stock concentration was 100 mg/ml in dH_2O; working concentration was 100 μg/ml

Chloramphenicol: stock concentration was 40 mg/ml in 100 % ethanol; working concentration was 40 μg/ml

Spectinomycin: stock concentration was 100 mg/ml in dH_2O; working concentration was 100 μg/ml

2.1.4 Molecular Biology

TSS buffer: 5 g PEG 8000 (Sigma 1546605), 0.3 g $MgCl_2$*H_2O, 2.5 ml Dimethyl sulfoxide (DMSO), add LB up to 50 mL.

E.Z.N.A. Plasmid Mini Kit I, (Q-spin): purchased from Omega Bio-Tek

OneTaq: OneTaq Quick-Load 2X Master Mix with Standard Buffer was purchased from NEB

Q5: 5X Q5 Reaction Buffer, 2 mM dNTPs and 2 U/μl Q5 High-Fidelity DNA Polymerase were purchased from NEB

Restriction enzymes: all were purchased from NEB

Agarose: purchased from Invitrogen

TAE (1X): 40 mM Tris, 20 mM acetate, 1 mM EDTA

Zymoclean - Gel DNA Recovery Kit: purchased from Zymoresearch

10X T4 DNA ligase buffer: purchased from NEB (B0202S)

T7 DNA ligase: purchased from NEB (M0318)

2.1.5 *S. cerevisiae* transformation

Salmon sperm DNA (10 mg/ml): purchased from Invitrogen (15632-011)

Lithium acetate (1 M): 5.101 g Lithium acetate dihydrate (Sigma 213195) dissolved in 50 ml dH_2O

PEG 3350, 50 % (w/v): 50 g PEG 3350 (Sigma 88276) dissolved in 100 ml dH_2O.

2.1.6 *S. cerevisisae* genomic DNA extraction

Chelex 100: purchased from Sigma

Acid washed glass beads: purchased from Sigma

2.1.7 GC-MS

GC/MS Free (Physiological) Amino Acid Analysis Kit: purchased from Phenomenex Inc. (KG0-7166)

D/L-Ethionine: purchased from Alfa Aesar (A1315406)

L-cysteine: purchased from Sigma Aldrich (30089-25G)

L-homoserine: purchased from Sigma Aldrich (H6515-250MG)

L-homocysteine: purchased from Sigma Aldrich (69453-50MG)

2.1.8 *S. cerevisiae* cell lysis

YeastBuster Protein extraction reagent: purchased from Merck (71186-3, including 100X THP solution)

Acid washed glass beads: 425-600 μm purchased from Sigma (G8772)

2.1.9 Microplate assays

All microplate assays were performed in a Tecan Sunrise plate reader.

96-well plates: purchased from Costar (3628)

Tape: electrical insulation tape, 12mm x 20m, RS Components 504-2380

2.2 Methods

2.2.1 Storage of *E. coli* and *S. cerevisiae* strains

For long term storage, *E. coli* and *S. cerevisiae* strains were stored at -80 °C in 25 % (v/v) glycerol. For short term storage, strains were kept on agar plates at 4 °C.
To prepare *E. coli* glycerol stocks, 5 ml LB containing the appropriate antibiotic was inoculated with the desired *E. coli* strain and grown overnight at 37 °C (shaking at 200 rpm). The overnight culture was diluted 1:10 into 5 ml LB containing the appropriate antibiotic and grown for 3 hr as above. To prepare *S. cerevisiae* glycerol stocks, 5 ml YPD was inoculated with the desired *S. cerevisiae* strain and grown overnight at 30 °C (shaking at 200 rpm). The overnight culture was diluted 1:10 into 5 ml YPD and grown for 4 hr as above. 750 μl of culture was mixed with 750 μl of 50 % (v/v) glycerol and stored -80 °C.

2.2.2 Preparation of chemically competent cells

Chemically competent *E. coli* cells were prepared using the TSS buffer method. 5 ml of LB was inoculated and grown overnight at 37 °C (200 rpm). 2.5 ml of the overnight culture was used to inoculate 250 ml of LB in a shake flask and the culture was grown until it reached OD_{600} of 0.4. Once the desired cell density was reached, the culture was placed on ice for 30 min and then centrifuged at 4,000 x g at 4 °C for 8 min. The pellet was resuspended in 20 ml ice-cold TSS buffer and aliquots of 100 μl were snap frozen in liquid nitrogen and stored at -80 °C.

2.2.3 Plasmid preparation

5 ml of LB containing the appropriate antibiotic was inoculated with a colony of *E. coli* containing the desired plasmid, and grown at 37 °C overnight (shaking at

200 rpm). Plasmid extraction was performed using the E.Z.N.A. Plasmid Mini Kit I according to manufacturers instructions, eluting in 50 μl dH_2O.

2.2.4 Polymerase Chain Reaction (PCR)

PCR reactions to amplify homology arms for gene deletions/promoter insertions or to amplify deleted/inserted regions for sequencing were performed using Q5 DNA Polymerase. The reaction mixture was 1X Q5 reaction buffer, 0.2 mM dNTPs, 0.5 μM each primer, 50 ng BY4742 gDNA template and 1 U Q5 High-Fidelity DNA Polymerase. The thermocycling programme was: 98 °C for 30 s; 35 cycles of 98 °C for 30 s, anneal for 30 s, extension at 72 °C (for 30 s/kbp); 72 °C for 2 min; hold at 16 °C. The annealing temperature started at 65 °C, was lowered by 1 °C each cycle for 10 cycles and remained at 55 °C for the remaining 25 cycles. The PCR products were purified by gel extraction.

2.2.5 Restriction digest

Restriction digests of plasmid minipreps were performed as follows. Mixed 43 μl plasmid, 2 μl of the restriction enzyme (NEB) and 1X CutSmart buffer (BsaI digest) or 1X NEBuffer 3.1 (BsmBI) in a final volume of 50 μl. The reaction was incubated at 37 °C (BsaI) or 55 °C (BsmBI) for at least 1 hr and analysed by agarose gel electrophoresis.

2.2.6 Agarose gel electrophoresis

Restriction digests or PCR reactions were mixed with 1X Gel Loading Dye, Purple (NEB B7024S) and loaded onto an agarose-TAE gel. PCR reactions that used OneTaq 2X Mastermix were loaded directly onto the gel. The percentage of agarose was typically 1 % but was adjusted based on the expected size of the bands. The gel was run at 100 V in 1X TAE buffer and imaged using a Gel Doc XR+ Gel Documentation System (BioRad).

2.2.7 Agarose gel extraction

PCR reactions were run on agarose-TAE gels and purified using the Zymoclean - Gel DNA Recovery Kit, according to the manufacturers instructions. Elution was in 30 μl dH_2O.

2.2.8 Sanger sequencing

Plasmids and linear PCR amplified DNA were sequenced by MRC PPU DNA Sequencing and Services (University of Dundee) using the Sanger sequencing method.

2.2.9 Plasmid construction

Plasmids were constructed using the Golden Gate assembly method described for the MoClo-Yeast-Toolkit (Lee et al., 2015).

The sequences of *10-kDa δ-zein*, *Ber e 1*, and *SFA8* were *S. cerevisiae* codon-optimised and ordered from IDT. The *10-kDa δ-zein* DNA template was PCR amplified with the primer pairs oDS0394/395 (N-terminal tag) & oDS0402/408 (C-terminal tag), respectively, and cloned into pCPS1UHA (2μ, *URA3*) with P_{GAL1} & T_{TDH1} as well as N- or C-terminal 3xFLAG-6xHIS-tags to generate the plasmids pDS089 (N-terminal tag) & pDS090 (C-terminal tag). The *Ber e 1* DNA template was PCR amplified with the primer pairs oDS0396/397 (N-terminal tag) & oDS0404/409 (C-terminal tag), respectively, and cloned into pCPS1UHA (2μ, *URA3*) with P_{GAL1} & T_{TDH1} as well as N- or C-terminal 3xFLAG-6xHIS-tags to generate the plasmids pDS091 (N-terminal tag) & pDS092 (C-terminal tag). The *SFA8* DNA template was PCR amplified with the primer pairs oDS0398/393 (N-terminal tag) & oDS0406/410 (C-terminal tag), respectively, and cloned into pCPS1UHA (2μ, *URA3*) with P_{GAL1} & T_{TDH1} as well as N- or C-terminal 3xFLAG-6xHIS-tags to generate the plasmids pDS093 (N-terminal tag) & pDS094 (C-terminal tag).

The sequences of *LmMetY* and *RsMetZ-M3* were *S. cerevisiae* codon-optimised and ordered from IDT. *LmMetY* was PCR amplified with the primer pair oDS0416/417 and *RsMetZ-M3* was PCR amplified with the primer pair oDS0418/419. Both were cloned into pCPS1UHA (2μ, *URA3*) with P_{CCW12} & T_{TDH1} to generate the plasmids pDS095 & pDS096. *MET17* was PCR amplified from BY4742 gDNA with the primer pair oDS0422/423 and cloned into pCPS1UHA (2μ, *URA3*) with P_{CCW12} & T_{TDH1} to generate pDS097.

The sequences of *CYS3* and *AQR1* were split into two parts in order to remove internal BsaI recognition sites in the genomic sequence. *CYS3* was PCR amplified from BY4742 gDNA with the primer pairs oDS0431/432 & oDS0433/434, respectively, and cloned into pCP12UHA (2μ, *URA3*) with P_{PGK1} & T_{ENO2} to generate pDS098. *AQR1* was PCR amplified from BY4742 gDNA with the primer pairs oDS0435/436 & oDS0437/438, respectively, and cloned into pCP23UHA (2μ, *URA3*) with P_{TEF1} & T_{PGK1} to generate pDS099. Two multi-cassette plasmids were constructed by cloning pDS096 & pDS098 into pMGSEUHS to generate pDS100 and cloning pDS096, pDS098 & pDS099 into pMGSEUHS to generate pDS101, respectively.

For constructing plasmids carrying a sgRNA expression cassette, two complementary DNA oligos were designed. The forward oligo was 5'-GACTTT$(N)_{20}$-3' and the reverse oligo 5'-AAAC$(N)_{20}$AA-3', whereas N_{20} represented the protospacer sequence and its reverse complementary sequence, respectively. The oligos were phophorylated (100 nmol each, T4 polynucleotide kinase, NEB M0201S) in a 10 μl reaction for 1 hr at 37 °C. Both reactions were mixed, 180 μl of ddH_2O added and 50 μl of the mixture were annealed in a thermocycler (96 °C for 6 min, then decrease the temperature at a rate of 0.1 °C per minute until 23 °C was

reached). Finally, 2 μl (20 fmol) of the annealed oligos were used for a Golden Gate assembly (BsmBI) into pWS082b.

2.2.10 *S. cerevisiae* transformation

Yeast transformation was performed as follows. Cells were grown overnight in YPD, diluted into the same media (5 ml per transformation) for an OD_{600} of 0.15, and grown until OD_{600} 0.4-0.6 ($\approx$ 4 hr). The culture was transferred to 50 ml Falcon tubes, pelleted (3000 RCF for 5 min), resuspended in the same volume dH_2O, pelleted again (3000 RCF for 2 min) and resuspended in 1/5th volume dH_2O. Cells were transferred to 1.5 ml microtubes (1 ml / tube), spun at 10,000 RCF for 1 min. Meanwhile, salmon sperm DNA was incubated at 100 °C for 5 min, briefly vortexed and stored on ice until later use. The pellet was resuspended in 34 μl of DNA and 286 μl of transformation mix (10 μl 10 mg/ml salmon sperm DNA, 36 μl 1 M lithium acetate and 240 μl 50 % PEG 3350) was added, and cells were mixed by vortexing. Cells were incubated at 42 °C for 40 min, pelleted (14,000 RCF, 1 min) and resuspended in 80 μl dH_2O, and 80 μl was plated onto appropriate selective media and incubated at 30 °C for $\approx$ 48 hr until colonies can be seen.

2.2.11 Verification of *S. cerevisiae* strains

DNA of individual colonies from the transformation was extracted using the GC prep method (Blount et al., 2016). An individual colony was picked from the plate, patched on a YPD agar plate, resuspended in 100 μl 5 % Chelex 100, and glass beads were added to approximately half sample volume. Cells were vortexed at maximum speed for 4 min, incubated at 100 °C for 2 min, pelleted (14,000 RCF, 1 min), and the supernatant (containing the DNA) was transferred to a fresh tube.

The extracts were analysed by PCR using OneTaq polymerase and a touch-down PCR programme. The forward primer was binding $\approx$550 bp upstream of the genomic target (outside of the homology flank region) and the reverse primer was binding either $\approx$100-150 bp downstream of the promoter region (for promoter insertions) or $\approx$100-150 bp downstream of the gene (for deletions). The reaction was set up as follows: 0.4 μl 1 μM each primer, 1 μl DNA extract, 10 μl OneTaq Quick-Load 2X Master Mix with Green Buffer (NEB M0485), 8.6 μl dH_2O. The cycling programme was: 94 °C for 30 s; 10 cycles of 94 °C for 30 s, 60 C for 30 s (decreasing by 1 °C per cycle), 68 °C for 1 min; 25 cycles of 94 °C for 30 s, 50 °C for 45 s, 68 °C for 1 min; 68 °C for 5 min; hold at 16 °C. 10 μl of PCR reaction was analysed by agarose gel electrophoresis.

Positive patched colonies were re-streaked on YPD plates and and single colonies were verified as above. Positive re-streaked colonies were chosen for 5 ml overnight cultures in YPD for long-term storage at -80 °C.

Additionally, for strains confirmed by PCR, the genomic regions containing promoter insertions or gene deletions were confirmed by Sanger sequencing. Genomic regions were amplified by PCR using Q5 (touch-down protocol as described above) with primers ≈50-100 bp binding up- and downstream of the homology flank region, respectively. The amplified linear DNA was sent out for Sanger sequencing.

2.2.12 *S. cerevisiae* cell lysis for GC-MS analysis

The cell lysis solution consisted of YeastBuster with 1X THP and 100 μM D/L-Ethionine (as an internal standard) added and was prepared freshly on the day. 1 ml of culture was pelleted (14,000 RCF, 1 min), the pellet resuspended in 100 μl of cell lysis solution and vortexed at maximum speed for 1 min. The mixture was gently shaking at room temperature for 15 min, before being vortexed at maximum speed for 1 min. The cell debris was pelleted (14,000 RCF, 1 min) and the supernatant was transferred to a new microcentrifuge tube.

2.2.13 Amino acid extraction and derivatisation for GC-MS analysis

Amino acids in the cell lysates were extracted and derivatised using the EZ:faast GC/MS Free (Physiological) Amino Acid Analysis Kit (Phenomenex, KG0-7166) according to the manufacturer's instructions. The samples were resuspended in 100 μl of Reagent 6 (iso-octane 80 %, chloroform 20 %, provided by the manufacturer).

2.2.14 Gas chromatography-mass spectrometry (GC-MS) analysis

Derivatised samples of amino acid extracts and amino acid calibration standards were analysed using a Shimadzu GCMS-QP2010-SE machine. Injection volume was 1 μl with a 1:10 split injection ratio. The column was a Phenomenex ZB-AAA column (10 m x 0.25 mm). The GC parameters were as follows: constant helium flow at 1.1 ml/min; injection at 300 °C; the oven was heated to initially 110 °C, then the temperature was increased to 320 °C at a rate of 30 °C / min, then held at 320 °C for 1 min. Ionisation was by electron ionisation (EI), and the MS parameters were: MS source at 240 °C, MS quad at 180 °C, scan range 45-450 m/z, acquisition rate of 3.5 scans/s.

Ion chromatograms and mass spectra were analysed and peak areas were calculated using the OpenChrom 1.3.0 software. Amino acid standards provided by the EZ:faast kit as well as bought in standards for D/L-ethionine, L-cysteine, L-homocysteine and L-homoserine were run in concentrations of 5-400 μM to create calibration curves for the quantification of samples. Peaks were identified by

their major ions, retention time and comparison to a library provided by the kit manufacturer. Peaks were integrated in the total ion chromatogramme (TIC), unless the compounds were in low abundance in the sample. For methionine, aspartic acid, serine, asparagine, cystathionine, cysteine and homocysteine, the TIC was processed by subtracting all ions except the major ions of the compound from the chromatogramme before integrating the peaks. The major ions for every compound are listed in table 2.1.

Table 2.1: List of amino acids detected by GC-MS and its corresponding major ions

Compound	**Abbr.**	**Major Ions (m/z)**
α-Aminoadipic acid	AAA	98, 244
α-Aminobutyric acid	ABA	102, 144
allo-Isoleucine	aILE	130, 172
Alanine	ALA	88, 130
α-Aminopimelic acid	APA	198, 258, 286
Asparagine	ASN	113, 155
Aspartic acid	ASP	130, 216
β-Aminobutyric acid	βAIB	116, 130, 158
Cysteine	CYS	162, 206, 248
Cystine	C-C	216, 248
Cystathionine	CTH	146, 203, 272
Ethionine	ETH	143, 203, 291
Glutamine	GLN	84, 112, 187
Glutamic acid	GLU	142, 170, 230
Glycine	GLY	116, 207
Glycil-proline	GPR	117, 144, 201
Histidine	HIS	136, 168, 282
Homocysteine	HCYS	142
Homoserine	HSER	102, 128, 143
Hydroxylysine	HLY	129, 169
3-Hydroxyproline	3HYP	130, 172, 259
Isoleucine	ILE	101, 130, 172
Leucine	LEU	86, 130, 172
Lysine	LYS	128, 153, 172
Methionine	MET	101, 203, 277
Norvaline	NOR	72, 116, 158
Ornithine	ORN	70, 114, 156
Phenylalanine	PHE	128, 147, 206
Proline-hydroxyproline	PHP	114, 156, 186
Proline	PRO	114, 156, 243

Continued on next page

Table 2.1 – *Continued from previous page*

Compound	Abbr.	Major Ions (m/z)
Sarcosine	SAR	130, 217
Serine	SER	101, 146, 203
Threonine	THR	101, 160
Thioproline	TPR	147, 174
Tryptophan	TRP	130
Tyrosine	TYR	107, 164, 206
Valine	VAL	98, 116, 158

2.2.15 Microplate assays

S. cerevisiae strains were grown overnight in 5 ml SC-MET + 2 % D-Glc and diluted to OD_{600} 0.2 in 100 μl SC-MET + 2 % D-Glc. Blanks contained only 100 μl SC-MET + 2 % D-Glc. A lid was placed on the plate and sealed with tape, and OD_{595} was read on a Tecan Sunrise plate reader every 15 min for 72 hr. Temperature was 30 °C, shaking mode was inside and shaking intensity was normal. Data was exported into Microsoft Excel and analysed using jupyterNotebook.

2.2.16 Ni-NTA purification

BY4742 carrying plasmids expressing methionine storage proteins (pDS089-94) were grown overnight in SC-URA + 2% glucose and back-diluted into fresh induction medium (OD_{600} 0.2, 5 ml of SC-URA + 2% galactose) and grown for 24 h at 30 °C, shaking at 200 rpm. The whole culture was centrifuged (4 °C, 3000 RCF) and the supernatant discarded. The cell pellet was resuspended in 400 μl YeastBuster (with added 1x THP and 1x cOmplete Protease Inhibitor Cocktail, Roche) and vortexed at maximum speed for 1 min. The mixture was gently shaking at room temperature for 15 min, before being vortexed at maximum speed for 1 min. The cell debris was pelleted (14,000 RCF, 1 min) and the supernatant (soluble fraction) was transferred to a new microcentrifuge tube. The cell debris (insoluble fraction) was resupspended in 400 μl YeastBuster.

The Ni-NTA slurry was prepared as followed. Four different buffers were prepared: Buffer A (10 mM Tris, pH 8.0, 100 mM NaCl, 25 mM imidazole), Buffer B (10 mM Tris, pH 8.0, 100 mM NaCl, 250 mM imidazole), Buffer C (10 mM Tris, pH 8.0, 100 mM NaCl, 25 mM imidazole, 8 M urea), Buffer D (10 mM Tris, pH 8.0, 100 mM NaCl, 250 mM imidazole, 8 M urea). The Ni Sepharose slurry (Ni Sepharose 6 Fast Flow, GE Healthcare GE17-5318-06) bottle was stirred gently before the slurry was transferred to a microcentrifuge tube (100 μl per sample). The slurry was centrifuged at 500x g for 5 min, the supernatant discarded and resuspended in 2.5x volumes of H_2O. The wash is repeated twice with Buffer

A (for the soluble fraction) or Buffer C (insoluble fraction) and the slurry was resuspended in 2x volumes of Buffer A or C, respectively.

The purification step using the prepared Ni Sepharose slurry was performed as followed. The soluble or insoluble fraction (400 μl each) were mixed with 100 μl of prepared slurry (slurry washed in Buffer A for the soluble fraction and slurry washed in Buffer C for the insoluble fraction) and incubated for 1 h at room temperature under gentle shaking. Centrifuge the mixture (500 x g, 5 min) and discard the supernatant. Add 500 μl of Buffer A or C, respectively, mix gently, centrifuge (500 x g, 5 min) and collect the supernatant. Repeat wash twice and resuspend the slurry in the elution buffer (Buffer B for soluble fraction and Buffer D for insoluble fraction). Centrifuge the mixture (500 x g, 5 min) and transfer the supernatant to a new microcentrifuge tube for analysis by Western Blot.

2.2.17 SDS-PAGE

Samples were mixed with the appropriate volume of 4x SDS loading buffer (200 mM Tris-Cl, pH 6.8; 400 mM DTT; 8% w/v SDS; 0.4% w/v bromophenol blue; 40% v/v glycerol) and boiled at 95 °C for 10 min. The samples were centrifuged (14,000 RCF, 1 min) and loaded together with a protein marker (NEB, Color Prestained Protein Standard, Broad Range, p7712) on a 415% Mini-PROTEAN TGX Precast Protein Gel (Bio-Rad, #4561086). The gel was run at 100 V for 15 min and then at 120 V for 60 min. The gel was subsequently stained using the InstantBlue stain (expedeon) or used for a Western blot.

2.2.18 Western Blot

After running an SDS-PAGE, the gel was transferred on a nitrocellulose membrane using a Bio-Rad Trans-Blot SD Semi-Dry Transfer Cell according to the manufacturer's specifications. The transfer buffer was 48 mM Tris, 39 mM Glycin in 20% MeOH, the transfer was performed at 10 V for 25 minutes. After the transfer, the membrane was incubated at room temperature in blocking buffer (1x PBS, 0.1% v/v Tween-20, 5% w/v milk powder) for 45 minutes under gentle shaking. The membrane was then transferred into a 50 ml falcon tube, 6 ml of blocking buffer and 0.6 μl of primary antibody (α-His, Sigma Aldrich, H1029 and α-actin, abcam, ab14128) were added, and the membrane was incubated under constant rolling at room temperature for 2 h. Then, the buffer was discarded, 10 ml of washing buffer (1x PBS, 0.1% v/v Tween-20) was added and incubated under constant rolling at room temperature for 10 min. The wash was repeated twice. The membrane was incubated as above with the secondary antibody (α-mouse IgGPeroxidase, Sigma Aldrich, A9044) for 1 h under constant rolling at room temperature. Finally, the membrane was washed three times as above.

The chemiluminescence reaction was performed with the WesternSure PREMIUM Chemiluminescent Substrate (Li-Cor) and the image was acquired using a

C-DiGit Chemiluminescent Western Blot Scanner (LiCor). Images were analysed using the Image Studio Lite (Li-Cor) software.

2.3 Yeast strains

S. cerevisiae strains used and their genotypes are listed below in table 2.2.

Table 2.2: List of *S. cerevisiae* strains used and generated in this work.

Strain	Genotype	Notes
BY4742	*MATα, his3Δ1, leu2Δ0, lys2Δ0, ura3Δ0*	wild-type strain
yDS059	BY4742, *met30-Δ0, met32-Δ0*	wild-type with *MET30* & *MET32* deleted
yDS085	BY4742, *ADO1(-1 to -155)Δ::P_{RPL18B}, sam1-Δ0, met30-Δ0, met32-Δ0*	DoE designed strain #2
yDS093	BY4742, *MET6(-1 to -50)Δ::P_{RPL18B}, STR3(-1 to -252)Δ::P_{RPL18B}, SAH1(-1 to -226)Δ::P_{RPL18B}, ADO1(-1 to -155)Δ::P_{TDH3}, sam2-Δ0*	DoE designed strain #10
yDS100	BY4742, *STR3(-1 to -252)Δ::P_{TDH3}, ADO1(-1 to -155)Δ::P_{RPL18B}, sam2-Δ0, met30-Δ0, met32-Δ0*	DoE designed strain #17
yDS107	BY4742, *MET6(-1 to -50)Δ::P_{TDH3}, STR3(-1 to -252)Δ::P_{REV1}, SAH1(-1 to -226)Δ::P_{RPL18B}, ADO1(-1 to -155)Δ::P_{RPL18B}, sam1-Δ0, met30-Δ0, met32-Δ0*	DoE designed strain #24
yDS110	BY4742, *ADO1(-1 to -155)Δ::P_{TDH3}, sam2-Δ0*	DoE designed strain #27
yDS111	BY4742, *STR3(-1 to -252)Δ::P_{REV1}, SAH1(-1 to -226)Δ::P_{TDH3}, ADO1(-1 to -155)Δ::P_{TDH3}, sam1-Δ0, met30-Δ0, met32-Δ0*	DoE designed strain #28
yDS113	BY4742, *MET6(-1 to -50)Δ::P_{TDH3}, ADO1(-1 to -155)Δ::P_{TDH3}, met30-Δ0, met32-Δ0*	DoE designed strain #30
yDS114	BY4742, *SAH1(-1 to -226)Δ::P_{TDH3}*	DoE designed strain #31
yDS122	BY4742, *MET6(-1 to -50)Δ::P_{RPL18B}, SAH1(-1 to -226)Δ::P_{RPL18B}, sam1-Δ0*	DoE designed strain #39

Continued on next page

Table 2.2 – *Continued from previous page*

Strain	Genotype	Notes
yDS124	BY4742, *STR3(-1 to -252)*Δ*::P_{TDH3}, sam1-*Δ*0*	DoE designed strain #41
yDS130	BY4742, *MET6(-1 to -50)*Δ*::P_{RPL18B}, STR3(-1 to -252)*Δ*::P_{TDH3}, ADO1(-1 to -155)*Δ*::P_{REV1}, sam2-*Δ*0*	DoE designed strain #47
yDS133	BY4742, *sam2-*Δ*0, met30-*Δ*0, met32-*Δ*0*	wild-type with *MET30*, *MET32* & *SAM2* deleted
yDS134	BY4742, *HOM3(A846T)*	Threonine feedback inhibition of native aspartate kinase removed
yDS136	BY4742, *MET6(-1 to -50)*Δ*::P_{TDH3}, STR3(-1 to -252)*Δ*::P_{TDH3}, sam2-*Δ*0, met30-*Δ*0, met32-*Δ*0*	Best L-met producer according to DoE model
yDS138	BY4742, *MET6(-1 to -50)*Δ*::P_{TDH3}, STR3(-1 to -252)*Δ*::P_{TDH3}, sam2-*Δ*0, met30-*Δ*0, met32-*Δ*0, HOM3(A846T), thr1-*Δ*0*	Best L-met producer with the aspartate kinase inhibition removed & *THR1* deleted
yDS139	BY4742, *MET6(-1 to -50)*Δ*::P_{TDH3}, STR3(-1 to -252)*Δ*::P_{TDH3}, sam2-*Δ*0, met30-*Δ*0, met32-*Δ*0, HOM3(A846T), thr1-*Δ*0, yct1-*Δ*0*	yDS138 (no aspartate kinase inhibition) with *YCT1* deleted

2.4 List of oligonucleotides

DNA oligonucleotides used are listed in table 2.3. All oligonucleotides were ordered from Integrated DNA Technologies (IDT).

Table 2.3: List of DNA oligonucleotides used in this work.

ID	Name	Sequence	Notes
oDS0019	pDS010 FWD	GACTTTTGGTTCAATCT GCTGTCTTA	Used for the construction of pDS010
oDS0020	pDS010 REV	AAACTAAGACAGCAGA TTGAACCAAA	Used for the construction of pDS010

Continued on next page

Table 2.3 – *Continued from previous page*

ID	Name	Sequence	Notes
oDS0039	pDS012 FWD	GACTTTGTCCGCTAAAC AAAAGATCT	Used for the construction of pDS012
oDS0040	pDS012 REV	AAACAGATCTTTTGTTT AGCGGACAA	Used for the construction of pDS012
oDS0074	MET6 homo left F	GGACCATCACGCCACA TCACGTG	Used for amplifying left homology flank of *MET6*
oDS0075	MET6 homo left/pTDH3 R	ggcagtattgataatgataaactcgaa ctgGTCAATGCTCTTAGA TGCTTGCTTTTTTAT	Used for amplifying left homology flank of *MET6* with homology to P_{TDH3}
oDS0076	MET6 homo right/pTDH3 F	gtttcgaataaacacacataaacaaa caaaATGGTTCAATCTGC TGTCTTAGGTTTCC	Used for amplifying right homology flank of *MET6* with homology to P_{TDH3}
oDS0077	MET6 homo right R	CCCAACAAGACAGGTC TAGTATGAATACCT	Used for amplifying right homology flank of *MET6*
oDS0096	MET6 screen F	GGTTTCCCACAGCCATT CAACTCAG	Used for screening *MET6* promoter integrations
oDS0185	pDS030 FWD	GACTTTGATGACTACCT AATTAGACA	Used for the construction of pDS030
oDS0186	pDS030 REV	AAACTGTCTAATTAGG TAGTCATCAA	Used for the construction of pDS030
oDS0189	pDS032 FWD	GACTTTCAATCTCTTAT TTAGTAACG	Used for the construction of pDS032
oDS0190	pDS032 REV	AAACCGTTACTAAATAA GAGATTGAA	Used for the construction of pDS032
oDS0191	pDS033 FWD	GACTTTTTTGTGGAAC CCATCTACCG	Used for the construction of pDS033

Continued on next page

Table 2.3 – *Continued from previous page*

ID	Name	Sequence	Notes
oDS0192	pDS033 REV	AAACCGGTAGATGGGT TCCACAAAAA	Used for the construction of pDS033
oDS0193	pDS034 FWD	GACTTTATTATTGTCGA CGCTTACGG	Used for the construction of pDS034
oDS0194	pDS034 REV	AAACCCGTAAGCGTCG ACAATAATAA	Used for the construction of pDS034
oDS0195	ADO1 homo left F	GATCTCGTAAGAGACA GTGGTTGG	Used for amplifying left homology flank of *ADO1*
oDS0196	ADO1 homo left/pTDH3 R	ggcagtattgataatgataaactcgaa ctgGCGACTCATCCATGT GAAAATTATCG	Used for amplifying left homology flank of *ADO1* with homology to P_{TDH3}
oDS0197	ADO1 homo right/pTDH3 F	gtttcgaataaacacacataaacaaa caaaATGACCGCACCATT GGTAGTATTG	Used for amplifying right homology flank of *ADO1* with homology to P_{TDH3}
oDS0198	ADO1 homo right R	CAAGTGGAAACCACCG ATGTAG	Used for amplifying right homology flank of *ADO1*
oDS0203	SAH1 homo left F	CCACTGAAACAACCCAT TTGAGTG	Used for amplifying left homology flank of *SAH1*
oDS0204	SAH1 homo left/pTDH3 R	ggcagtattgataatgataaactcgaa ctgCAACGAGATCACGTG CACAG	Used for amplifying left homology flank of *SAH1* with homology to P_{TDH3}
oDS0205	SAH1 homo right/pTDH3 F	gtttcgaataaacacacataaacaaa caaaATGTCTGCTCCAGC TCAAAACTAC	Used for amplifying right homology flank of *SAH1* with homology to P_{TDH3}

Continued on next page

Table 2.3 – *Continued from previous page*

ID	Name	Sequence	Notes
oDS0206	SAH1 homo right R	CCATTCTGTATAAGTG GTGAACACC	Used for amplifying right homology flank of *SAH1*
oDS0207	SAM1 homo left F	CCTCTTTGTTCAGTTTA GCAACGATGG	Used for amplifying left homology flank of *SAM1*
oDS0208	SAM1 homo left/KO R	GCAAATGAAAACATGG GAGGTTGAAGGCAGCG AAGCTAACCGAAAAAC AACGATG	Used for amplifying left homology flank for deleting *SAM1*
oDS0209	SAM1 homo right/KO F	TTATTCATCGTTGTTTT TCGGTTAGCTTCGCTG CCTTCAACCTCCCATGT TTTC	Used for amplifying right homology flank for deleting *SAM1*
oDS0210	SAM1 homo right R	CGAAGATGCAATAACA AAAGACGAACAAC	Used for amplifying right homology flank of *SAM1*
oDS0211	SAM2 homo left F	CTTCATTCTCAGGTAAC AACTGGAGC	Used for amplifying left homology flank of *SAM2*
oDS0212	SAM2 homo left/KO R	GGGACCAGCCTAGCAT AAAGAAAGGGATTGTG TCGTAAATACTGGATA TATTGAAGACAG	Used for amplifying left homology flank for deleting *SAM2*
oDS0213	SAM2 homo right/KO F	CTGTCTTCAATATATCC AGTATTTACGACACAA TCCCTTTCTTTATGCTA GGCTGG	Used for amplifying right homology flank for deleting *SAM2*
oDS0214	SAM2 homo right R	CGTCTGGCAAGCCATT AGAAG	Used for amplifying right homology flank of *SAM2*
oDS0215	pDS035 FWD	GACTTTGTATATGGGA CTTATTCACG	Used for the construction of pDS035
oDS0216	pDS035 REV	AAACCGTGAATAAGTC CCATATACAA	Used for the construction of pDS035
oDS0217	pDS036 FWD	GACTTTGTTGATATAA ATAGTCAAGG	Used for the construction of pDS036

Continued on next page

Table 2.3 – *Continued from previous page*

ID	Name	Sequence	Notes
oDS0218	pDS036 REV	AAACCCTTGACTATTTA TATCAACAA	Used for the construction of pDS036
oDS0219	MET30 homo left F	GCATGTGCATGATAAT GATAAGTGATGATG	Used for amplifying left homology flank of *MET30*
oDS0220	MET30 homo left/KO R	CAGGTCCTAATCATTG AGATCGAATTTGTACG CCCTTCTCCTTTATAAA TCACCAAAC	Used for amplifying left homology flank for deleting *MET30*
oDS0221	MET30 homo right/KO F	GTGTTTGGTGATTTAT AAAGGAGAAGGGCGTA CAAATTCGATCTCAATG ATTAGGACCTG	Used for amplifying left homology flank for deleting *MET30*
oDS0222	MET30 homo right R	GCCTCAACTGTTGGGT TCTTG	Used for amplifying right homology flank of *MET30*
oDS0223	MET32 homo left F	CGCCAGATGCTTTCTAT GCTTCTAATC	Used for amplifying left homology flank of *MET30*
oDS0224	MET32 homo left/KO R	CACGCTATTTACTCTTT CAGCCATTACTGCGCAT CCTGATCCTCCATTTGG TAC	Used for amplifying left homology flank for deleting *MET32*
oDS0225	MET32 homo right/KO F	CAAAAAAGTACCAAAT GGAGGATCAGGATGCG CAGTAATGGCTGAAAG AGTAAATAGCG	Used for amplifying left homology flank for deleting *MET32*
oDS0226	MET32 homo right R	CAGCAGCAAACAAAGT TGGTGG	Used for amplifying right homology flank of *MET32*
oDS0252	pDS055 FWD	GACTTTTCTGAGACCT GGTTGAAATG	Used for the construction of pDS055
oDS0253	pDS055 REV	AAACCATTTCAACCAG GTCTCAGAAA	Used for the construction of pDS055
oDS0258	STR3 homo left F	GAAAGCATTAGATGGG ATGCAGC	Used for amplifying left homology flank of *STR3*

Continued on next page

Table 2.3 – *Continued from previous page*

ID	Name	Sequence	Notes
oDS0259	STR3 homo left/pTDH3 R	ggcagtattgataatgataaactcgaa ctgCTTTTGAGATGCGAT GAGTCTTCC	Used for amplifying left homology flank of *STR3* with homology to P_{TDH3}
oDS0260	STR3 homo right/pTDH3 F	gtttcgaataaacacacataaacaaa caaaATGCCGATCAAGAG ATTAGATACAGTTG	Used for amplifying right homology flank of *STR3* with homology to P_{TDH3}
oDS0261	STR3 homo right R	CTAGGGATATCTACAA CCTTGCAAAGC	Used for amplifying right homology flank of *STR3*
oDS0280	MET6 homo right/pREV1 F	tcgatactgcatttctaggcatatcca gcgATGGTTCAATCTGCT GTCTTAGGTTTCC	Used for amplifying right homology flank of *MET6* with homology to P_{pREV1}
oDS0281	MET6 homo right/pRPL18B F	aaaatcaattagaagaaaacaaaaaa caaaATGGTTCAATCTGC TGTCTTAGGTTTCC	Used for amplifying right homology flank of *MET6* with homology to $P_{pRPL18B}$
oDS0282	MET6 homo left/pREV1 R	aaaatatccggttgtatcggataacaa cacGTCAATGCTCTTAGA TGCTTGCTTTTTTAT	Used for amplifying left homology flank of *MET6* with homology to P_{REV1}
oDS0283	MET6 homo left/pRPL18B R	ttccttaaaaaaaatattggacatcct cttGTCAATGCTCTTAGA TGCTTGCTTTTTTAT	Used for amplifying left homology flank of *MET6* with homology to P_{RPL18B}
oDS0284	SAH1 homo right/pREV1 F	tcgatactgcatttctaggcatatcca gcgATGTCTGCTCCAGCT CAAAACTAC	Used for amplifying right homology flank of *SAH1* with homology to P_{pREV1}

Continued on next page

Table 2.3 – *Continued from previous page*

ID	Name	Sequence	Notes
oDS0285	SAH1 homo right/pRPL18B F	aaaatcaattagaagaaaacaaaaaa caaaATGTCTGCTCCAGC TCAAAACTAC	Used for amplifying right homology flank of *SAH1* with homology to $P_{pRPL18B}$
oDS0286	SAH1 homo left/pREV1 R	aaaatatccggttgtatcggataacaa cacCAACGAGATCACGT GCACAG	Used for amplifying left homology flank of *SAH1* with homology to P_{REV1}
oDS0287	SAH1 homo left/pRPL18B R	ttccttaaaaaaaatattggacatcct cttCAACGAGATCACGTG CACAG	Used for amplifying left homology flank of *SAH1* with homology to P_{RPL18B}
oDS0288	ADO1 homo right/pREV1 F	tcgatactgcatttctaggcatatcca gcgATGACCGCACCATTG GTAGTATTG	Used for amplifying right homology flank of *ADO1* with homology to P_{pREV1}
oDS0289	ADO1 homo right/ pRPL18B F	aaaatcaattagaagaaaacaaaaaa caaaATGACCGCACCATT GGTAGTATTG	Used for amplifying right homology flank of *ADO1* with homology to $P_{pRPL18B}$
oDS0290	ADO1 homo left/pREV1 R	aaaatatccggttgtatcggataacaa cacGCGACTCATCCATGT GAAAATTATCG	Used for amplifying left homology flank of *ADO1* with homology to P_{REV1}
oDS0291	ADO1 homo left/pRPL18B R	ttccttaaaaaaaatattggacatcct cttGCGACTCATCCATGT GAAAATTATCG	Used for amplifying left homology flank of *ADO1* with homology to P_{RPL18B}
oDS0292	STR3 homo right/pREV1 F	tcgatactgcatttctaggcatatcca gcgATGCCGATCAAGAG ATTAGATACAGTTG	Used for amplifying right homology flank of *STR3* with homology to P_{REV1}

Continued on next page

Table 2.3 – *Continued from previous page*

ID	Name	Sequence	Notes
oDS0293	STR3 homo right/ pRPL18B F	aaaatcaattagaagaaaacaaaaaacaaaATGCCGATCAAGAGATTAGATACAGTTG	Used for amplifying right homology flank of *STR3* with homology to P_{RPL18B}
oDS0294	STR3 homo left/ pREV1 R	aaaatatccggttgtatcggataacaacacCTTTTGAGATGCGATGAGTCTTCC	Used for amplifying left homology flank of *STR3* with homology to P_{REV1}
oDS0295	STR3 homo left/ pRPL18B R	ttccttaaaaaaaatattggacatcctcttCTTTTGAGATGCGATGAGTCTTCC	Used for amplifying left homology flank of *STR3* with homology to P_{RPL18B}
oDS0296	pREV1 screen R	gtattcaattggaatctgtgaacgc	Used for screening of the successful integration of P_{REV1}
oDS0297	pRPL18B screen R	gacaaggcacttcttgaatacttcc	Used for screening of the successful integration of P_{RPL18B}
oDS0298	pTDH3 screen R	gcatgtacgggttacagcag	Used for screening of the successful integration of P_{TDH3}
oDS0329	STR3 screen F	CATACAATAGGGAGGCTCTACTGG	Used for screening & sequencing of the *STR3* gene
oDS0330	STR3 screen R	GAGTCCACTCATCATAGTATTATCAACGAC	Used for screening & sequencing of the *STR3* gene
oDS0331	SAH1 screen F	CATTTCCATTGTATCAGTCTTCAATTC	Used for screening & sequencing of the *SAH1* gene
oDS0332	SAH1 screen R	CGTACAAGTTGTCAAACTTGGACTTAG	Used for screening & sequencing of the *SAH1* gene

Continued on next page

Table 2.3 – *Continued from previous page*

ID	Name	Sequence	Notes
oDS0333	ADO1 screen F	GGCATCTCCAAACTCATGAATG	Used for screening & sequencing of the *ADO1* gene
oDS0334	ADO1 screen R	GAAAGGAGCACTAAAGTTCAACACG	Used for screening & sequencing of the *ADO1* gene
oDS0335	MET6 screen R	CAGTGTATAGAGGCAACAATTGTTCC	Used for screening & sequencing of the *MET6* gene
oDS0336	MET30 screen F	CGTTCTAGAAATGCCTCACACC	Used for screening & sequencing of the *MET30* gene
oDS0337	MET30 screen R	CTGTTATTAGGAAGATTTAAAGGTTCATCC	Used for screening & sequencing of the *MET30* gene
oDS0338	MET32 screen F	GTACATAGTTATCTTCAAGCCGTAATTCG	Used for screening & sequencing of the *MET32* gene
oDS0339	MET32 screen R	GCTGTGACAGAAACAATTAAGTTGC	Used for screening & sequencing of the *MET32* gene
oDS0340	SAM1 screen F	GATTGCCCAATTTGATGTCG	Used for screening & sequencing of the *SAM1* gene deletion
oDS0341	SAM1 screen R	GAAGATGTTGATCACCAGACAAGC	Used for screening & sequencing of the *SAM1* gene deletion
oDS0342	SAM2 screen F	CGAAAAGAGACATACTTCCTTCACC	Used for screening & sequencing of the *SAM2* gene deletion
oDS0343	SAM2 screen R	GCAAAACATCAATTCCAACACTTC	Used for screening & sequencing of the *SAM2* gene deletion
oDS0346	pDS061 FWD	GACTTTCGTAAAAGGATGTATAACTT	Used for the construction of pDS061

Continued on next page

Table 2.3 – *Continued from previous page*

ID	Name	Sequence	Notes
oDS0347	pDS061 REV	AAACAAGTTATACATCC TTTTACGAA	Used for the construction of pDS061
oDS0348	HOM3 mut ultra F	CACGTTTGCTAGACAG TGTTACTCCAGAAGAA GCTTCTGAtTTAACATA TTATGGTTCtGAAGTTA TACATCCTTTTACGATG GAACAAG	Used for annealing with oDS0349 as a repair template to introduce the A1210T mutation in *HOM3*
oDS0349	HOM3 mut ultra R	CTTGTTCCATCGTAAAA GGATGTATAACTTCaGA ACCATAATATGTTAAaT CAGAAGCTTCTTCTGG AGTAACACTGTCTAGC AAACGTG	Used for annealing with oDS0348 as a repair template to introduce the A1210T mutation in *HOM3*
oDS0350	pDS062 FWD	GACTTTATAACCGCTGC TATGATGGG	Used for the construction of pDS062
oDS0351	pDS062 REV	AAACCCCATCATAGCA GCGGTTATAA	Used for the construction of pDS062
oDS0352	THR1 homo left F	CTCCAACGTCTCTGCCA TTG	Used for amplifying left homology flank of *THR1*
oDS0353	THR1 homo left/KO R	CTAGGGGTAAAGGACA TTTCATTGCTGTTCGCG AACCATTTTCTGTAGTC CGTATATC	Used for amplifying left homology flank for deleting *THR1*
oDS0354	THR1 homo right/KO F	GTAGATATACGGACTA CAGAAAATGGTTCGCG AACAGCAATGAAATGT CCTTTAC	Used for amplifying right homology flank for deleting *THR1*
oDS0355	THR1 homo right R	CTTAACAAGAACTTCCC GAAATTAATGTC	Used for amplifying right homology flank of *THR1*
oDS0356	THR1 screen F	CTCACAGTTTCTGACAT TAATTGAAGC	Used for screening & sequencing of the *THR1* gene deletion

Continued on next page

Table 2.3 – *Continued from previous page*

ID	Name	Sequence	Notes
oDS0357	THR1 screen R	GACGGGTAACGGAAGA AGACTC	Used for screening of the *THR1* gene deletion
oDS0374	HOM3 screen F	GTTTCTACACTTTCCTG GTTCAAGC	Used for screening & sequencing of the *HOM3* A1210T mutation
oDS0375	HOM3 screen R	GGATAAGTTCTCAGGA GGATGTGG	Used for screening & sequencing of the *HOM3* A1210T mutation
oDS0393	SFA8 R	CTAGCACGTCTCCggtcG GTCTCAGGATTTACATC TGGCAAGGCTGG	Used for amplifying Type 3 *SFA8* by PCR
oDS0394	10kDaZein 3b F	CTAGCACGTCTCAtcggG GTCTCATTCTACACATA TACCGGGCCATTTG	Used for adding Type 3b overhangs to *10kDaZein* by PCR
oDS0395	10kDaZein 3b R	CTAGCACGTCTCCggtcG GTCTCAGGATTTAGAA CGCCGCTCCGAC	Used for adding Type 3b overhangs to *10kDaZein* by PCR
oDS0396	Ber e 1 3b F	CTAGCACGTCTCAtcggG GTCTCATTCTTTCAGAG CTACAGTTACAACAAC GG	Used for adding Type 3b overhangs to *Ber e 1* by PCR
oDS0397	Ber e 1 3b R	CTAGCACGTCTCCggtcG GTCTCAGGATTTAGAA GCCAGCCATAGACCC	Used for adding Type 3b overhangs to *Ber e 1* by PCR
oDS0398	SFA8 3b F	CTAGCACGTCTCAtcggG GTCTCATTCTCCCTATG GCAGAGGTAG	Used for adding Type 3b overhangs to *SFA8* by PCR
oDS0402	10kDaZein 3 F	CTAGCACGTCTCAtcggG GTCTCATATGACACATA TACCGGGCCATTTG	Used for amplifying Type 3 *10kDaZein* by PCR
oDS0404	Ber e 1 3 F	CTAGCACGTCTCAtcggG GTCTCATATGTTCAGA GCTACAGTTACAACAA CGG	Used for amplifying Type 3 *Ber e 1* by PCR

Continued on next page

Table 2.3 – *Continued from previous page*

ID	Name	Sequence	Notes
oDS0406	SFA8 3 F	CTAGCACGTCTCAtcggG GTCTCATATGCCCTATG GCAGAGGTAGGACC	Used for amplifying Type 3 *SFA8* by PCR
oDS0408	10kDaZein no stop R	CTAGCACGTCTCCggtcG GTCTCAGGATCCGAAC GCCGCTCCGAC	Used for amplifying Type 3 *10kDaZein* without a stop codon by PCR
oDS0409	Ber e 1 no stop R	CTAGCACGTCTCCggtcG GTCTCAGGATCCGAAG CCAGCCATAGACCCTG	Used for amplifying Type 3 *Ber e 1* without a stop codon by PCR
oDS0410	SFA8 no stop R	CTAGCACGTCTCCggtcG GTCTCAGGATCCCATCT GGCAAGGCTGGC	Used for amplifying Type 3 *SFA8* without a stop codon by PCR
oDS0411	Con1 seq R	GTCATCATGCAGTCATC CGAGC	Used for sequencing plasmids with the Con1 sequence
oDS0412	10kDa seq F	CAGCTTGATGTTGCAG CAACTG	Used for sequencing *10kDaZein*
oDS0415	THR1 screen R2	CCAATCATGGATGAAC CAGTAATG	Used for screening & sequencing of the *THR1* gene deletion
oDS0416	LmMetY Type 3 F	CTAGCACGTCTCAtcggG GTCTCATATGGTCGGT CCTTCAGGC	Used for adding Type 3 overhangs to *LmMetY* by PCR
oDS0417	LmMetY Type 3 R	CTAGCACGTCTCCggtcG GTCTCAGG	Used for adding Type 3 overhangs to *LmMetY* by PCR
oDS0418	RsMetZ-M3 Type 3 F	CTAGCACGTCTCAtcggG GTCTC	Used for adding Type 3 overhangs to *RsMetZ-M3* by PCR

Continued on next page

Table 2.3 – *Continued from previous page*

ID	Name	Sequence	Notes
oDS0419	RsMetZ-M3 Type 3 R	CTAGCACGTCTCCggtcG GTCTCAGGATTTATAT GACTGCCAGTGCCTGT TTC	Used for adding Type 3 overhangs to *RsMetZ-M3* by PCR
oDS0420	LmMetY seq 1	GGACACTGATCACGCA GCTAG	Used for sequencing *LmMetY*
oDS0421	RsMetZ-M3 seq 1	CTGACTCAGGGCTTCG TATATGATTC	Used for sequencing *RsMetZ-M3*
oDS0422	MET17 Type 3 F	CTAGCACGTCTCAtcggG GTCTCATATGCCATCTC ATTTCGATACTGTTC	Used for adding Type 3 overhangs to *MET17* by PCR
oDS0423	MET17 Type 3 R	CTAGCACGTCTCCggtcG GTCTCAGGATTCATGG TTTTTGGCCAGC	Used for adding Type 3 overhangs to *MET17* by PCR
oDS0424	MET17 seq 1	GGTCTAGAAGTTCCAG GTTACGTCTATTC	Used for sequencing *MET17*
oDS0431	CYS3 1 Type 3 F	CTAGCACGTCTCAtcggG GTCTCATATGACTCTAC AAGAATCTGATAAATT TGC	Used for adding Type 3 overhangs to *CYS3* by PCR
oDS0432	CYS3 1 Type 3 R	CCggtcGGTCTCACCGAT AGAGACAGCATGGGAG	Used for adding Type 3 overhangs to *CYS3* by PCR
oDS0433	CYS3 2 Type 3 F	CAtcggGGTCTCATCGGT GATGTGTACGGTGG	Used for adding Type 3 overhangs to *CYS3* by PCR
oDS0434	CYS3 2 Type 3 R	CTAGCACGTCTCCggtcG GTCTCAGGATTTAGTT GGTGGCTTGTTTCAAG G	Used for adding Type 3 overhangs to *CYS3* by PCR
oDS0435	AQR1 1 Type 3 F	CTAGCACGTCTCAtcggG GTCTCATATGTCACGA AGTAACAGTATATACA CAGAAG	Used for adding Type 3 overhangs to *AQR1* by PCR
oDS0436	AQR1 1 Type 3 R	CCggtcGGTCTCAGTCTA CGTCCAAAGCAATCCG	Used for adding Type 3 overhangs to *AQR1* by PCR
oDS0437	AQR1 2 Type 3 F	CAtcggGGTCTCAAGACC TATAATTTTAGCAGGT ATGCTGATATAC	Used for adding Type 3 overhangs to *AQR1* by PCR

Continued on next page

Table 2.3 – *Continued from previous page*

ID	Name	Sequence	Notes
oDS0438	AQR1 2 Type 3 F	CTAGCACGTCTCCggtcG GTCTCAGGATTTAATT ATGATTATCGTTCTGAT CTCTTTTTG	Used for adding Type 3 overhangs to *AQR1* by PCR
oDS0439	pDS102 FWD	GACTTTTGTTACGCTA GCATTCATGG	Used for the construction of pDS102
oDS0440	pDS102 REV	AAACCCATGAATGCTA GCGTAACAAA	Used for the construction of pDS102
oDS0441	YCT1 homo left F	GTGATGTTACGGAGTC TTTGGTCTG	Used for amplifying left homology flank of *YCT1*
oDS0442	YCT1 homo left/KO R	GATAGAACATTTACAC AACAAAACATCAATATT CTTGATGTTTTGTTCAA CCTTCAAG	Used for amplifying left homology flank for deleting *YCT1*
oDS0443	YCT1 homo right/KO F	CTTGAAGGTTGAACAA AACATCAAGAATATTG ATGTTTTGTTGTGTAA ATGTTCTATCTG	Used for amplifying right homology flank for deleting *YCT1*
oDS0444	YCT1 homo right R	CCGAGGTATGTAATTT CAGCAAACTC	Used for amplifying right homology flank of *YCT1*
oDS0445	YCT1 screen F	CAAGCTCGGATGCAAA TCAC	Used for screening & sequencing of the *YCT1* gene deletion
oDS0446	YCT1 screen R	CAGTTGACATTCCAAG AACTATGGTTAC	Used for screening & sequencing of the *YCT1* gene deletion
oDS0447	AQR1 seq 1	GAATGGTTGCAATTCT AACAATGTG	Used for sequencing *AQR1*

2.5 List of plasmids

All plasmids used are listed below in table 2.4.

Table 2.4: List of plasmids used and generated in this work.

Name	Description	Source
pCPS1UHA	Empty yeast plasmid for Golden Gate reactions. *URA3*-marker, 2μ yeast origin of replication	M. Dale doctoral thesis
pCP12UHA	Empty yeast plasmid for Golden Gate reactions. *URA3*-marker, 2μ yeast origin of replication	M. Dale doctoral thesis
pCP23UHA	Empty yeast plasmid for Golden Gate reactions. *URA3*-marker, 2μ yeast origin of replication	M. Dale doctoral thesis
pMGSEUHS	Empty yeast plasmid for Golden Gate reactions. *URA3*-marker, 2μ yeast origin of replication. Backbone for multi-cassette plasmids.	M. Dale doctoral thesis
pWS082b	Plasmid for constructing sgRNA expressing plasmids	M. Dale doctoral thesis
pWS158b	CRISPR/Cas9 plasmid. *URA3*-marker, 2μ yeast origin of replication, P_{PGK1}-Cas9	M. Dale doctoral thesis
pWS171b	CRISPR/Cas9 plasmid. *LEU2*-marker, 2μ yeast origin of replication, P_{PGK1}-Cas9	M. Dale doctoral thesis
pWS172b	CRISPR/Cas9 plasmid. *HIS3*-marker, 2μ yeast origin of replication, P_{PGK1}-Cas9	M. Dale doctoral thesis
pDS010	sgRNA plasmid targeting *MET6*	This work
pDS030	sgRNA plasmid targeting *ADO1*	This work
pDS032	sgRNA plasmid targeting *SAH1*	This work
pDS033	sgRNA plasmid targeting *SAM1*	This work
pDS034	sgRNA plasmid targeting *SAM2*	This work
pDS035	sgRNA plasmid targeting *MET30*	This work
pDS036	sgRNA plasmid targeting *MET32*	This work
pDS055	sgRNA plasmid targeting *STR3*	This work
pDS061	sgRNA plasmid targeting *HOM3*	This work
pDS062	sgRNA plasmid targeting *THR1*	This work
pDS089	P_{GAL1}-3xFLAG-6xHis-*10kDaZein*-T_{TDH1} cloned into pCPS1UHA, 2μ, *URA3*	This work
pDS090	P_{GAL1}-*10kDaZein*-3xFLAG-6xHis-T_{TDH1} cloned into pCPS1UHA, 2μ, *URA3*	This work

Continued on next page

Table 2.4 – *Continued from previous page*

Name	**Description**	**Source**
pDS091	P_{GAL1}-3xFLAG-6xHis-*Ber e 1*-T_{TDH1} cloned into pCPS1UHA, 2μ, *URA3*	This work
pDS092	P_{GAL1}-*Ber e 1*-3xFLAG-6xHis-T_{TDH1} cloned into pCPS1UHA, 2μ, *URA3*	This work
pDS093	P_{GAL1}-3xFLAG-6xHis-*SFA8*-T_{TDH1} cloned into pCPS1UHA, 2μ, *URA3*	This work
pDS094	P_{GAL1}-*SFA8*-3xFLAG-6xHis-T_{TDH1} cloned into pCPS1UHA, 2μ, *URA3*	This work
pDS095	P_{CCW12}-*LmMetY*-T_{TDH1} cloned into pCPS1UHA, 2μ, *URA3*	This work
pDS096	P_{CCW12}-*RsMetZ-M3*-T_{TDH1} cloned into pCPS1UHA, 2μ, *URA3*	This work
pDS097	P_{CCW12}-*MET17*-T_{TDH1} cloned into pCPS1UHA, 2μ, *URA3*	This work
pDS098	P_{PGK1}-*CYS3*-T_{ENO2} cloned into pCP12UHA, 2μ, *URA3*	This work
pDS099	P_{TEF1}-*AQR1*-T_{PGK1} cloned into pCP23UHA, 2μ, *URA3*	This work
pDS100	P_{CCW12}-*RsMetZ-M3*-T_{TDH1} & P_{PGK1}-*CYS3*-T_{ENO2} cloned into pMGEUHS, 2μ, *URA3*	This work
pDS101	P_{CCW12}-*RsMetZ-M3*-T_{TDH1}, P_{PGK1}-*CYS3*-T_{ENO2} & P_{TEF1}-*AQR1*-T_{PGK1} cloned into pMGEUHS, 2μ, *URA3*	This work
pDS102	sgRNA plasmid targeting *YCT1*	This work

Chapter 3

Design of Experiments for Improving *Saccharomyces cerevisiae* Methionine Titres

3.1 Introduction

Methionine biosynthesis in *S. cerevisiae* is tightly regulated. Methionine homeostasis is maintained by transcriptional control of enzymes involved in its biosynthesis as well as feedback inhibition of these enzymes by either methionine or other metabolites involved in amino acid biosynthesis. In the biosynthesis of methionine (see also Figure 3.1), inorganic sulphur in the form of sulphate is transported through the plasma membrane to the cytosol (by Sul1p or Sul2p) and subsequently reduced to sulphide (by Met3p, Met14p, Met16p and Met5p/Met10p), before being transferred to O-acetylhomoserine by Met17p to generate homocysteine. Homocysteine is either converted to methionine by Met6p in the methyl cycle or to cysteine via cystathionine in the transsulphuration pathway (by Cys4p and Cys3p). Methionine is both a product of the pathway and a substrate for the synthesis of methionyl-tRNA and S-adenosyl-methionine through the methyl cycle (Thomas and Surdin-Kerjan, 1997; Ljungdahl and Daignan-Fornier, 2012).

The leucine-zipper transcriptional activator Met4p together with combinations of the auxiliary factors Cbf1p, Met28p, Met31p and Met32p regulates the transcriptional response to low levels of sulphur metabolites and heavy metal stress. Restricted internal methionine as well as high levels of arsenic or cadmium causes activation of Met4p, which in turn initiates the transcription of genes involved in methionine biosynthesis or heavy metal stress response. Full activation of Met4p induces transcription of all genes controlled by Met4p and triggers cell cycle arrest. Met4p is fully activated in *met30*Δ strains, but Met32p mediated lethality can be bypassed by deleting *MET32* (Patton et al., 2000; Su et al., 2008; Ouni et al., 2011). Nevertheless, full activation of Met4p leads to the increased expression of enzymes producing methionine (e. g. Met6p), but also

enzymes using methionine as a substrate (Sam1p & Sam2p) and enzymes using homocysteine, a methionine precursor, as a substrate (Cys4p).

In order to elucidate the influence of individual genetic and environmental factors and combinations of those on methionine titres, a Design of Experiments (DOE) approach was chosen to minimise the number of experiments needed to be performed. Traditional optimisation approaches often change a single factor while the other factors remain constant. This approach, often called one-factor-at-a-time (OFAT), can prove to be inefficient for understanding multi-factorial biological systems with potentially non-linear interactions between several factors. Statistical methods like DOE can help to avoid biases and reduce the use of experimental resources. DOE was successfully applied previously for strain engineering to increase violacein titres in *E. coli* (Xu et al., 2017) and ethanol production in *S. cerevisiae* (Brown et al., 2018).

For the initial design of DOE strains, six genetic factors were chosen. The expression of four genes (*MET6*, *STR3*, *SAH1* & *ADO1*) was changed by inserting a low, medium or high expressing constitutive promoter from the MoClo toolkit (Lee et al., 2015) in front of the start codon. *MET6* was overexpressed previously to increase methionine levels in S-adenosyl-methionine (SAM) producing *S. cerevisiae* strains (Chen, Wang, Wang, Dou and Zhou, 2016; Kanai, Mizunuma, Fujii and Iefuji, 2017), while SAM levels were elevated in a *S. cerevisiae* strain carrying an *sah1-1* mutation that impairs the S-adenosyl-homocysteine activity (Mizunuma et al., 2004). In another study, Kanai et al. (2013) overexpressed *SAH1* and deleted *ADO1*, which increased SAM levels. Finally, *STR3* encodes a cystathionine β-lyase that synthesises homocysteine from cystathionine.

The deletion of either *SAM1* or *SAM2* was chosen as the fifth genetic factor and aimed to reduce the accumulation of SAM. A high-throughput study identified *sam1* and *sam2* mutants as accumulating almost fourfold more intracellular methionine than the BY4742 strain during exponential growth (Mülleder et al., 2016). Nevertheless, deleting both genes is not desirable, because *sam1*/*sam2* double mutants result in SAM auxotrophy (Cherest et al., 1978).

The final genetic factor involves the constitutive activation of Met4p by the deletion of *MET30* and *MET32*. While the constitutive activation of Met4p eliminates the transcriptional repression of methionine biosynthetic genes by methionine, it also induces the expression of genes encoding enzymes that use methionine or methionine precursors as substrates (*SAM1*, *SAM2* & *CYS4*).

JMP (SAS Institute) is a statistical software package that includes a DOE application (JMP and Proust, 2018). A total of 48 strains containing different combinations of genetic factors was designed using the JMP software and cloned using CRISPR/Cas9 technology. Methionine production was quantified using gas chromatography-mass spectrometry (GC-MS), before methionine levels were used to create a linear regression model and determine the most important factors for the production of methionine in *S. cerevisiae*. Growth curves were recorded using

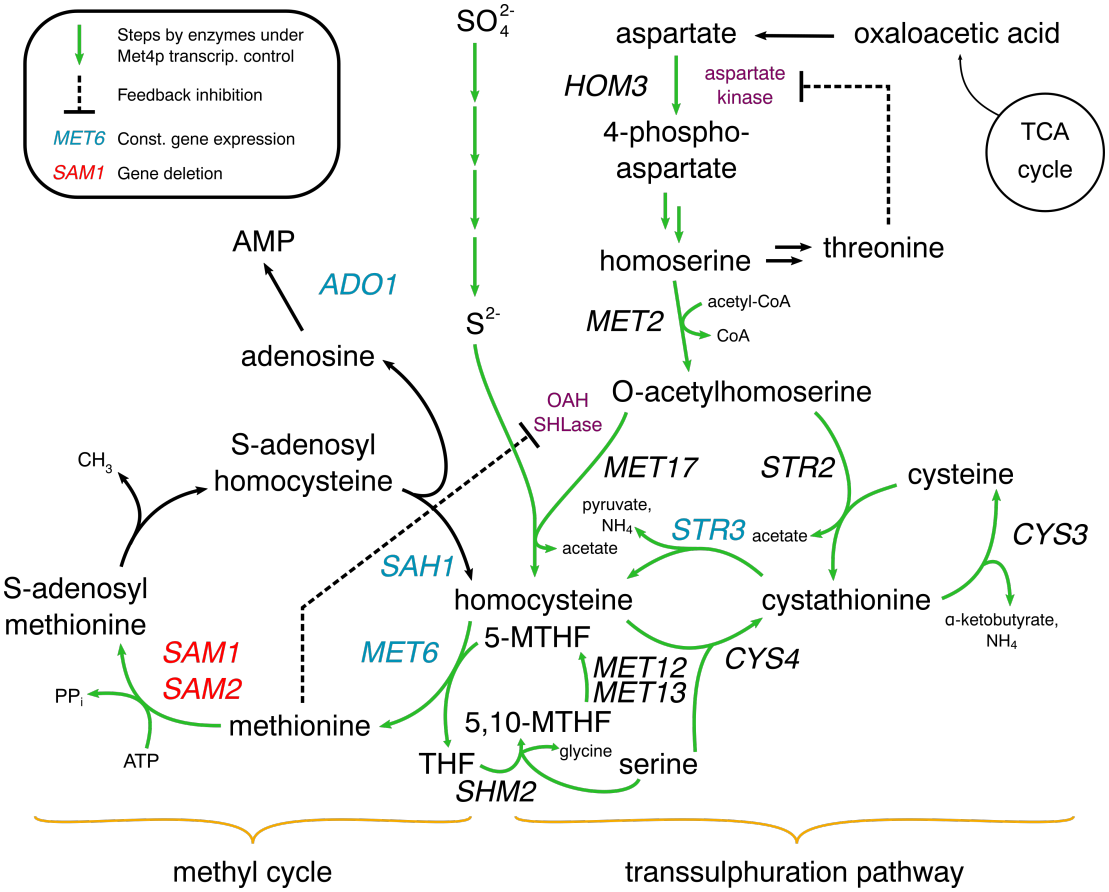

Figure 3.1: Methionine biosynthesis in S. cerevisiae and DOE targets. Enzymes involved in the biosynthesis of methionine and other sulphur metabolites are encoded by genes whose expression is controlled by the transcriptional activator Met4p (green arrows). Deletion of *MET30* and *MET32* fully activated Met4p. Four genes (*MET6*, *STR3*, *SAH1* & *ADO1*, blue) were chosen for the insertion of constitutive promoters in front of the coding sequence. Either *SAM1* or *SAM2* (red) were chosen as targets for deletion in order to reduce S-adenosyl-methionine (SAM) accumulation.

a microplate assay to investigate any detrimental effects of the strain engineering on cell growth.

3.2 Design of strains for DOE analysis

The JMP software package was used for designing the strains to be tested. Since the design included a mixture of continuous (infinite number of numerical variables between two values) and categorical (finite number of non-numerical categories) factors, the Custom Design function of JMP was used. Custom Design uses a D-Optimal Design approach, where an iterative algorithm with random starting points is used for finding optimal factor combinations (Meyer and Nachtsheim, 1995). D-Optimal Design is most desirable in screening designs, where the active factors are to be identified (JMP and Proust, 2018). It should be noted that due to the nature of the D-Optimal Design approach, re-running the Custom Design Function can lead to a different but equivalent set of factor combinations.

Table 3.1: Numerical values of promoters used in DOE model

Promoter	**Numerical value**
P_{REV1}	84
P_{RPL18B}	353
P_{TDH3}	7163
P_{MET6}	4082
P_{STR3}	1826
P_{SAH1}	459
P_{ADO1}	395

MET6, *STR3*, *SAH1* and *ADO1* were defined as continuous factors where factor levels corresponded to expression levels of the genes. Gene expression levels in *S. cerevisiae* may vary depending on environmental factors, genotype and growth phase (Lewis et al., 2014; Reider Apel et al., 2017), thus complicating the choice of numerical values for the factors chosen. Considering the experimental set-up (growth in SC-MET + 2% glucose) and the aim of the designed experiment, it was assumed that the expression levels were comparable to those of a methionine restricted environment. P_{REV1}, P_{RPL18B} and P_{TDH3} were not characterised in a methionine restricted environment by Lee et al. (2015), but they had been shown to have weak, medium and strong expression, respectively, when glucose was the carbon source. The numerical values for each promoter (P_{REV1}, P_{RPL18B}, P_{TDH3} or the native promoters P_{MET6}, P_{STR3}, P_{SAH1} and P_{ADO1}) were based on the mRNA normalised reads under methionine restriction from the dataset published by Zou

et al. (2017) and are listed in Table 3.1. Using that dataset has limitations, since it measured only the immediate transcriptional response to methionine starvation. Nevertheless, defining the promoter strength as numerical factors (rather than categorical) and assuming a methionine restricted environment enables the design to contain a smaller number of strains tested and a better representation of relative promoter strength.

The two other genetic factors were defined as categorical factors. *SAM1*/*SAM2* had three factor levels corresponding to deletions influencing SAM synthesis: wild-type (*SAM1*, *SAM2*); SAM1 KO (*sam1*Δ, *SAM2*); *SAM2* KO (*SAM1*/*sam2*Δ). *MET30*/*MET32* had two factor levels corresponding to deletions activating Met4p: wild-type (*MET30*/*MET32*); KO (*met30*Δ, *me32*Δ). All factors of the design, their role (continous or categorical) and factor levels (numerical values for promoter insertions or category for deletions) are listed in Table 3.2.

Table 3.2: Experimental factors and the associated levels of each chosen for evaluation for their impact on methionine production

Factor	**Role**	**Factor level**		
MET6	Continuous	84		7163
STR3	Continuous	84		7163
SAH1	Continuous	84		7163
ADO1	Continuous	84		7163
SAM1/SAM2	Categorical	wild-type	*SAM1* KO	*SAM2* KO
MET30/MET32	Categorical	wild-type	KO	

If every possible combination of low, medium, high or wild-type promoters in front of *MET6*, *STR3*, *SAH1* or *ADO1* as well as wild-type or deleted versions of *SAM1*, *SAM2* and *MET30*/*MET32* were to be tested, the total number of strains to be cloned would have been 1536 (4*4*4*4*3*2). The D-Optimal Design approach allowed to optimise the use of experimental resources while gaining the maximal amount of information about the influence of indiviual factors. The number of strains to be cloned was reduced to 48 and all strains of the design are listed in Table 3.3.

Table 3.3: List of DOE generated strains

MET6	**STR3**	**SAH1**	**ADO1**	**SAM1/SAM2**	**MET30/MET32**	**ID**
P_{RPL18B}	P_{TDH3}	P_{REV1}	P_{RPL18B}	SAM2 KO	KO	yDS084
wt	wt	wt	P_{RPL18B}	SAM1 KO	KO	yDS085
wt	P_{RPL18B}	P_{RPL18B}	wt	SAM2 KO	KO	yDS086
P_{REV1}	P_{REV1}	P_{REV1}	P_{REV1}	SAM1 KO	KO	yDS087
P_{RPL18B}	P_{REV1}	wt	wt	SAM2 KO	KO	yDS088
wt	P_{REV1}	wt	P_{RPL18B}	wt	wt	yDS089
P_{TDH3}	P_{REV1}	P_{RPL18B}	P_{TDH3}	SAM2 KO	wt	yDS090
P_{TDH3}	P_{RPL18B}	P_{RPL18B}	P_{RPL18B}	wt	wt	yDS091
wt	P_{REV1}	P_{REV1}	P_{REV1}	SAM2 KO	wt	yDS092
P_{RPL18B}	P_{RPL18B}	P_{RPL18B}	P_{TDH3}	SAM2 KO	wt	yDS093
P_{TDH3}	wt	P_{RPL18B}	P_{REV1}	SAM1 KO	wt	yDS094
P_{RPL18B}	P_{REV1}	P_{TDH3}	P_{RPL18B}	wt	wt	yDS095
P_{TDH3}	P_{RPL18B}	P_{TDH3}	wt	SAM2 KO	wt	yDS096
P_{REV1}	P_{TDH3}	wt	P_{TDH3}	SAM2 KO	KO	yDS097
P_{REV1}	P_{TDH3}	P_{RPL18B}	wt	SAM1 KO	KO	yDS098
P_{REV1}	P_{RPL18B}	wt	P_{REV1}	wt	wt	yDS099
wt	P_{TDH3}	wt	P_{RPL18B}	SAM2 KO	KO	yDS100
P_{TDH3}	P_{TDH3}	P_{TDH3}	wt	wt	KO	yDS101
P_{TDH3}	P_{REV1}	P_{REV1}	P_{REV1}	wt	wt	yDS102
P_{REV1}	P_{RPL18B}	P_{TDH3}	P_{RPL18B}	SAM1 KO	KO	yDS103
P_{RPL18B}	P_{RPL18B}	wt	P_{RPL18B}	SAM1 KO	wt	yDS104
P_{RPL18B}	P_{TDH3}	P_{TDH3}	P_{REV1}	SAM1 KO	wt	yDS105
P_{RPL18B}	P_{RPL18B}	wt	P_{REV1}	wt	KO	yDS106
P_{TDH3}	P_{REV1}	P_{RPL18B}	P_{RPL18B}	SAM1 KO	KO	yDS107
P_{REV1}	wt	P_{REV1}	wt	wt	KO	yDS108
P_{TDH3}	P_{TDH3}	P_{TDH3}	P_{TDH3}	SAM1 KO	wt	yDS109
wt	wt	wt	P_{TDH3}	SAM2 KO	wt	yDS110
wt	P_{REV1}	P_{TDH3}	P_{TDH3}	SAM1 KO	KO	yDS111
P_{REV1}	P_{TDH3}	P_{RPL18B}	P_{RPL18B}	wt	wt	yDS112
P_{TDH3}	wt	wt	P_{TDH3}	wt	KO	yDS113
wt	wt	P_{TDH3}	wt	wt	wt	yDS114
P_{RPL18B}	P_{REV1}	P_{RPL18B}	P_{TDH3}	SAM1 KO	KO	yDS115
wt	P_{RPL18B}	P_{TDH3}	P_{REV1}	SAM1 KO	wt	yDS116
P_{TDH3}	wt	P_{REV1}	P_{RPL18B}	SAM2 KO	wt	yDS117
wt	P_{TDH3}	P_{REV1}	P_{REV1}	wt	KO	yDS118
P_{REV1}	wt	P_{TDH3}	P_{REV1}	SAM2 KO	KO	yDS119
P_{REV1}	P_{REV1}	P_{REV1}	wt	SAM2 KO	wt	yDS120
wt	P_{RPL18B}	P_{REV1}	P_{TDH3}	wt	wt	yDS121
P_{RPL18B}	wt	P_{RPL18B}	wt	SAM1 KO	wt	yDS122
P_{REV1}	P_{RPL18B}	P_{REV1}	P_{TDH3}	SAM2 KO	KO	yDS123
wt	P_{TDH3}	wt	wt	SAM1 KO	wt	yDS124
P_{REV1}	P_{REV1}	P_{RPL18B}	P_{TDH3}	wt	KO	yDS125
P_{RPL18B}	wt	P_{TDH3}	P_{TDH3}	wt	KO	yDS126
P_{TDH3}	P_{RPL18B}	P_{TDH3}	P_{TDH3}	SAM1 KO	KO	yDS127
P_{RPL18B}	P_{TDH3}	P_{REV1}	wt	wt	wt	yDS128
P_{REV1}	wt	P_{TDH3}	P_{TDH3}	SAM1 KO	wt	yDS129
P_{RPL18B}	wt	wt	P_{REV1}	SAM2 KO	wt	yDS130
P_{TDH3}	P_{TDH3}	P_{RPL18B}	P_{REV1}	SAM2 KO	KO	yDS131

3.3 Construction and growth characteristics of DOE strains

The library of DOE strains was constructed from the haploid *S. cerevisiae* strain BY4742. Using a CRISPR/Cas9 approach instead of classical homologous recombination allowed targeting more than one locus at a time and going through several cycles of cloning without having to remove the auxotrophic marker from the genome for the next round. The the Cas9 and sgRNA plasmids used were described by Shaw (2016). In short, a linearised Cas9 plasmid (pWS158b, pWS171b or pWS172b), restriction enzyme digested sgRNA plasmids and donor DNA for the repair of double strand breaks (DSB) by homologous recombination were transformed together into *S. cerevisiae* strains and plated on agar plates with the correct drop-out media conferring to the Cas9 plasmid used (SC-URA, SC-LEU or SC-HIS). Colonies were screened by genomic PCR and the correct promoter insertions and/or gene deletions was confirmed by Sanger sequencing of the DNA junction (Figure 3.2).

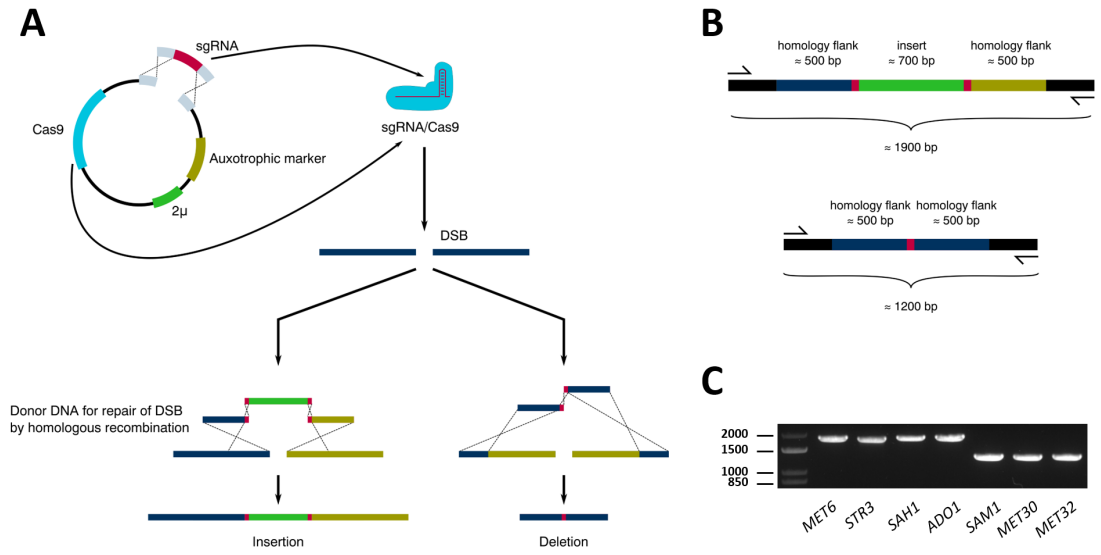

Figure 3.2: Generating DOE strains using CRISPR/Cas9. *S. cerevisiae* strains were transformed with **(A)** the linearised Cas9 expression plasmid as well as the sgRNA expression cassette. The Cas9/sgRNA complex induced targeted doublestrand breaks (DSB) which were repaired with co-transformed linear donor DNA by homologous recombination to result in either insertions or deletions. Strains were confirmed by **(B)** PCR from genomic DNA with primers binding approximately 100 bp outside the homology regions. PCR products **(C)** were purified and sent off for Sanger sequencing. A representative agarose gel of genomic PCR products of several gene loci changed in yDS107 is shown. The size of the DNA ladder denoted in bp.

Up to two genes were targeted per transformation. Strains with more than

two insertions/deletions underwent several rounds of CRISPR/Cas9 cloning using a different Cas9 plasmid until all genetic changes were confirmed. Typically, transformation plates contained between 10 - 50 colonies and 8 colonies were chosen for screening. For the strains that were able to be cloned, usually between 50 - 100% were positive in the first genomic PCR screen and the genetic changes of one colony that was positive after restreaking were confirmed by Sanger sequencing. Nevertheless, only 11 strains out of 48 were able to be cloned (Figure 3.3). A strain was deemed to be unable to be cloned, if no positive colonies were be confirmed after three consecutive attempts (plates were typically incubated for up to 72 h).

	MET6	*STR3*	*SAH1*	*ADO1*	*SAM1*	*SAM2*	*MET30* *MET32*
yDS085	wild-type	wild-type	wild-type	medium	deletion	wild-type	deletion
yDS093	medium	medium	medium	high	wild-type	deletion	wild-type
yDS100	wild-type	high	wild-type	medium	wild-type	deletion	deletion
yDS107	high	low	medium	medium	deletion	wild-type	deletion
yDS110	wild-type	wild-type	wild-type	high	wild-type	deletion	wild-type
yDS111	wild-type	low	high	high	deletion	wild-type	deletion
yDS113	high	wild-type	wild-type	high	wild-type	wild-type	deletion
yDS114	wild-type	wild-type	high	wild-type	wild-type	wild-type	wild-type
yDS122	medium	wild-type	medium	wild-type	deletion	wild-type	wild-type
yDS124	wild-type	high	wild-type	wild-type	deletion	wild-type	wild-type
yDS130	medium	wild-type	wild-type	low	wild-type	deletion	wild-type

Figure 3.3: List of DOE strains being able to be constructed using CRISPR/Cas9. Methionine metabolic genes were expressed either from the native (wild-type) or from a low (P_{REV1}), medium (P_{RPL18B}) or strong (P_{TDH3}) constitutive promoter. Strains with P_{REV1} inserted in front of the *MET6* or *SAH1* ORF couldn't be cloned.

The promoter strengths were derived from the characterisation by Lee et al. (2015) and the expression data under methionine restriction (Zou et al., 2017). P_{REV1} was the weakest, P_{TDH3} the strongest and P_{RPL18B} a medium strong promoter in the set of promoter characterised by Lee et al. (2015). The relative expression of the genes expressed by these promoters was similar under methionine restriction (Zou et al., 2017). Notably, no strain having P_{REV1}, the weakest constitutive promoter, inserted in front of either the *MET6* or the *SAH1* open reading frame (ORF) could be cloned (19 total). High-throughput studies showed null mutants of *MET6* to be of decreased competitiveness in synthetic media, while null mutants of *SAH1* were shown in the same studies to have reduced

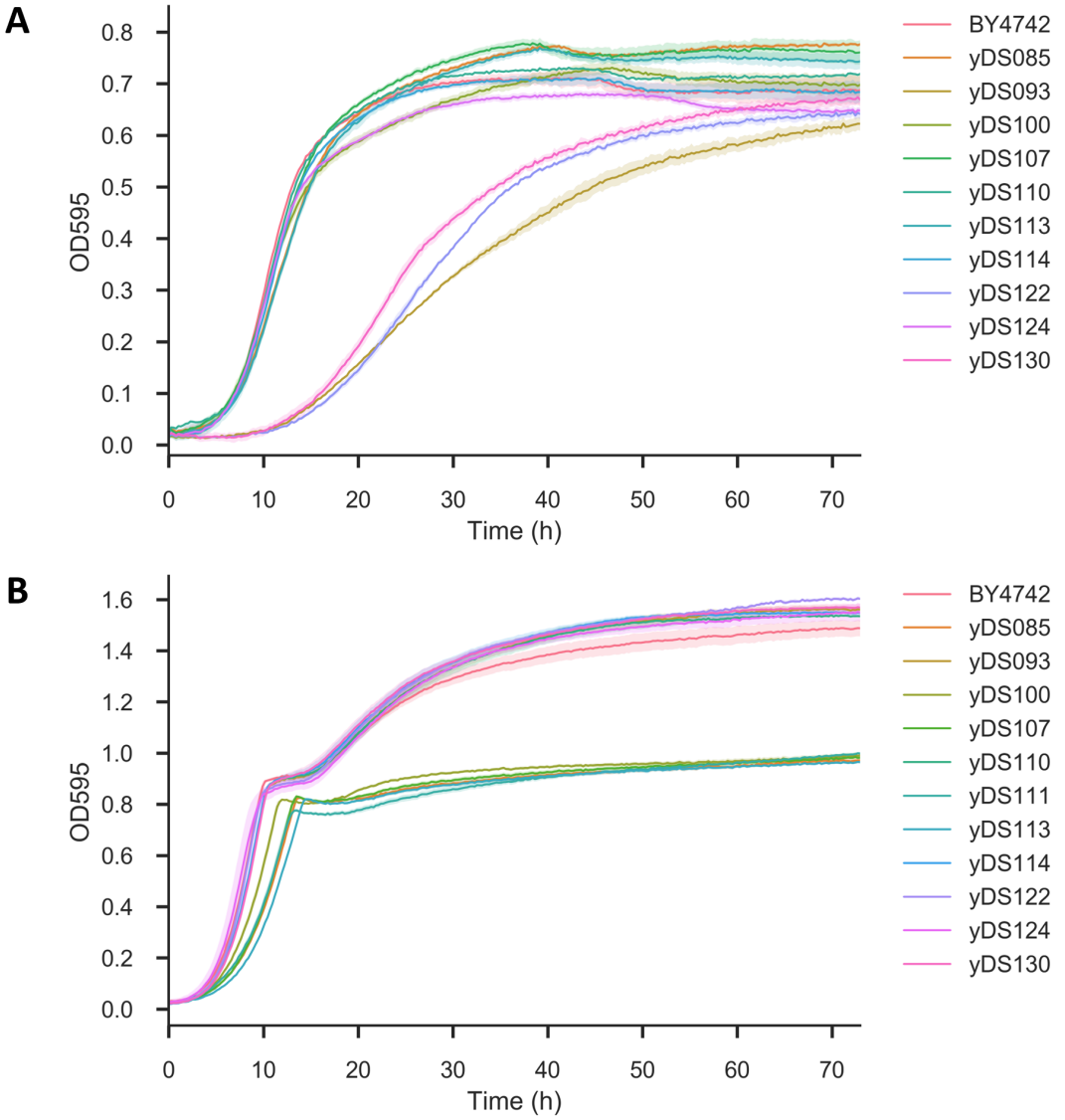

Figure 3.4: Growth curves of DOE strains in synthetic and rich media. DOE strains as well as the wild-type BY4742 strain were grown in **(A)** SC-MET + 4% glucose or **(B)** YPD media in 96-well microtitre plates. OD_{595} was measured every 15 minutes for 72 h in a Tecan Sunrise plate reader. Lines represent the mean of three biological replicates and confidence bands represent the standard deviation.

competitiveness, a significantly more oxidised cytosol or be inviable (Giaever et al., 2002; Breslow et al., 2008; Ayer et al., 2012).

In order to investigate the influence of the genetic changes on the competitive fitness of the DOE strains, growth in synthetic media without methionine (SC-MET + 4% glucose) or in rich media (YPD) was monitored in 96-well microtitre plates for 72 hours (Figure 3.4). DOE strains having P_{RPL18B} inserted in front of the *MET6* ORF (yDS093, yDS122 and yDS130) had prolonged lag phases and slower growth rates compared to BY4742 in synthetic media, but all other DOE strains did not exhibit a reduction in growth. The difference in growth characteristics suggests that lowered *MET6* expression levels are growth rate limiting in SC-MET media.

When growing in rich media (YPD), strains carrying a *MET30*/*MET32* double deletion (yDS085, yDS100, yDS107, yDS111 and yDS113) had slightly longer lag phases, reduced growth after the diauxic shift and lower final optical densities after 72 h.

3.4 Methionine production in DOE strains

Even though only 11 DOE strains could to be cloned, those strains covered several combinations of factors. Nevertheless, when evaluating those combinations it should be kept in mind that they might have been skewed in favour of strains easier to generate or growing faster.

Given the lack of strains, two more environmental factors were considered in the initial DOE experiments: the amount of glucose in the medium (2% and 4%) and culturing time (24 h and 72 h). BY4742 and all DOE strains were grown in biological triplicates in glass tubes in SC-MET with either 2% or 4% glucose for either 24 h or 72 h. Cells were collected by centrifugation and lysed with YeastBuster before analysis with GC-MS. Media samples were not collected for analysis since no methionine exporters were reported in *S. cerevisiae* and therefore no methionine was expected in the media. All methionine titres reported here refer to free methionine measured in the cell lysates only, while the unit (in μg/l) refers to the volume of the whole culture.

The results of the initial DOE experiments are summarised in Figure 3.5. Increasing the glucose concentration increased the methionine titres in most strains and most strains had lower methionine titres after 72 h (Figure 3.5 A and B). Interestingly, the methionine titre of BY4742 decreased at 72 h compared with 24 h when grown in 4 % glucose; this was not observed with 2 % glucose.

As seen in the microplate growth assays, yDS093, yDS122 and yDS130 grew to considerably lower OD_{600} than the other strains, and after 72 h most strains reached very similar OD_{600} (Figure 3.5 E and F). It should be noted that the absolute OD values measured in a plate reader and a spectrophotometer differ and only relative changes should be compared. Due to their low OD_{600}, the specific methionine titres (Figure 3.5 C and D) for yDS093, yDS122 and yDS130

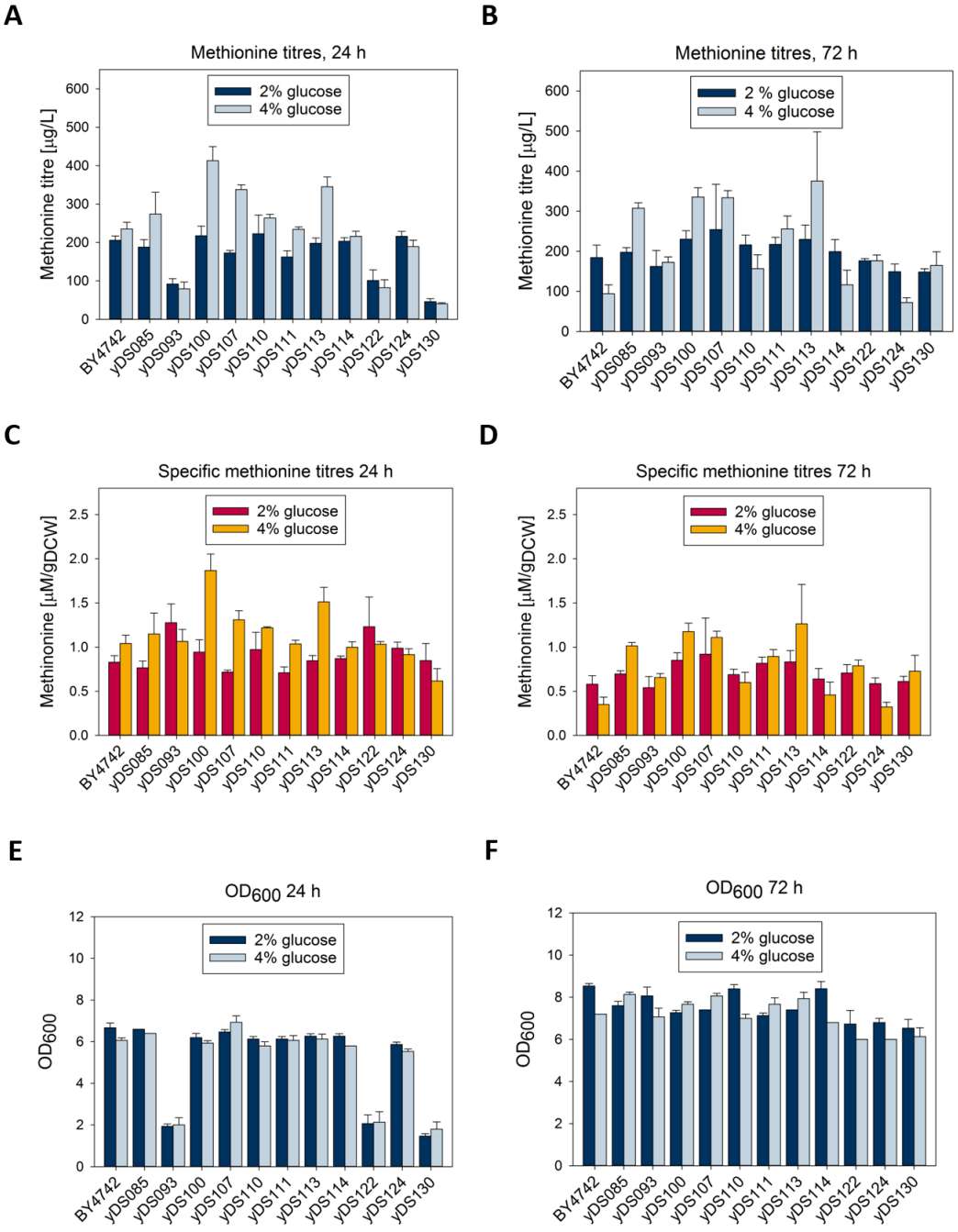

Figure 3.5: Methionine production of DOE strains. Methionine titres of DOE strains and BY4742 after 24 h **(A)** and 72 h **(B)**. Specific methionine titres after 24 h **(C)** and 72 h **(D)** were calculated by dividing methionine concentrations by the estimated dry cell weight. The final OD_{600} after 24 h **(E)** were similar for all strains except yDS093, yDS122 and yDS124 and similar for all strains after 72 h **(F)**. Bars represent the mean of three biological replicates, error bars the standard deviation.

were similar to the other strains at 24 h, whereas their total titres were much lower. Nevertheless, after 72 h, the specific titres of all strains showed the same relative pattern as the total titres.

The highest methionine titre of 413 μg/l was reached by yDS100 after 24 h of growth in 4% glucose, which is only a 1.7 fold increase compared to BY4742 in the same conditions. The three highest methionine producers, yDS100, yDS113 (345 μg/l), and yDS107 (337 μg/l) carried a double deletion of *MET30/MET32* and *MET6* was expressed either from the native (yDS100) or P_{TDH3} (yDS113 & yDS107) promoter.

By adding two additional environmental factors to the DOE experiment the range of responses (methionine titres) had been increased. The methionine titres ranged 10-fold from 40 μg/l (yDS130, 24 h, 4% glucose) to 413 μg/l (yDS100, 24 h, 4% glucose). The data was used to build a linear regression model in JMP.

3.5 DOE linear regression model

As stated above, not all strains from the initial design could be cloned. Therefore, the design was augmented with two additional factors: Fermentation time (h) and the amount of glucose in the fermentation medium (%). The factors in the augmented model are listed in Table 3.4.

Table 3.4: Experimental factors and the associated levels of each chosen for evaluation for their impact on methionine production in the augmented design

Factor	Role	Factor level		
MET6	Continuous	84		7163
STR3	Continuous	84		7163
SAH1	Continuous	84		7163
ADO1	Continuous	84		7163
SAM1/SAM2	Categorical	wild-type	*SAM1* KO	*SAM2* KO
MET30/MET32	Categorical	wild-type	KO	
Time (h)	Continuous	24		72
% Glucose	Continuous	2		4

Regression analysis was performed using the "Fit Model" function in the JMP software. A total of 31 Effect Terms (the mathematical terms representing the effect of factors on the modelled response) were chosen for the model (see Appendix for full list). The initial model Effect Terms were chosen on the following criteria: (1) All factors chosen for the design in the augmented design, (2) all two-factor-interactions (3) all interactions between two-factor-interactions and *MET30/MET32*, Time or Percentage glucose and (4) all interactions between

three-factor-interactions and *MET30/MET32*, Time or Percentage glucose. The aim was to be very broad in the first approach and include all interactions between two factors as well as interactions between those two factor interactions and factors likely to have global influence (*MET30/MET32*, Time and Percentage glucose). Transcription of all methionine biosynthetic genes was expected to be influenced by a *MET30/MET32* deletion and all strains were cultured in all combinations of time and glucose concentrations.

Afterwards, the initial model fit was run (Standard Least Squares) and Effect Terms were removed in iterative steps until the model with the highest R^2 was found. A summary of the best model fit can be found in Figure 3.6. Figure 3.6 A shows the plot of the actual data points by the predicted data points and the R^2 value. The full equation of the Prediction Expression can be found in the Appendix.

Figure 3.6 B shows the 11 effect terms with the biggest scaled estimated influence (Scaled Estimate) on the modelled methionine titres. The largest effect term was the Intercept of the Prediction Expression equation (blue line in the Actual by Predicted Plot, Figure 3.6 A). The next three effect terms with the highest Scaled Estimate were *MET6*, *MET6*STR3* and *MET6*SAM2*(knock-out). Nevertheless, the t-Ratios (Scaled Estimate / Standard Error), a measure of confidence that the effect is real and not noise (high values indicate high confidence and low noise), were not very high for most terms. Besides the Intercept, only the *MET30/MET32* (knock-out) term had a t-Ratio above 10, even though the Scaled Estimate of the effect was comparably small (38.6).

The utilisation of the Prediction Profiler tool (Figure 3.6 C) in JMP is an useful way to inspect the modelled data graphically. The model suggested that in a *SAM2* and *MET30/MET32* deletion background, increasing the expression of *MET6* and *STR3* while increasing the glucose content to 4% and decreasing the fermentation time to 24 h would result in a methionine titre of 794 ($\pm$221) μg/l, which would be a 3.4 fold increase compared to BY4742 in the same growth conditions. Changing the expression of *SAH1* or *ADO1* didn't influence methionine titres in one way or another. The model still included very broad confidence intervals, reflecting the low t-Ratios of the Effect Terms. It remained unclear whether Standard Errors could have been decreased by testing more strains or whether the uncertainty is intrinsic to the regulation of sulphur metabolism.

Even though the model had large uncertainties, the predictions of the model can be explained by previously published work and the results of this work. Overexpression of *MET6* improved SAM production in *S. cerevisiae* by increasing the methionine availability in SAM producing strains (Chen, Wang, Wang, Dou and Zhou, 2016). *MET30/MET32* strains accumulated elevated levels of cystathionine (Figure 3.7 A), increasing the expression levels of *STR3* would be expected to increase the amounts of the methionine precursor and *MET6* substrate, homocysteine. Increased expression of *STR3* only improved methionine

A

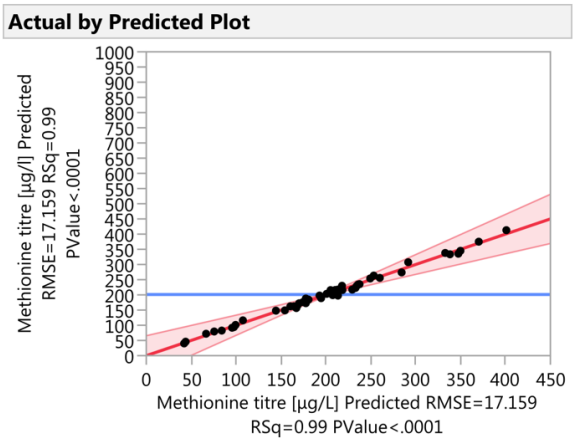

B

Scaled Estimates

Nominal factors expanded to all levels

Term	Scaled Estimate	Std Error	t Ratio	Prob>|t|
Intercept	199.39989	10.0976	19.75	<.0001*
MET6(353,7163)	158.1201	48.35109	3.27	0.0114*
MET6*STR3	125.90887	49.08265	2.57	0.0334*
MET6*SAM1/SAM2[SAM2 knock-out]	70.878286	13.81251	5.13	0.0009*
SAM1/SAM2[wild-type]*MET30/MET32[knock-out]*Time [h]	41.284514	13.2714	3.11	0.0144*
SAM1/SAM2[SAM2 knock-out]	41.057882	13.23753	3.10	0.0146*
MET30/MET32[knock-out]*Percentage glucose [%]	38.592685	3.837239	10.06	<.0001*
SAM1/SAM2[SAM1 knock-out]*MET30/MET32[wild-type]*Time [h]	35.914622	17.75774	2.02	0.0778
MET30/MET32[knock-out]	31.175373	6.083785	5.12	0.0009*
MET6*MET30/MET32[knock-out]	27.735549	12.15633	2.28	0.0519
MET30/MET32[knock-out]*Time [h]	26.814922	12.52378	2.14	0.0647

C

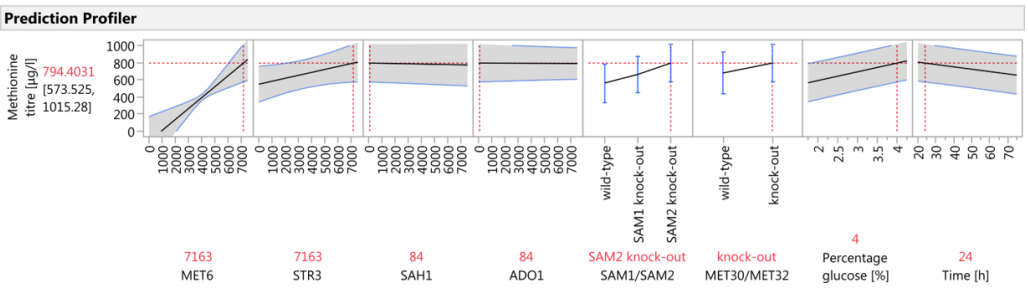

Figure 3.6: Summary of the DOE model. **(A)** The actual data points (black dots) were plotted against the predicted data points by the model (red line), the intercept of the Prediction Expression is marked by the blue line. **(B)** The Effect Terms with the largest Scaled Estimated effects, the graphical representation of the Scaled Estimate, its Standard Errors, t-Ratios and probabilities are listed. **(C)** The Prediction Profiler is an interactive graphical representation of the model predictions. The best predicted methionine titres are in a strain with high *MET6* and *STR3* expression in a *sam2*Δ, *met30*Δ/*met32*Δ background when grown in SC-MET + 4% glucose for 24 h.

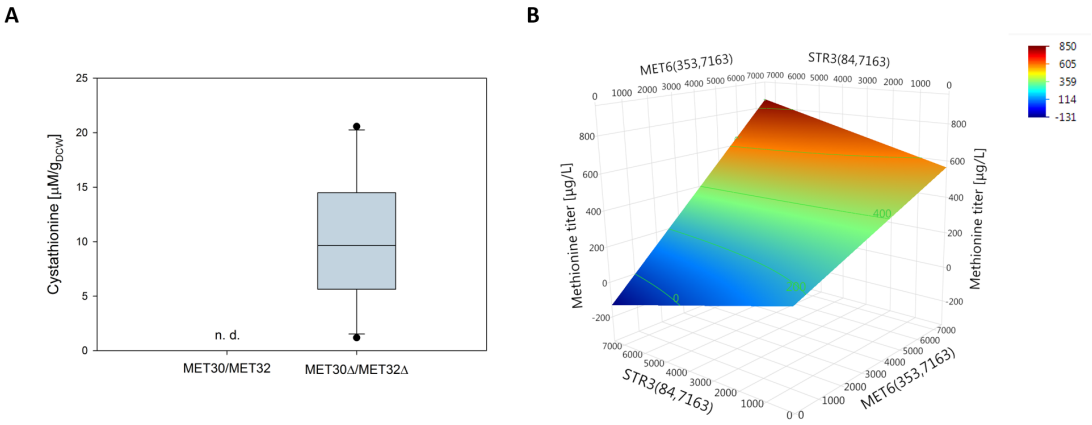

Figure 3.7: Influence of STR3 expression on methionine titres. (A) Box-and-whisker plot of strains with a *MET30*/*MET32* double deletion accumulating internal cystathionine. No cystathionine was detected in strains with functional copies of *MET30* and *MET32*. **(B)** Surface plot of modelled methionine titres (z axis) depending on *MET6* (x axis) and *STR3* (y axis) expression. The other model factors are set to: *SAH1*[84], *ADO1*[84], *sam2*Δ, *met30*Δ/*met32*Δ, Percentage glucose [4], Time(h)[24]. At low *MET6* expression levels, increasing *STR3* expresssion was predicted to decrease methionine titres, while the opposite was true for high *MET6* expression levels.

titres when *MET6* expression was increased as well in the model, but had the opposite effect at lower *MET6* expression levels (Figure 3.7 B). The deletion of either *SAM1* or *SAM2* was shown to lead to elevated internal methionine levels (Mülleder et al., 2016) and Zou et al. (2017) found higher expression levels of *SAM2* compared to *SAM1* under methionine restriction conditions, which are mimicked in the *MET30*/*MET32* deletion strains. Therefore, the preference of a *SAM2* deletion over a *SAM1* deletion in the model could be explained.

In summary, the DOE experiments and the model built on the experimental data suggested that increased expression of *MET6* and *STR3* as well as deletions of *SAM2*, *MET30* and *MET32* would give the greatest increase in methionine titres. Subsequently, the model was validated by implementing the suggested changes in a new methionine production strain.

3.6 Validation of the DOE model

The DOE model was validated by implementing the suggested changes in a new methionine production strain, yDS136(P_{TDH3}-*MET6*, P_{TDH3}-STR3, *sam2*Δ and *met30*Δ/*met32*Δ). The strain was generated using CRISPR/Cas9 as described above and confirmed by genomic DNA PCR and Sanger sequencing of the introduced changes. The expected pathway activation of yDS136 is summarised in Figure 3.8 A.

The engineered DOE strain yDS136 and wild-type BY4742 were grown in glass tubes with 5 ml of SC-MET + 4% glucose for 24 or 72 h and the samples were analysed using GC-MS. The methionine titres are shown in Figure 3.8 B.

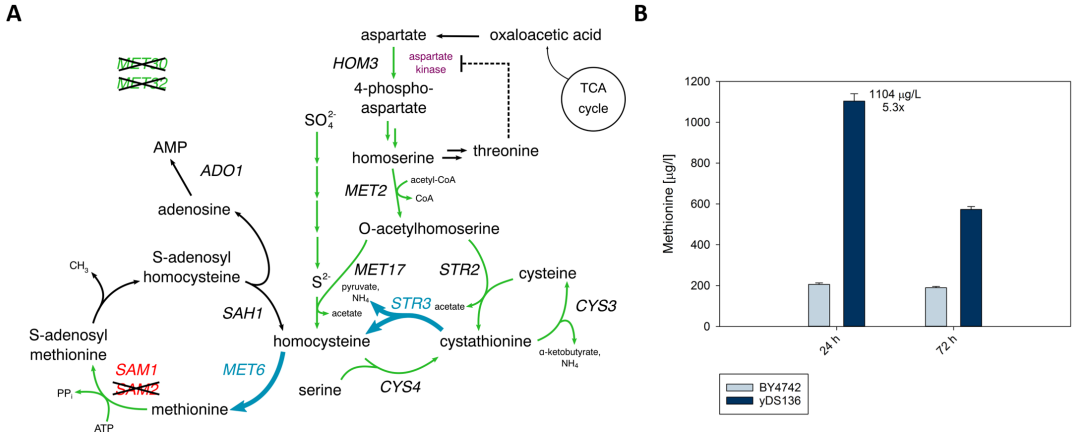

Figure 3.8: Validation of the DOE model. (A) The expression of *MET6* and *STR3* was increased by inserting P_{TDH3} before the ORF (wide blue arrows). *MET30* and *MET32* were deleted to increase the expression of genes encoding the enzymes catalysing the reactions represented by the green arrows. *SAM2* was deleted in order to reduce metabolic flux to SAM. **(B)** Methionine titres in DOE strain yDS136 increased after 24 h of culturing to 5.3-fold compared to the wild-type strain BY4742. Methionine titres in yDS136 decreased after 72 h of culturing compared to 24 h of culturing. The bars represent the mean of three biological replicates, standard deviation is indicated by the error bars. Only methionine inside the cells was considered for the calculation of titres.

The methionine titre after 24 h of culturing increased to 1104 ±29 μg/l, a 5.3-fold increase compared to BY4742 in the same conditions. The measured methionine titre for yDS136 was higher than the modelled outcome (794 μg/l), but only slightly higher than the upper confidence limit (1015 μg/l). While the methionine titre decreased after 72 h in yDS136, as the DOE model predicted, it didn't change in BY4742 as was observed in the initial DOE experiments in the same conditions (Figure 3.5 B). No homoserine or homocysteine was deteceted in either BY4742 or yDS136.

In summary, even though only a fraction of the designed DOE strains were able to be cloned and therefore the model had broad confidence bands, key factors influencing methionine production were identified. The predicted changes for increasing methionine titres were confirmed in the production strain yDS136. By applying the changes predicted in the DOE model, the methionine titre could be increased by 5.3-fold compared to the wild-type.

3.7 Discussion

The JMP software was used to design a DOE approach to identify the main genetic and environmental factors influencing the production of methionine in *S. cerevisiae*. DOE leverages statistical methods to reduce the number experiments to be performed for covering the design space while avoiding biases introduced when using an OFAT approach. A total of 48 strains were designed.

Unfortunately, only eleven strains could be cloned. It is not clear in every case, why the CRISPR/Cas9 approach was unsuccessful, but it is notable that no strain was able to be constructed with P_{REV1} in front of either the *MET6* or *SAH1* ORF. P_{REV1} is the weakest promoter described by Lee et al. (2015) and was driving gene expression several orders of magnitude lower than strong promoters such as P_{TDH3}. Gene expression, especially of genes with fairly strong native promoters, from very weak promoters could cause phenotypes that are indistinguishable from actual null mutants. Inserting P_{REV1} in front of the *MET6* or *SAH1* ORF could have caused null mutant phenotypes and therefore prohibited successful cloning.

MET6 null mutants are methionine auxotrophs (Masselot and de Robichon-Szulmajster, 1975). Methionine was added to the transformation plates, but high-throughput studies found diminuished competitive fitness in *MET6* null mutants in synthetic media (Giaever et al., 2002; Breslow et al., 2008) and the microplate growth assays in this work showed prolonged lag phases and lower growth rates for P_{RPL18B}-*MET6* strains, allbeit in SC-MET media. It is possible, that no positive colonies were found, because P_{REV1}-*MET6* strains grew very slowly and were not visible after 72 h of incubation, while false positive colonies grew fast and therefore were picked and screened.

The literature on *SAH1* is more mixed. Giaever et al. (2002) found null mutants to be inviable, while Breslow et al. (2008) reported reduced competitive fitness of mutants with a reduced *SAH1* function grown in minimal medium. Ishtar Snoek and Yde Steensma (2006) identified *SAH1* as essential for aerobic growth, and Ayer et al. (2012) measured a significantly more oxidised cytosol when *SAH1* expression was repressed and the strains were grown in synthetic defined medium. Similarly to P_{REV1}-*MET6* strains, strains expressing *SAH1* at very low levels could be phenotypically equivalent to null mutants, thus being either inviable (under aerobic growth conditions) or growing very slowly and difficult to identify.

Nevertheless, the failure of constructing the remaining 18 strains couldn't be explained by these circumstances. It is possible that certain combinations of expression levels could have influenced intracellular glutathione levels, which plays pivotal roles in maintaining basic cellular functions and protection against oxidative stress (Penninckx, 2002), and subsequently induced inviable or slow-growing phenotypes. DOE methodology does not take biological feasibility into account and since the D-optimal Design option in JMP uses an alghorithm, another design would have produced a slightly different but equivalent set of

strains and a different number of strains might have been unable to be cloned. When designing a set of DOE experiments, especially for changes to central metabolism, one should perform a scoping experiment and test whether all factor ranges (and possibly several factor combinations) are physically and biologically possible.

The limited number of strains made it possible to test all strains (and the BY4742 wild-type) in two different environmental conditions. Even without any modelling, it was obvious that methionine titres increased with higher glucose concentrations and, to a lesser extent, shorter fermentation times. The only strains increasing their methionine titre markedly whith increased fermentation times were the slow-growing P_{RPL18B}-*MET6* strains, even though their specific methionine titres differed less distinctly. Methionine biosynthesis is ATP intensive (Hayakawa et al., 2018) and some of the additional ATP from increased cellular respiration in higher glucose concentrations might have been used for it. On the other hand, free intracellular methionine is also a substrate for SAM and protein biosynthesis, which might explain the decreased methionine titres after 72 h compared with 24 h. Taking more timepoints between 24 h and 72 h would enable a better understanding of methionine levels over the culturing period.

The DOE strain titres ranged 10-fold, but the lower methionine titres were only reached by the slow-growing strains and most data points centred around the wild-type titres. Methionine is one of the lowest abundance amino acids in *S. cerevisiae* (Mülleder et al., 2016) and methionine pools are maintained within narrow boundaries. Furthermore, following the failure to clone all designed strains, the composition of the DOE strains tested might have been skewed towards faster growing strains. Considering these circumstances the narrow spread was not surprising, but linear regression models benefit from a broad range of responses rather than clustering around a certain value.

Another issue in the DOE model is the correct denomination of the genetic input factors. The expression levels for the constitutive promoters were characterised as a single timepoint in the exponential growth phase by Lee et al. (2015) while the fermentations in this work were performed over 24 h and 72 h. Reider Apel et al. (2017) showed that the activity of P_{TDH3} can drop by as much as 50% after 48 h of growth in synthetic media, but it is unclear whether the drop in activity over time would be the same in different glucose concentrations (Tdh3p is a glycolytic enzyme) or whether other promoters have similar changes in activity. Additionally, the gene expression values taken from Zou et al. (2017) were measured one hour after methionine restriction, but Met4p regulates the expression of sulphur compound biosynthetic genes dynamically in response to intracellular methionine (Ouni et al., 2011). Deletion of *MET30* and *MET32* set Met4p active constitutively (Su et al., 2008), but it is unclear whether Met4p stays active at similar levels over longer fermentation times. It also means that the actual activities of the native promoters of *MET6* and *STR3* are dependent on whether or not *MET30* and *MET32* were deleted. Therefore, many factor levels defined in the

linear regression model are more flexible than the numerical values imply and in some cases dependent on other factor levels, which introduces further uncertainty to the model. Measurements of actual gene expression levels in the DOE strains prior to building the model would help to reduce that uncertainty.

Despite these flaws, the model was able to elucidate the influence of key factors on methionine titres. Changing the expression of *SAH1* or *ADO1* did not influence methionine titres. Increasing the expression of *MET6* and deleting *SAM2* was expected to elevate internal methionine levels (Chen, Wang, Wang, Dou and Zhou, 2016; Kanai, Mizunuma, Fujii and Iefuji, 2017; Mülleder et al., 2016). While the data from Mülleder et al. (2016) implied that both *sam1*Δ and *sam2*Δ would have a similar influence on methionine levels, Zou et al. (2017) transcriptional data showed higher expression levels of *SAM2*, suggesting that deleting *SAM2* would have a bigger influence on methionine titres.

The influence of a *MET30*/*MET32* on methionine titres was discerned successfully by the application of DOE and the construction of a linear regression model. *A priori*, it was not clear, whether *met30*Δ/*met32*Δ strains would accumulate increased amounts of methionine, because higher transcription of sulphur biosynthesis genes would produce enzymes both pulling flux away and pushing flux into the direction of methionine. Indeed, not all *met30*Δ/*met32*Δ strains showed increased methionine titres, but the linear regression model helped discerning the net positive effect of a *MET30*/*MET32* deletion with high confidence. While the transcriptional changes in *met30*Δ/*met32*Δ double mutants have been described extensively (Patton et al., 2000; Su et al., 2008), to my knowledge this work represents the first characterisation of amino acid levels in *met30*Δ/*met32*Δ strains. Most notably, the elevated cystathionine levels hint at its central role in the transsulphuration pathway and sulphur amino acid homeostasis.

DOE also enabled to correctly predict the influence of *STR3* expression on methionine titres. Increasing *STR3* expression increased methionine titres only when *MET6* expression was high as well. If an OFAT were chosen and the expression levels of *STR3* were changed first, one might have come to the conclusion that *STR3* has no influence on methionine titres and increased expression might even reduce titres. Considering the accumulation of cystathionine in *met30*Δ/*met32*Δ strains, additional copies of *STR3* and/or reduced expression of *CYS4* could elevate methionine titres even more.

The methionine titre of the newly constructed strain yDS136, which was designed based on the model predictions, was close to the upper limit of the confidence interval of the predicted titre, increasing the titre 5.3-fold compared to BY4742. Two studies sought to increase methionine production in yeast by isolating mutants resistant to DL-ethionine, which is a toxic analogue of methionine. Brigidi et al. (1988) reported a titre of 20 mg/l methionine in strains formed through protoplast fusion of DL-ethionine resistant *Saccharomyces uvarum* and *S. cerevisiae*. Brigidi et al. (1988) measured methionine in the

supernatant, but it is unclear what fermentation medium was used, therefore obfuscating whether extracellular methionine was introduced by the choice of fermentation medium containing yeast extract or whether *S. uvarum* expresses a native methionine exporter. Martinez-Force and Benitez (1992) grew an industrial strain in continuous culture and increasing DL-ethionine concentrations. Mutants isolated from these cultures accumulated up to 32.6 mM intracellular methionine (up from 0.2 mM in the starting strain). Interestingly, methionine accumulating strains also had increased intracellular homoserine concentrations (compared to no detectable homoserine in the starting strain). Neither Brigidi et al. (1988) nor Martinez-Force and Benitez (1992) characterised the methionine producing strains genetically. Given that no homoserine or homocysteine was detected in yDS136, methionine titres could be increased by increasing methionine precursor levels (see Chapter 4).

Chapter 4

Improving Precursor Supply for Sulphur Amino Acid Biosynthesis

4.1 Introduction

Biosynthesis of the methionine precursors homoserine and homocysteine is not only controlled by transcriptional regulation, but also feedback inhibitions of the enzymes.

The first step of homoserine biosynthesis involves the phosphorylation of aspartate by an aspartate kinase, which is encoded by *HOM3* in *S. cerevisiae*. Homoserine itself is then either phosphorylated by a homoserine kinase (*THR1*) in the first step of threonine biosynthesis or converted to O-acetylhomoserine, the substrate for homocysteine biosynthesis, by a homoserine O-trans-acetylase (*MET2*, Figure 4.2). Both, the aspartate kinase and homoserine kinase, are inhibited by threonine (Martínez-Force and Benítez, 1993) and methionine overproducing strains, obtained through random mutagenesis, also accumulated elevated levels of intracellular homoserine and threonine (Martinez-Force and Benitez, 1992). However, high levels of homoserine can cause toxicity, possibly by acting as a toxic threonine analogue or by accumulating high levels of the toxic precursor aspartate β-semialdehyde, and therefore tight regulation of homoserine biosynthesis is required in yeast strains (Arevalo-Rodriguez et al., 2004; Kingsbury and McCusker, 2010).

Several studies have investigated the mechanism of the allosteric inhibition of the aspartate kinase and identified several mutations reducing the sensitivity to inhibition by threonine (Arévalo-Rodríguez et al., 1999; Bareich and Wright, 2003). Overexpression of *HOM3* variants with some of these mutations were successfully applied for overproducing threonine (Farfán et al., 1999; Farfán and Calderón, 2000).

Bacterial sulfhydration (transfer of a thiol group) of activated homoserine uses a different combinations of substrates to synthesise homocysteine, cystathionine or methionine (Figure 4.1). Most bacterial enzymes use either O-acetylhomoserine

or O-succinylhomoserine and depending on the thiol substrate synthesise either homocysteine (with hydrogen sulphide), cystathionine (with cysteine) or methionine (with methanethiol). Most enzymes have a preference for certain substrates and some are allosterically inhibited by methionine or SAM (Ferla and Patrick, 2014). *MET17* encodes the *S. cerevisiae* O-acetylhomoserine sulfhydrylase (OAH-SHLase), which uses hydrogen sulphide as a donor to synthesise homocysteine *in vivo* but is also able to use methanethiol as a substrate to produce methionine *in vitro*. *S. cerevisiae* OAH-SHLase in cell lysates was shown to be inhibited strongly by methionine (Yamagata, 1971). *S. cerevisiae* synthesises cysteine exclusively through the transsulphuration pathway via homocysteine and cystathionine *in vivo* (Cherest et al., 1993). Even though some strains have detectable serine O-acetyltransferase activity, no cysteine seems to be synthesised via O-acetylserine *in vivo* (Takagi et al., 2003). Another enzyme with sulfhydration activity, cystathionine γ-synthase encoded by *STR2*, uses O-acetylhomoserine as a substrate to synthesise cystathionine from cysteine (Hansen and Johannesen, 2000).

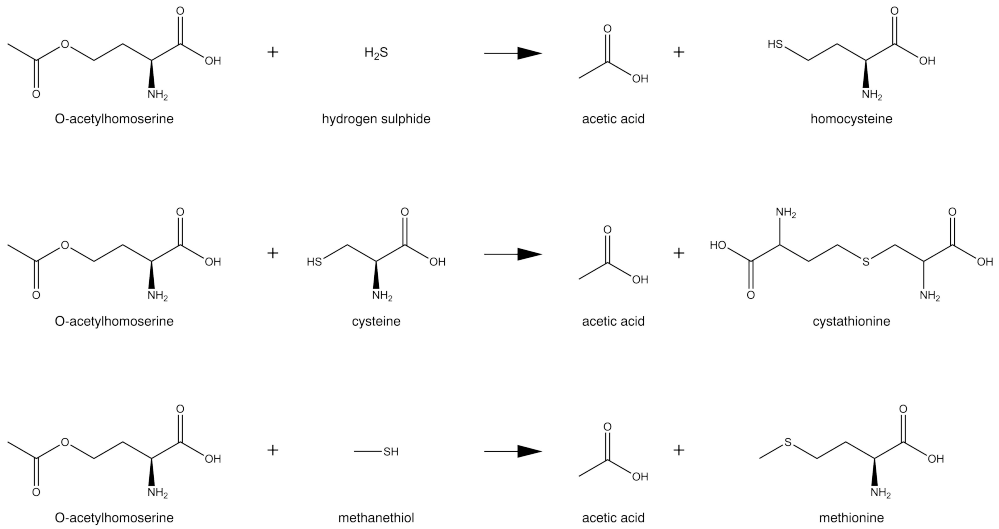

Figure 4.1: Sulfhydration reactions. OAH-SHLases generally catalyse three different reactions of O-acetylhomoserine: the synthesis of homocysteine with hydrogen sulphide, the synthesis of cystathionine with cysteine and the synthesis of methionine with methanethiol.

Previously, a DOE approach was used to generate a methionine overproducing strain, yDS136 (P_{TDH3}-*MET6*, P_{TDH3}-*STR3*, *sam2*Δ, *met30*Δ, *met32*Δ). The characterisation of the internal amino acid composition revealed that yDS136 accumulated large amounts of cystathionine, but no measurable amounts of homoserine. An E282D mutation in Hom3p, which greatly reduced threonine feedback inhibition (Velasco et al., 2005), was introduced in the native copy of *HOM3* (by mutating A846T in the ORF) and the *THR1* gene was deleted in yDS136, to attempt to increase methionine precursor supply (Figure 4.2). The

resulting strain yDS138 was characterised for its methionine production as well as general amino acid composition and compared to BY4742 and yDS136, as well.

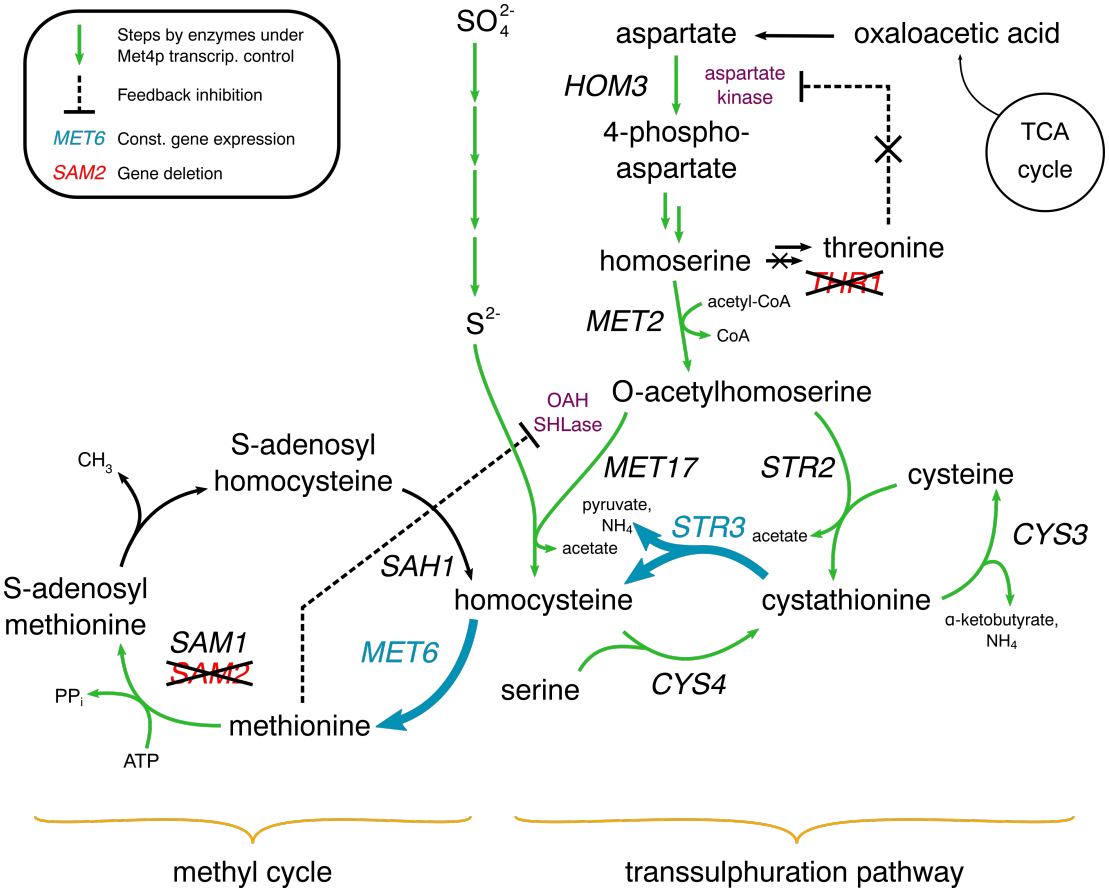

Figure 4.2: Pathway map of yDS138. Based on the background strain yDS136 (P_{TDH3}-*MET6*, P_{TDH3}-*STR3*, *sam2*Δ, *met30*Δ, *met32*Δ), *HOM3* was mutated to ease the feedback inhibition of the aspartate kinase by threonine while *THR1* was deleted to increase the availability of homoserine, a methionine precursor. The blue arrows indicate the increased expression of *MET6* and *STR3* by inserting the strong promoter P_{TDH3} in front of the ORF. Green arrows indicate the biosynthetic steps catalysed by enzymes encoded by genes under transcriptional control by Met4p.

Given the strong inhibition of the *S. cerevisiae* OAH-SHLase Met17p by methionine, two bacterial OAH-SHLases were chosen for overexpression to elevate intracellular homocysteine levels and thereby increase methionine production. Belfaiza et al. (1998) described *metY*, an OAH-SHLase from *Leptospira meyeri*, as being inhibited by only very high concentrations (10 mM) of methionine or SAM. Kim et al. (2011) introduced three mutations into *MetZ*, an OAH-SHLase from *Rhodobacter sphaeroides*, for the effective production of methionine from O-acetylhomoserine and methanethiol (*RsMetZ* and RsMetZp will be referred from hereon as the gene and protein containing the three mutations, I3N,

F65Y and V104A). In this chapter, both OAH-SHLases were expressed by strong constitutive promoters from high-copy plasmids in the yDS138 strain and characterised for their effect to increase methionine titres and/or its precursor levels.

Since *met30*Δ/*met32*Δ strains accumulate cystathionine, another possible branching point of the central sulphur metabolism was investigated: *CYS3* involved in the synthesis of cysteine and encoding the *S. cerevisiae* cystathionine γ-lyase, was co-expressed with an OAH-SHLase lacking feedback inhibition in the yDS138 strain to investigate whether *S. cerevisiae* could be engineered as a platform for cysteine production. *YCT1*, encoding an *S. cerevisiae* cysteine importer (Kaur and Bachhawat, 2007), was deleted and the amino acid exporter *AQR1* (Velasco et al., 2005) was overexpressed as well in this work. It was investigated, whether both measures could elevate cysteine accumulation in the growth medium by preventing cysteine reimport and/or increase cysteine export.

4.2 Eliminating aspartate kinase feedback inhibition and blocking threonine biosynthesis

HOM3 and *THR1* were targeted in yDS136 using CRISPR/Cas9. In order to introduce the A846T point mutation in the ORF of *HOM3*, the linearised Cas9 and sgRNA plasmids were co-transformed with two annealed complementary 90 nt oligonucleotides (oDS0348 & oDS0349, see also Materials section) that spanned the targeted region and included the desired mutation as well as a mutation in the PAM motif that didn't change the translated sequence. The correctly mutated *HOM3* would produce Hom3p containing the E282D mutation. *THR1* was deleted by co-transforming linearised Cas9 and sgRNA plasmids as well as donor DNA with homology to either sides of the genome introducing the gene deletion. The point mutation in *HOM3* and deletion of *THR1* in the resulting strain yDS138 were confirmed by genomic PCR and Sanger sequencing.

The wild-type strain, BY4742, the DOE strain, yDS136 ((P_{TDH3}-*MET6*, P_{TDH3}-*STR3*, *sam2*Δ, *met30*Δ, *met32*Δ), and the DOE strain without aspartate kinase feedback inhibition, yDS138 ((P_{TDH3}-*MET6*, P_{TDH3}-*STR3*, *sam2*Δ, *met30*Δ, *met32*Δ, *HOM3(A846T)*, *thr1*Δ), were cultured in SC-MET + 4% glucose. All strains were grown for 24 h or 48 h in glass tubes (5 ml medium) or 100 ml shake flasks (20 ml medium) to elucidate different culturing times and conditions on methionine titres. The cell lysates (for internal amino acid compositions) and media samples (for external amino acid concentrations) were analysed using GC-MS. The results are summarised in Figure 4.3.

The methionine titres in yDS138, the strain without aspartate kinase feedback inhibition, were higher than in BY4742 but lower than in yDS136, the most productive strain as predicted by the DOE model, in all conditions (Figure 4.3 A & B). Generally, titres did not change with prolonged culturing times or being

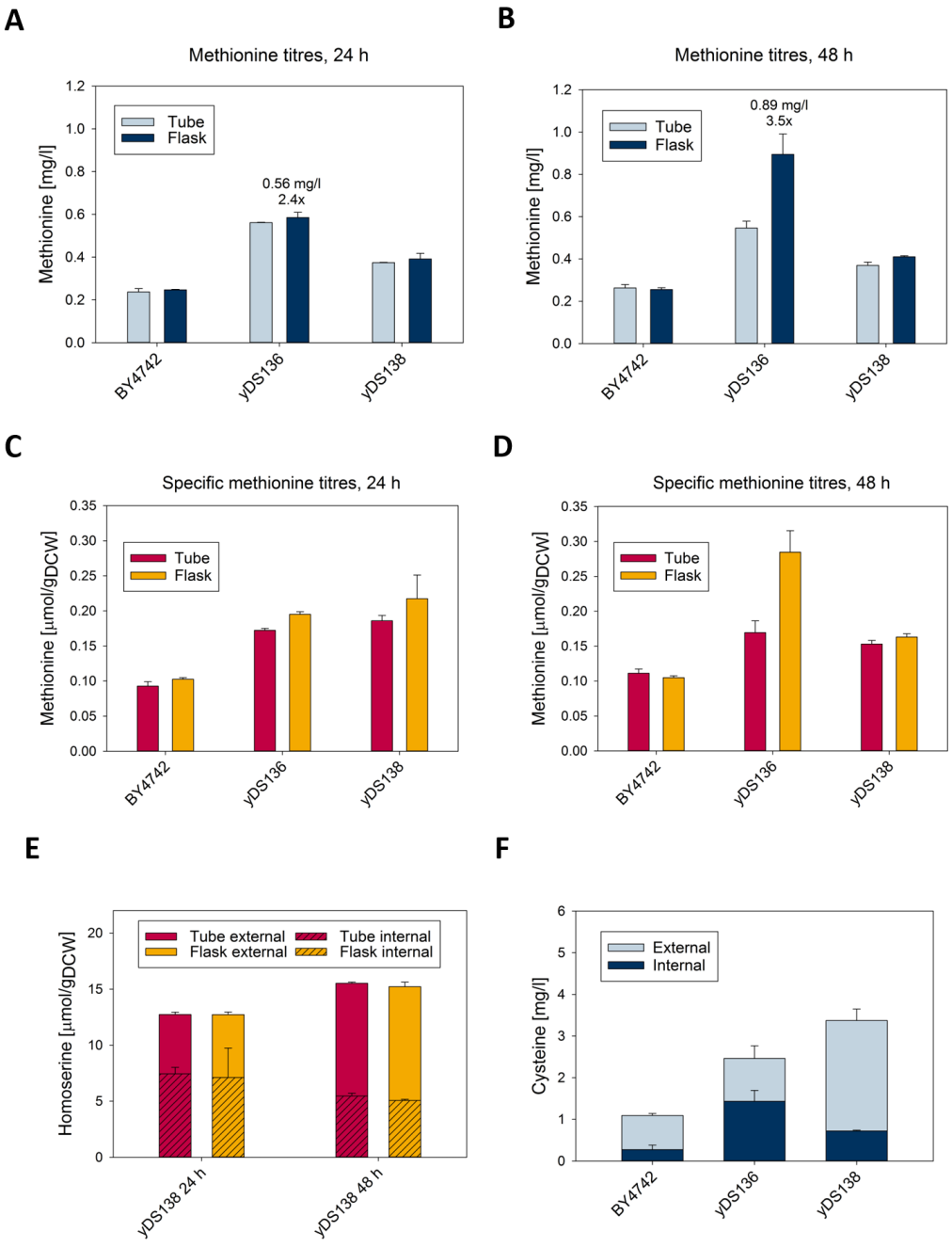

Figure 4.3: Methionine titres of BY4742, yDS136 & yDS138 and homoserine accumulation in yDS138. Methionine titres after 24 h **(A)** and 48 h **(B)** as well as specific methionine titres after 24 h **(C)** and 48 h **(D)**. **(E)** Homoserine levels in yDS138. Strains accumulated elevated levels of **(F)** cysteine (48 h, shake flasks). All bars represent the mean of biological triplicates, error bars represent standard deviation.

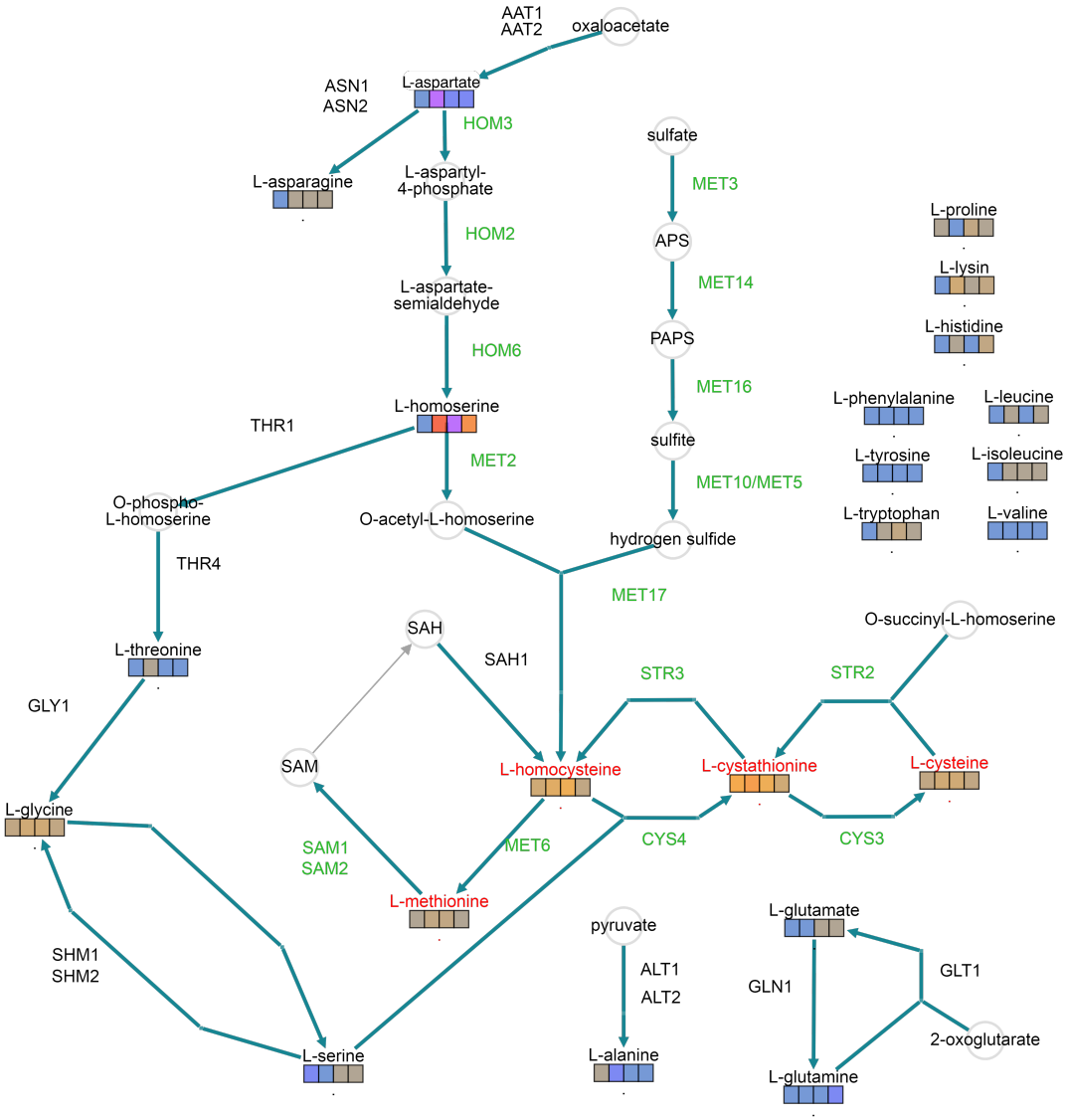

Figure 4.4: Relative changes of amino acid pools in yDS136 & yDS138 compared to BY4742. Relative changes of internal amino acid pools in yDS136 and yDS138 (after 24 h and 48 h) compared to BY4742 were calculated from the means of biological triplicates. Colour codes represent log2 of relative changes. Genes under transcriptional control of Met4p are marked in green, amino acids containing a sulphur atom are marked in red. APS: adenosine 5'-phosphosulphate; PAPS: 3'-phosphoadenylyl-sulphate; SAM: S-adenosylmethionine; SAH: S-adenosylhomocysteine. The figure was generated using Pathway Tools v22.5 software.

shaken in glass tubes or shake flasks. The only exception is the methionine titre in yDS136 grown for 48 h in a shake flask, which reached 0.89 mg/l, a 3.5-fold increase compared to BY4742 under the same conditions. The methionine titre of yDS136 under the same conditions as during the initial experiment characterising yDS136 (SC-MET + 4% glucose, grown for 24 h in glass tubes) was 0.56 mg/l, which is only a 2.4-fold increase compared to BY4742 under the same conditions, and considerably lower than the 1.1 mg/l reached previously by yDS136 (Figure 3.8).

Methionine titres in yDS138 were lower than in yDS136, but the yDS138 specific methionine titres (in μmol/g_{DCW}, Figure 4.3 C & D) were similar to yDS136 (except yDS136 after 48 h growth in shake flasks). The difference in methionine titres despite similar specific methionine titres was reflected in the final OD_{600} values: yDS136 had final OD_{600} values of 6.6 - 7.8, while yDS138 final OD_{600} values reached 4.4 - 5.6 (after 24 h) and 6.4 - 6.8 (after 48 h), indicating that yDS138 grew slower and was still growing between 24 and 48 h.

BY4742 and yDS136 accumulated homoserine below the linear detection range, whereas yDS138 accumulated 12.7 μmol/g_{DCW} (after 24 h) and 15.4 μmol/g_{DCW} (after 48 h) of homoserine in total (Figure 4.3 E). More homoserine was found in the media than inside the cells after 48 h, suggesting an export mechanism, since no homoserine was added to the media. Interestingly, yDS136 and yDS138 accumulated increased amounts of cysteine, another sulphur containing amino acid, with a combined titre of 3.4 mg/l for yDS138 and the majority of cysteine (79%) was detected in the media (Figure 4.3 F). Unlike BY4742 and yDS138, yDS136 accumulated more cysteine inside the cells (58%) than in the medium.

The relative changes of internal amino acid pools in yDS136 and yDS138 compared to BY4742 are shown in Figure 4.4. Most amino acid concentrations were largely unaffected in both strains, with the exception being several amino acids involved in the sulphur amino acid biosynthesis pathway. Internal aspartic acid levels were markedly lower in yDS138 after 24 h (4.1-fold decrease), but recovered to not as much reduced levels after 48 h (2.40-fold decrease). Aspartic acid was supplied in the growth medium at 80 mg/l and the steep reduction (log2 of less than -2) after 24 h indicate a highly active aspartate kinase (Hom3p) in yDS138. Homoserine levels saw large increases in yDS138 and homoserine levels seemed to decrease in yDS136, but homoserine levels were very low in BY4742 (below the linear range of detection) and these changes don't necessarily reflect big absolute changes. Homocysteine, cystathionine and cysteine levels were increased in all strains. The increase of homocysteine was similar in yDS136 (7.8-fold increase) and yDS138 after 24 h (8.4-fold increase), while homocysteine levels after 48 h were markedly higher in yDS136 (26.0-fold increase) compared to yDS136 (3.3-fold increase). Cystathionine and cysteine levels were raised markedly in both yDS136 and yDS138 compared to BY4742, but the rise was more pronounced in yDS138 after 24 h, but the opposite was the case after 48 h. Notably, yDS138

accumulated higher levels of cysteine (Figure 4.3 F) as well as cystathionine (3.5 compared to 2.0 μmol/g_{DCW} after 48 h growth in shake flasks) outside the cells than yDS136 did.

4.3 Overexpression of bacterial OAH-SHLases without methionine inhibition

Since the GC-MS method did not enable the measurement of O-acetylhomoserine, it was unknown whether O-acetylhomoserine accumulated in any of the strains; therefore, the measured homoserine levels could have higher than the actual levels, because the acidification of samples during the extraction step might have hydrolysed the O-acetylhomoserine pools to form homoserine. Nevertheless, it was hypothesised that a feedback inhibition of Met17p by methionine could have caused the accumulation of homoserine in yDS138 (Yamagata, 1971).

In order to investigate similarities between different enzymes using O-acetylhomoserine as a substrate and find conserved residues, the protein sequences of the *S. cerevisiae* cystathionine γ-synthase (Str2p), and three OAH-SHLases (RsMetZp, Met17p & LmMetYp) were aligned using the Clustal Omega tool (www.ebi.ac.uk/Tools/msa/clustalo/; see Figure 4.5). Despite several regions of conservation among these enzymes, they all possess low similarity overall, with Str2p being the least similar to the other three enzymes. Of the three mutations in RsMetZ described by Kim et al. (2011) to increase activity, only the V104A mutation is found in the other enzymes and conserved across all enzymes. Notably, the Str2p sequence is markedly longer than the three other enzyme sequences and the Str2p N-terminal sequence did not align with the other three sequences. The InterProScan tool (www.ebi.ac.uk/interpro/beta/) combines several predictive models for the analysis of protein sequences and the tool was used to analyse the sequence of Str2p. The analysis revealed that the first 270 amino acids of Str2p did not show any homology to any known domains. The remaining amino acids showed homology to the superfamily of pyridoxal phosphate-dependent transferases, to which the other three OAH-SHLases belong as well.

The genes encoding the bacterial enzymes, *LmMetY* and *RsMetZ*, were *S. cerevisiae* codon optimised and their synthesised DNA sequences were ordered from IDT; the sequence of *MET17* was amplified by PCR from BY4742 genomic DNA. All genes were cloned into a high-copy plasmid (pCPS1UHA) and their expression was driven by a strong constitutive promoter (P_{CCW12}) from the MoClo kit (Lee et al., 2015). The plasmids carrying either *LmMetY* (pDS095), *RsMetZ* (pDS096), *MET17* (pDS097) cassettes or an empty plasmid (pCPS1UHA) were transformed into yDS138. All transformed strains were grown for 24 h or 48 h in glass tubes with SC-MET-URA + 4% glucose. The cell pellets and media supernatants were analysed by GC-MS as before. Methionine and cysteine titres,

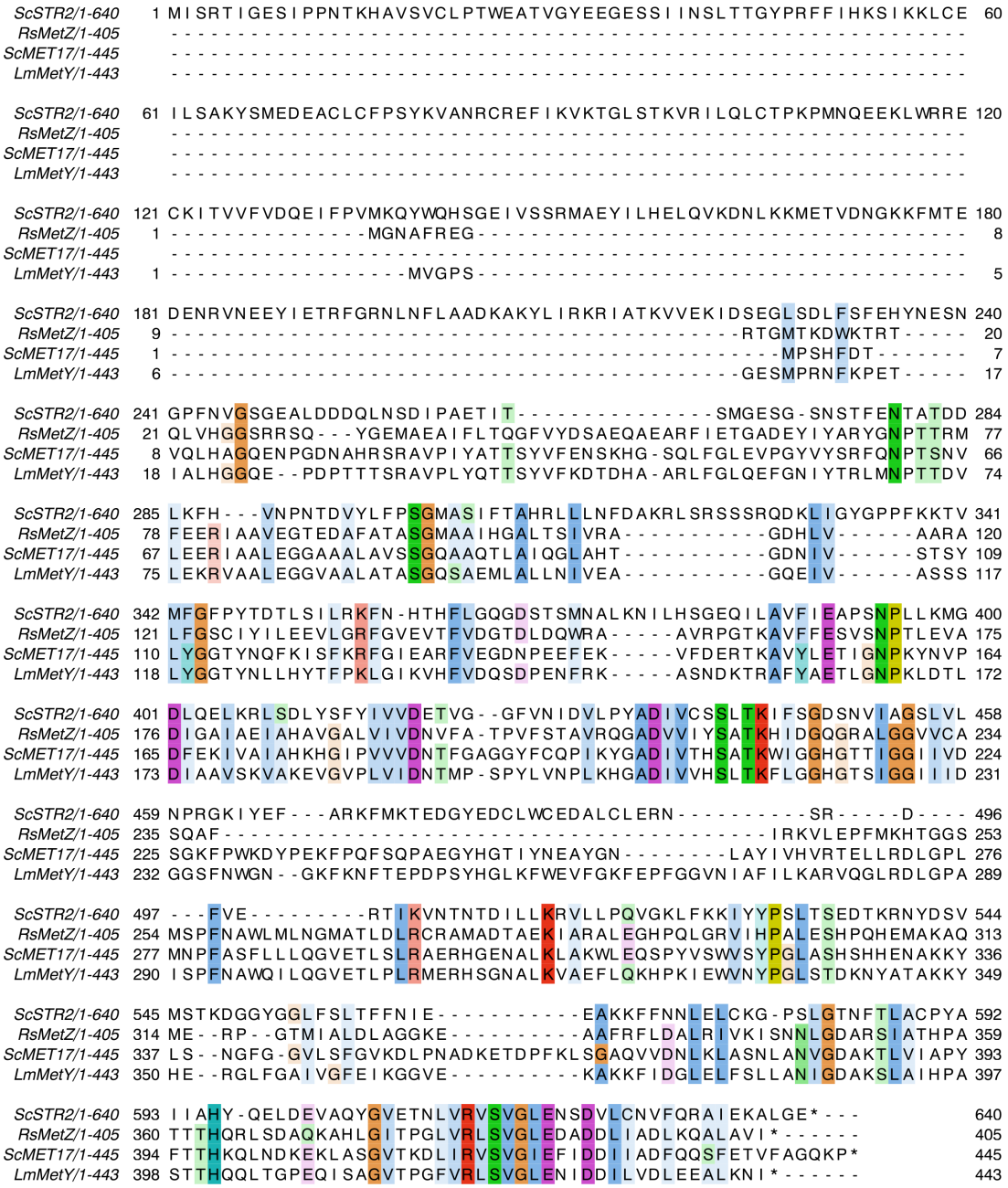

Figure 4.5: Multiple sequence alignment of different OAH-SHLases. Protein sequences were aligned using Clustal Omega with default parameters. Conserved sequences are highlighted in colour. ScSTR2: *Saccharomyces cerevisiae* cystathionine γ-synthase; RsMetZ: *Rhodobacter sphaeroides* OAH-SHLase (Kim et al., 2011); ScMET17: *Saccharomyces cerevisiae* OAH-SHLase; LmMetY: *Leptospira meyeri* OAH-SHLase.

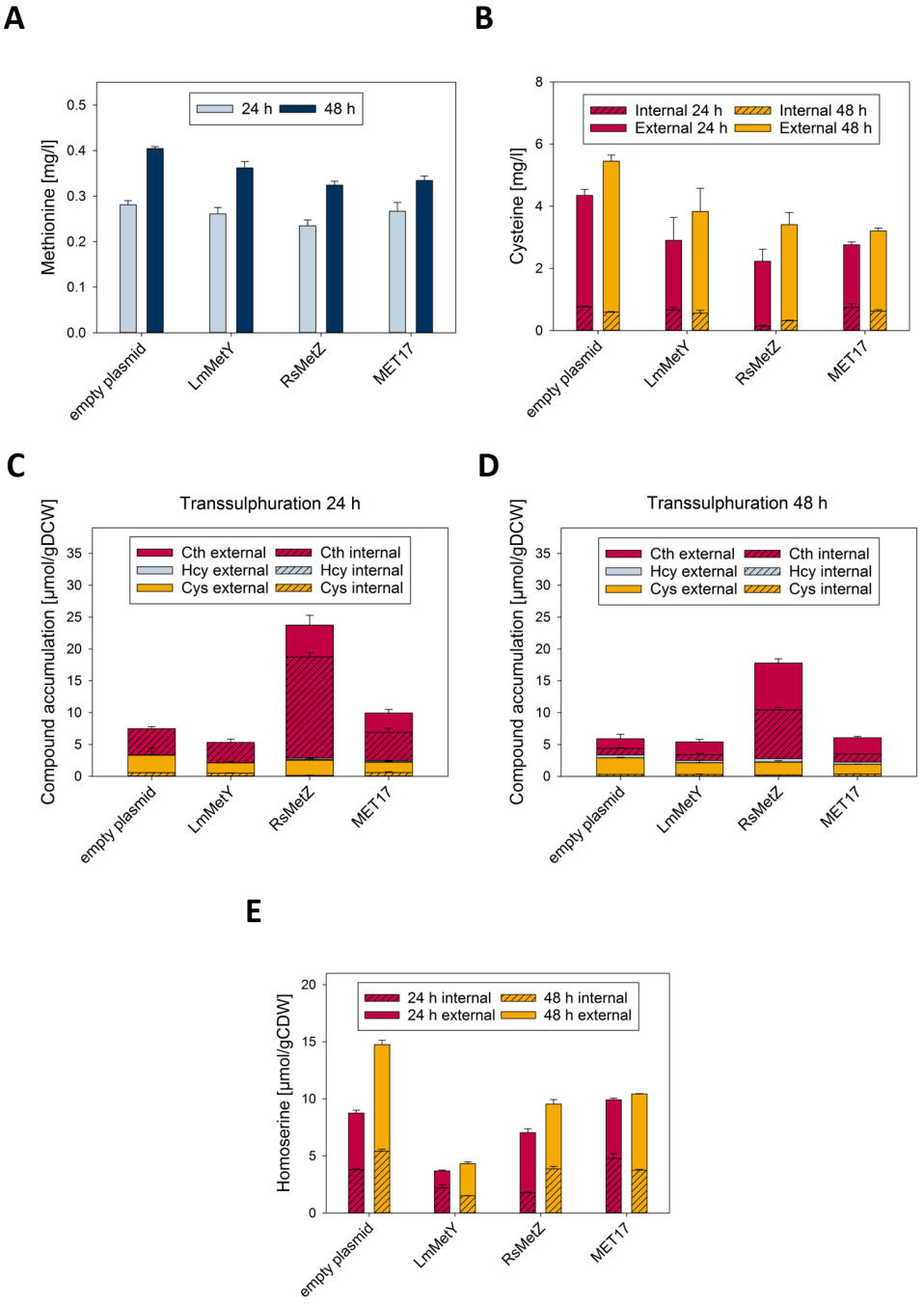

Figure 4.6: Characterisation of yDS138 overexpressing bacterial OAH-SHLases. (A) Methionine and **(B)** cysteine titres after 24 h and 48 h. Compound accumulation in the transsulphuration pathway after 24 h **(C)** and 48 h **(D)**. Cth: cystathionine; Hcy: homocysteine; Cys: cysteine. **(E)** Homoserine levels after 24 h and 48 h. Bars represent the mean of biological triplicates, error bars represent standard deviation.

compound accumulation in the transsulphuration pathway as well as homoserine accumulation in the generated strains are summarised in Figure 4.6.

Methionine titres were not changed significantly by the overexpression of either the bacterial OAH-SHLases or *MET17*, but titres comparable to yDS138 in SC-MET were not reached until after 48 h (Figure 4.6 A); no methionine was detected in the media. Cysteine titres were not changed either by the overexpression of bacterial OAH-SHLases but yDS138 carrying an empty plasmid accumulated 5.5 mg/l of cysteine, mostly in the media, which was higher than cysteine titres in yDS138 growing in SC-MET (Figure 4.6 B).

Differences between the OAH-SHLases emerged after the accumulation of compounds in the transsulphuration pathway was analysed (homocysteine, cystathionine and cysteine, Figure 4.6 C & D). Expression of *RsMetZ* caused yDS138 to accumulate large amounts of cystathionine after 24 h (24% outside the cells). The total amount of cystathionine decreased after 48 h, but a larger fraction (49%) was found in the media. Notably, specific cysteine levels after 48 h were very similar across all strains, suggesting that the higher cysteine titre of the yDS138 strain carrying an empty plasmid was due to a higher final OD_{600}. The only notable exception was the specific internal cysteine titre after 24 h: the yDS138-*RsMetZ* strain accumulated much lower internal cysteine levels (0.16 $\mu mol/g_{DCW}$) than the other strains (0.48 - 0.59 $\mu mol/g_{DCW}$). Homocysteine levels were much lower compared to cysteine and cystathionine and highest in the *RsMetZ* expressing strain after 48 h (0.56 $\mu mol/g_{DCW}$), where the majority (91%) was found in the media.

Homoserine accumulated in yDS138 carrying an empty plasmid to similar levels as in yDS138 grown in SC-MET after 48 h, whereas the overexpression of any OAH-SHLase reduced homoserine levels in all cases, up to a 3.4-fold decrease in the strain overexpressing *LmMetY* (Figure 4.6 E). It remains unclear what caused the homoserine reduction in *LmMetY* expressing strains, because threonine biosynthesis was blocked and no increased compound accumulation in the transsulphuration pathway or increased methionine titres were observed.

4.4 Increasing metabolic flux towards cysteine biosynthesis and export

Overexpressing *RsMetZ* in yDS138 did not influence methionine titres, but drastically increased the amount of cystathionine, which is the substrate for the *S. cerevisiae* cystathionine γ-lyase (Cys3p) catalysing the synthesis of cysteine. It was therefore hypothesised that co-expressing *RsMetZ* and *CYS3* would increase cysteine titres. Similarly, it was investigated whether deleting the cysteine importer *YCT1* and/or co-expressing the amino acid exporter *AQR1* would lead to enhanced cysteine accumulation outside the cells.

A new strain, yDS139, was constructed by deleting the coding sequence of

YCT1 in the yDS138 background using CRISPR/Cas9. *YCT1* was deleted by co-transforming linearised Cas9 and sgRNA plasmids targeting the gene as well as donor DNA with homology to either sides of the genome introducing the gene deletion.

Two new plasmids, pDS100 and pDS101, were constructed using Golden Gate assembly. A P_{CCW12}-*RsMetZ* cassette and a cassette with *CYS3* being expressed from a strong constitutive P_{PGK1} promoter were cloned into a high-copy plasmid to generate pDS100. The *RsMetZ* and *CYS3* cassettes together with *AQR1* expressed from a P_{TEF1} promoter were cloned into a high-copy plasmid to generate pDS101.

Both plasmids as well as an empty plasmid control (pCPS1UHA) were transformed into either yDS138 or newly cloned yDS139. All strains were grown for 48 h in glass tubes with SC-MET-URA + 4% glucose. The cell pellets and media samples were analysed by GC-MS as above. The results are summarised in Figure 4.7.

Cysteine titres did not increase in strains overexpressing either *RsMetZ* & *CYS3* or *RsMetZ*, *CYS3* & *AQR1*. Indeed, only in yDS138-*RsMetZ*-*CYS3* methionine titres were similar to the empty plasmid controls, while all other combinations decreased the total cysteine titre (Figure 4.7 A). Deleting the cysteine specific importer *YCT1* did not decrease internal cysteine titres or increase extracellular cysteine concentrations.

Co-expressing *RsMetZ* and *CYS3* markedly reduced homoserine accumulation compared to yDS138 (in SC-MET), yDS138 or yDS139 carrying an empty plasmid or yDS138 expressing *RsMetZ* alone. Notably, overexpression of *AQR1*, which also exports homoserine, did not increase homoserine levels detected in the media (Figure 4.7 B and C). The homoserine precursor aspartic acid was supplemented in the media at concentrations of 80 mg/l, but after 48 h of culturing $\leq$1.3 mg/l of aspartic acid were measured in all media samples.

The compound composition in the transsulphuration pathway changed considerably from yDS138 overexpressing *RsMetZ* alone (Figure 4.6 D & Figure 4.7 D). Deletion of the cysteine importer *YCT1* alone did not change the overall transsulphuration profile in yDS138 or yDS139 carrying an empty plasmid.

The total cystathionine accumulation observed in yDS138-*RsMetZ* was greatly lowered by co-expressing *CYS3* (from 15.0 μmol/g_{DCW} in yDS138-*RsMetZ* to 4.7 μmol/g_{DCW} in yDS138-*RsMetZ*-*CYS3*). Nevertheless, cysteine levels did not rise equally (from 2.2 μmol/g_{DCW} in yDS138-*RsMetZ* to 3.9 μmol/g_{DCW} in yDS138-*RsMetZ*-*CYS3*).

All strains held very similar low pools of intracellular cysteine (0.20 - 0.28 μmol/g_{DCW}) and differed only in how much cysteine was detected in the media. The highest amounts of total cysteine accumulated in yDS138-*RsMetZ*-*CYS3*, but since the yDS138-*RsMetZ*-*CYS3* strain reached a lower OD_{600} than yDS138 carrying an empty plasmid, the total combined cysteine titres were similar.

Similarly, all strains retained very small pools of internal homocysteine and

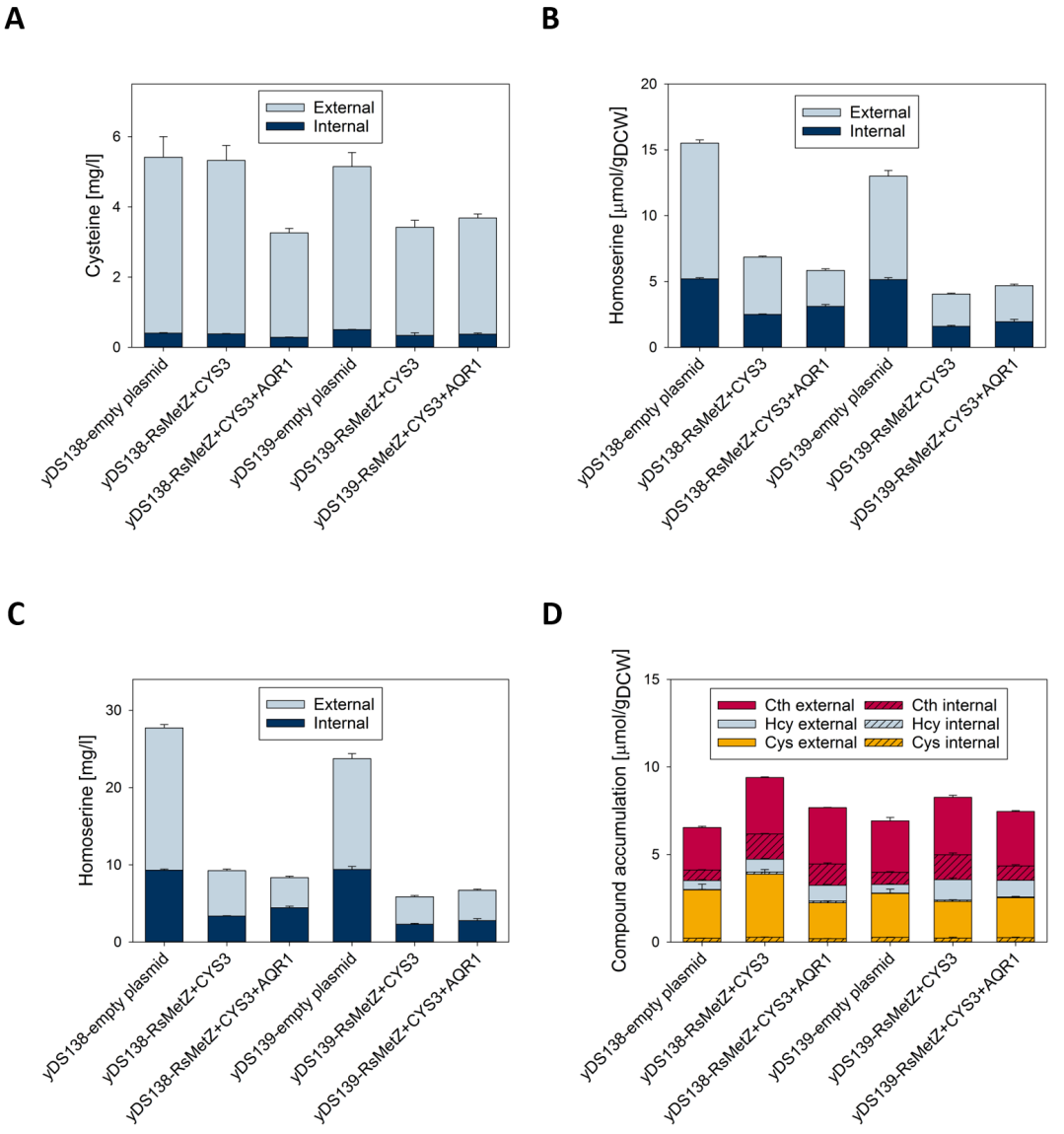

Figure 4.7: Cysteine titres, homoserine accumulation and transsulphuration pathway of cysteine producing strains. An empty plasmid or plasmids overexpressing *RsMetZ*/*CYS3* or *RsMetZ*/*CYS3*/*AQR1* were transformed into yDS138 (P_{TDH3}-*MET6*, P_{TDH3}-*STR3*, *sam2*Δ, *met30*Δ, *met32*Δ, *HOM3(A846T)*, *thr1*Δ) or yDS139 (P_{TDH3}-*MET6*, P_{TDH3}-*STR3*, *sam2*Δ, *met30*Δ, *met32*Δ, *HOM3(A846T)*, *thr1*Δ, *yct1*Δ). **(A)** Cysteine titres, **(B)** homoserine specific titres (per gram dry cell weight), **(C)** homoserine titres and **(D)** compound accumulation in the transsulphuration pathway. Cth: cystathionine; Hcy: homocysteine; Cys: cysteine. All strains were cultured for 48 h in SC-MET-URA + 4% glucose. Bars represent the mean of biological triplicates, error bars represent standard deviation.

differing levels of homocysteine in the media. The highest extracellular amounts of homocysteine were found in yDS139-*RsMetZ-CYS3*.

4.5 Discussion

Mutating *HOM3* and blocking threonine biosynthesis by deleting *THR1* was successfully applied for increasing the amount of homoserine, a precursor in methionine and cysteine biosynthesis. In fact, yDS138 accumulated large amounts of homoserine, more than 18 mg/l in the medium, which is remarkable because Kingsbury and McCusker (2010) reported that just 1 mg/l of homoserine in the medium (YPD, growth on plates) could inhibit growth of *thr1* mutants. While yDS138 did show decreased final optical densities compared to BY4742 or yDS136, the toxicity of homoserine might have been mediated by either the difference in growth media or activation of the sulphur amino acid pathway by the deletion of *MET30*/*MET32* that would have also increased the expression of *HOM6* and thereby prohibited the accumulation of the toxic intermediate β-aspartate-semialdehyde. It should be noted, that about a third of total homoserine was detected inside the cells.

The lack of reproducibility of methionine titres in yDS136 is concerning for the development of *S. cerevisiae* as a platform for the fermentative production of methionine. The titres varied between repeats and depended on the growth conditions, which could have been caused by slightly different metabolic states of the overnight starter cultures. It indicates that levels of free methionine were more influenced by the growth state than any genetic changes in the strain, thus complicating any future attempts for upscaling the fermentation process. Yoshida et al. (2011) reported indeed methionine levels in wild-type strains peaking after about 8 h of growth, while cysteine and cystathionine levels did not change greatly. The absence of any methionine in the media of any strains in this work might indicate that *S. cerevisiae* does not export excess methionine but rather converts it into SAM and regenerates it through the methyl cycle. Additionally, methionine production might be restricted through the export of compounds in the transsulphuration pathway, homocysteine, cystathionine and cysteine. Down-regulating the expression of *SAM1* and *CYS4* in yDS136 (a deletion would cause the strain to be auxotrophic for SAM and cysteine, respectively) could decrease the utilisation of methionine but also negatively impact growth rates. More measurements of internal metabolites at earlier timepoints as well as qPCR experiments could clarify the time-dependent accumulation of methionine and whether *met30*Δ/*met32*Δ mutants have indeed increased transcription of genes involved in methionine biosynthesis as is the case under methionine restricting conditions.

Farfán et al. (1999) measured much higher amounts of homoserine (up to 187 μmol/g_{DCW} total compared to 15 μmol/g_{DCW} in yDS138) by expressing a different feedback resistant *HOM3* mutant from a high expression promoter (P_{GAL1}) on a

high-copy 2μ plasmid. *HOM3* in yDS138 was expressed from its native promoter on the genome, but the upregulation of native *HOM3* by deleting *MET30* and *MET32* seemed to be enough to accumulate significant amounts of homoserine. Farfán et al. (1999) and others such as Farfán and Calderón (2000) and Velasco et al. (2005) aimed to overproduce threonine and therefore did not delete *THR1*, which could explain higher tolerance to homoserine.

Nevertheless, excess homoserine did not lead to increased methionine titres even after blocking its conversion to threonine by deleting *THR1*. A possible reason could have been additional enzymatic inhibitions in the pathway. The *S. cerevisiae* homoserine-O-acetyltransferase (Met2p) had been described as being post-transcriptionally inhibited under high expression conditions (Forlani et al., 1991) and the purified enzyme was inhibited partially by O-acetylhomoserine, homocysteine and cysteine but not methionine (Yamagata, 1987). The *S. cerevisiae* OAH-SHLase (Met17p) on the other hand was shown to be enzymatically inhibited by methionine and, to a lesser degree, homoserine (Yamagata, 1971). Homocysteine levels were elevated in yDS136 and yDS138 compared to BY4742, where homocysteine synthesis is regulated by methionine levels via *MET17* transcription and enzymatic repression of Met17p. Lower homocysteine levels in yDS138 compared to yDS136 might have been caused by heightened Met17p repression due to high intracellular homoserine and therefore homocysteine synthesis became the bottleneck for methionine production. Therefore, the overexpression of bacterial OAH-SHLases with reduced feedback inhibition was deemed as an option for overcoming this metabolic bottleneck.

Overexpression of OAH-SHLases did not increase methionine titres and slightly decreased cysteine titres. Nevertheless, overexpression of *RsMetZ* drastically changed the composition of compounds in the transsulphuration pathway, with large amounts of cystathionine accumulating inside and outside the cells. It might have been caused by lowered feedback inhibition of RsMetZp by methionine compared to LmMetYp and Met17p. It remains unclear why the overexpression of *RsMetZ* did not lead to similar increases of methionine or homocysteine even though the strain had strong promoters inserted in front of the native *MET6* and *STR3* ORF. Neither Met6p nor Str3p were tested for enzymatic inhibition by methionine, but Str3p localises to the peroxisome (Schäfer et al., 2001) and is the target of Skp2p-dependent degradation (Yoshida et al., 2011), which might limit its potential to convert cystathionine into homocysteine. Str3p, but also Cys3p and Str2p were stabilised in *skp2* mutants, therefore a deletion of *SKP2* could help to push flux into the direction of methionine.

The cystathionine accumulation might also be explained by a higher specificity of RsMetZp for the reaction synthesising cystathionine from O-acetylhomoserine and cysteine. Kim et al. (2011) aimed to find enzymes synthesising methionine directly from methanethiol and O-acetylhomoserine, but they also described cysteine as a suitable substrate and used cysteine as a substrate in the assays characterising mutant RsMetZp. Interestingly, the *S. cerevisiae* cystathionine

γ-synthase, Str2p, is expressed at comparatively low levels (Zou et al., 2017) and overexpression of *STR2* could increase cystathionine levels in similar ways as *RsMetZ*. It remains unclear, what function the long N-terminal sequence of Str2p possesses and how it might influence its substrate specificity, sensitivity to feedback inhibition and/or protein stability.

Curiously, homoserine levels markedly decrease in *LmMetY* expressing strains but did not lead to increased amounts of methionine or any compound in the transsulphuration pathway. The homoserine dehydrogenase (Hom6p) was shown to be weakly inhibited by methionine and threonine (Yumoto et al., 1991; Jacques et al., 2001). The β-aspartate-semialdehyde dehydrogenase (Hom2p) was described as being not feedback inhibited by methionine or threonine and the reverse reaction was weakly inhibited by cysteine and homocysteine (Surdin, 1967). Since all reactions in the pathway converting aspartate to homoserine are reversible, differences in the equilibrium of those reactions could have influenced the amount of homoserine generated.

The large amounts of cystathionine encouraged the assumption that overexpression of *CYS3* could elevate cysteine titres. Therefore, it was not surprising that co-expressing *RsMetZ* and *CYS3* lowered cystathionine levels, but it was not expected that cysteine titres either did not change or dropped (depending on the background strain and whether *AQR1* was expressed as well), while homoserine levels were lowered drastically. Cysteine titres were higher than in yDS138 expressing *RsMetZ* alone, suggesting that *CYS3* was indeed expressed and cystathionine converted into cysteine, but the combined amount of cysteine and cystathionine (and all compounds in the transsulphuration pathway) was lower in *RsMetZ* & *CYS3* co-expressing strains. Glutathione levels were not measured using the GC-MS method. However, it is conceivable that increased *GSH1* expression, which encodes the rate-limiting enzyme in glutathione biosynthesis, due to the *MET30*/*MET32* deletion gave rise to elevated intracellular glutathione (Ask et al., 2013; Zou et al., 2017). The decreased homoserine levels also indicate that flux into the transsulphuration pathway was indeed increased.

Overexpression of *AQR1* did not greatly enhance amino acid excretion. Velasco et al. (2004) showed that Aqr1p mediated secretion is more pronounced in strains lacking amino acid permeases and that Aqr1p efficiently exports amino acids that are highly abundant in the cytosol. Cysteine precursors such as homoserine and cystathionine might have been constantly exported by overexpressed *AQR1* products and reimported by general or specific amino acid permeases, thus reducing the available preursor amount and subsequently cysteine titres. Interestingly, yDS136 was the only strain that maintained larger pools of internal than external cysteine, while the extracellular concentrations remained similar to BY4742. Velasco et al. (2004) showed that the basal *AQR1* gene expression was very low and could be increased by adding γ-aminobutyric acid (GABA), glutamic acid and proline to the medium but no other amino acid, even though it should be noted that the effect of homoserine on *AQR1* gene

expression was not investigated by the authors. Internal levels of glutamic acid and proline did not differ between yDS136 and yDS138, therefore it is possible that basal *AQR1* expression in yDS136 was too low to effectively secrete cysteine into the medium, but yDS138 had increased *AQR1* expression caused by elevated homoserine levels. Another possibility is that Aqr1p - which cycles between the cytosol, vacuole, plasma membrane and the cell surface (Tkach et al., 2012) - activity is mediated by an unknown post-transcriptional mechanism or that Aqr1p export is not specific for cysteine.

Deleting the cysteine importer *YCT1* did not lead to increased levels of extracellular cysteine. That was surprising since the general amino acid permeases have much lower affinities for cysteine than Yct1p, even though indirect evidence suggests that other amino acid permeases such as Agp1p, Gnp1p and Mup1p also import cysteine (Huang, Walker, Fedrizzi, Gardner and Jiranek, 2017). On the contrary, the cysteine titres of strains co-expressing *RsMetZ* and *CYS3* in a *yct1*Δ background fell markedly, while the yDS139-*RsMetZ-CYS3* strain accumulated the highest amounts of extracellular homocysteine. Kaur and Bachhawat (2007) demonstrated the high affinity of Yct1p for cysteine and given the structural similarity it is possible that *yct1*Δ strains failed to effectively import extracellular homocysteine and therefore reduced the availability of homocysteine in the transsulphuration pathway.

Homocysteine is toxic in humans (Perła-Kaján et al., 2007) and since both yeast and humans share the transsulphuration pathway, *S. cerevisiae* has been used in the past to investigate mechanisms of homocysteine toxicity. High extracellular concentrations (5 mM) of cysteine and homocysteine were shown to inhibit growth in yeast (Kumar et al., 2006) and Christopher et al. (2002) indicated that high levels of S-adenosyl homocysteine rather than homocysteine itself cause toxicity. All strains overexpressing *RsMetZ* and *CYS3* exported the majority of cysteine and homocysteine into the media and the additional overexpression of *AQR1* did not increase the amount of cysteine and homocysteine found in the media. It remains unclear, whether Aqr1p is not exporting cysteine or homocysteine, whether the export is dependent on internal concentrations or whether another unknown exporter is responsible for the extracellular accumulation of cysteine and homocysteine. Deleting the native copy of *AQR1* in yDS138 could help elucidating that question. The slightly higher extracellular concentrations of homocysteine in yDS139 (*yct1*Δ) indicates that Yct1p might not only import cysteine but homocysteine as well.

It should be noted that only one timepoint of 48 h was measured in the case of strains overexpressing *RsMetZ*, *CYS3* and *AQR1*. It is unclear, how and whether cysteine titres changed before and after 48 h. The reduced but still high amounts of homoserine and cystathionine should open the opportunity to producing more cysteine and supplementing more glucose might improve the conversion by supplying more ATP for the synthesis of acetyl-CoA.

In summary, *S. cerevisiae* proved to be an unsuitable host for overproducing

free methionine. The lack of a native methionine exporter could be overcome by either expressing a methionine specific exporter from another organism or mutate one of the multidrug transporters native to *S. cerevisiae* to be specific for methionine. Another approach could be to increase the total amount of methionine by expressing a methionine storage protein high in methionine content (see Chapter 5).

Measuring more key metabolites such as SAM, S-adenosylhomocysteine, sulphide and glutathione will allow a better understanding of the fate sulphur metabolites. Proteomics studies or measurements of total hydrolysed amino acid content could help investigate whether the engineering efforts changed the proteome and lead to the accumulation of protein bound methionine or cysteine. Since cysteine is exported to the medium and cysteine precursors were produced in high quantities, targeting this sulphur amino acid for overproduction seems to be more promising. Future engineering approaches will need to address the efficient conversion of precursors into cysteine, and ensure the export of only cysteine into the medium and not its precursors while prohibiting the reimport of cysteine by specific or non-specific amino acid permeases.

Chapter 5

Expression of a Methionine Storage Protein

5.1 Introduction

Several studies demonstrated the advantage of using either D-methionine, which needs to racemised to L-methionine by the body prior to protein synthesis, or a commercially available methionine dimer as an additive to animal feeds (Sveier et al., 2001; Niu et al., 2018). The studies' authors reasoned that a slower uptake of other methionine sources compared to crystalline L-methionine contributed to a better bioavailability of L-methionine and thus better utilisation of the sulphur source. It was therefore hypothetised in this work that the expression of a methionine storage protein in *S. cerevisiae* could generate nutritionally valuable yeast.

The 2S albumins are watersoluble storage proteins, which take up between 20% - 60% of the soluble protein deposit in developing seeds and serve as nutrient source (Youle and Huang, 1981; Shewry and Pandya, 1999), with some 2S albumins showing anti-fungal properties through cell wall permeabilisation (Agizzio et al., 2006). Their conserved structure is characterised by four helices connected by four disulphide bonds forming a superhelical structure (Rico et al., 1996; Pantoja-Uceda et al., 2004; Rundqvist et al., 2012). Zeins are a class of insoluble maize storage proteins belonging to the family of prolamins (storage proteins with high prolin content) and have commercial uses as coatings or fibres (Lawton, 2002). Zeins are classified by their solubility properties into α-, β-, γ- and δ-zeins, with the only structurally described α-zeins forming disulphide bridged dimers (Momany et al., 2006). Aqueous alcohol solutions can be used to extract α-zeins, while β-, γ- and δ-zeins need to be treated with reducing agents first to disrupt the disulphide bonds. Structural studies by atomic force microscopy (AFM) described zeins as forming mesh-like structures (Guo et al., 2005; Zhang et al., 2018).

In order to overcome the low abundance of sulphur amino acids in common

food crops, several studies expressed genes encoding methionine rich proteins in transgenic plants. Among other examples, Lee et al. (2003) increased the methionine content of rice plants by up to 75% by expressing a sesame seed albumin and Molvig et al. (1997) expressed a sunflower seed albumin in *Lupinus angustifolius* L. to increase the seed methionine content by 94%. Nevertheless, some 2S seed albumins were shown to be potential allergens, reducing their biotechnological applicability (Galili and Amir, 2013). Furthermore, the elevated levels of methionine in storage protein expressing plants can be at the expense of other sulphur containing proteins and therefore not increase the total sulphur amino acid content (Hagan et al., 2003; Chiaiese et al., 2004). Other groups of methionine-rich storage proteins derived from maize, β-, γ- and/or δ-zeins, have been successfully expressed in tobacco and soybean plants (Bagga et al., 1997; Dinkins et al., 2001).

The expression of a methionine storage protein in *S. cerevisiae* could be beneficial in two ways: (i) Free methionine would be sequestered into a protein body inside the cell (as opposed to being exported outside the cell) and thus the transcriptional down-regulation of methionine biosynthesis genes as well as feedback inhibitions of enzymes in the pathway could be avoided; (ii) protein bound methionine could have a higher bioavailability and therefore better efficiency when used in animal feeds.

In this chapter, three seed methionine storage proteins were expressed from high copy plasmids in BY4742: the 10-kDa δ-zein from *Zea mays* (Wu et al., 2009), Ber e 1, a 2S albumin from *Bertholletia excelsa* (Brazil nut) (Rundqvist et al., 2012), and SFA8, a 2S albumin from *Helianthus anuus* L. (sunflower) (Pantoja-Uceda et al., 2004). The expression was investigated using a Western blot.

Furthermore, the truncated sequence of a methionine rich 10-kDa δ-zein from *Zea mays* was expressed from a high-copy plasmid in three different *S. cerevisiae* strains: BY4742, yDS136 & yDS138. In order to elucidate whether methionine and/or cysteine overproducing strains are able to better express the methionine-rich 10-kDa δ-zein, a Western blot was performed. Finally, the structures of the truncated and full protein was modelled and compared to find out whether the truncation might have influenced protein folding.

5.2 Cloning and expression of three methionine storage proteins

The protein sequences of 10-kDa δ-zein, Ber e 1 and SFA8 were analysed using the InterProScan tool (www.ebi.ac.uk/interpro/beta/) and all three proteins were predicted to contain an N-terminal signal peptide (the predictions were confirmed using SignalP 5.0 (Almagro Armenteros et al., 2019)). The predicted signal peptides were the residues 1-21 (10-kDa δ-zein), 1-22 (Ber e 1) and 1-38 (SFA8).

Therefore, the *S. cerevisiae* codon optimised DNA sequences corresponding to the translated protein lacking signal peptide residues but containing a methionine start codon and the correct overhangs for Golden Gate cloning, were ordered from IDT. The genes were cloned into a high-copy copy plasmid (pCPS1UHA) with a P_{GAL1} promoter and either an N- or C-terminal 3x-FLAG-6x-His-tag (containing a single GS linker) using Golden Gate to generate the plasmids pDS089 (3x-FLAG-6x-His-10-kDa δ-zein), pDS090 (10-kDa δ-zein-3x-FLAG-6x-His), pDS091 (3x-FLAG-6x-His-Ber e 1), pDS092 (Ber e 1-3x-FLAG-6x-His), pDS093 (3x-FLAG-6x-His-SFA8) and pDS094 (SFA8-3x-FLAG-6x-His). The molecular weights and methionine content of the proteins are listed in Table 5.1.

Table 5.1: Molecular weight and methionine content of three methionine storage proteins.

Protein	Molecular Weight (kDa)	Methionine residues
10-kDa δ-zein	14.6	30/130 (23.1%)
Ber e 1	14.8	24/124 (19.4%)
SFA8	12.3	17/104 (16.3%)

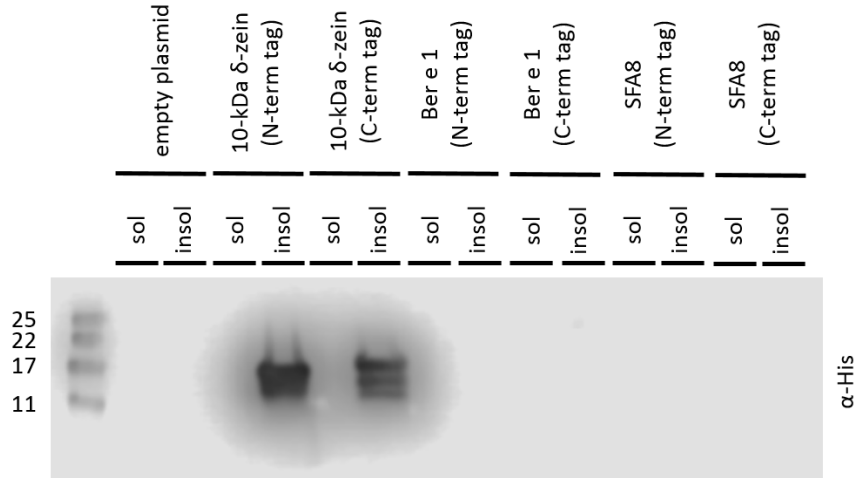

Figure 5.1: Western blot of methionine storage proteins in BY4742 Primary antibody: anti-His. Secondary antibody: Anti-Mouse IgGPeroxidase. The image was acquired using a C-DiGit Chemiluminescent Western Blot Scanner (Licor). Marker sizes in kDa. Sol: Soluble fraction. Insol: Insoluble fraction.

All generated plasmids and an empty plasmid control (pCPS1UHA) were transformed into BY4742. All strains were grown in 5 ml of SC-URA + 4% galactose for 24 h. After 24 h, the final OD_{600} values were lower for most strains carrying plasmids expressing Ber e 1 (OD_{600} 4.6 & 5.6) or SFA8 (OD_{600} 4.8 & 8.4) compared to strains carrying the empty plasmid control (OD_{600} 7.6) or expressing 10-kDa δ-zein (OD_{600} 6.0 & 7.2).

The whole cell culture was lysed using YeastBuster and the lysate (soluble fraction) as well as the centrifuged cell debris (insoluble fraction) were purified using a Ni-NTA slurry in order to enrich the target protein. The eluted fractions were analysed using a Western blot (Figure 5.1). The expected molecular weights for the tagged proteins were 18.6 kDa (10-kDa δ-zein), 18.8 kDa (Ber e 1) and 16.3 kDa (SFA8).

Neither Ber e 1 nor SFA8 were detected in the Western blot. Both, the N- as well as the C-terminally 10-kDa δ-zein were detected solely in the insoluble fraction and both samples had two more bands below the expected band at around 18.6 kDa. All further experiments were performed with 10-kDa δ-zein only.

5.3 Expression of 10-kDa δ-zein in different strain backgrounds

Subsequently, the 10-kDa δ-zein sequence was analysed. The protein parameters of the truncated and untagged 10-kDa δ-zein were calculated using the ExPASy ProtParam Webtool (https://web.expasy.org/protparam/). The results were compared to TDH3p, one of the most abundant proteins in *S. cerevisiae* (Ho et al., 2018), and both are listed in Table 5.2.

Table 5.2: Amino acid, molecular weight, amino acid composition and expected hydropathy of 10-kDa δ-zein and TDH3p.

Property	**10-kDa δ-zein**	TDH3p
Number of amino acids	130	332
Molecular weight (kDa)	14.6	35.7
Methionine residues (Percentage)	30 (23.1%)	7 (2.1%)
Cysteine residues (Percentage)	5 (3.8%)	2 (0.6%)
Alanine residues (Percentage)	7 (5.4%)	32 (9.6%)
Arginine residues (Percentage)	0 (0%)	11 (3.3%)
Asparagine residues (Percentage)	3 (2.3%)	13 (3.9%)
Aspartic acid residues (Percentage)	1 (0.8%)	24 (7.2%)
Glutamine residues (Percentage)	15 (11.5%)	5 (1.5%)
Glutamic acid residues (Percentage)	0 (0%)	15 (4.5%)
Glycine residues (Percentage)	4 (3.1%)	26 (7.8%)
Histidine residues (Percentage)	3 (2.3%)	8 (2.4%)
Isoleucine residues (Percentage)	3 (2.3%)	19 (5.7%)
Leucine residues (Percentage)	15 (11.5%)	21 (6.3%)
Lysine residues (Percentage)	0 (0%)	21 (6.3%)
Phenylalanine residues (Percentage)	5 (3.8%)	10 (3.0%)
Proline residues (Percentage)	20 (15.4%)	12 (3.6%)
Serine residues (Percentage)	8 (6.2%)	26 (7.8%)

Continued on next page

Table 5.2 – *Continued from previous page*

Property	**10-kDa δ-zein**	TDH3p
Threonine residues (Percentage)	5 (3.8%)	24 (7.2%)
Tryptophan residues (Percentage)	0 (0%)	3 (0.9%)
Tyrosine residues (Percentage)	1 (0.8%)	11 (3.3%)
Valine residues (Percentage)	5 (3.8%)	37 (11.1%)
GRAVY (Grand Average of Hydropathy)	0.513	-0.107

The 10-kDa δ-zein protein consists of 130 amino acids and has a molecular weight of 14.6 kDa, with 30 methionine and 5 cysteine residues and a percentage of sulphur amino acids of 26.9% in the protein. The next most abundant amino acid residues are proline (20 residues, 15.4%), glutamine (15, 11.5%), leucine (15, 11.5%) and serine (8, 6.2%). The GRAVY (Grand Average of Hydropathy) (Kyte and Doolittle, 1982) score of a protein is calculated as the sum of hydropathy values of all the amino acids, divided by the number of residues in the sequence, where higher values indicate higher hydrophobicity. The GRAVY score of 10-kDa δ-zein is 0.513, indicating that the protein is hydrophobic. It should be noted that the 3xFLAG-6xHis-tagged 10-kDa δ-zein has a GRAVY score of -0.208, as the affinity tags are much more hydrophilic than the rest of the protein.

An empty plasmid control (pCPS1UHA) and pDS090 (10-kDa δ-zein with C-terminal tag) were transformed into BY4742, yDS136 (P_{TDH3}-*MET6*, P_{TDH3}-*STR3*, *sam2*Δ, *met30*Δ, *met32*Δ) and yDS138 (P_{TDH3}-*MET6*, P_{TDH3}-*STR3*, *sam2*Δ, *met30*Δ, *met32*Δ, *HOM3(A846T)*, *thr1*Δ) and grown in 5 ml of SC-MET-URA + 4% galactose for 48 h. After lysis, equal amounts of the lysate (soluble fraction) or the centrifuged cell debris resuspended in YeastBuster (insoluble fraction) were used for analysis by SDS-PAGE and Western blot. The results are summarised in Figure 5.2.

All strains were able to express 10-kDa δ-zein, as detected by Western blotting, and the protein was found in the insoluble fraction only (Figure 5.2 A). Notably, the Western blot using the resuspended cell debris did not show additional bands (as opposed to the Western bot using samples concentrated by a Ni-NTA slurry). The loading control antibody (anti-actin) could not be detected by the secondary antibody (anti-mouse IgG-peroxidase), which prevented a quantification by direct comparison of actin to 10-kDa δ-zein ratios. Visual inspection of the band intensities did not suggest drastic differences in expression between strains.

The Coomassie Blue stained SDS-PAGE gel indicated that similar amounts of the soluble or insoluble fraction, respectively, were loaded for each strain (Figure 5.2 B). An additional band at the size of around 17-18 kDa can be seen in the insoluble fractions of the 10-kDa δ-zein expressing strains (compared to strains carrying an empty plasmid control).

Despite failing to detect the loading control, the band intensities were semi-quantitatively analysed using the Image Studio Lite (Licor) software. The

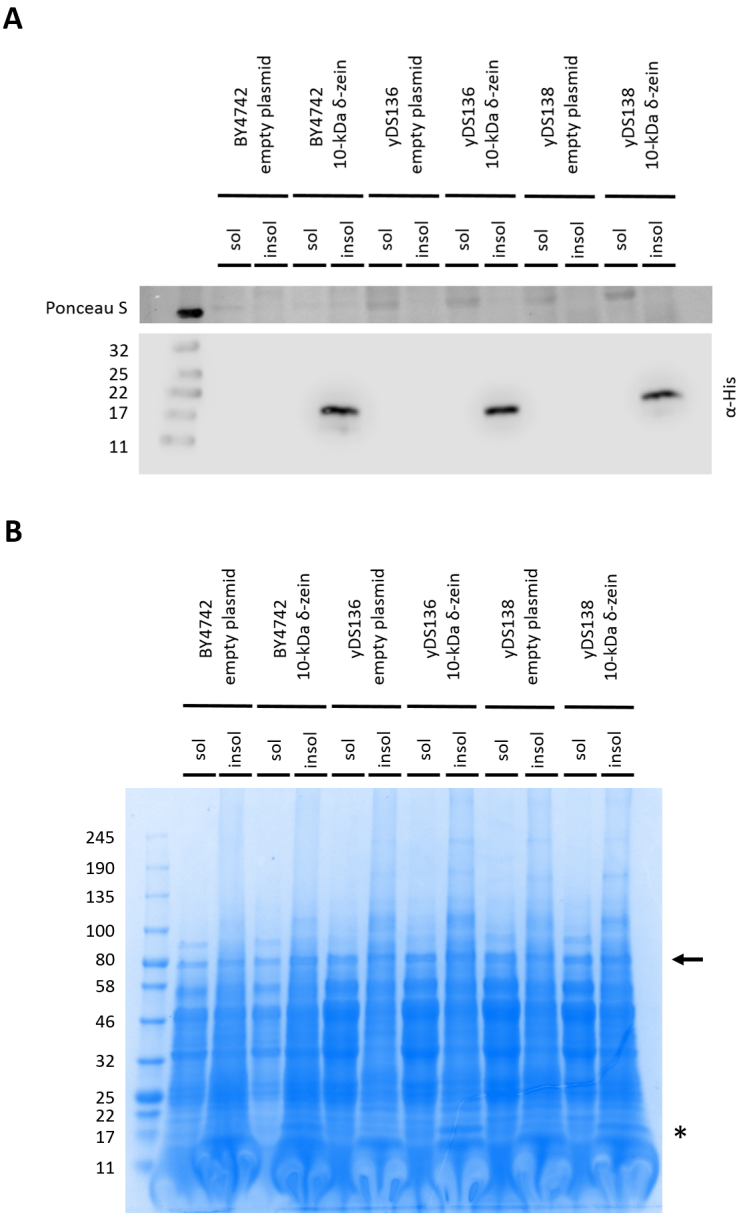

Figure 5.2: Western blot and Coomassie Blue stained SDS-PAGE of strains expressing 10-kDa δ-zein. (A) Western blot of 10-kDa δ-zein(-3x-FLAG-6xHis) expressing strains. Primary antibodies: anti-His & anti-actin. Secondary antibody: Anti-Mouse IgGPeroxidase. The image was acquired using a C-DiGit Chemiluminescent Western Blot Scanner (Licor). **(B)** Coomassie Blue stained SDS-PAGE gel. The asterisk indicates 10-kDa δ-zein(-3x-FLAG-6xHis). The arrow indicates the 80 kDa reference band. Equal amounts of the soluble (sol) and insoluble (insol) fraction of each strain, respectively, were loaded on the gel.

intensity of each band in the Western blot was divided by the intensity of a typical band in either the Ponceau S stained membrane (reference band size around 50 kDa) or in a Coomassie Blue stained SDS-PAGE gel that was loaded with the same amount of sample as in the Western Blot (reference band size around 80 kDa). The results of the analysis were normalised to the band intensity in BY4742 and are listed in Table 5.3.

Table 5.3: Relative band intensities of 10-kDa δ-zein(-3x-FLAG-6xHis) detected by Western blot in BY4742, yDS136 or yDS138. The table shows values of the raw band intensities of the Western blot (Western), normalised to a representative band in the Ponceau S (Western/Ponceau S) or normalised to a representative band in the Coomassie Blue stained SDS-PAGE gel (Western/Comassie Blue). The values of yDS136 and yDS136 were divided by the value of BY4742.

Strain	Western	Western/Ponceau S	Western/Coomassie Blue
BY4742	1	1	1
yDS136	0.94	0.62	0.89
yDS138	0.82	1.26	0.77

In all cases, the expression of 10-kDa δ-zein was lower in yDS136 and yDS138 than in BY4742. The only exception was yDS138, when the intensity of the Western Blot band was divided by the intensity of a representative band in the Ponceau S stained membrane. The quantification of the Western blot alone and the Western blot normalised to a reference band in the Coomassie Blue stained SDS-PAGE gel indicated that 10-kDa δ-zein was less highly expressed in yDS138 than in yDS136 and BY4742. The quantification of the Western blot normalised to the Ponceau S stained membrane indicated the highest expression of the protein in yDS138, but it should be noted that the Ponceau S stain of the membrane was uneven.

5.4 Structural analysis of the full and truncated 10-kDa δ-zein protein

The N-terminal sequence of 10-kDa δ-zein, which was predicted to be a signal peptide, contained a cysteine residue (Ber e 1 and SFA8 did not contain a cysteine in their predicted signal peptide). In order to investigate, whether the truncation of 10-kDa δ-zein influenced protein stability by disrupting one or more disulphide bonds, the three-dimensional model of the full and truncated protein was predicted using the I-TASSER web server (Yang and Zhang, 2015). The predicted models are shown in Figure 5.3.

The predicted structure for the truncated protein (Figure 5.3 A) showed two longer helical structures connected by a single disulphide bond (Cys24-Cys91). The predicted structure for the full protein (Figure 5.3 B) did not exhibit a

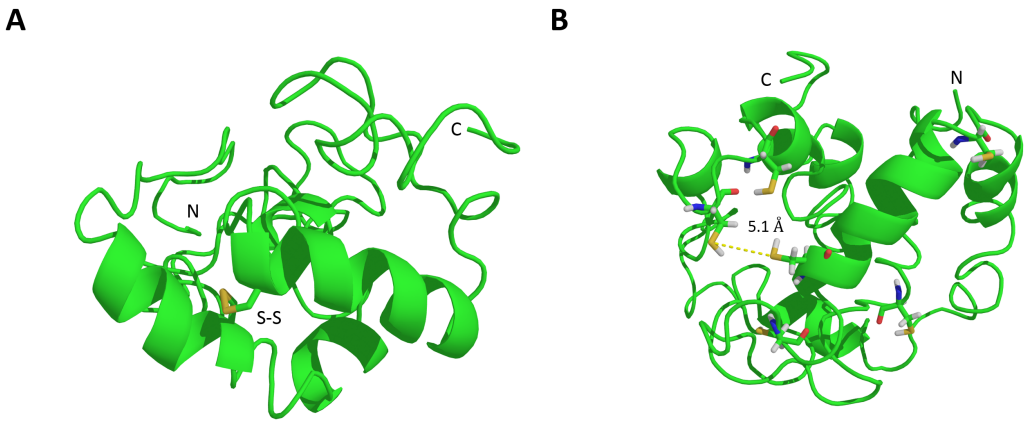

Figure 5.3: Cartoon representation of I-TASSER models for the truncated and full 10-kDa δ-zein protein. (A) The truncated protein; the disulphide bond (S-S) between Cys24 and Cys91 is shown in stick representation. **(B)** The full protein. All cysteine residues are shown in stick representation. The distance between the two cysteine residues corresponding to the disulphide bond in the truncated protein (Cys44 & Cys111) is marked by a dotted line. The N-terminus and C-terminus are marked by the letters N and C, respectively.

disulphide bond, but the same cysteine residues (Cys44 & Cys111) were in close proximity (5.1 $\AA$). Both models had low large unstructured regions and low confidence scores (C-scores below -3.8), indicating low quality models. The I-TASSER modelling started from structure templates identified in the PDB library and three (for the truncated 10-kDa δ-zein protein) and four (full protein) of the highest scoring structures used for modelling were structures of 2S albumins.

5.5 Discussion

In this work, three different seed methionine storage proteins were expressed in *S. cerevisiae*, but only 10-kDa δ-zein was able to be detected. It remained unclear, why neither Ber e 1 nor SFA8 were detected: Both proteins were expected to be soluble and the addition of an affinity tag might have influenced protein fold and subsequently stability and/or the ability to be translated. On the other hand, the initial expression experiment involved a purification step using Ni-NTA slurry, in which the His-tags might not have been exposed to the nickel matrix of the slurry, since both structures were stabilised by four disulphide bonds (Rundqvist et al., 2012; Pantoja-Uceda et al., 2004) and only the insoluble fraction was treated with a reducing agent. Furthermore, most strains expressing a 2S albumin grew to a lower final OD_{600}. Inspecting cell morphology by microscopy could reveal, whether the expression of Ber e 1 or SFA8 could be toxic via the permeabilisation of the cell wall, which has been described previously to be an effect of other 2S albumins (Agizzio et al., 2006).

Interestingly, the 10-kDa δ-zein showed extra bands in the initial bands that were not visible in the later Western blot of 10-kDa δ-zein in the insoluble fraction of BY4742, yDS136 and yDS138. Two possible explanations of the additional bands seem unlikely: Unspecific binding of the antibody (the bands were not observed in the other samples) or degradation of the protein while binding to the nickel matrix (protease inhibitor was added to the solution). Notably, the samples were taken at different timepoints (after 24 h in the initial screen versus after 48 h when comparing different strain backgrounds). Measuring expression at different timepoints could reveal, whether a degradation inside the cells occurred in a time-dependent manner.

The 10-kDa δ-zein protein was successfully expressed in the wild-type BY4742 strain as well as methionine and cysteine overproducing strains yDS136 and yDS138. Nevertheless, the results were ambiguous and it remained unclear, whether the engineered strains increased the expression significantly.

The large number of non-polar amino acids such as methionine and leucine and a high GRAVY score indicated that 10-kDa δ-zein might not be soluble in the cytosol. Indeed, no protein was found in the soluble fraction of cells expressing the protein, but it remained unclear, where exactly inside the cell it accumulated. It is possible that that either the protein was inserted into cellular membranes, even though no transmembrane domains have been predicted, or it formed insoluble protein aggregates and was targeted to the Insoluble Protein Deposit (IPOD) for degradation (Rothe et al., 2018). The 10-kDa δ-zein localisation should be investigated using immunofluorescence microscopy because a fusion with a fluorescent protein, which would be larger than 10-kDa δ-zein itself, could influence the solubility and stability of the protein. If the protein is being degraded in the vacuole, deleting vacuolar proteinases might increase the stability of the protein (Liao et al., 2005; Arendt et al., 2017).

Since methionine levels were expected to be higher in yDS136 and yDS138

(Figure 4.3), it was surprising that these strains were less able to express 10-kDa δ-zein. It should be noted that the actual methionine levels were not measured in BY4742, yDS136, and yDS138 when utilising galactose instead of glucose as a carbon source. Utilisation of galactose through the Leloir pathway is less efficient than utilisation of glucose, which could have impeded the ATP intensive biosynthesis of methionine (Nilsson and Nielsen, 2016). Additionally, other highly abundant amino acids in the 10-kDa δ-zein protein such as leucine and proline are present at low concentrations in the *S. cerevisiae* cytosol (Mülleder et al., 2016) and might have become limiting for protein synthesis as well (see also Figure 4.4).

The stability of the 10-kDa δ-zein protein remains an open question. Removing the N-terminal sequence might have reduced protein stability by disrupting one or two disulphide bonds and monitoring protein production at more timepoint would help elucidating protein production and degradation dynamics. The homology modelling of the truncated and full 10-kDa δ-zein protein did not reveal conclusively, whether the structure is stabilised by internal disulphide bonds or whether the protein forms stable dimers similar to α-zeins in maize. Nevertheless, the quality of the models was poor due to a lack of similar structures in the PDB library. Structurally similar 2S albumin proteins possess several disulphide bonds, which contribute to their remarkable stability and resistance to heat and enzymatic degradation (Pantoja-Uceda et al., 2004; Rundqvist et al., 2012). Secreting 10-kDa δ-zein by fusing it to the preprosegment of the α-factor precursor might also prevent degradation of the protein (Brake et al., 1984; Zsebo et al., 1986).

On the other hand, 2S albumins are major allergens and stabilising the 10-kDa δ-zein structure might reduce their degradation in the animal gut and increase the possibility of being an allergen in humans (Moreno and Clemente, 2008). The only maize allergen identified was is a lipid transfer protein with structural similarities to 2S albumins (Pastorello et al., 2000). Future experiments should try to heterologously express and purify the protein for the characterisation of its physicochemical properties.

Chapter 6

Final discussion

The aim of this work was to overproduce the sulphur amino acid methionine in *Saccharomyces cerevisiae*, which is a generally recognised as safe (GRAS) organism that has broad applicability in food additives or livestock feeds (Bekatorou et al., 2006). Methionine biosynthesis is native to *S. cerevisiae*: Inorganic sulphur in the form of sulphate is imported into the cell and reduced to sulphide. Sulphide is transferred to O-acetylhomoserine to yield homocysteine, which is the central branching point in the biosynthesis of sulphur amino acids, methionine and cysteine (via the transsulphuration pathway). Sulphur amino acid levels are tightly controlled by transcriptional regulation of biosynthetic enzyme synthesis and feedback inhibitions of enzymes in the pathway (Ljungdahl and Daignan-Fornier, 2012).

In chapter 3, a Design of Experiments (DOE) approach was used to increase methionine titres. In chapter 4, the feedback inhibitions of the aspartate kinase and O-acetylhomoserine sulfhydrylase (OAH-SHLase) were overcome and their effect on methionine and cysteine production assessed. In chapter 5, a methionine storage protein from maize was expressed in *S. cerevisiae*.

In this chapter, the following are discussed: (i) the usefulness of DOE for strain improvement and the comparison of improved strains to other work in *S. cerevisiae* and other organisms, (ii) addressing feedback inhibitions in the pathway and the implications on the accumulation of other sulphur compounds in *S. cerevisiae*, (iii) the potential of expressing a methionine storage protein for the improvement of *S. cerevisiae* nutritional value, and (iv) future work, especially the potential of *S. cerevisiae* for the semisynthetic production of unnatural amino acids.

6.1 DOE is a powerful tool for discerning the main factors in the production of methionine

The DOE approach for increasing methionine titres chosen in chapter 3 was able to discern the major influences on methionine production and increase the methionine titre up to 5.3-fold.

The DOE approach identified the increased expression of *MET6* and *STR3* as well as the deletion of *SAM2* and *MET30*/*MET32* as the most important genetic factors in engineering a methionine overproducing strain. At the same time the model predicted that increasing the glucose concentration and decreasing the fermentation time would increase methionine titres (Figure 3.6). Even though only a limited dataset was used to build a linear regression model, the predictions could be explained by previously published data and general biological context. *MET6* was overxpressed previously to increase methionine availability for the production of S-adenosylmethionine (SAM) (Chen, Wang, Cai and Zhou, 2016; Kanai, Mizunuma, Fujii and Iefuji, 2017) and it is not surprising that increasing the precursor supply of homocysteine by increasing *STR3* expression is only effective if *MET6* expression is elevated as well. Similarly, it could have been expected that a deletion of *SAM2* would have increased methionine levels more than a *SAM1* deletion, since *SAM2* is more highly expressed than *SAM1* in a methionine restricted environment (Zou et al., 2017). Furthermore, the DOE approach could give insights about biological processes: It was unclear *a priori*, whether activating the transcriptional activator Met4p by deleting *MET30* and *MET32* would have increased or decreased methionine levels since it would have induced the production of enzymes that push metabolic flux both towards methionine and away from it. By applying DOE it was inferred that deleting *MET30* and *MET32* had a net positive effect on methionine titres (Figure 3.6 B).

Considering all of the flaws in the specific DOE approach chosen here, the successful application might be regarded as unexpected. Only eleven of the designed strains were able to be generated (Figure 3.3) and the transcriptional data used for building the model was collected in a similar but different experimental context compared to this work (Lee et al., 2015; Zou et al., 2017). Those main drawbacks could have been overcome by two measures: (i) a set of scoping experiments to investigate, whether all intended genetic manipulations (of genes in yeast central metabolism) would result in viable strains, and (ii) a set of experiments measuring the transcriptional dynamics in the context of this experiment. Brown et al. (2018) successfully created DOE aided libraries of alcohol dehydrogenases deletion strains in *S. cerevisiae* and Xu et al. (2017) created and characterised a T7 promoter library before choosing promoters for the DOE aided improvement of a heterologously expressed violacein in *E. coli*. Applying these measures would have drastically improved the quality of the DOE approach used in this work.

Nevertheless, the newly constructed strain yDS136 (Figure 3.8) performed better than the wild-type and every single strain during the DOE experiments. However, the failure to reproduce in chapter 4 the yDS136 methionine titres measured in chapter 3, raises the question, whether the generated strain is suitable for the fermentative production of methionine. Yoshida et al. (2011) measured a steep drop of internal methionine concentrations after reaching its peak around 8 hours of culturing. Similarly, the higher methionine titres after shorter growth times of the DOE strains (Figure 3.5) and the variability of methionine titres in yDS136 measured in this work indicates that levels of intracellular methionine are tightly linked to the growth phase of yeast and internal pools of free methionine are being depleted for protein and/or SAM biosynthesis. It remained unclear, how growth in a fermenter might influence the productivity of the strain.

Engineering approaches in other organisms combined the overexpression of a methionine exporter with the deletion of a methionine importer (Huang, Liu, Jin, Tang, Shen, Yin and Zheng, 2017). Accumulation of methionine in the medium is highly desirable since it prevents the organism from utilising it for growth while simplifying the purification in a downstream process. Applying that strategy to *S. cerevisiae* would require the deletion of genes encoding the methionine permeases Mup1p and Mup3p (Isnard et al., 1996) as well as general amino acid permeases such as Gap1p, Agp1p and Gnp1p (Ljungdahl and Daignan-Fornier, 2012), all of which could reduce the competitive fitness of strains. Unfortunately, the presence of a methionine specific exporter has not been reported in *S. cerevisiae* and the measurements of media samples in this work imply no active export of methionine.

Interestingly, Brigidi et al. (1988) measured methionine outside of yeast cells. The authors subjected *Saccharomyces uvarum* to chemical mutagenesis and isolated strains resistant to ethionine, a structurally similar to methionine and toxic amino acid. Unfortunately, Brigidi et al. (1988) did not identify the mutation(s) conferring ethionine resistance. Another ethionine resistance conferring mutation, which restores the functionality of the multi-drug and toxin extrusion (MATE) exporter Erc1p, caused the accumulation of SAM inside the cells (Shiomi et al., 1991; Kanai, Kawata, Yoshida, Kita, Ogawa, Mizunuma, Watanabe, Shimoi, Mizuno, Yamada, Fujii and Iefuji, 2017). Weak evidence suggested that Erc1p localises to the vacuole (Shiomi et al., 1991) and SAM accumulated inside the cells, therefore it seems unlikely that functional Erc1p directly exports methionine into the medium. Thus, the export of methionine in ethionine resistant *S. uvarum* strains described by Brigidi et al. (1988) could have two likely explanations: (i) the strains were lacking amino acid permeases and intracellular methionine accumulated to levels high enough to cause excretion via an unspecific amino acid exporter (e. g. Aqr1p), or (ii) one or several mutations caused a native exporter to be more specific for methionine. Future work trying to export methionine should focus on deleting amino permeases and mutating the gene of a native amino acid exporter, e. g. *AQR1* (Velasco et al., 2004), to increase the exporter's specificity for methionine.

Direct comparisons between methionine titres of yDS136 and methionine production in yeasts reported in past literature are not possible, because the strains, culturing conditions, and sampling times differed. Compared to methionine titres reported by Brigidi et al. (1988) and in this work, several groups and companies were much more successful in producing methionine in other organisms such as *E. coli* or *C. glutamicum*. The company Metabolic Explorer filed a patent (Dischert and Figge, 2013) for an *E. coli* strain reaching methionine yield of 0.24 (g/g glucose) (Metabolic Explorer reported a methionine yield of 0.29 g/g and a methionine titre of 63 g/l, which is the solubility limit of methionine, at the Metabolic Engineering 12 conference in 2018), Li et al. (2016) produced 6.85 g/l methionine in *C. glutamicum* and Huang, Liu, Jin, Tang, Shen, Yin and Zheng (2017) produced 9.75 g/l methionine in *E. coli*.

In summary, the DOE approach was able to increase methionine titres compared to the wild-type strain. Nevertheless, the titres were low compared to titres reported previously in other organisms, which could be explained by several limitations (export and feedback inhibitions of pathway enzymes) not addressed during the DOE approach. The implications of addressing the feedback inhibitions are discussed below.

6.2 Feedback inhibitions play a crucial role in the biosynthesis of sulphur amino acids

The low levels of homoserine in yDS136 suggested that homoserine biosynthesis was a crucial bottleneck in the biosynthesis of methionine. Homoserine levels were successfully increased by introducing a mutation in *HOM3* removing the feedback inhibition of Hom3p, and by blocking threonine biosynthesis through the deletion of *THR1*. Nevertheless, the resulting strain yDS138 did not have increased methionine titres (Figure 4.3). This result suggests that methionine biosynthesis is regulated at several steps after homoserine in *S. cerevisiae*.

It remained unclear, why increased levels of homoserine did not increase methionine titres. Met17p was described as being feedback inhibited by methionine (Yamagata, 1971) and Met2p was partially inhibited *in vitro* by O-acetylhomoserine, homocysteine and cysteine (Yamagata, 1987). While feedback inhibitions might have played a role, it seems unlikely that they are the sole explanation for lower methionine titres in yDS138. Martinez-Force and Benitez (1992) isolated ethionine resistant and fast-growing mutants from a pH controlled continuous culture and several isolated strains had drastically elevated levels of aspartic acid, homoserine and methionine (up to a 160-fold increase of methionine for the highest producing strain). On the contrary, threonine overproducers expressing a copy of feedback insensitive *HOM3* were shown to reach lower optical densities at the end of fermentation (Farfán and Calderón, 2000), which was also the case for yDS138. The biosynthesis of methionine is ATP intensive and requires large

amounts of reducing equivalents in the form of NADH/NADPH for the synthesis of homoserine and the reduction of sulphate to sulphide. Activating the homoserine biosynthesis and the sulphur assimilation pathways might have severely lowered the ratios of cytosolic NADPH/NADP and thereby reducing the ability to effectively synthesise homocysteine and methionine. Measuring the amount of intracellular sulphide (Linderholm et al., 2008) and the NADPH/NADP ratios (Zhang et al., 2016) could reveal new possible bottlenecks.

Given the failure to increase methionine titres by genetic manipulation and increase of homoserine supply, it seems probable that a change in the culturing conditions could improve methionine titres further. Carbon flux analysis showed that *S. cerevisiae* strains grown on ethanol accumulated more ATP, methionine and SAM (Hayakawa et al., 2018). Growth on thiosulphate as a sulphur source reduces the NADPH consumption of sulphur assimilation but also decreases flux through the TCA cycle and increases ethanol production when growing on glucose (Funahashi et al., 2015; Chen et al., 2018). Each of these changes or a combination of both tested in a fermenter have the potential to increase the methionine titres of yDS138 above yDS136.

The overexpression of bacterial OAH-SHLases proved to be not sufficient for improving methionine titres. OAH-SHLases can have different substrate specificities and inhibition kinetics, and the two bacterial OAH-SHLases used in this work, *LmMetY* & *RsMetZ*, were characterised *in vitro* (Belfaiza et al., 1998; Kim et al., 2011). Different behaviour of *LmMetY in vivo* could explain, why its overexpression reduced homoserine but did not increase homocysteine or methionine levels. At the same time, some of the experimental evidence point towards *RsMetZ* having a higher preference for cysteine rather than sulphide. It is possible that increasing internal sulphide levels would increase the specificity of *RsMetZ* it as a substrate, leading to higher levels of homocysteine.

To my knowledge, this work presents the first evidence that cystathionine accumulates inside *met30*Δ/*met32*Δ strains and is exported into the medium as well. Current literature described cystathionine accumulation to occur in *cys3* mutant strains but did not measure, whether accumulation occurred outside the cells (Ono et al., 1984). The high levels of cystathionine in the yDS138-*RsMetZ* strain (Figure 4.6 C & D) and the export to the medium (Figure 4.6 B) suggested the possibility of overproducing cysteine in *S. cerevisiae*. Co-expressing *CYS3* indeed reduced the accumulation of the cysteine precursors homoserine and cystathionine (Figure 4.7 B & D), but did not increase cysteine titres. Furthermore, the conversion of of precursors homoserine and cystathionine was incomplete, indicating an imbalance of co-factors needed for the synthesis of precursors. Given the the preference of *RsMetZ* for cysteine as a substrate and the cystathionine accumulation of yDS138 itself (Figure 4.6 C & D), the overexpression of *CYS3* alone might prove more successful for overproducing cysteine.

The mechanism of cysteine secretion in *S. cerevisiae* remains unclear. Neither

the overexpression of *AQR1* nor the deletion of *YCT1* did increase extracellular cysteine accumulation. While it is unknown whether Aqr1p exports either cysteine or homocysteine, deleting the gene encoding Str3p, which converts cystathionine to homocysteine, might prevent the extracellular accumulation of homocysteine in strains overexpressing *RsMetZ*. Similarly, deleting genes encoding amino acid permeases responsible for cysteine uptake (Düring-Olsen et al., 1999) as well as the highly specific cysteine transporter Yct1p (Kaur and Bachhawat, 2007) might prove more successful in prohibiting the reimport of cysteine.

It is worth noting that the engineered strain yDS138 and the overexpression of *RsMetZ* did not suggest an increase in cysteine titres: The increased expression of *MET6* and *STR3* and the preference of RsMetZp would imply flux being pushed away from cysteine. Nevertheless, yDS138-*RsMetZ*-*CYS3* reached cysteine titres of more than 5 mg/l, with the majority of cysteine measured in the medium (Figure 4.7 A). Compared to cysteine reached in other organisms, the titres described in this work were low: Wei, Wang, Xu, Zhou, Ju, Liu and Ma (2019) produced about 1 g/l in *C. glutamicum*, Takumi et al. (2017) reached titres of 2 g/l in *Pantoea ananatis* and the highest titre of 5.1 g/l in *E. coli* was reported by Liu et al. (2018). Applying the strategies described above could improve cysteine titres in *S. cerevisiae* to comparable levels. Interestingly, Maier (2003) utilised the cysteine biosynthesis pathway of *E. coli* and its O-acetylserine sulfhydrylase to produce unnatural amino acids (UAA) by feeding it synthetic thiol substrates. Similarly, the strains described in this work could be used as a platform for the semisynthetic production of UAA. The different amino acid backbone used for the sulfhydrylation (O-acetylhomoserine instead of O-acetylserine) would produce a different set of UAA with the same substrates while *S. cerevisiae* might be more resistant to the toxic effects of some substrates.

The substrate promiscuity of many OAS-SHLases and OAH-SHLases has been applied succesfully for the synthesis of unnatural amino acids (UAA) by providing different nucleophiles as co-substrates with acetylated amino acid backbones (Salvo et al., 2012). Omura et al. (2003) purified a thermostable OAH-SHLase from *Bacillus stearothermophilus* and used it to synthesise γ-cyano-α-aminobutyric acid from O-acetylhomoserine and cyanide. Other studies utilised a *C. glutamicum* OAH-SHLase to produce methionine analogues, azidohomoalanine and S-allyl-homocysteine, inside *E. coli* and incorporate them into proteins for labelling (Ma et al., 2014; Nojoumi et al., 2019). Similarly, Maier (2003) generated a broad range of UAA semi-synthetically exploiting an *E. coli* O-acetylserine sulfhydrylase and feeding various nucleophile substrates.

In summary, mutating *HOM3* and removing the feedback inhibition of its gene product proved crucial for improving the availability of the sulphur amino acid precursor homoserine. Nevertheless, conversion of homoserine into methionine or cysteine was incomplete, possibly because of co-factor imbalances. The accumulation cystathionine in a OAH-SHLase expressing strain points towards

the potential of *S. cerevisiae* as an alternative platform for the semisynthetic production of new UAA.

6.3 Expression of a methionine storage protein

Of three different methionine storage proteins, only the expression of a *Zea mays* methionine storage protein in *S. cerevisiae* was possible. However, several questions about its feasibility to increase the nutritional value of yeast remained unanswered.

It is unclear, why neither Ber e 1 nor SFA8 were able to be detected. The studies characterising their structures either expressed the protein in *Pichia pastoris* and purified it on a heparin column (Lin et al., 2004) or purified directly it from sunflower seeds (Alcocer et al., 2002). Therefore, it seems likely that both storage proteins might not have been detected because during the concentration step using a Ni-NTA slurry the His-tag was not exposed and the proteins did not bind to the Ni matrix.

The 10-kDa δ-zein was able to be expressed in different *S. cerevisiae* strains (Figure 5.2). Previous literature described zeins as not water soluble (Lawton, 2002) and the calculated GRAVY (Grand Average of Hydropathy) score (Table 5.2) suggested the protein to be not soluble. Unsurprisingly, 10-kDa δ-zein was detected only in the insoluble fraction of all strains. Nevertheless, BY4742 seemingly produced more of the protein than yDS136 and yDS138, which produced more methionine in previous experiments (Figure 4.3 A), throwing up the question what factors might have been limiting. It should be noted, that only one successful Western blot was performed and several experiments will need to be repeated, but a few possible reasons for the differences in strains are discussed below.

Since the free amino acid composition was not measured in the growth conditions used for the expression of 10-kDa δ-zein, it remained unclear, whether yDS136 or yDS138 produced the same amounts of methionine using galactose (instead of glucose) as a carbon source. ATP supply could have become limiting as it is needed for both, methionine biosynthesis and protein synthesis as well. Switching to a strong constitutive promoter for the expression of 10-kDa δ-zein instead of the inducible P_{GAL1} promoter would circumvent the need for galactose in the growth medium. On the other hand, if the availability of proline was limiting, further strain engineering would be necessary for improving protein production.

Expression of a methionine storage protein offered the opportunity to overcome transcriptional regulation and feedback inhibition of biosynthetic enzymes by free methionine. Sequestering methionine in a storage protein (instead of exporting it to the medium) would deplete intracellular free methionine and thereby activate transcription of methionine biosynthetic enzymes. Attempts to express storage proteins in crop plants did not always increase the overall sulphur content as the

amount of other sulphur containing proteins was lowered (Hagan et al., 2003; Chiaiese et al., 2004). Therefore, any strains expressing 10-kDa δ-zein will have to be tested for the total methionine content and any changes to the proteome.

Another limiting factor might have been the stability of 10-kDa δ-zein. The initial expression of 10-kDa δ-zein was investigated after 24 h of growth and two additional smaller bands were detected, indicating a degradation of the protein. Intriguingly, the two additional bands were not detected after 48 h of expression in either BY4742, yDS136 or yDS138. If intracellular degradation occurred, it happened most likely the Insoluble Protein Deposit (IPOD), since the protein does not contain a lysine residue that could be target it for ubiquitination. Previous studies increased protein stability by deleting vacuolar proteinases (Liao et al., 2005; Arendt et al., 2017), which could be a promising approach for enhancing 10-kDa δ-zein production.

Given the lack of any zein protein structure published in the protein database, homology modelling of the full and truncated 10-kDa δ-zein could produce only very low quality structure models (Figure 5.3). The only published (but not deposited in a protein database) zein structure was of an α-zein (Momany et al., 2006), which has a different amino acid composition and forms a mesh-like structure stabilised by disulphide cross-links (Lawton, 2002; Guo et al., 2005; Zhang et al., 2018). Therefore, it seems reasonable that the 10-kDa δ-zein structure is more similar to 2S albumins, which are stabilised by four internal disulphide bonds. The full 10-kDa δ-zein sequence has six cysteine residues and the homology modelling could not discern, whether the protein is stabilised by three internal disulphide bonds, respectively, but the full protein could be more stable when expressed in *S. cerevisiae*. On the other hand, the increased stability could also lead to it being a food allergen since the allergenic properties of 2S albumins are thought be mediated by their stable structure (Moreno and Clemente, 2008). However, previous studies identified maize α- and β-zeins as potential allergens, but not the 10-kDa δ-zein (Pastorello et al., 2000, 2009).

In summary, the methionine storage protein 10-kDa δ-zein was successfully expressed in various *S. cerevisiae* strain, hinting at its potential to increase the sulphur amino acid content and thereby nutritional value of yeast. Nevertheless, more experimentation is needed to ascertain, which strain engineering approach could improve protein production, and whether the expression of the protein can increase the total methionine content.

6.4 Future work

6.4.1 Further characterisation of amino acid producing strains

Despite being able to measure every proteinogenic amino acid and many non-proteinogenic amino acids, many cellular conditions during methionine production remained unclear.

This work used a DOE approach to design and generate a range of strains with a changed expression of key genes in the methionine biosynthesis pathway. The expression was changed by inserting a constitutive promoter in front of the ORF and/or activating Met4p by deleting *MET30* and *MET32*. For constructing a linear regression model, it was assumed that gene expression was comparable to a methionine restricted environment as described by Zou et al. (2017).

However, gene expression in those strains was not measured. Genetic context is known to influence the strength of promoters (Redden et al., 2014) and Met4p (in wild-type *MET30* and *MET32* strains) regulates gene expression in response to methionine levels. It is therefore very likely that the expression values used in the linear regression model were significantly different from the expression in the context of the experiments measuring methionine titres. Transcriptional levels of methionine biosynthesis genes should be measured in a set of representative strains using RT-qPCR and those results could be used in turn to optimise the predictions of the DOE model.

More transcriptional data could also elucidate, whether a *MET30*/*MET32* deletion induces gene transcription in a similar way as sulphur or methionine starvation. Several critical genes in methionine biosynthesis (e. g. *HOM3*) were reported to be induced under methionine restriction conditions (Zou et al., 2017), even though they do not possess cofactor binding sites in their promoter regions needed for Met4p activation (Lee et al., 2010). Previous studies investigated the transcriptional responses on a time scale of up to 90 minutes after starvation or induction of a phenotype (Lee et al., 2010; Zou et al., 2017). It would be of interest to know, how transcription changes in *met30*Δ/*met32*Δ strains on a larger time scale over several hours, which is more comparable to typical fermentation timespans.

Beyond the transcriptional response of genes in the methionine biosynthesis pathway, protein levels could also have been influenced by the rewiring of central sulphur metabolism. Methionine biosynthesis is energy intensive and its precursors are either other proteinogenic amino acids (aspartic acid) or substrates for the biosynthesis of other proteinogenic amino acids (homoserine, homocysteine). Pushing flux towards methionine could lead to amino acid imbalances and indirectly causing a change in global protein biosynthesis. An untargeted proteomics approach could discern global relative protein changes compared to the wild-type BY4742 strain.

Since cytosolic levels of free methionine might peak during exponential growth

phases (Yoshida et al., 2011), measuring amino acid levels at several timepoints before the 24 h mark would provide insights into metabolite dynamics. Similarly, quantifying other key metabolites such as ATP, NADPH and hydrogen sulphide would help to ascertain, whether the supply of ATP and/or NADPH became a limiting factor in methionine production. If that would prove to be the case, ATP supply could be increased by switching the carbon source to ethanol while the use of thiosulphate as a sulphur source should reduce the need for NADPH in the sulphur assimilation pathway. Additionally, a ^{13}C flux analysis of sulphur amino acid overproducing strains could reveal in more detail, how different carbon sources change the availability of cofactors.

Finally, glutathione levels should be measured to explore, whether excess cysteine was used for the synthesis of glutathione. Glutathione levels can be measured easily by enzymatic assays (Forman et al., 2009) and glutathione is known to increase the resistance to oxidative stress (Izawa et al., 1995). Measuring oxidative stress beyond the glutathione levels itself is also important, since the the deletion of *MET30* and *MET32* might influence the stress response of those strains (Jamieson, 1998; Jamnik and Raspor, 2005). *S. cerevisiae* with elevated amounts of glutathione have the potential to increase the robustness to inhibitors in pretreated lignocellulosic materials (Ask et al., 2013).

6.4.2 Transport of metabolites across membranes

The successful production of sulphur amino acids calls for the export of the product into the fermentation medium while blocking the reimport in the cell and utilisation for growth.

Methionine and cysteine import into *S. cerevisiae* has been well described previously (Isnard et al., 1996; Düring-Olsen et al., 1999; Kosugi et al., 2001; Kaur and Bachhawat, 2007; Ljungdahl and Daignan-Fornier, 2012). Besides genes encoding the methionine (*MUP1* & *MUP3*) and cysteine (*YCT1*) specific permeases, several genes encoding general amino acid permeases (*GAP1*, *AGP1*, *GNP1*) would be targets for gene deletions. Nevertheless, those genetic changes would need to be performed in a strain background without any amino acid auxotrophies in order to ensure optimal growth.

Establishing specific export of methionine and/or across the plasma membrane would be desirable in import-deficient strains. The only described exporter, Aqr1p, would be an obvious option for overexpression, but its broad amino acid specificity means the export of other amino acids such as aspartic acid and homoserine as well (Tenreiro et al., 2002; Velasco et al., 2004). Several methionine exporters have been described in *E. coli* and *C. glutamicum* (Trotschel et al., 2005; Liu et al., 2015), but it seems unlikely that prokaryotic exporters will be functionally equivalent when expressed in the eukaryotic *S. cerevisiae*. On the other hand, Brigidi et al. (1988) and this work (Figure 4.3 B) demonstrated the ability of *S. cerevisiae* to export methionine or cysteine, respectively, even though the mechanism was unknown in both cases. *AQR1* and/or its paralogue *QDR1*

could be mutated (e. g. by error-prone PCR) in order to find mutants that are specific for the export of either methionine or cysteine.

6.4.3 Exploring the possibility of *S. cerevisiae* as a platform for the production of Unnatural amino acids (UAA)

The production of methionine and cysteine encountered the issue that the product of the fermentation process is at the same time a substrate for other cellular processes and reactions while methionine and cysteine might inhibit enzymes in the pathway. This issue could be overcome by focusing on a bioorthogonal product such as unnatural amino acids (UAA).

UAA are important building blocks for many active pharmaceutical ingredients (APIs) and are usually produced by chemical synthesis (Renata et al., 2015). Maier (2003) utilised *E. coli* O-acetylserine sulfhydrylases (OAS-SLases) to semisynthetically produce UAA by adding different thiol substrates to the growth medium, but so far no study attempted to imitate the whole range of reactions using O-acetylhomoserine (instead of O-acetylserine) as a substrate. The general feasibility of such an approach was demonstrated by Ma et al. (2014), who synthesised L-azidohomoalanine from O-acetylhomoserine and sodium azide by expressing a *C. glutamicum* OAH-SHLase in *E. coli*.

The accumulation of cystathionine in *met30*Δ/*met32*Δ strains and especially *RsMetZ* overexpressing strains indicate that *S. cerevisiae* is capable of effectively producing O-acetylhomoserine in yDS138. Therefore, first scoping experiments for the production of UAA would involve feeding thiol compounds as well as sodium azide in order to assess, whether the *S. cerevisiae* OAH-SHLases (Met17p & Str2p) are able to synthesise homoserine based UAA. Particular consideration should be given to the analysis of the transport of substrates and UAA products across the plasma membrane. UAA analysis should involve LC-MS as well as NMR characterisation of novel UAA.

Depending on the results of the initial experiments, other OAH-SHLases from other organisms, such as *LmMetY*, *RsMetZ* or the *C. glutamicum* OAH-SHLase (Ma et al., 2014), could be expressed in *S. cerevisiae* to test them for their subtrate specificity and efficacy to synthesise UAA *in vivo*. Alternatively, homology models of the enzymes could be used for identifying the active sites and subsequently engineer the enzyme for substrate specificity and increased efficiency.

Simultaneously, the accumulation of homoserine in yDS138 suggests that the supply of O-acetylhomoserine could become rate-limiting in the synthesis of UAA. A recent study used a structure-guided engineering approach to improve the specific activity of the *E. coli* homoserine acetyltransferase, MetX (Wei, Wang, Xu, Cheng, Zhou, Han, Jiang, Liu and Ma, 2019). A similar approach could be chosen to improve the specific activity of the *S. cerevisiae* homoserine acetylase (Met2p) or the improved MetX enzyme described by the authors could be

expressed in *S. cerevisiae* to increase O-acetylhomoserine levels. Simultaneously, the availability of acetyl-CoA, the crucial cofactor in this reaction, should be increased by applying strategies described before (Nielsen and Keasling, 2016).

Thus, the strains described in this work present the opportunity to transform *S. cerevisiae* into a production platform for novel UAA. Several metabolic engineering approaches can be taken to effectively produce a variety of novel UAA with high efficiency.

6.4.4 Assessing the potential of expressing a methionine storage protein for increased sulphur amino acid contents in *S. cerevisiae*

The experiments quantifying the expression of 10-kDa δ-zein lacked definitive conclusions. The Western blots should be repeated with a functional loading control to be able to semi-quantitatively determine the expression in different strains. Western blots of more timepoints before the 48 h might reveal the presence of degradation products and provide insights about the stability of the protein over time.

Knowledge of the internal metabolite levels is crucial for understanding potential bottlenecks in the synthesis of 10-kDa δ-zein. Amino acid levels could be measured by GC-MS and very low levels of methionine or proline would hint at the possibility that those amino acids were rate-limiting. Similarly, measurements of ATP and NADPH would elucidate, whether a switch of the carbon source (to ethanol for increased ATP yield) or sulphur source (to thiosulphate for reduced NADPH consumption) could improve protein production.

A central aim of sequestering methionine into a storage protein was to mimic a methionine restricted environment and thereby induce the Met4p-mediated transcription of methionine biosynthesis genes. Measuring gene expression by RT-qPCR would help elucidate the transcriptional dynamics in strains expressing 10-kDa δ-zein. Similarly, untargeted proteomics experiments as well as quantifying the total methionine content of the hydrolysed proteome would indicate, whether the expression of a methionine storage protein can increase the total sulphur content or reduce the expression of other sulphur containing proteins.

Further future experiments should focus on the cellular localisation of 10-kDa δ-zein. Immunofluorescence microscopy would be a promising approach since a fusion with fluorescent proteins might influence the solubility and localisation.

Finally, more structural information about 10-kDa δ-zein would promote the understanding of protein stability and solubility *in vivo*. Both, the full and truncated variant of 10-kDa δ-zein should be expressed in *S. cerevisiae* and compared for their stability and ability to be expressed *in vivo* by Western blotting. Additionally, protein (carrying a poly-histidine-affinity tag) should be purified using ion affinity chromatography (IMAC). Given the expected insolubility of 10-kDa δ-zein, that approach migh prove difficult, but purified protein could be structurally

characterised by circular dichroism (CD) spectroscopy and possibly more precise methodology such as X-ray crystallography or cryogenic electron microscopy (cryo-EM).

6.5 Concluding remarks

In this work, a DOE approach was utilised to investigate the main influencing factors on the production of methionine in *S. cerevisiae*. Even though most DOE designed strains were not able to be generated, the resulting linear regression model identified key factors and the newly constructed strain yDS136 exhibited increased methionine titres. The key intermediate homoserine proved to be rate-limiting and strains with a feedback resistant aspartate kinase accumulated large amounts of homoserine but not methionine, hinting that a lack of an effective export mechanism for methionine might be a crucial hindrance for the production of methionine in *S. cerevisiae*. On the other hand, cysteine was produced in larger amounts than methionine and found mostly in the medium. However, the accumulation of methionine and cysteine precursors calls for more metabolic engineering efforts to effectively convert homoserine into sulphur amino acids.

The expression of the 10-kDa δ-zein methionine storage protein presented the possibility to increase the nutritional value of *S. cerevisiae*. More experiments are needed to confirm the efficacy of 10-kDa δ-zein expression and its safety as an animal feed additive.

Strains with a deletion of *MET30* and *MET32* accumulated intra- and extracellular cystathionine, which is to my knowledge to have been reported in this work for the first time. The even larger amounts of cystathionine in strains expressing *RsMetZ* opens the possibility to engineer *S. cerevisiae* as a platform for the production of novel unnatural amino acids.

References

Agizzio, A. P., Da Cunha, M., Carvalho, A. O., Oliveira, M. A., Ribeiro, S. F. and Gomes, V. M. (2006), 'The antifungal properties of a 2S albumin-homologous protein from passion fruit seeds involve plasma membrane permeabilization and ultrastructural alterations in yeast cells', *Plant Science* **171**(4), 515–522.
URL: *https://linkinghub.elsevier.com/retrieve/pii/S0168945206001737*

Alarcón, C. M. and Heitman, J. (1997), 'FKBP12 physically and functionally interacts with aspartokinase in Saccharomyces cerevisiae.', *Mol Cell Biol* **17**(10), 5968–5975.

Alcocer, M. J., Murtagh, G. J., Bailey, K., Dumoulin, M., Sarabia Meseguer, A., Parker, M. J. and Archer, D. B. (2002), 'The Disulphide Mapping, Folding and Characterisation of Recombinant Ber e 1, an Allergenic Protein, and SFA8, Two Sulphur-rich 2S Plant Albumins', *Journal of Molecular Biology* **324**(1), 165–175.
URL: *https://linkinghub.elsevier.com/retrieve/pii/S0022283602010616*

Almagro Armenteros, J. J., Tsirigos, K. D., Sønderby, C. K., Petersen, T. N., Winther, O., Brunak, S., von Heijne, G. and Nielsen, H. (2019), 'SignalP 5.0 improves signal peptide predictions using deep neural networks', *Nature Biotechnology* **37**(4), 420–423.
URL: *http://www.nature.com/articles/s41587-019-0036-z*

Alonso-Gutierrez, J., Kim, E.-M., Batth, T. S., Cho, N., Hu, Q., Chan, L. J. G., Petzold, C. J., Hillson, N. J., Adams, P. D., Keasling, J. D., Garcia Martin, H. and Lee, T. S. (2015), 'Principal component analysis of proteomics (PCAP) as a tool to direct metabolic engineering', *Metabolic Engineering* **28**, 123–133.
URL: *https://linkinghub.elsevier.com/retrieve/pii/S109671761400161X*

Altenbach, S. B., Kuo, C. C., Staraci, L. C., Pearson, K. W., Wainwright, C., Georgescu, A. and Townsend, J. (1992), 'Accumulation of a Brazil nut albumin in seeds of transgenic canola results in enhanced levels of seed protein methionine', *Plant Molecular Biology* **18**(2), 235–245.

Altenbach, S. B., Pearson, K. W., Meeker, G., Staraci, L. C. and Sun, S. S. M. (1989), 'Enhancement of the methionine content of seed proteins by the

expression of a chimeric gene encoding a methionine-rich protein in transgenic plants', *Plant Molecular Biology* **13**(5), 513–522.
URL: *http://link.springer.com/10.1007/BF00027311*

Anstee, Q. M. and Day, C. P. (2012), 'S-adenosylmethionine (SAMe) therapy in liver disease: A review of current evidence and clinical utility', *Journal of Hepatology* **57**(5), 1097–1109.
URL: *https://linkinghub.elsevier.com/retrieve/pii/S0168827812004096*

Anupama and Ravindra, P. (2000), 'Value-added food:', *Biotechnology Advances* **18**(6), 459–479.
URL: *https://linkinghub.elsevier.com/retrieve/pii/S0734975000000458*

Arendt, P., Miettinen, K., Pollier, J., De Rycke, R., Callewaert, N. and Goossens, A. (2017), 'An endoplasmic reticulum-engineered yeast platform for overproduction of triterpenoids', *Metabolic Engineering* **40**(February), 165–175.
URL: *https://linkinghub.elsevier.com/retrieve/pii/S1096717616302373*

Arévalo-Rodríguez, M., Calderón, I. L. and Holmberg, S. (1999), 'Mutations that cause threonine sensitivity identify catalytic and regulatory regions of the aspartate kinase of Saccharomyces cerevisiae.', *Yeast (Chichester, England)* **15**(13), 1331–45.
URL: *https://www.ncbi.nlm.nih.gov/pubmed/10509015*

Arevalo-Rodriguez, M., Pan, X., Boeke, J. D. and Heitman, J. (2004), 'FKBP12 Controls Aspartate Pathway Flux in Saccharomyces cerevisiae To Prevent Toxic Intermediate Accumulation', *Eukaryotic Cell* **3**(5), 1287–1296.
URL: *http://ec.asm.org/cgi/doi/10.1128/EC.3.5.1287-1296.2004*

Ask, M., Mapelli, V., Höck, H., Olsson, L. and Bettiga, M. (2013), 'Engineering glutathione biosynthesis of Saccharomyces cerevisiae increases robustness to inhibitors in pretreated lignocellulosic materials', *Microbial Cell Factories* **12**(1), 1.
URL: *Microbial Cell Factories*

Avraham, T. and Amir, R. (2005), 'The expression level of threonine synthase and cystathionine-γ-synthase is influenced by the level of both threonine and methionine in Arabidopsis plants', *Transgenic Research* **14**(3), 299–311.
URL: *http://link.springer.com/10.1007/s11248-005-0273-4*

Ayer, A., Fellermeier, S., Fife, C., Li, S. S., Smits, G., Meyer, A. J., Dawes, I. W. and Perrone, G. G. (2012), 'A Genome-Wide Screen in Yeast Identifies Specific Oxidative Stress Genes Required for the Maintenance of Sub-Cellular Redox Homeostasis', *PLoS ONE* **7**(9), e44278.
URL: *https://dx.plos.org/10.1371/journal.pone.0044278*

Bagga, S., Adams, H., Kemp, J. D. and Sengupta-Gopalan, C. (1995), 'Accumulation of 15-Kilodalton Zein in Novel Protein Bodies in Transgenic Tobacco', *Plant Physiology* **107**(1), 13–23.
URL: *http://www.plantphysiol.org/lookup/doi/10.1104/pp.107.1.13*

Bagga, S., Adams, H. P., Rodriguez, F. D., Kemp, J. D. and Sengupta-Gopalan, C. (1997), 'Coexpression of the maize delta-zein and beta-zein genes results in stable accumulation of delta-zein in endoplasmic reticulum-derived protein bodies formed by beta-zein.', *The Plant Cell* **9**(9), 1683–1696.
URL: *http://www.plantcell.org/lookup/doi/10.1105/tpc.9.9.1683*

Bagga, S., Potenza, C., Ross, J., Martin, M. N., Leustek, T. and Sengupta-Gopalan, C. (2005), 'A transgene for high methionine protein is posttranscriptionally regulated by methionine', *In Vitro Cellular & Developmental Biology - Plant* **41**(6), 731–741.
URL: *http://link.springer.com/10.1079/IVP2005709*

Bailey, J. (1991), 'Toward a science of metabolic engineering', *Science* **252**(5013), 1668–1675.
URL: *http://www.sciencemag.org/cgi/doi/10.1126/science.2047876*

Bansal, A. S., Chee, R., Nagendran, V., Warner, A. and Hayman, G. (2007), 'Dangerous liaison: sexually transmitted allergic reaction to Brazil nuts.', *Journal of investigational allergology & clinical immunology* **17**(3), 189–91.
URL: *http://www.ncbi.nlm.nih.gov/pubmed/17583107*

Bao, A., Burritt, D. J., Chen, H., Zhou, X., Cao, D. and Tran, L.-S. P. (2019), 'The CRISPR/Cas9 system and its applications in crop genome editing', *Critical Reviews in Biotechnology* **39**(3), 321–336.
URL: *https://www.tandfonline.com/doi/full/10.1080/07388551.2018.1554621*

Bareich, D. C. and Wright, G. D. (2003), 'Functionally important amino acids in Saccharomyces cerevisiae aspartate kinase', *Biochemical and Biophysical Research Communications* **311**(3), 597–603.
URL: *http://linkinghub.elsevier.com/retrieve/pii/S0006291X03021107*

Bartlem, D., Lambein, I., Okamoto, T., Itaya, A., Uda, Y., Kijima, F., Tamaki, Y., Nambara, E. and Naito, S. (2000), 'Mutation in the Threonine Synthase Gene Results in an Over-Accumulation of Soluble Methionine in Arabidopsis', *Plant Physiology* **123**(1), 101–110.
URL: *http://www.plantphysiol.org/lookup/doi/10.1104/pp.123.1.101*

Bekatorou, A., Psarianos, C. and Koutinas, A. A. (2006), 'Production of food grade yeasts', *Food Technology and Biotechnology* **44**(3), 407–415.

Belfaiza, J., Martel, A., Margarita, D. and Saint Girons, I. (1998), 'Direct sulfhydrylation for methionine biosynthesis in Leptospira meyeri.', *Journal of*

bacteriology **180**(2), 250–5.
URL: *http://www.ncbi.nlm.nih.gov/pubmed/9440513 http://www.pubmedcentral.nih.gov/articlerender.fcgi?artid=PMC106879*

Bellucci, M., Alpini, A. and Arcioni, S. (2002), 'Zein accumulation in forage species (Lotus corniculatus and Medicago sativa) and co-expression of the γ-zein:KDEL and β-zein:KDEL polypeptides in tobacco leaf', *Plant Cell Reports* **20**(9), 848–856.
URL: *http://link.springer.com/10.1007/s00299-001-0413-0*

Bestel-Corre, G., Chateau, M., Figge, R., Raynaud, C. and Soucaille, P. (2014), 'Recombinant enzyme with altered feedback sensitivity'.

Blaiseau, P.-L. and Thomas, D. (1998), 'Multiple transcriptional activation complexes tether the yeast activator Met4 to DNA', *The EMBO Journal* **17**(21), 6327–6336.
URL: *http://emboj.embopress.org/cgi/doi/10.1093/emboj/17.21.6327*

Blount, B. A., Driessen, M. R. M. and Ellis, T. (2016), 'GC Preps: Fast and Easy Extraction of Stable Yeast Genomic DNA.', *Scientific reports* **6**, 26863.
URL: *http://www.ncbi.nlm.nih.gov/pubmed/27240644*

Boer, V. M., Crutchfield, C. A., Bradley, P. H., Botstein, D. and Rabinowitz, J. D. (2010), 'Growth-limiting Intracellular Metabolites in Yeast Growing under Diverse Nutrient Limitations', *Molecular Biology of the Cell* **21**(1), 198–211.
URL: *https://www.molbiolcell.org/doi/10.1091/mbc.e09-07-0597*

Box, G. E. P. and Behnken, D. W. (1960), 'Some New Three Level Designs for the Study of Quantitative Variables', *Technometrics* **2**(4), 455–475.
URL: *http://www.tandfonline.com/doi/abs/10.1080/00401706.1960.10489912*

Brake, A. J., Merryweather, J. P., Coit, D. G., Heberlein, U. A., Masiarz, F. R., Mullenbach, G. T., Urdea, M. S., Valenzuela, P. and Barr, P. J. (1984), 'Alpha-factor-directed synthesis and secretion of mature foreign proteins in Saccharomyces cerevisiae.', *Proceedings of the National Academy of Sciences* **81**(15), 4642–4646.
URL: *http://www.pnas.org/cgi/doi/10.1073/pnas.81.15.4642*

Breslow, D. K., Cameron, D. M., Collins, S. R., Schuldiner, M., Stewart-Ornstein, J., Newman, H. W., Braun, S., Madhani, H. D., Krogan, N. J. and Weissman, J. S. (2008), 'A comprehensive strategy enabling high-resolution functional analysis of the yeast genome', *Nature Methods* **5**(8), 711–718.
URL: *http://www.nature.com/articles/nmeth.1234*

Brigidi, P., Matteuzzi, D. and Fava, F. (1988), 'Use of protoplast fusion to introduce methionine overproduction into Saccharomyces cerevisiae', *Applied*

Microbiology and Biotechnology **28**(3), 268–271.
URL: *http://link.springer.com/10.1007/BF00250453*

Brown, S. R., Staff, M., Lee, R., Love, J., Parker, D. A., Aves, S. J. and Howard, T. P. (2018), 'Design of Experiments Methodology to Build a Multifactorial Statistical Model Describing the Metabolic Interactions of Alcohol Dehydrogenase Isozymes in the Ethanol Biosynthetic Pathway of the Yeast Saccharomyces cerevisiae', *ACS Synthetic Biology* **7**(7), 1676–1684.
URL: *http://pubs.acs.org/doi/10.1021/acssynbio.8b00112*

Cai, P., Gao, J. and Zhou, Y. (2019), 'CRISPR-mediated genome editing in non-conventional yeasts for biotechnological applications', *Microbial Cell Factories* **18**(1), 63.
URL: *https://doi.org/10.1186/s12934-019-1112-2 https://microbialcellfactories.biomedcentral.com/articles/10.1186/s12934-019-1112-2*

Calvert, J. (2010), 'Synthetic Biology: Constructing Nature?', *The Sociological Review* **58**(1_suppl), 95–112.
URL: *http://journals.sagepub.com/doi/10.1111/j.1467-954X.2010.01913.x*

Cao, X., Yang, M., Xia, Y., Dou, J., Chen, K., Wang, H., Xi, T. and Zhou, C. (2012), 'Strain improvement for enhanced production of S-adenosyl-L-methionine in Saccharomyces cerevisiae based on ethionine-resistance and SAM synthetase activity', *Annals of Microbiology* **62**(4), 1395–1402.
URL: *http://link.springer.com/10.1007/s13213-011-0389-0*

Carbonell, P., Jervis, A. J., Robinson, C. J., Yan, C., Dunstan, M., Swainston, N., Vinaixa, M., Hollywood, K. A., Currin, A., Rattray, N. J. W., Taylor, S., Spiess, R., Sung, R., Williams, A. R., Fellows, D., Stanford, N. J., Mulherin, P., Le Feuvre, R., Barran, P., Goodacre, R., Turner, N. J., Goble, C., Chen, G. G., Kell, D. B., Micklefield, J., Breitling, R., Takano, E., Faulon, J.-L. and Scrutton, N. S. (2018), 'An automated Design-Build-Test-Learn pipeline for enhanced microbial production of fine chemicals', *Communications Biology* **1**(1), 66.
URL: *https://www.nature.com/articles/s42003-018-0076-9*

Carrillo, E., Ben-Ari, G., Wildenhain, J., Tyers, M., Grammentz, D. and Lee, T. A. (2012), 'Characterizing the roles of Met31 and Met32 in coordinating Met4-activated transcription in the absence of Met30', *Molecular Biology of the Cell* **23**(10), 1928–1942.
URL: *https://www.molbiolcell.org/doi/10.1091/mbc.e11-06-0532*

Cashion, T., Le Manach, F., Zeller, D. and Pauly, D. (2017), 'Most fish destined for fishmeal production are food-grade fish', *Fish and Fisheries* **18**(5), 837–844.
URL: *http://doi.wiley.com/10.1111/faf.12209*

Caspeta, L., Chen, Y., Ghiaci, P., Feizi, A., Buskov, S., Hallström, B. M., Petranovic, D. and Nielsen, J. (2014), 'Altered sterol composition renders yeast thermotolerant', *Science* **346**(6205), 75–78.
URL: *http://www.sciencemag.org/lookup/doi/10.1126/science.1258137*

Chen, H., Wang, Z., Cai, H. and Zhou, C. (2016), 'Progress in the microbial production of S-adenosyl-l-methionine', *World Journal of Microbiology and Biotechnology* **32**(9), 1–8.

Chen, H., Wang, Z., Wang, Z., Dou, J. and Zhou, C. (2016), 'Improving methionine and ATP availability by MET6 and SAM2 co-expression combined with sodium citrate feeding enhanced SAM accumulation in Saccharomyces cerevisiae', *World Journal of Microbiology and Biotechnology* **32**(4), 56.
URL: *http://link.springer.com/10.1007/s11274-016-2010-y*

Chen, X., Zhu, P. and Liu, L. (2016), 'Modular optimization of multi-gene pathways for fumarate production', *Metabolic Engineering* **33**, 76–85.
URL: *https://linkinghub.elsevier.com/retrieve/pii/S1096717615000968*

Chen, Z., Zhang, X., Li, H., Liu, H., Xia, Y. and Xun, L. (2018), 'The Complete Pathway for Thiosulfate Utilization in Saccharomyces cerevisiae', *Applied and Environmental Microbiology* **84**(22), 1–15.
URL: *http://aem.asm.org/lookup/doi/10.1128/AEM.01241-18*

Cherest, H., Davidian, J. C., Thomas, D., Benes, V., Ansorge, W. and Surdin-Kerjan, Y. (1997), 'Molecular characterization of two high affinity sulfate transporters in Saccharomyces cerevisiae.', *Genetics* **145**(3), 627–35.
URL: *http://www.ncbi.nlm.nih.gov/pubmed/9055073*

Cherest, H. and Surdin-Kerjan, Y. (1992), 'Genetic analysis of a new mutation conferring cysteine auxotrophy in Saccharomyces cerevisiae: updating of the sulfur metabolism pathway.', *Genetics* **130**(1), 51–8.
URL: *http://www.ncbi.nlm.nih.gov/pubmed/1732168*

Cherest, H., Surdin-Kerjan, Y., Exinger, F. and Lacroute, F. (1978), 'S-adenosyl methionine requiring mutants in Saccharomyces cerevisiae: Evidences for the existence of two methionine adenosyl transferases', *MGG Molecular & General Genetics* **163**(2), 153–167.
URL: *http://link.springer.com/10.1007/BF00267406*

Cherest, H., Thomas, D. and Surdin-Kerjan, Y. (1993), 'Cysteine biosynthesis in Saccharomyces cerevisiae occurs through the transsulfuration pathway which has been built up by enzyme recruitment.', *Journal of Bacteriology* **175**(17), 5366–5374.
URL: *http://jb.asm.org/lookup/doi/10.1128/jb.175.17.5366-5374.1993*

Chiaiese, P., Ohkama-Ohtsu, N., Molvig, L., Godfree, R., Dove, H., Hocart, C., Fujiwara, T., Higgins, T. J. and Tabe, L. M. (2004), 'Sulphur and nitrogen nutrition influence the response of chickpea seeds to an added, transgenic sink for organic sulphur', *Journal of Experimental Botany* **55**(404), 1889–1901.

Christopher, S. A., Melnyk, S., Jill James, S. and Kruger, W. D. (2002), 'S-Adenosylhomocysteine, but not homocysteine, is toxic to yeast lacking cystathionine β-synthase', *Molecular Genetics and Metabolism* **75**(4), 335–343.
URL: *https://linkinghub.elsevier.com/retrieve/pii/S1096719202000033*

Costello, Z. and Martin, H. G. (2018), 'A machine learning approach to predict metabolic pathway dynamics from time-series multiomics data', *npj Systems Biology and Applications* **4**(1), 19.
URL: *http://www.nature.com/articles/s41540-018-0054-3*

Csete, M. and Doyle, J. (2004), 'Bow ties, metabolism and disease', *Trends in Biotechnology* **22**(9), 446–450.
URL: *https://linkinghub.elsevier.com/retrieve/pii/S0167779904002008*

Dancs, G., Kondrák, M. and Bánfalvi, Z. (2008), 'The effects of enhanced methionine synthesis on amino acid and anthocyanin content of potato tubers', *BMC Plant Biology* **8**(1), 65.
URL: *http://bmcplantbiol.biomedcentral.com/articles/10.1186/1471-2229-8-65*

de Aguiar, P., Bourguignon, B., Khots, M., Massart, D. and Phan-Than-Luu, R. (1995), 'D-optimal designs', *Chemometrics and Intelligent Laboratory Systems* **30**(2), 199–210.
URL: *https://linkinghub.elsevier.com/retrieve/pii/016974399400076X*

Di, R., Kim, J., Martin, M. N., Leustek, T., Jhoo, J., Ho, C.-T. and Tumer, N. E. (2003), 'Enhancement of the Primary Flavor Compound Methional in Potato by Increasing the Level of Soluble Methionine', *Journal of Agricultural and Food Chemistry* **51**(19), 5695–5702.
URL: *https://pubs.acs.org/doi/10.1021/jf030148c*

DiCarlo, J. E., Norville, J. E., Mali, P., Rios, X., Aach, J. and Church, G. M. (2013), 'Genome engineering in Saccharomyces cerevisiae using CRISPR-Cas systems', *Nucleic Acids Research* **41**(7), 4336–4343.
URL: *https://academic.oup.com/nar/article/41/7/4336/1075252*

Dinkins, R. D., Srinivasa Reddy, M. S., Meurer, C. A., Yan, B., Trick, H., Thibaud-Nissen, F., Finer, J. J., Parrott, W. A. and Collins, G. B. (2001), 'Increased sulfur amino acids in soybean plants overexpressing the maize 15 kDa zein protein', *In Vitro Cellular and Developmental Biology - Plant* **37**(6), 742–747.

Dischert, W. and Figge, R. (2013), 'A Microorganism For Methionine Production With Enhanced Glucose Import'.
URL: *https://lens.org/020-106-199-231-181*

Düring-Olsen, L., Regenberg, B., Gjermansen, C., Kielland-Brandt, M. C. and Hansen, J. (1999), 'Cysteine uptake by Saccharomyces cerevisiae is accomplished by multiple permeases', *Current Genetics* **35**(6), 609–617.
URL: *http://link.springer.com/10.1007/s002940050459*

Endy, D. (2005), 'Foundations for engineering biology', *Nature* **438**(7067), 449–453.
URL: *http://www.nature.com/articles/nature04342*

Exley, K., Reynolds, C. R., Suckling, L., Chee, S. M., Tsipa, A., Freemont, P. S., McClymont, D. and Kitney, R. I. (2019), 'Utilising datasheets for the informed automated design and build of a synthetic metabolic pathway', *Journal of Biological Engineering* **13**(1), 8.
URL: *https://jbioleng.biomedcentral.com/articles/10.1186/s13036-019-0141-z*

Farfán, M. j., Aparicio, L. and Calderón, I. L. (1999), 'Threonine overproduction in yeast strains carrying the HOM3-R2 mutant allele under the control of different inducible promoters.', *Applied and environmental microbiology* **65**(1), 110–6.
URL: *http://www.ncbi.nlm.nih.gov/pubmed/9872767*

Farfán, M.-J. and Calderón, I. L. (2000), 'Enrichment of threonine content in Saccharomyces cerevisiae by pathway engineering', *Enzyme and Microbial Technology* **26**(9-10), 763–770.
URL: *http://linkinghub.elsevier.com/retrieve/pii/S0141022900001691*

Farzadfard, F., Perli, S. D. and Lu, T. K. (2013), 'Tunable and Multifunctional Eukaryotic Transcription Factors Based on CRISPR/Cas', *ACS Synthetic Biology* **2**(10), 604–613.
URL: *http://pubs.acs.org/doi/10.1021/sb400081r*

Ferla, M. P. and Patrick, W. M. (2014), 'Bacterial methionine biosynthesis', *Microbiology* **160**(Pt_8), 1571–1584.
URL: *http://mic.microbiologyresearch.org/content/journal/micro/10.1099/mic.0.077826-0*

Flick, K., Ouni, I., Wohlschlegel, J. a., Capati, C., McDonald, W. H., Yates, J. R. and Kaiser, P. (2004), 'Proteolysis-independent regulation of the transcription factor Met4 by a single Lys 48-linked ubiquitin chain.', *Nature cell biology* **6**(7), 634–41.
URL: *http://www.ncbi.nlm.nih.gov/pubmed/15208638*

Foglino, M., Borne, F., Bally, M., Ball, G. and Patte, J. C. (1995), 'A direct sulfhydrylation pathway is used for methionine biosynthesis in Pseudomonas aeruginosa', *Microbiology* **141**(2), 431–439.
URL: *https://www.microbiologyresearch.org/content/journal/micro/10.1099/13500872-141-2-431*

Forlani, N., Martegani, E. and Alberghina, L. (1991), 'Posttranscriptional regulation of the expression of MET2 gene of Saccharomyces cerevisiae', *Biochimica et Biophysica Acta (BBA) - Gene Structure and Expression* **1089**(1), 47–53.
URL: *https://linkinghub.elsevier.com/retrieve/pii/016747819190083X*

Forman, H. J., Zhang, H. and Rinna, A. (2009), 'Glutathione: Overview of its protective roles, measurement, and biosynthesis', *Molecular Aspects of Medicine* **30**(1-2), 1–12.
URL: *https://linkinghub.elsevier.com/retrieve/pii/S0098299708000617*

Funahashi, E., Saiki, K., Honda, K., Sugiura, Y., Kawano, Y., Ohtsu, I., Watanabe, D., Wakabayashi, Y., Abe, T., Nakanishi, T., Suematsu, M. and Takagi, H. (2015), 'Finding of thiosulfate pathway for synthesis of organic sulfur compounds in Saccharomyces cerevisiae and improvement of ethanol production', *Journal of Bioscience and Bioengineering* **120**(6), 666–669.
URL: *http://dx.doi.org/10.1016/j.jbiosc.2015.04.011*

Galili, G. and Amir, R. (2013), 'Fortifying plants with the essential amino acids lysine and methionine to improve nutritional quality', *Plant Biotechnology Journal* **11**(2), 211–222.
URL: *http://doi.wiley.com/10.1111/pbi.12025*

Galili, G., Amir, R., Hoefgen, R. and Hesse, H. (2005), 'Improving the levels of essential amino acids and sulfur metabolites in plants', *Biological Chemistry* **386**(9), 817–831.
URL: *http://www.degruyter.com/view/j/bchm.2005.386.issue-9/bc.2005.097/bc.2005.097.xml*

Galili, G. and Höfgen, R. (2002), 'Metabolic engineering of amino acids and storage proteins in plants', *Metabolic Engineering* **4**(1), 3–11.

Giaever, G., Chu, A. M., Ni, L., Connelly, C., Riles, L., Véronneau, S., Dow, S., Lucau-Danila, A., Anderson, K., André, B., Arkin, A. P., Astromoff, A., El Bakkoury, M., Bangham, R., Benito, R., Brachat, S., Campanaro, S., Curtiss, M., Davis, K., Deutschbauer, A., Entian, K.-D., Flaherty, P., Foury, F., Garfinkel, D. J., Gerstein, M., Gotte, D., Güldener, U., Hegemann, J. H., Hempel, S., Herman, Z., Jaramillo, D. F., Kelly, D. E., Kelly, S. L., Kötter, P., LaBonte, D., Lamb, D. C., Lan, N., Liang, H., Liao, H., Liu, L., Luo, C., Lussier, M., Mao, R., Menard, P., Ooi, S. L., Revuelta, J. L., Roberts, C. J., Rose, M., Ross-Macdonald, P., Scherens, B., Schimmack, G., Shafer, B.,

Shoemaker, D. D., Sookhai-Mahadeo, S., Storms, R. K., Strathern, J. N., Valle, G., Voet, M., Volckaert, G., Wang, C.-y., Ward, T. R., Wilhelmy, J., Winzeler, E. A., Yang, Y., Yen, G., Youngman, E., Yu, K., Bussey, H., Boeke, J. D., Snyder, M., Philippsen, P., Davis, R. W. and Johnston, M. (2002), 'Functional profiling of the Saccharomyces cerevisiae genome', *Nature* **418**(6896), 387–391.
URL: *http://www.nature.com/articles/nature00935*

Gierest, H., Thao, N. N. and Surdin-Kerjan, Y. (1985), 'Transcriptional regulation of the MET3 gene of Saccharomyces cerevisiae', *Gene* **34**(2-3), 269–281.
URL: *https://linkinghub.elsevier.com/retrieve/pii/0378111985901362*

Gilbert, L. A., Larson, M. H., Morsut, L., Liu, Z., Brar, G. A., Torres, S. E., Stern-Ginossar, N., Brandman, O., Whitehead, E. H., Doudna, J. A., Lim, W. A., Weissman, J. S. and Qi, L. S. (2013), 'CRISPR-Mediated Modular RNA-Guided Regulation of Transcription in Eukaryotes', *Cell* **154**(2), 442–451.
URL: *http://dx.doi.org/10.1016/j.cell.2013.06.044*
https://linkinghub.elsevier.com/retrieve/pii/S009286741300826X

Golan, A., Matityahu, I., Avraham, T., Badani, H., Galili, S. and Amir, R. (2005), 'Soluble methionine enhances accumulation of a 15 kDa zein, a methionine-rich storage protein, in transgenic alfalfa but not in transgenic tobacco plants', *Journal of Experimental Botany* **56**(419), 2443–2452.
URL: *http://academic.oup.com/jxb/article/56/419/2443/532009/Soluble-methionine-enhances-accumulation-of-a-15*

Guo, Y., Liu, Z., An, H., Li, M. and Hu, J. (2005), 'Nano-structure and properties of maize zein studied by atomic force microscopy', *Journal of Cereal Science* **41**(3), 277–281.
URL: *https://linkinghub.elsevier.com/retrieve/pii/S0733521005000123*

Hacham, Y., Matityahu, I., Schuster, G. and Amir, R. (2008), 'Overexpression of mutated forms of aspartate kinase and cystathionine γ-synthase in tobacco leaves resulted in the high accumulation of methionine and threonine', *The Plant Journal* **54**(2), 260–271.
URL: *http://doi.wiley.com/10.1111/j.1365-313X.2008.03415.x*

Hacham, Y., Schuster, G. and Amir, R. (2006), 'An in vivo internal deletion in the N-terminus region of Arabidopsis cystathionine γ -synthase results in CGS expression that is insensitive to methionine', *The Plant Journal* **45**(6), 955–967.
URL: *http://doi.wiley.com/10.1111/j.1365-313X.2006.02661.x*

Hagan, N. D., Upadhyaya, N., Tabe, L. M. and Higgins, T. J. (2003), 'The redistribution of protein sulfur in transgenic rice expressing a gene for a foreign, sulfur-rich protein', *Plant Journal* **34**(1), 1–11.

Hansen, J., Cherest, H. and Kielland-Brandt, M. C. (1994), 'Two divergent MET10 genes, one from Saccharomyces cerevisiae and one from Saccharomyces carlsbergensis, encode the alpha subunit of sulfite reductase and specify potential binding sites for FAD and NADPH.', *Journal of Bacteriology* **176**(19), 6050–6058.
URL: *http://jb.asm.org/lookup/doi/10.1128/jb.176.19.6050-6058.1994*

Hansen, J. and Johannesen, P. F. (2000), 'Cysteine is essential for transcriptional regulation of the sulfur assimilation genes in Saccharomyces cerevisiae', *Molecular and General Genetics MGG* **263**(3), 535–542.
URL: *http://link.springer.com/10.1007/s004380051199*

Hansen, J., Muldbjerg, M., Chérest, H. and Surdin-Kerjan, Y. (1997), 'Siroheme biosynthesis in Saccharomyces cerevisiae requires the products of both the MET1 and MET8 genes', *FEBS Letters* **401**(1), 20–24.
URL: *https://doi.org/10.1016/S0014-5793(96)01423-8*

Hayakawa, K., Matsuda, F. and Shimizu, H. (2016), 'Metabolome analysis of Saccharomyces cerevisiae and optimization of culture medium for S-adenosyl-l-methionine production', *AMB Express* **6**(1), 38.
URL: *http://amb-express.springeropen.com/articles/10.1186/s13568-016-0210-3*

Hayakawa, K., Matsuda, F. and Shimizu, H. (2018), '13C-metabolic flux analysis of ethanol-assimilating Saccharomyces cerevisiae for S-adenosyl-l-methionine production', *Microbial Cell Factories* **17**(1), 82.
URL: *http://link.springer.com/10.1186/s12934-018-0935-6*

Henchion, M., Hayes, M., Mullen, A., Fenelon, M. and Tiwari, B. (2017), 'Future Protein Supply and Demand: Strategies and Factors Influencing a Sustainable Equilibrium', *Foods* **6**(7), 53.
URL: *http://www.mdpi.com/2304-8158/6/7/53*

Hillson, N., Caddick, M., Cai, Y., Carrasco, J. A., Chang, M. W., Curach, N. C., Bell, D. J., Le Feuvre, R., Friedman, D. C., Fu, X., Gold, N. D., Herrgård, M. J., Holowko, M. B., Johnson, J. R., Johnson, R. A., Keasling, J. D., Kitney, R. I., Kondo, A., Liu, C., Martin, V. J. J., Menolascina, F., Ogino, C., Patron, N. J., Pavan, M., Poh, C. L., Pretorius, I. S., Rosser, S. J., Scrutton, N. S., Storch, M., Tekotte, H., Travnik, E., Vickers, C. E., Yew, W. S., Yuan, Y., Zhao, H. and Freemont, P. S. (2019), 'Building a global alliance of biofoundries', *Nature Communications* **10**(1), 2040.
URL: *http://www.nature.com/articles/s41467-019-10079-2*

Ho, B., Baryshnikova, A. and Brown, G. W. (2018), 'Unification of Protein Abundance Datasets Yields a Quantitative Saccharomyces cerevisiae Proteome', *Cell*

Systems **6**(2), 192–205.
URL: *https://linkinghub.elsevier.com/retrieve/pii/S240547121730546X*

Hong, S. W., Hwang, I. S., Lee, S. M., Lee, Y. J., Jung, J. Y. and Eyal, A. (2017), 'Methods for production of L-methionine and related products'.

Horwitz, A. A., Walter, J. M., Schubert, M. G., Kung, S. H., Hawkins, K., Platt, D. M., Hernday, A. D., Mahatdejkul-Meadows, T., Szeto, W., Chandran, S. S. and Newman, J. D. (2015), 'Efficient Multiplexed Integration of Synergistic Alleles and Metabolic Pathways in Yeasts via CRISPR-Cas', *Cell Systems* **1**(1), 88–96.
URL: *https://linkinghub.elsevier.com/retrieve/pii/S2405471215000034*

Hua, X., Shui, C., He, Y., Xing, S., Yu, N., Zhu, Z. and Zhao, C. (2015), 'Effects of different feed stimulants on freshwater crayfish (Procambarus clarkii), fed diets with or without partial replacement of fish meal by biofeed', *Aquaculture Nutrition* **21**(1), 113–120.
URL: *http://doi.wiley.com/10.1111/anu.12148*

Huang, C.-W., Walker, M. E., Fedrizzi, B., Gardner, R. C. and Jiranek, V. (2017), 'Yeast genes involved in regulating cysteine uptake affect production of hydrogen sulfide from cysteine during fermentation', *FEMS Yeast Research* **17**(5), 1–26.
URL: *http://academic.oup.com/femsyr/article/doi/10.1093/femsyr/fox046/3934655/Yeast-genes-involved-in-regulating-cysteine-uptake*

Huang, J.-F., Liu, Z.-Q., Jin, L.-Q., Tang, X.-L., Shen, Z.-Y., Yin, H.-H. and Zheng, Y.-G. (2017), 'Metabolic engineering of Escherichia coli for microbial production of L-methionine', *Biotechnology and Bioengineering* **114**(4), 843–851.
URL: *http://doi.wiley.com/10.1002/bit.26198*

Hummel, W., Geueke, B., Osswald, S., Weckbecker, C. and Huthmacher, K. (2007), 'Method for the preparation of L-amino acids from D-amino acids'.

Humphries, W., Miller, D. L. and Wildnauer, R. H. (1972), 'The thermomechanical analysis of natural and chemically modified human hair', *Journal of the Society of Cosmetic Chemists* **23**(6), 359–370.

Hwang, B.-J., Yeom, H.-J., Kim, Y. and Lee, H.-S. (2002), 'Corynebacterium glutamicum Utilizes both Transsulfuration and Direct Sulfhydrylation Pathways for Methionine Biosynthesis', *Journal of Bacteriology* **184**(5), 1277–1286.
URL: *http://jb.asm.org/cgi/doi/10.1128/JB.184.5.1277-1286.2002*

Inoue, Y., Sugiyama, K.-i., Izawa, S. and Kimura, A. (1998), 'Molecular identification of glutathione synthetase (GSH2) gene from Saccharomyces cerevisiae', *Biochimica et Biophysica Acta (BBA) - Gene Structure and Expression*

1395(3), 315–320.
URL: *https://linkinghub.elsevier.com/retrieve/pii/S0167478197001991*

Iorizzo, M., Piraccini, B. M. and Tosti, A. (2007), 'Nail cosmetics in nail disorders', *Journal of Cosmetic Dermatology* **6**(1), 53–58.
URL: *http://doi.wiley.com/10.1111/j.1473-2165.2007.00290.x*

Ishtar Snoek, I. and Yde Steensma, H. (2006), 'Why does Kluyveromyces lactis not grow under anaerobic conditions? Comparison of essential anaerobic genes of Saccharomyces cerevisiae with the Kluyveromyces lactis genome', *FEMS Yeast Research* **6**(3), 393–403.
URL: *https://academic.oup.com/femsyr/article-lookup/doi/10.1111/j.1567-1364.2005.00007.x*

Isnard, A.-D., Thomas, D. and Surdin-Kerjan, Y. (1996), 'The Study of Methionine Uptake inSaccharomyces cerevisiaeReveals a New Family of Amino Acid Permeases', *Journal of Molecular Biology* **262**(4), 473–484.
URL: *https://linkinghub.elsevier.com/retrieve/pii/S002228369690529X*

Izawa, S., Inoue, Y. and Kimura, A. (1995), 'Oxidative stress response in yeast: effect of glutathione on adaptation to hydrogen peroxide stress in Saccharomyces cerevisiae', *FEBS Letters* **368**(1), 73–76.
URL: *https://www.sciencedirect.com/science/article/pii/0014579395006037*

Jacques, S. L., Ejim, L. J. and Wright, G. D. (2001), 'Homoserine dehydrogenase from Saccharomyces cerevisiae: kinetic mechanism and stereochemistry of hydride transfer', *Biochimica et Biophysica Acta (BBA) - Protein Structure and Molecular Enzymology* **1544**(1-2), 42–54.
URL: *https://linkinghub.elsevier.com/retrieve/pii/S0167483800002028*

Jakočiūnas, T., Bonde, I., Herrgård, M., Harrison, S. J., Kristensen, M., Pedersen, L. E., Jensen, M. K. and Keasling, J. D. (2015), 'Multiplex metabolic pathway engineering using CRISPR/Cas9 in Saccharomyces cerevisiae', *Metabolic Engineering* **28**, 213–222.
URL: *http://www.sciencedirect.com/science/article/pii/S1096717615000105*

Jakočiunas, T., Rajkumar, A. S., Zhang, J., Arsovska, D., Rodriguez, A., Jendresen, C. B., Skjødt, M. L., Nielsen, A. T., Borodina, I., Jensen, M. K. and Keasling, J. D. (2015), 'CasEMBLR: Cas9-Facilitated Multiloci Genomic Integration of in Vivo Assembled DNA Parts in Saccharomyces cerevisiae', *ACS Synthetic Biology* **4**(11), 1226–1234.
URL: *http://pubs.acs.org/doi/abs/10.1021/acssynbio.5b00007*

Jamieson, D. J. (1998), 'Oxidative stress responses of the yeast Saccharomyces cerevisiae', *Yeast* **14**(16), 1511–1527.

Jamnik, P. and Raspor, P. (2005), 'Methods for monitoring oxidative stress response in yeasts', *Journal of Biochemical and Molecular Toxicology* **19**(4), 195–203.
URL: *http://doi.wiley.com/10.1002/jbt.20091*

Jankowski, J., Kubińska, M. and Zduńczyk, Z. (2014), 'Nutritional and immunomodulatory function of methionine in poultry diets a review', *Annals of Animal Science* **14**(1), 17–32.
URL: *http://content.sciendo.com/view/journals/aoas/14/1/article-p17.xml*

Jinek, M., Chylinski, K., Fonfara, I., Hauer, M., Doudna, J. A. and Charpentier, E. (2012), 'A Programmable Dual-RNA-Guided DNA Endonuclease in Adaptive Bacterial Immunity', *Science* **337**(6096), 816–821.
URL: *http://www.sciencemag.org/cgi/doi/10.1126/science.1225829*

JMP, A. and Proust, M. (2018), *Design of Experiments Guide*, SAS Institute: Cary, NC, USA.
URL: *https://support.sas.com/documentation/onlinedoc/jmp/14.0/DOE-Guide.pdf*

Joo, Y. C., Hyeon, J. E. and Han, S. O. (2017), 'Metabolic Design of Corynebacterium glutamicum for Production of l -Cysteine with Consideration of Sulfur-Supplemented Animal Feed', *Journal of Agricultural and Food Chemistry* **65**(23), 4698–4707.

Kaiser, P., Flick, K., Wittenberg, C. and Reed, S. I. (2000), 'Regulation of Transcription by Ubiquitination without Proteolysis', *Cell* **102**(3), 303–314.
URL: *https://linkinghub.elsevier.com/retrieve/pii/S0092867400000362*

Kaiser, P., Su, N.-Y., Yen, J. L., Ouni, I. and Flick, K. (2006), 'The yeast ubiquitin ligase SCFMet30: connecting environmental and intracellular conditions to cell division.', *Cell division* **1**(3), 16.
URL: *http://www.ncbi.nlm.nih.gov/pubmed/16895602*

Kanai, M., Kawata, T., Yoshida, Y., Kita, Y., Ogawa, T., Mizunuma, M., Watanabe, D., Shimoi, H., Mizuno, A., Yamada, O., Fujii, T. and Iefuji, H. (2017), 'Sake yeast YHR032W/ERC1 haplotype contributes to high S-adenosylmethionine accumulation in sake yeast strains', *Journal of Bioscience and Bioengineering* **123**(1), 8–14.
URL: *http://dx.doi.org/10.1016/j.jbiosc.2016.07.007*

Kanai, M., Masuda, M., Takaoka, Y., Ikeda, H., Masaki, K., Fujii, T. and Iefuji, H. (2013), 'Adenosine kinase-deficient mutant of Saccharomyces cerevisiae accumulates S-adenosylmethionine because of an enhanced methionine biosynthesis pathway', *Applied Microbiology and Biotechnology* **97**(3), 1183–1190.

Kanai, M., Mizunuma, M., Fujii, T. and Iefuji, H. (2017), 'A genetic method to enhance the accumulation of S-adenosylmethionine in yeast', *Applied Microbiology and Biotechnology* **101**(4), 1351–1357.
URL: *http://link.springer.com/10.1007/s00253-017-8098-7*

Karimian, A., Azizian, K., Parsian, H., Rafieian, S., ShafieiIrannejad, V., Kheyrollah, M., Yousefi, M., Majidinia, M. and Yousefi, B. (2019), 'CRISPR/Cas9 technology as a potent molecular tool for gene therapy', *Journal of Cellular Physiology* **234**(8), 12267–12277.
URL: *https://onlinelibrary.wiley.com/doi/abs/10.1002/jcp.27972*

Kaur, J. and Bachhawat, A. K. (2007), 'Yct1p, a Novel, High-Affinity, Cysteine-Specific Transporter From the Yeast Saccharomyces cerevisiae', *Genetics* **176**(2), 877–890.
URL: *http://www.genetics.org/lookup/doi/10.1534/genetics.107.070342*

Kim, J., Lee, M., Chalam, R., Martin, M. N., Leustek, T. and Boerjan, W. (2002), 'Constitutive Overexpression of Cystathionine γ-Synthase in Arabidopsis Leads to Accumulation of Soluble Methionine and S -Methylmethionine', *Plant Physiology* **128**(1), 95–107.
URL: *http://www.plantphysiol.org/lookup/doi/10.1104/pp.101801*

Kim, S. Y., Shin, Y. U., Seo, C. I., Son, S. K., Heo, I. K., Lee, H. J., Kim, J. E., Kim, H. A., BAE, J. Y. and Na, K. H. (2011), 'Novel o-acetylhomoserine sulfhydrylase or variant thereof, and method for transforming methionine using same'.
URL: *https://patents.google.com/patent/EP2657249A2/pt-PT*

Kingsbury, J. M. and McCusker, J. H. (2010), 'Homoserine Toxicity in Saccharomyces cerevisiae and Candida albicans Homoserine Kinase (thr1 Δ) Mutants', *Eukaryotic Cell* **9**(5), 717–728.
URL: *http://ec.asm.org/lookup/doi/10.1128/EC.00044-10*

Kinoshita, S. (2017), *Amino Acid Fermentation*, Vol. 159 of *Advances in Biochemical Engineering/Biotechnology*, Springer Japan, Tokyo.
URL: *http://link.springer.com/10.1007/978-4-431-56520-8*

Kistler, M., Maier, K. and Eckardt-Schupp, F. (1990), 'Genetic and biochemical analysis of glutathione-deficient mutants of Saccharomyces cerevisiae', *Mutagenesis* **5**(1), 39–44.
URL: *https://academic.oup.com/mutage/article-lookup/doi/10.1093/mutage/5.1.39*

Kitano, H. (2004), 'Biological robustness', *Nature Reviews Genetics* **5**(11), 826–837.
URL: *http://www.nature.com/articles/nrg1471*

Kodaki, T., Tsuji, S., Otani, N., Yamamoto, D., Rao, K. S., Watanabe, S., Tsukatsune, M. and Makino, K. (2003), 'Differential transcriptional regulation of two distinct S-adenosylmethionine synthetase genes (SAM1 and SAM2) of Saccharomyces cerevisiae.', *Nucleic acids research. Supplement (2001)* **3**(3), 303–4.
URL: *http://www.ncbi.nlm.nih.gov/pubmed/15102835*

Koga, R., Miyoshi, Y., Sakaue, H., Hamase, K. and Konno, R. (2017), 'Mouse d-Amino-Acid Oxidase: Distribution and Physiological Substrates', *Frontiers in Molecular Biosciences* **4**(DEC), 1–10.
URL: *http://journal.frontiersin.org/article/10.3389/fmolb.2017.00082/full*

Kondoh, M. and Hirasawa, T. (2019), 'l-Cysteine production by metabolically engineered Corynebacterium glutamicum', *Applied Microbiology and Biotechnology* **103**(6), 2609–2619.
URL: *http://dx.doi.org/10.1007/s00253-019-09663-9 http://link.springer.com/10.1007/s00253-019-09663-9*

Kosugi, A., Koizumi, Y., Yanagida, F. and Udaka, S. (2001), 'MUP1, High Affinity Methionine Permease, is Involved in Cysteine Uptake by Saccharomyces cerevisiae', *Bioscience, Biotechnology, and Biochemistry* **65**(3), 728–731.
URL: *http://www.tandfonline.com/doi/full/10.1271/bbb.65.728*

Kosuri, S. and Church, G. M. (2014), 'Large-scale de novo DNA synthesis: technologies and applications', *Nature Methods* **11**(5), 499–507.
URL: *http://www.nature.com/articles/nmeth.2918*

Krömer, J. O., Wittmann, C., Schröder, H. and Heinzle, E. (2006), 'Metabolic pathway analysis for rational design of L-methionine production by Escherichia coli and Corynebacterium glutamicum', *Metabolic Engineering* **8**(4), 353–369.
URL: *https://linkinghub.elsevier.com/retrieve/pii/S1096717606000097*

Kumar, A., John, L., Alam, M. M., Gupta, A., Sharma, G., Pillai, B. and Sengupta, S. (2006), 'Homocysteine- and cysteine-mediated growth defect is not associated with induction of oxidative stress response genes in yeast', *Biochemical Journal* **396**(1), 61–69.
URL: *http://www.biochemj.org/cgi/doi/10.1042/BJ20051411*

Kumar, V., Bhalla, A. and Rathore, A. S. (2014), 'Design of experiments applications in bioprocessing: Concepts and approach', *Biotechnology Progress* **30**(1), 86–99.

Kuras, L., Rouillon, A., Lee, T., Barbey, R., Tyers, M. and Thomas, D. (2002), 'Dual regulation of the Met4 transcription factor by ubiquitin-dependent degradation and inhibition of promoter recruitment', *Molecular Cell* **10**(1), 69–80.

Kurihara, S., Shibahara, S., Arisaka, H. and Akiyama, Y. (2007), 'Enhancement of Antigen-Specific Immunoglobulin G Production in Mice by Co-Administration of L-Cystine and L-Theanine', *Journal of Veterinary Medical Science* **69**(12), 1263–1270.
URL: *http://joi.jlc.jst.go.jp/JST.JSTAGE/jvms/69.1263?from=CrossRef*

Kyte, J. and Doolittle, R. F. (1982), 'A simple method for displaying the hydropathic character of a protein', *Journal of Molecular Biology* **157**(1), 105–132.
URL: *https://linkinghub.elsevier.com/retrieve/pii/0022283682905150*

Lambert, I. A. and Kokini, J. L. (2001), 'Effect of ¡scp¿l¡/scp¿ -Cysteine on the Rheological Properties of Wheat Flour', *Cereal Chemistry Journal* **78**(3), 226–230.
URL: *http://doi.wiley.com/10.1094/CCHEM.2001.78.3.226*

Lawton, J. W. (2002), 'Zein: A History of Processing and Use', *Cereal Chemistry Journal* **79**(1), 1–18.
URL: *http://doi.wiley.com/10.1094/CCHEM.2002.79.1.1*

Leavitt, J. M., Wagner, J. M., Tu, C. C., Tong, A., Liu, Y. and Alper, H. S. (2017), 'Biosensor-Enabled Directed Evolution to Improve Muconic Acid Production in Saccharomyces cerevisiae', *Biotechnology Journal* **12**(10), 1600687.
URL: *http://doi.wiley.com/10.1002/biot.201600687*

Lee, C. M.-S. (1988), 'Constrained optimal designs', *Journal of Statistical Planning and Inference* **18**(3), 377–389.
URL: *https://linkinghub.elsevier.com/retrieve/pii/0378375888901140*

Lee, M. E., Aswani, A., Han, A. S., Tomlin, C. J. and Dueber, J. E. (2013), 'Expression-level optimization of a multi-enzyme pathway in the absence of a high-throughput assay', *Nucleic Acids Research* **41**(22), 10668–10678.
URL: *https://academic.oup.com/nar/article-lookup/doi/10.1093/nar/gkt809*

Lee, M. E., DeLoache, W. C., Cervantes, B. and Dueber, J. E. (2015), 'A Highly Characterized Yeast Toolkit for Modular, Multipart Assembly', *ACS Synthetic Biology* **4**(9), 975–986.
URL: *http://pubs.acs.org/doi/10.1021/sb500366v*

Lee, T. A., Jorgensen, P., Bognar, A. L., Peyraud, C., Thomas, D. and Tyers, M. (2010), 'Dissection of Combinatorial Control by the Met4 Transcriptional Complex', *Molecular Biology of the Cell* **21**(3), 456–469.
URL: *https://www.molbiolcell.org/doi/10.1091/mbc.e09-05-0420*

Lee, T. T. T., Wang, M. M. C., HOU, R. C. W., Chen, L.-J., Su, R.-C., Wang, C.-S. and Tzen, J. T. C. (2003), 'Enhanced Methionine and Cysteine Levels in Transgenic Rice Seeds by the Accumulation of Sesame 2S Albumin', *Bioscience,*

Biotechnology, and Biochemistry **67**(8), 1699–1705.
URL: *http://www.tandfonline.com/doi/full/10.1271/bbb.67.1699*

Lewis, J. A., Broman, A. T., Will, J. and Gasch, A. P. (2014), 'Genetic Architecture of Ethanol-Responsive Transcriptome Variation in Saccharomyces cerevisiae Strains', *Genetics* **198**(1), 369–382.
URL: *http://www.genetics.org/lookup/doi/10.1534/genetics.114.167429*

Li, Y., Cong, H., Liu, B., Song, J., Sun, X., Zhang, J. and Yang, Q. (2016), 'Metabolic engineering of Corynebacterium glutamicum for methionine production by removing feedback inhibition and increasing NADPH level', *Antonie van Leeuwenhoek* **109**(9), 1185–1197.
URL: *http://link.springer.com/10.1007/s10482-016-0719-0*

Lian, J., Bao, Z., Hu, S. and Zhao, H. (2018), 'Engineered CRISPR/Cas9 system for multiplex genome engineering of polyploid industrial yeast strains', *Biotechnology and Bioengineering* **115**(6), 1630–1635.
URL: *http://doi.wiley.com/10.1002/bit.26569*

Lian, J., HamediRad, M., Hu, S. and Zhao, H. (2017), 'Combinatorial metabolic engineering using an orthogonal tri-functional CRISPR system', *Nature Communications* **8**(1), 1688.
URL: *http://www.nature.com/articles/s41467-017-01695-x*

Liao, M., Zgoda, V. G., Murray, B. P. and Correia, M. A. (2005), 'Vacuolar Degradation of Rat Liver CYP2B1 in Saccharomyces cerevisiae : Further Validation of the Yeast Model and Structural Implications for the Degradation of Mammalian Endoplasmic Reticulum P450 Proteins', *Molecular Pharmacology* **67**(5), 1460–1469.
URL: *http://molpharm.aspetjournals.org/lookup/doi/10.1124/mol.104.009654*

Lin, J., Fido, R., Shewry, P., Archer, D. B. and Alcocer, M. J. (2004), 'The expression and processing of two recombinant 2S albumins from soybean (Glycine max) in the yeast Pichia pastoris', *Biochimica et Biophysica Acta (BBA) - Proteins and Proteomics* **1698**(2), 203–212.
URL: *https://linkinghub.elsevier.com/retrieve/pii/S1570963903003881*

Linderholm, A. L., Findleton, C. L., Kumar, G., Hong, Y. and Bisson, L. F. (2008), 'Identification of Genes Affecting Hydrogen Sulfide Formation in Saccharomyces cerevisiae', *Applied and Environmental Microbiology* **74**(5), 1418–1427.
URL: *http://aem.asm.org/cgi/doi/10.1128/AEM.01758-07*

Liu, H., Fang, G., Wu, H., Li, Z. and Ye, Q. (2018), 'L-Cysteine Production in Escherichia coli Based on Rational Metabolic Engineering and Modular Strategy', *Biotechnology Journal* **13**(5), 1700695.
URL: *http://doi.wiley.com/10.1002/biot.201700695*

Liu, Q., Liang, Y., Zhang, Y., Shang, X., Liu, S. and Wen, J. (2015), 'YjeH Is a Novel Exporter of L -Methionine and Branched-Chain Amino Acids in Escherichia coli', *Applied and Environmental Microbiology* **81**(22), 7753–7766.

Liu, W., Tang, D., Shi, R., Lian, J., Huang, L., Cai, J. and Xu, Z. (2019), 'Efficient production of SadenosylLmethionine from DLmethionine in metabolic engineered Saccharomyces cerevisiae', *Biotechnology and Bioengineering* **53**(9), bit.27157.
URL: *https://onlinelibrary.wiley.com/doi/abs/10.1002/bit.27157*

Liu, Z., Zhang, Y. and Nielsen, J. (2019), 'Synthetic Biology of Yeast', *Biochemistry* **58**(11), 1511–1520.
URL: *https://pubs.acs.org/doi/10.1021/acs.biochem.8b01236*

Ljungdahl, P. O. (2009), 'Amino-acid-induced signalling via the SPS-sensing pathway in yeast', *Biochemical Society Transactions* **37**(1), 242–247.
URL: *http://www.biochemsoctrans.org/cgi/doi/10.1042/BST0370242*

Ljungdahl, P. O. and Daignan-Fornier, B. (2012), 'Regulation of Amino Acid, Nucleotide, and Phosphate Metabolism in Saccharomyces cerevisiae', *Genetics* **190**(3), 885–929.
URL: *http://www.genetics.org/lookup/doi/10.1534/genetics.111.133306*

Lussling, T., Muller, K.-P., Schreyer, G. and Theissen, F. (1981), 'Process for the recovery of methionine and potassium bicarbonate'.

Ma, Y., Biava, H., Contestabile, R., Budisa, N. and di Salvo, M. (2014), 'Coupling Bioorthogonal Chemistries with Artificial Metabolism: Intracellular Biosynthesis of Azidohomoalanine and Its Incorporation into Recombinant Proteins', *Molecules* **19**(1), 1004–1022.
URL: *http://www.mdpi.com/1420-3049/19/1/1004*

Maier, T. H. P. (2003), 'Semisynthetic production of unnatural L-α-amino acids by metabolic engineering of the cysteine-biosynthetic pathway', *Nature Biotechnology* **21**(4), 422–427.
URL: *http://www.nature.com/articles/nbt807*

Malanovic, N., Streith, I., Wolinski, H., Rechberger, G., Kohlwein, S. D. and Tehlivets, O. (2008), 'S -Adenosyl-L-homocysteine Hydrolase, Key Enzyme of Methylation Metabolism, Regulates Phosphatidylcholine Synthesis and Triacylglycerol Homeostasis in Yeast', *Journal of Biological Chemistry* **283**(35), 23989–23999.
URL: *http://www.jbc.org/lookup/doi/10.1074/jbc.M800830200*

Mandenius, C.-F. and Brundin, A. (2008), 'Bioprocess optimization using design-of-experiments methodology.', *Biotechnology progress* **24**(6), 1191–203.
URL: *http://www.ncbi.nlm.nih.gov/pubmed/19194932*

Mannhaupt, G., Pohlenz, H.-D., Seefluth, A. K., Pilz, U. and Feldmann, H. (1990), 'Yeast homoserine kinase. Characteristics of the corresponding gene, THR1, and the purified enzyme, and evolutionary relationships with other enzymes of threonine metabolism', *European Journal of Biochemistry* **191**(1), 115–122.
URL: *http://doi.wiley.com/10.1111/j.1432-1033.1990.tb19100.x*

Martinez-Force, E. and Benitez, T. (1992), 'Selection of amino-acid overproducer yeast mutants', *Current Genetics* **21**(3), 191–196.
URL: *http://link.springer.com/10.1007/BF00336840*

Martínez-Force, E. and Benítez, T. (1993), 'Regulation of aspartate-derived amino acid biosynthesis in the yeast Saccharomyces cerevisiae', *Current Microbiology* **26**(6), 313–322.
URL: *http://link.springer.com/10.1007/BF01576262*

Masselot, M. and de Robichon-Szulmajster, H. (1975), 'Methionine biosynthesis in Saccharomyces cerevisiae', *Molecular and General Genetics MGG* **139**(2), 121–132.
URL: *http://link.springer.com/10.1007/BF00264692*

Matityahu, I., Godo, I., Hacham, Y. and Amir, R. (2013), 'Tobacco seeds expressing feedback-insensitive cystathionine gamma-synthase exhibit elevated content of methionine and altered primary metabolic profile', *BMC Plant Biology* **13**(1), 206.
URL: *http://bmcplantbiol.biomedcentral.com/articles/10.1186/1471-2229-13-206*

McCarty, N. S., Shaw, W. M., Ellis, T. and Ledesma-Amaro, R. (2019), 'Rapid Assembly of gRNA Arrays via Modular Cloning in Yeast', *ACS Synthetic Biology* **8**(4), 906–910.
URL: *http://pubs.acs.org/doi/10.1021/acssynbio.9b00041*

Menant, A., Barbey, R. and Thomas, D. (2006), 'Substrate-mediated remodeling of methionine transport by multiple ubiquitin-dependent mechanisms in yeast cells', *The EMBO Journal* **25**(19), 4436–4447.
URL: *http://emboj.embopress.org/cgi/doi/10.1038/sj.emboj.7601330*

Meyer, R. K. and Nachtsheim, C. J. (1995), 'The Coordinate-Exchange Algorithm for Constructing Exact Optimal Experimental Designs', *Technometrics* **37**(1), 60–69.
URL: *http://www.tandfonline.com/doi/abs/10.1080/00401706.1995.10485889*

Millea, P. J. (2009), 'N-acetylcysteine: Multiple clinical applications', *American Family Physician* **80**(3), 265–269.

Mitsui, R., Yamada, R. and Ogino, H. (2019), 'CRISPR system in the yeast Saccharomyces cerevisiae and its application in the bioproduction of useful chemicals', *World Journal of Microbiology and Biotechnology* **35**(7), 111.
URL: *http://link.springer.com/10.1007/s11274-019-2688-8*

Mizunuma, M., Miyamura, K., Hirata, D., Yokoyama, H. and Miyakawa, T. (2004), 'Involvement of S-adenosylmethionine in G1 cell-cycle regulation in Saccharomyces cerevisiae', *Proceedings of the National Academy of Sciences* **101**(16), 6086–6091.
URL: *http://www.pnas.org/cgi/doi/10.1073/pnas.0308314101*

Molvig, L., Tabe, L. M., Eggum, B. O., Moore, A. E., Craig, S., Spencer, D. and Higgins, T. J. V. (1997), 'Enhanced methionine levels and increased nutritive value of seeds of transgenic lupins (Lupinus angustifolius L.) expressing a sunflower seed albumin gene', *Proceedings of the National Academy of Sciences* **94**(16), 8393–8398.
URL: *http://www.pnas.org/cgi/doi/10.1073/pnas.94.16.8393*

Momany, F. A., Sessa, D. J., Lawton, J. W., Selling, G. W., Hamaker, S. A. H. and Willett, J. L. (2006), 'Structural Characterization of α-Zein', *Journal of Agricultural and Food Chemistry* **54**(2), 543–547.
URL: *https://pubs.acs.org/doi/10.1021/jf058135h*

Moreno, F. J. and Clemente, A. (2008), '2S Albumin Storage Proteins: What Makes them Food Allergens?', *The Open Biochemistry Journal* **2**, 16–28.
URL: *http://benthamopen.com/ABSTRACT/TOBIOCJ-2-16*

Morse, N. J., Gopal, M. R., Wagner, J. M. and Alper, H. S. (2017), 'Yeast Terminator Function Can Be Modulated and Designed on the Basis of Predictions of Nucleosome Occupancy', *ACS Synthetic Biology* **6**(11), 2086–2095.
URL: *http://pubs.acs.org/doi/10.1021/acssynbio.7b00138*

Mountain, H. A., Bystrom, A. S., Tang Larsen, J. and Korch, C. (1991), 'Four major transcriptional responses in the methionine/threonine biosynthetic pathway of Saccharomyces cerevisiae', *Yeast* **7**(8), 781–803.

Mülleder, M., Calvani, E., Alam, M. T., Wang, R. K., Eckerstorfer, F., Zelezniak, A. and Ralser, M. (2016), 'Functional Metabolomics Describes the Yeast Biosynthetic Regulome', *Cell* **167**(2), 553–565.
URL: *http://linkinghub.elsevier.com/retrieve/pii/S0092867416312375*

Muller, O. (2005), 'Malnutrition and health in developing countries', *Canadian Medical Association Journal* **173**(3), 279–286.
URL: *http://www.cmaj.ca/cgi/doi/10.1503/cmaj.050342*

Nakamori, S., Kobayashi, S., Nishimura, T. and Takagi, H. (1999), 'Mechanism of l -methionine overproduction by Escherichia coli : the replacement of Ser-54 by

Asn in the MetJ protein causes the derepression of l -methionine biosynthetic enzymes', *Applied Microbiology and Biotechnology* **52**(2), 179–185.
URL: *http://link.springer.com/10.1007/s002530051506*

Natarajan, K., Meyer, M. R., Jackson, B. M., Slade, D., Roberts, C., Hinnebusch, A. G. and Marton, M. J. (2001), 'Transcriptional Profiling Shows that Gcn4p Is a Master Regulator of Gene Expression during Amino Acid Starvation in Yeast', *Molecular and Cellular Biology* **21**(13), 4347–4368.
URL: *http://mcb.asm.org/cgi/doi/10.1128/MCB.21.13.4347-4368.2001*

Ni, J., Zhang, G., Qin, L., Li, J. and Li, C. (2019), 'Simultaneously down-regulation of multiplex branch pathways using CRISPRi and fermentation optimization for enhancing β-amyrin production in Saccharomyces cerevisiae', *Synthetic and Systems Biotechnology* **4**(2), 79–85.
URL: *https://linkinghub.elsevier.com/retrieve/pii/S2405805X18301078*

Nielsen, J. and Keasling, J. D. (2016), 'Engineering Cellular Metabolism', *Cell* **164**(6), 1185–1197.
URL: *https://linkinghub.elsevier.com/retrieve/pii/S0092867416300708*

Nilsson, A. and Nielsen, J. (2016), 'Metabolic Trade-offs in Yeast are Caused by F1F0-ATP synthase', *Scientific Reports* **6**(1), 22264.
URL: *http://www.nature.com/articles/srep22264*

Niu, J., Lemme, A., He, J.-Y., Li, H.-Y., Xie, S.-W., Liu, Y.-J., Yang, H.-J., Figueiredo-Silva, C. and Tian, L.-X. (2018), 'Assessing the bioavailability of the Novel Met-Met product (AQUAVI® Met-Met) compared to dl-methionine (dl-Met) in white shrimp (Litopenaeus vannamei)', *Aquaculture* **484**(March 2017), 322–332.
URL: *https://doi.org/10.1016/j.aquaculture.2017.08.021 https://linkinghub.elsevier.com/retrieve/pii/S0044848617305021*

Nojoumi, S., Ma, Y., Schwagerus, S., Hackenberger, C. P. R. and Budisa, N. (2019), 'In-Cell Synthesis of Bioorthogonal Alkene Tag S-Allyl-Homocysteine and Its Coupling with Reprogrammed Translation', *International Journal of Molecular Sciences* **20**(9), 2299.
URL: *https://www.mdpi.com/1422-0067/20/9/2299*

Nunes, P. A., Tenreiro, S. and Sa-Correia, I. (2001), 'Resistance and Adaptation to Quinidine in Saccharomyces cerevisiae: Role of QDR1 (YIL120w), Encoding a Plasma Membrane Transporter of the Major Facilitator Superfamily Required for Multidrug Resistance', *Antimicrobial Agents and Chemotherapy* **45**(5), 1528–1534.
URL: *http://aac.asm.org/cgi/doi/10.1128/AAC.45.5.1528-1534.2001*

Ohtake, Y. and Yabuuchi, S. (1991), 'Molecular cloning of the γ-glutamylcysteine synthetase gene ofSaccharomyces cerevisiae', *Yeast* **7**(9), 953–961.
URL: *http://doi.wiley.com/10.1002/yea.320070907*

Oliva-Teles, A. (2012), 'Nutrition and health of aquaculture fish', *Journal of Fish Diseases* **35**(2), 83–108.
URL: *http://doi.wiley.com/10.1111/j.1365-2761.2011.01333.x*

Omura, H., Ikemoto, M., Kobayashi, M., Shimizu, S., Yoshida, T. and Nagasawa, T. (2003), 'Purification, characterization and gene cloning of thermostable O-acetyl-l-homoserine sulfhydrylase forming γ-cyano-α-aminobutyric acid', *Journal of Bioscience and Bioengineering* **96**(1), 53–58.
URL: *https://linkinghub.elsevier.com/retrieve/pii/S138917230390096X*

Ono, B.-I., Kijima, K., Inoue, T., Miyoshi, S.-I., Matsuda, A. and Shinoda, S. (1994), 'Purification of properties ofSaccharomyces cerevisiae cystathionine β-synthase', *Yeast* **10**(3), 333–339.
URL: *http://doi.wiley.com/10.1002/yea.320100306*

Ono, B., Suruga, T., Yamamoto, M., Yamamoto, S., Murata, K., Kimura, A., Shinoda, S. and Ohmori, S. (1984), 'Cystathionine accumulation in Saccharomyces cerevisiae.', *Journal of bacteriology* **158**(3), 860–5.
URL: *http://www.ncbi.nlm.nih.gov/pubmed/6373742*

Ono, B., Tanaka, K., Naito, K., Heike, C., Shinoda, S., Yamamoto, S., Ohmori, S., Oshima, T. and Toh-e, A. (1992), 'Cloning and characterization of the CYS3 (CYI1) gene of Saccharomyces cerevisiae.', *Journal of Bacteriology* **174**(10), 3339–3347.
URL: *http://jb.asm.org/lookup/doi/10.1128/jb.174.10.3339-3347.1992*

Oomuro, M., Watanabe, D., Sugimoto, Y., Kato, T., Motoyama, Y., Watanabe, T. and Takagi, H. (2018), 'Accumulation of intracellular S-adenosylmethionine increases the fermentation rate of bottom-fermenting brewer's yeast during high-gravity brewing', *Journal of Bioscience and Bioengineering* **xx**(xx), 1–6.
URL: *https://doi.org/10.1016/j.jbiosc.2018.05.027*

Österlund, T., Bordel, S. and Nielsen, J. (2015), 'Controllability analysis of transcriptional regulatory networks reveals circular control patterns among transcription factors', *Integrative Biology* **7**(5), 560–568.
URL: *https://academic.oup.com/ib/article/7/5/560-568/5193016*

Ouni, I., Flick, K. and Kaiser, P. (2010), 'A Transcriptional Activator Is Part of an SCF Ubiquitin Ligase to Control Degradation of Its Cofactors', *Molecular Cell* **40**(6), 954–964.
URL: *https://linkinghub.elsevier.com/retrieve/pii/S109727651000883X*

Ouni, I., Flick, K. and Kaiser, P. (2011), 'Ubiquitin and transcription', *Transcription* **2**(3), 135–139.
URL: *http://www.tandfonline.com/doi/abs/10.4161/trns.2.3.15903*

Oz, H. S., Chen, T. S. and Neuman, M. (2008), 'Methionine Deficiency and Hepatic Injury in a Dietary Steatohepatitis Model', *Digestive Diseases and Sciences* **53**(3), 767–776.
URL: *http://link.springer.com/10.1007/s10620-007-9900-7*

OBrien, E. J., Monk, J. M. and Palsson, B. O. (2015), 'Using Genome-scale Models to Predict Biological Capabilities', *Cell* **161**(5), 971–987.
URL: *https://linkinghub.elsevier.com/retrieve/pii/S0092867415005681*

Pantoja-Uceda, D., Shewry, P. R., Bruix, M., Tatham, A. S., Santoro, J. and Rico, M. (2004), 'Solution Structure of a Methionine-Rich 2S Albumin from Sunflower Seeds: Relationship to Its Allergenic and Emulsifying Properties , ', *Biochemistry* **43**(22), 6976–6986.
URL: *http://pubs.acs.org/doi/abs/10.1021/bi0496900*

Park, S.-D., Lee, J.-Y., Sim, S.-Y., Kim, Y. and Lee, H.-S. (2007), 'Characteristics of methionine production by an engineered Corynebacterium glutamicum strain', *Metabolic Engineering* **9**(4), 327–336.
URL: *https://linkinghub.elsevier.com/retrieve/pii/S1096717607000286*

Pastorello, E. A., Farioli, L., Pravettoni, V., Ispano, M., Scibola, E., Trambaioli, C., Giuffrida, M. G., Ansaloni, R., Godovac-Zimmermann, J., Conti, A., Fortunato, D. and Ortolani, C. (2000), 'The maize major allergen, which is responsible for food-induced allergic reactions, is a lipid transfer protein', *Journal of Allergy and Clinical Immunology* **106**(4), 744–751.
URL: *https://linkinghub.elsevier.com/retrieve/pii/S0091674900867391*

Pastorello, E. A., Farioli, L., Pravettoni, V., Scibilia, J., Conti, A., Fortunato, D., Borgonovo, L., Bonomi, S., Primavesi, L. and Ballmer-Weber, B. (2009), 'Maize food allergy: lipid-transfer proteins, endochitinases, and alpha-zein precursor are relevant maize allergens in double-blind placebo-controlled maize-challenge-positive patients', *Analytical and Bioanalytical Chemistry* **395**(1), 93–102.
URL: *http://link.springer.com/10.1007/s00216-009-2945-z*

Patton, E., Peyraud, C., Rouillon, A., Surdin-Kerjan, Y., Tyers, M. and Thomas, D. (2000), 'SCFMet30-mediated control of the transcriptional activator Met4 is required for the G1-S transition', *The EMBO Journal* **19**(7), 1613–1624.
URL: *http://emboj.embopress.org/cgi/doi/10.1093/emboj/19.7.1613*

Penninckx, M. J. (2002), 'An overview on glutathione in Saccharomyces versus non-conventional yeasts', *FEMS Yeast Research* **2**(3), 295–305.

Perła-Kaján, J., Twardowski, T. and Jakubowski, H. (2007), 'Mechanisms of homocysteine toxicity in humans', *Amino Acids* **32**(4), 561–572.
URL: *http://link.springer.com/10.1007/s00726-006-0432-9*

Pickar-Oliver, A. and Gersbach, C. A. (2019), 'The next generation of CRISPRCas technologies and applications', *Nature Reviews Molecular Cell Biology* **20**(8), 490–507.
URL: *http://www.nature.com/articles/s41580-019-0131-5*

Plackett, R. L. and Burman, J. P. (1946), 'The Design of Optimum Multifactorial Experiments', *Biometrika* **33**(4), 305–325.
URL: *https://academic.oup.com/biomet/article-lookup/doi/10.1093/biomet/33.4.305*

Presnell, K. V. and Alper, H. S. (2019), 'Systems Metabolic Engineering Meets Machine Learning: A New Era for DataDriven Metabolic Engineering', *Biotechnology Journal* **14**(9), 1800416.
URL: *https://onlinelibrary.wiley.com/doi/abs/10.1002/biot.201800416*

Qin, T., Hu, X., Hu, J. and Wang, X. (2015), 'Metabolic engineering of Corynebacterium glutamicum strain ATCC13032 to produce l -methionine', *Biotechnology and Applied Biochemistry* **62**(4), 563–573.
URL: *http://doi.wiley.com/10.1002/bab.1290*

Rabeh, W. M. and Cook, P. F. (2004), 'Structure and Mechanism of O -Acetylserine Sulfhydrylase', *Journal of Biological Chemistry* **279**(26), 26803–26806.
URL: *http://www.jbc.org/lookup/doi/10.1074/jbc.R400001200*

Rafalski, J. A. and Falco, S. C. (1988), 'Structure of the yeast HOM3 gene which encodes aspartokinase.', *The Journal of biological chemistry* **263**(5), 2146–51.
URL: *http://www.ncbi.nlm.nih.gov/pubmed/2892836*

Rajakumar, P. D., Gowers, G.-O. F., Suckling, L., Foster, A., Ellis, T., Kitney, R. I., McClymont, D. W. and Freemont, P. S. (2018), 'Rapid Prototyping Platform for Saccharomyces cerevisiae Using Computer-Aided Genetic Design Enabled by Parallel Software and Workcell Platform Development', *SLAS TECHNOLOGY: Translating Life Sciences Innovation* p. 247263031879830.
URL: *http://journals.sagepub.com/doi/10.1177/2472630318798304*

Ramos, C., Delgado, M. A. and Calderon, I. L. (1991), 'Inhibition by different amino acids of the aspartate kinase and the homoserine kinase of the yeast Saccharomyces cerevisiae', *FEBS Letters* **278**(1), 123–126.
URL: *https://doi.org/10.1016/0014-5793(91)80098-N*

Raymond, R. K., Kastanos, E. K. and Appling, D. R. (1999), 'Saccharomyces cerevisiae Expresses Two Genes Encoding Isozymes of Methylenetetrahydrofolate Reductase', *Archives of Biochemistry and Biophysics* **372**(2), 300–308.
URL: *https://linkinghub.elsevier.com/retrieve/pii/S0003986199914984*

Redden, H., Morse, N. and Alper, H. S. (2014), 'The synthetic biology toolbox for tuning gene expression in yeast', *FEMS Yeast Research* **15**(1), n/a–n/a.
URL: *https://academic.oup.com/femsyr/article-lookup/doi/10.1111/1567-1364.12188*

Redding-Johanson, A. M., Batth, T. S., Chan, R., Krupa, R., Szmidt, H. L., Adams, P. D., Keasling, J. D., Soon Lee, T., Mukhopadhyay, A. and Petzold, C. J. (2011), 'Targeted proteomics for metabolic pathway optimization: Application to terpene production', *Metabolic Engineering* **13**(2), 194–203.
URL: *https://linkinghub.elsevier.com/retrieve/pii/S1096717610001254*

Regenberg, B., Düring-Olsen, L., Kielland-Brandt, M. C. and Holmberg, S. (1999), 'Substrate specificity and gene expression of the amino-acid permeases in Saccharomyces cerevisiae', *Current Genetics* **36**(6), 317–328.
URL: *http://link.springer.com/10.1007/s002940050506*

Regenberg, B., Grotkjær, T., Winther, O., Fausbøll, A., Åkesson, M., Bro, C., Hansen, L. K., Brunak, S. and Nielsen, J. (2006), 'Growth-rate regulated genes have profound impact on interpretation of transcriptome profiling in Saccharomyces cerevisiae', *Genome Biology* **7**(11).
URL: *https://genomebiology.biomedcentral.com/articles/10.1186/gb-2006-7-11-r107*

Reider Apel, A., D'Espaux, L., Wehrs, M., Sachs, D., Li, R. A., Tong, G. J., Garber, M., Nnadi, O., Zhuang, W., Hillson, N. J., Keasling, J. D. and Mukhopadhyay, A. (2017), 'A Cas9-based toolkit to program gene expression in Saccharomyces cerevisiae', *Nucleic Acids Research* **45**(1), 496–508.
URL: *https://academic.oup.com/nar/article-lookup/doi/10.1093/nar/gkw1023*

Renata, H., Wang, Z. J. and Arnold, F. H. (2015), 'Expanding the Enzyme Universe: Accessing Non-Natural Reactions by Mechanism-Guided Directed Evolution', *Angewandte Chemie International Edition* **54**(11), 3351–3367.
URL: *http://doi.wiley.com/10.1002/anie.201409470*

Rico, M., Bruix, M., González, C., Monsalve, R. I. and Rodríguez, R. (1996), '1 H NMR Assignment and Global Fold of Napin BnIb, a Representative 2S Albumin Seed Protein ', *Biochemistry* **35**(49), 15672–15682.
URL: *https://pubs.acs.org/doi/10.1021/bi961748q*

Rothe, S., Prakash, A. and Tyedmers, J. (2018), 'The Insoluble Protein Deposit (IPOD) in Yeast', *Frontiers in Molecular Neuroscience* **11**(July), 1–9.
URL: *https://www.frontiersin.org/article/10.3389/fnmol.2018.00237/full*

Rouillon, A., Barbey, R., Patton, E., Tyers, M. and Thomas, D. (2000), 'Feedback-regulated degradation of the transcriptional activator Met4 is triggered by the SCFMet30 complex', *The EMBO Journal* **19**(2), 282–294.
URL: *http://emboj.embopress.org/cgi/doi/10.1093/emboj/19.2.282*

Rouillon, A., Surdin-Kerjan, Y. and Thomas, D. (1999), 'Transport of Sulfonium Compounds', *Journal of Biological Chemistry* **274**(40), 28096–28105.
URL: *http://www.jbc.org/lookup/doi/10.1074/jbc.274.40.28096*

Rundqvist, L., Tengel, T., Zdunek, J., Björn, E., Schleucher, J., Alcocer, M. J. C. and Larsson, G. (2012), 'Solution Structure, Copper Binding and Backbone Dynamics of Recombinant Ber e 1The Major Allergen from Brazil Nut', *PLoS ONE* **7**(10), e46435.
URL: *http://dx.plos.org/10.1371/journal.pone.0046435*

Ryan, O. W., Skerker, J. M., Maurer, M. J., Li, X., Tsai, J. C., Poddar, S., Lee, M. E., DeLoache, W., Dueber, J. E., Arkin, A. P. and Cate, J. H. D. (2014), 'Selection of chromosomal DNA libraries using a multiplex CRISPR system.', *eLife* p. e03703.
URL: *http://www.ncbi.nlm.nih.gov/pubmed/25139909*

Ryu, O. H., Jae Yeong Ju and Shin, C. S. (1997), 'Continuous l-cysteine production using immobilized cell reactors and product extractors', *Process Biochemistry* **32**(3), 201–209.
URL: *https://linkinghub.elsevier.com/retrieve/pii/S0032959296000611*

Saalbach, I., Waddell, D., Pickardt, T., Schieder, O. and Müntz, K. (1995), 'Stable Expression of the Sulphur-rich 2S Albumin Gene in Transgenic Vicia narbonensis Increases the Methionine Content of Seeds', *Journal of Plant Physiology* **145**(5-6), 674–681.
URL: *https://linkinghub.elsevier.com/retrieve/pii/S0176161711812800*

Saint-Marc, C., Hürlimann, H. C., Daignan-Fornier, B. and Pinson, B. (2015), 'Serine hydroxymethyltransferase: a key player connecting purine, folate and methionine metabolism in Saccharomyces cerevisiae', *Current Genetics* **61**(4), 633–640.
URL: *http://link.springer.com/10.1007/s00294-015-0489-7*

Salvo, M. L., Budisa, N. and Contestabile, R. (2012), 'PLP-dependent Enzymes : a Powerful Tool for Metabolic Synthesis of Non-Canonical Amino Acids', *Beilstein Bozen Symposium on Molecular Engineering and Control* pp. 27–66.
URL: *https://pdfs.semanticscholar.org/e215/d42f14b4987d0fdf2918bab393cfaf172dbb.pdf*

Sánchez, B. J., Zhang, C., Nilsson, A., Lahtvee, P., Kerkhoven, E. J. and Nielsen, J. (2017), 'Improving the phenotype predictions of a yeast genomescale metabolic model by incorporating enzymatic constraints', *Molecular Systems*

Biology **13**(8), 935.
URL: *https://onlinelibrary.wiley.com/doi/abs/10.15252/msb.20167411*

Sano, K. and Mitsugi, K. (1978), 'Enzymatic production of L-cysteine from DL-2-amino-.DELTA.2-thiazoline-4-carboxylic acid by Pseudomonas thiazolinophilum: Optimal conditions for the enzyme formation and enzymatic reaction.', *Agricultural and Biological Chemistry* **42**(12), 2315–2321.
URL: *http://joi.jlc.jst.go.jp/JST.Journalarchive/bbb1961/42.2315?from=CrossRef*

Schäfer, H., Nau, K., Sickmann, A., Erdmann, R. and Meyer, H. E. (2001), 'Identification of peroxisomal membrane proteins of Saccharomyces cerevisiae by mass spectrometry', *ELECTROPHORESIS* **22**(14), 2955–2968.
URL: *https://www.ncbi.nlm.nih.gov/pubmed/11565790*

Scheller, L. and Fussenegger, M. (2019), 'From synthetic biology to human therapy: engineered mammalian cells', *Current Opinion in Biotechnology* **58**, 108–116.
URL: *https://linkinghub.elsevier.com/retrieve/pii/S0958166918302167*

Schwenn, J. D., Krone, F. A. and Husmann, K. (1988), 'Yeast PAPS reductase: properties and requirements of the purified enzyme.', *Archives of microbiology* **150**(4), 313–9.
URL: *http://www.ncbi.nlm.nih.gov/pubmed/3060034*

Serrano, L. (2007), 'Synthetic biology: promises and challenges', *Molecular Systems Biology* **3**(1), 158.
URL: *https://onlinelibrary.wiley.com/doi/abs/10.1038/msb4100202*

Shaw, W. M. (2016), 'Quick and easy CRISPR engineering in Saccharomyces cerevisiae'.
URL: *https://benchling.com/pub/ellis-crispr-tools*

Shewry, P. R. and Pandya, M. J. (1999), The 2S Albumin Storage Proteins, *in* 'Seed Proteins', Springer Netherlands, Dordrecht, pp. 563–586.

Shi, S., Liang, Y., Zhang, M. M., Ang, E. L. and Zhao, H. (2016), 'A highly efficient single-step, markerless strategy for multi-copy chromosomal integration of large biochemical pathways in Saccharomyces cerevisiae', *Metabolic Engineering* **33**, 19–27.
URL: *https://linkinghub.elsevier.com/retrieve/pii/S1096717615001391*

Shiomi, N. and Fukuda, H. (1990), 'Production of S-Adenosyl-Methionine by Saccharomyces cerevisiae Cells Carrying a Gene for Ethionine Resistance', *Biotechnology and Bioengineering* **35**, 1120–1124.

Shiomi, N., Fukuda, H., Fukuda, Y. and Murata, K. (1991), 'Nucleotide sequence and characterization of a gene conferring resistance to ethionine in yeast

Saccharomyces cerevisiae', *Journal of fermentation* **71**(4), 211–215.
URL: *http://www.sciencedirect.com/science/article/pii/0922338X9190269M*

Shiomi, N., Fukuda, H., Murata, K. and Kimura, A. (1995), 'Improvement of S-adenosylmethionine production by integration of the ethionine-resistance gene into chromosomes of the yeast Saccharomyces cerevisiae', *Applied Microbiology and Biotechnology* **42**(5), 730–733.

Si, T., Chao, R., Min, Y., Wu, Y., Ren, W. and Zhao, H. (2017), 'Automated multiplex genome-scale engineering in yeast', *Nature Communications* **8**(1), 15187.
URL: *http://www.nature.com/articles/ncomms15187*

Storici, F., Durham, C. L., Gordenin, D. A. and Resnick, M. A. (2003), 'Chromosomal site-specific double-strand breaks are efficiently targeted for repair by oligonucleotides in yeast', *Proceedings of the National Academy of Sciences* **100**(25), 14994–14999.
URL: *http://www.pnas.org/cgi/doi/10.1073/pnas.2036296100*

Su, N. Y., Flick, K. and Kaiser, P. (2005), 'The F-Box Protein Met30 Is Required for Multiple Steps in the Budding Yeast Cell Cycle', *Molecular and Cellular Biology* **25**(10), 3875–3885.
URL: *http://mcb.asm.org/cgi/doi/10.1128/MCB.25.10.3875-3885.2005*

Su, N.-Y., Ouni, I., Papagiannis, C. V. and Kaiser, P. (2008), 'A Dominant Suppressor Mutation of the met30 Cell Cycle Defect Suggests Regulation of the Saccharomyces cerevisiae Met4-Cbf1 Transcription Complex by Met32', *Journal of Biological Chemistry* **283**(17), 11615–11624.
URL: *http://www.jbc.org/lookup/doi/10.1074/jbc.M708230200*

Suliman, H. S., Sawyer, G. M., Appling, D. R. and Robertus, J. D. (2005), 'Purification and properties of cobalamin-independent methionine synthase from Candida albicans and Saccharomyces cerevisiae', *Archives of Biochemistry and Biophysics* **441**(1), 56–63.
URL: *https://linkinghub.elsevier.com/retrieve/pii/S0003986105002651*

Surdin, Y. (1967), 'La semi-aldehyde aspartique deshydrogenase chez Saccharomyces cerevisiae: proprietes et regulation', *European Journal of Biochemistry* **2**(3), 341–348.
URL: *http://doi.wiley.com/10.1111/j.1432-1033.1967.tb00144.x*

Sveier, H., Nordås, H., Berge, G. E. and Lied, E. (2001), 'Dietary inclusion of crystalline D- and L-methionine: Effects on growth, feed and protein utilization, and digestibility in small and large Atlantic salmon (Salmon salar L.)', *Aquaculture Nutrition* **7**(3), 169–181.

Tabe, L. M. and Droux, M. (2002), 'Limits to Sulfur Accumulation in Transgenic Lupin Seeds Expressing a Foreign Sulfur-Rich Protein', *Plant Physiology*

128(3), 1137–1148.
URL: *http://www.plantphysiol.org/lookup/doi/10.1104/pp.010935*

Tabor, C. W. and Tabor, H. (1984), 'Methionine adenosyltransferase (S-adenosylmethionine synthetase) and S-adenosylmethionine decarboxylase.', *Advances in enzymology and related areas of molecular biology* **56**, 251–82.
URL: *http://www.ncbi.nlm.nih.gov/pubmed/6364703*

Takagi, H. and Ohtsu, I. (2016), L-Cysteine metabolism and fermentation in microorganisms, *in* 'Amino Acid Fermentation', Springer, pp. 129–151.

Takagi, H., Yoshioka, K., Awano, N., Nakamori, S. and Ono, B.-i. (2003), 'Role of Saccharomyces cerevisiae serine O -acetyltransferase in cysteine biosynthesis', *FEMS Microbiology Letters* **218**(2), 291–297.
URL: *https://academic.oup.com/femsle/article-lookup/doi/10.1111/j.1574-6968.2003.tb11531.x*

Takumi, K., Ziyatdinov, M. K., Samsonov, V. and Nonaka, G. (2017), 'Fermentative Production of Cysteine by Pantoea ananatis', *Applied and Environmental Microbiology* **83**(5), 1–14.
URL: *http://aem.asm.org/lookup/doi/10.1128/AEM.02502-16*

Tan, Q., Liu, Q., Chen, X., Wang, M. and Wu, Z. (2013), 'Growth performance, biochemical indices and hepatopancreatic function of grass carp, Ctenopharyngodon idellus, would be impaired by dietary rapeseed meal', *Aquaculture* **414-415**, 119–126.
URL: *https://linkinghub.elsevier.com/retrieve/pii/S0044848613003748*

Tan, Q., Song, D., Chen, X., Xie, S. and Shu, X. (2018), 'Replacing fish meal with vegetable protein sources in feed for juvenile red swamp crayfish, Procambarus clarkii: Effects of amino acids supplementation on growth and feed utilization', *Aquaculture Nutrition* **24**(2), 858–864.

Tehlivets, O., Hasslacher, M. and Kohlwein, S. D. (2004), 'S -Adenosyl- l -homocysteine hydrolase in yeast: key enzyme of methylation metabolism and coordinated regulation with phospholipid synthesis', *FEBS Letters* **577**(3), 501–506.
URL: *http://doi.wiley.com/10.1016/j.febslet.2004.10.057*

Tenreiro, S., Nunes, P. A., Viegas, C. A., Neves, M. S., Teixeira, M. C., Cabral, M. and Sá-Correia, I. (2002), 'AQR1 Gene (ORF YNL065w) Encodes a Plasma Membrane Transporter of the Major Facilitator Superfamily That Confers Resistance to Short-Chain Monocarboxylic Acids and Quinidine in Saccharomyces cerevisiae', *Biochemical and Biophysical Research Communications* **292**(3), 741–748.
URL: *https://linkinghub.elsevier.com/retrieve/pii/S0006291X02967033*

Thomas, D., Barbey, R. and Surdin-Kerjan, Y. (1990), 'Gene-enzyme relationship in the sulfate assimilation pathway of Saccharomyces cerevisiae. Study of the 3'-phosphoadenylylsulfate reductase structural gene.', *The Journal of biological chemistry* **265**(26), 15518–24.
URL: *http://www.ncbi.nlm.nih.gov/pubmed/2203779*

Thomas, D. and Surdin-Kerjan, Y. (1989), 'Structure of the HOM2 gene of Saccharomyces cerevisiae and regulation of its expression', *MGG Molecular & General Genetics* **217**(1), 149–154.
URL: *http://link.springer.com/10.1007/BF00330954*

Thomas, D. and Surdin-Kerjan, Y. (1991), 'The synthesis of the two S-adenosylmethionine synthetases is differently regulated in Saccharomyces cerevisiae', *MGG Molecular & General Genetics* **226-226**(1-2), 224–232.
URL: *http://link.springer.com/10.1007/BF00273607*

Thomas, D. and Surdin-Kerjan, Y. (1997), 'Metabolism of sulfur amino acids in Saccharomyces cerevisiae.', *Microbiology and molecular biology reviews : MMBR* **61**(4), 503–32.
URL: *http://www.pubmedcentral.nih.gov/articlerender.fcgi?artid=PMC232622*

Tkach, J. M., Yimit, A., Lee, A. Y., Riffle, M., Costanzo, M., Jaschob, D., Hendry, J. A., Ou, J., Moffat, J., Boone, C., Davis, T. N., Nislow, C. and Brown, G. W. (2012), 'Dissecting DNA damage response pathways by analysing protein localization and abundance changes during DNA replication stress', *Nature Cell Biology* **14**(9), 966–976.
URL: *http://www.nature.com/articles/ncb2549*

Trotschel, C., Deutenberg, D., Bathe, B., Burkovski, A. and Kramer, R. (2005), 'Characterization of Methionine Export in Corynebacterium glutamicum', *Journal of Bacteriology* **187**(11), 3786–3794.
URL: *http://jb.asm.org/cgi/doi/10.1128/JB.187.11.3786-3794.2005*

Ullrich, T. C., Blaesse, M. and Huber, R. (2001), 'Crystal structure of ATP sulfurylase from Saccharomyces cerevisiae, a key enzyme in sulfate activation', *The EMBO Journal* **20**(3), 316–329.
URL: *http://emboj.embopress.org/cgi/doi/10.1093/emboj/20.3.316*

Velasco, I., Arévalo-Rodríguez, M., Marina, P. and Calderón, I. L. (2005), 'A new mutation in the yeast aspartate kinase induces threonine accumulation in a temperature-regulated way', *Yeast* **22**(2), 99–110.

Velasco, I., Tenreiro, S., Calderon, I. L. and André, B. (2004), 'Saccharomyces cerevisiae Aqr1 Is an Internal-Membrane Transporter Involved in Excretion of Amino Acids', *Eukaryotic Cell* **3**(6), 1492–1503.
URL: *http://ec.asm.org/lookup/doi/10.1128/EC.3.6.1492-1503.2004*

Verwaal, R., Buiting-Wiessenhaan, N., Dalhuijsen, S. and Roubos, J. A. (2018), 'CRISPR/Cpf1 enables fast and simple genome editing of Saccharomyces cerevisiae', *Yeast* **35**(2), 201–211.
URL: *http://doi.wiley.com/10.1002/yea.3278*

Wada, M. and Takagi, H. (2006), 'Metabolic pathways and biotechnological production of l-cysteine', *Applied Microbiology and Biotechnology* **73**(1), 48–54.
URL: *http://link.springer.com/10.1007/s00253-006-0587-z*

Wang, G., Xu, M., Wang, W. and Galili, G. (2017), 'Fortifying Horticultural Crops with Essential Amino Acids: A Review', *International Journal of Molecular Sciences* **18**(6), 1306.
URL: *http://www.mdpi.com/1422-0067/18/6/1306*

Wei, L., Wang, H., Xu, N., Zhou, W., Ju, J., Liu, J. and Ma, Y. (2019), 'Metabolic engineering of Corynebacterium glutamicum for l-cysteine production', *Applied Microbiology and Biotechnology* **103**(3), 1325–1338.
URL: *http://link.springer.com/10.1007/s00253-018-9547-7*

Wei, L., Wang, Q., Xu, N., Cheng, J., Zhou, W., Han, G., Jiang, H., Liu, J. and Ma, Y. (2019), 'Combining Protein and Metabolic Engineering Strategies for High-Level Production of O -Acetylhomoserine in Escherichia coli', *ACS Synthetic Biology* **8**(5), 1153–1167.
URL: *http://pubs.acs.org/doi/10.1021/acssynbio.9b00042*

Wendisch, V. F. (2019), 'Metabolic engineering advances and prospects for amino acid production', *Metabolic Engineering* (March), 0–1.
URL: *https://linkinghub.elsevier.com/retrieve/pii/S1096717619301004*

Williams, A.-l., Girard, C., Jui, D., Sabina, A. and Katz, D. L. (2005), 'S-adenosylmethionine (SAMe) as treatment for depression: a systematic review.', *Clinical and investigative medicine. Medecine clinique et experimentale* **28**(3), 132–9.
URL: *http://www.ncbi.nlm.nih.gov/pubmed/16021987*

Willke, T. (2014), 'Methionine production - a critical review', *Applied Microbiology and Biotechnology* **98**(24), 9893–9914.

Wöltinger, J., Karau, A., Leuchtenberger, W. and Drauz, K. (2005), Membrane Reactors at Degussa, *in* 'Advances in Biochemical Engineering/Biotechnology', Vol. 92, pp. 289–316.
URL: *http://link.springer.com/10.1007/b98909*

Wu, W., Yang, Y. and Lei, H. (2019), 'Progress in the application of CRISPR: From gene to base editing', *Medicinal Research Reviews* **39**(2), 665–683.
URL: *https://onlinelibrary.wiley.com/doi/abs/10.1002/med.21537*

Wu, Y., Goettel, W. and Messing, J. (2009), 'Non-Mendelian regulation and allelic variation of methionine-rich delta-zein genes in maize', *Theoretical and Applied Genetics* **119**(4), 721–731.
URL: *http://link.springer.com/10.1007/s00122-009-1083-5*

Xu, P., Rizzoni, E. A., Sul, S.-Y. and Stephanopoulos, G. (2017), 'Improving Metabolic Pathway Efficiency by Statistical Model-Based Multivariate Regulatory Metabolic Engineering', *ACS Synthetic Biology* **6**(1), 148–158.
URL: *http://pubs.acs.org/doi/10.1021/acssynbio.6b00187*

Yamagata, S. (1971), 'Homocysteine synthesis in yeast. Partial purification and properties of O-acetylhomoserine sulfhydrylase.', *Journal of biochemistry* **70**(6), 1035–45.
URL: *http://www.ncbi.nlm.nih.gov/pubmed/4947307*

Yamagata, S. (1981), 'Low-molecular-weight O-acetylserine sulfhydrylase and serine sulfhydrylase of Saccharomyces cerevisiae are the same protein.', *Journal of bacteriology* **147**(2), 688–90.
URL: *http://www.ncbi.nlm.nih.gov/pubmed/7021536*

Yamagata, S. (1987), 'Partial purification and some properties of homoserine O-acetyltransferase of a methionine auxotroph of Saccharomyces cerevisiae.', *Journal of Bacteriology* **169**(8), 3458–3463.
URL: *http://jb.asm.org/lookup/doi/10.1128/jb.169.8.3458-3463.1987*

Yamagata, S. (1989), 'Roles of O-acetyl-l-homoserine sulfhydrylases in microorganisms', *Biochimie* **71**(11-12), 1125–1143.
URL: *https://linkinghub.elsevier.com/retrieve/pii/0300908489900163*

Yamagata, S., Isaji, M., Nakamura, K., Fujisaki, S., Doi, K., Bawden, S. and D'Andrea, R. (1994), 'Overexpression of the Saccharomyces cerevisiae MET17/MET25 gene in Escherichia coli and comparative characterization of the product with O-acetylserine · O-acetylhomoserine sulfhydrylase of the yeast', *Applied Microbiology and Biotechnology* **42**(1), 92–99.
URL: *http://link.springer.com/10.1007/BF00170230*

Yang, J. and Zhang, Y. (2015), 'I-TASSER server: new development for protein structure and function predictions', *Nucleic Acids Research* **43**(W1), W174–W181.
URL: *https://academic.oup.com/nar/article-lookup/doi/10.1093/nar/gkv342*

Yoshida, S., Imoto, J., Minato, T., Oouchi, R., Kamada, Y., Tomita, M., Soga, T. and Yoshimoto, H. (2011), 'A novel mechanism regulates H2S and SO2 production in Saccharomyces cerevisiae', *Yeast* **28**(2), 109–121.
URL: *http://doi.wiley.com/10.1002/yea.1823*

Youle, R. J. and Huang, A. H. C. (1981), 'Occurrence of Low Molecular Weight and High Cysteine Containing Albumin Storage Proteins in Oilseeds of Diverse Species', *American Journal of Botany* **68**(1), 44.
URL: *http://doi.wiley.com/10.1002/j.1537-2197.1981.tb06354.x*

Young, E. M., Zhao, Z., Gielesen, B. E., Wu, L., Benjamin Gordon, D., Roubos, J. A. and Voigt, C. A. (2018), 'Iterative algorithm-guided design of massive strain libraries, applied to itaconic acid production in yeast', *Metabolic Engineering* **48**(May), 33–43.
URL: *https://linkinghub.elsevier.com/retrieve/pii/S1096717618301186*

Yu, T., Dabirian, Y., Liu, Q., Siewers, V. and Nielsen, J. (2019), 'Strategies and challenges for metabolic rewiring', *Current Opinion in Systems Biology* **15**, 30–38.
URL: *https://linkinghub.elsevier.com/retrieve/pii/S2452310019300010*

Yu, T., Zhou, Y. J., Huang, M., Liu, Q., Pereira, R., David, F. and Nielsen, J. (2018), 'Reprogramming Yeast Metabolism from Alcoholic Fermentation to Lipogenesis', *Cell* **174**(6), 1549–1558.
URL: *https://linkinghub.elsevier.com/retrieve/pii/S0092867418309073*

Yumoto, N., Kawata, Y., Noda, S. and Tokushige, M. (1991), 'Rapid purification and characterization of homoserine dehydrogenase from Saccharomyces cerevisiae', *Archives of Biochemistry and Biophysics* **285**(2), 270–275.
URL: *https://linkinghub.elsevier.com/retrieve/pii/000398619190359Q*

Zalatan, J. G., Lee, M. E., Almeida, R., Gilbert, L. A., Whitehead, E. H., La Russa, M., Tsai, J. C., Weissman, J. S., Dueber, J. E., Qi, L. S. and Lim, W. A. (2015), 'Engineering Complex Synthetic Transcriptional Programs with CRISPR RNA Scaffolds', *Cell* **160**(1-2), 339–350.
URL: *https://linkinghub.elsevier.com/retrieve/pii/S0092867414015700*

Zeh, M., Casazza, A. P., Kreft, O., Roessner, U., Bieberich, K., Willmitzer, L., Hoefgen, R. and Hesse, H. (2001), 'Antisense Inhibition of Threonine Synthase Leads to High Methionine Content in Transgenic Potato Plants', *Plant Physiology* **127**(3), 792–802.
URL: *http://www.plantphysiol.org/lookup/doi/10.1104/pp.010438*

Zetsche, B., Gootenberg, J. S., Abudayyeh, O. O., Slaymaker, I. M., Makarova, K. S., Essletzbichler, P., Volz, S. E., Joung, J., van der Oost, J., Regev, A., Koonin, E. V. and Zhang, F. (2015), 'Cpf1 Is a Single RNA-Guided Endonuclease of a Class 2 CRISPR-Cas System', *Cell* **163**(3), 759–771.
URL: *https://linkinghub.elsevier.com/retrieve/pii/S0092867415012003*

Zhang, J., Sonnenschein, N., Pihl, T. P. B., Pedersen, K. R., Jensen, M. K. and Keasling, J. D. (2016), 'Engineering an NADPH/NADP+ redox biosensor in

yeast', *ACS Synthetic Biology* p. acssynbio.6b00135.
URL: *http://pubs.acs.org/doi/abs/10.1021/acssynbio.6b00135*

Zhang, J., Wen, C., Zhang, H., Zandile, M., Luo, X., Duan, Y. and Ma, H. (2018), 'Structure of the zein protein as treated with subcritical water', *International Journal of Food Properties* **21**(1), 128–138.
URL: *https://doi.org/10.1080/10942912.2017.1414839*

Zhou, H., Vonk, B., Roubos, J. A., Bovenberg, R. A. and Voigt, C. A. (2015), 'Algorithmic co-optimization of genetic constructs and growth conditions: application to 6-ACA, a potential nylon-6 precursor', *Nucleic Acids Research* **43**(21), gkv1071.
URL: *https://academic.oup.com/nar/article-lookup/doi/10.1093/nar/gkv1071*

Zhou, Y., Li, G., Dong, J., Xing, X.-h., Dai, J. and Zhang, C. (2018), 'MiYA, an efficient machine-learning workflow in conjunction with the YeastFab assembly strategy for combinatorial optimization of heterologous metabolic pathways in Saccharomyces cerevisiae', *Metabolic Engineering* **47**(January), 294–302.
URL: *https://linkinghub.elsevier.com/retrieve/pii/S1096717618300144*

Zou, K., Ouyang, Q., Li, H. and Zheng, J. (2017), 'A global characterization of the translational and transcriptional programs induced by methionine restriction through ribosome profiling and RNA-seq', *BMC Genomics* **18**(1), 189.
URL: *http://bmcgenomics.biomedcentral.com/articles/10.1186/s12864-017-3483-2*

Zsebo, K. M., Lu, H. S., Fieschko, J. C., Goldstein, L., Davis, J., Duker, K., Suggs, S. V., Lai, P. H. and Bitter, G. A. (1986), 'Protein secretion from Saccharomyces cerevisiae directed by the prepro-alpha-factor leader region.', *The Journal of biological chemistry* **261**(13), 5858–65.
URL: *http://www.ncbi.nlm.nih.gov/pubmed/3009432*

Appendix

sgRNA sequences

The target genes, sgRNA plasmid name and the guide sequence of the sgRNA are listed below.

Target	Plasmid	Sequence
MET6	pDS010	TGGTTCAATCTGCTGTCTTA
STR3	pDS055	TCTGAGACCTGGTTGAAATG
SAH1	pDS032	CAATCTCTTATTTAGTAACG
ADO1	pDS030	GATGACTACCTAATTAGACA
SAM1	pDS033	TTTGTGGAACCCATCTACCG
SAM2	pDS034	ATTATTGTCGACGCTTACGG
MET30	pDS035	GTATATGGGACTTATTCACG
MET32	pDS036	GTTGATATAAATAGTCAAGG
HOM3	pDS061	CGTAAAAGGATGTATAACTT
THR1	pDS062	ATAACCGCTGCTATGATGGG
YCT1	pDS102	TGTTACGCTAGCATTCATGG

Prediction expression

The full prediction expression of the DOE model is found below.

$$
\begin{aligned}
&199.39988867 \\
&+158.12009918 \cdot \left(\frac{(\text{MET6} - 3758)}{3405}\right) \\
&+-23.54118398 \cdot \left(\frac{(\text{STR3} - 3623.5)}{3539.5}\right) \\
&+1.9791776252 \cdot \left(\frac{(\text{SAH1} - 3758)}{3405}\right) \\
&+-17.68766119 \cdot \left(\frac{(\text{ADO1} - 3623.5)}{3539.5}\right) \\
&+\text{Match}(\text{SAM1/SAM2}) \begin{pmatrix} \text{"wild-type"} & \Rightarrow -17.1259891 \\ \text{"SAM1 knock-out"} & \Rightarrow -23.9318933 \\ \text{"SAM2 knock-out"} & \Rightarrow 41.057882404 \\ \text{else} & \Rightarrow . \end{pmatrix} \\
&+\text{Match}(\text{MET30/MET32}) \begin{pmatrix} \text{"wild-type"} & \Rightarrow -31.17537313 \\ \text{"knock-out"} & \Rightarrow 31.175373134 \\ \text{else} & \Rightarrow . \end{pmatrix} \\
&+\left(\frac{(\text{MET6} - 3758)}{3405}\right) \cdot \left(\left(\frac{(\text{STR3} - 3623.5)}{3539.5}\right) \cdot 125.90886576\right) \\
&+\left(\frac{(\text{MET6} - 3758)}{3405}\right) \cdot \text{Match}(\text{SAM1/SAM2}) \begin{pmatrix} \text{"wild-type"} & \Rightarrow -40.89868453 \\ \text{"SAM1 knock-out"} & \Rightarrow -29.97960117 \\ \text{"SAM2 knock-out"} & \Rightarrow 70.878285706 \\ \text{else} & \Rightarrow . \end{pmatrix} \\
&+\left(\frac{(\text{MET6} - 3758)}{3405}\right) \cdot \text{Match}(\text{MET30/MET32}) \begin{pmatrix} \text{"wild-type"} & \Rightarrow -27.73554919 \\ \text{"knock-out"} & \Rightarrow 27.735549194 \\ \text{else} & \Rightarrow . \end{pmatrix} \\
&+17.232435824 \cdot (\text{Percentage glucose [\%]} - 3) \\
&+-19.60814879 \cdot \left(\frac{(\text{Time [h]} - 48)}{24}\right) \\
&+\text{Match}(\text{MET30/MET32}) \begin{pmatrix} \text{"wild-type"} & \Rightarrow (\text{Percentage glucose [\%]} - 3) \cdot -38.59268452 \\ \text{"knock-out"} & \Rightarrow (\text{Percentage glucose [\%]} - 3) \cdot 38.592684516 \\ \text{else} & \Rightarrow . \end{pmatrix}
\end{aligned}
$$

$$
\begin{aligned}
&+\left(\frac{(\text{STR3}-3623.5)}{3539.5}\right)\cdot\left(\left(\frac{(\text{Time [h]}-48)}{24}\right)\cdot -57.16246775\right)\\
&+\left(\frac{(\text{ADO1}-3623.5)}{3539.5}\right)\cdot\left(\left(\frac{(\text{Time [h]}-48)}{24}\right)\cdot -23.77184193\right)\\
&+\left(\frac{(\text{MET6}-3758)}{3405}\right)\cdot\left(\left(\frac{(\text{Time [h]}-48)}{24}\right)\cdot -34.16967606\right)\\
&+\text{Match}(\text{SAM1/SAM2})\begin{pmatrix}
\text{"wild-type"} & \Rightarrow \text{Match}(\text{MET30/MET32})\begin{pmatrix}\text{"wild-type"} & \Rightarrow \left(\frac{(\text{Time [h]}-48)}{24}\right)\cdot -41.28451413\\ \text{"knock-out"} & \Rightarrow \left(\frac{(\text{Time [h]}-48)}{24}\right)\cdot 41.28451413\\ \text{else} & \Rightarrow .\end{pmatrix}\\
\text{"SAM1 knock-out"} & \Rightarrow \text{Match}(\text{MET30/MET32})\begin{pmatrix}\text{"wild-type"} & \Rightarrow \left(\frac{(\text{Time [h]}-48)}{24}\right)\cdot 35.914621946\\ \text{"knock-out"} & \Rightarrow \left(\frac{(\text{Time [h]}-48)}{24}\right)\cdot -35.91462195\\ \text{else} & \Rightarrow .\end{pmatrix}\\
\text{"SAM2 knock-out"} & \Rightarrow \text{Match}(\text{MET30/MET32})\begin{pmatrix}\text{"wild-type"} & \Rightarrow \left(\frac{(\text{Time [h]}-48)}{24}\right)\cdot 5.369892184\\ \text{"knock-out"} & \Rightarrow \left(\frac{(\text{Time [h]}-48)}{24}\right)\cdot -5.369892184\\ \text{else} & \Rightarrow .\end{pmatrix}\\
\text{else} & \Rightarrow .
\end{pmatrix}\\
&+\text{Match}(\text{SAM1/SAM2})\begin{pmatrix}
\text{"wild-type"} & \Rightarrow (\text{Percentage glucose [\%]}-3)\cdot -3.22914757\\
\text{"SAM1 knock-out"} & \Rightarrow (\text{Percentage glucose [\%]}-3)\cdot -15.00964971\\
\text{"SAM2 knock-out"} & \Rightarrow (\text{Percentage glucose [\%]}-3)\cdot 18.238797277\\
\text{else} & \Rightarrow .
\end{pmatrix}\\
&+\text{Match}(\text{MET30/MET32})\begin{pmatrix}
\text{"wild-type"} & \Rightarrow \left(\frac{(\text{Time [h]}-48)}{24}\right)\cdot\left((\text{Percentage glucose [\%]}-3)\cdot -7.690775669\right)\\
\text{"knock-out"} & \Rightarrow \left(\frac{(\text{Time [h]}-48)}{24}\right)\cdot\left((\text{Percentage glucose [\%]}-3)\cdot 7.6907756691\right)\\
\text{else} & \Rightarrow .
\end{pmatrix}\\
&+\text{Match}(\text{MET30/MET32})\begin{pmatrix}
\text{"wild-type"} & \Rightarrow \left(\frac{(\text{Time [h]}-48)}{24}\right)\cdot -26.81492231\\
\text{"knock-out"} & \Rightarrow \left(\frac{(\text{Time [h]}-48)}{24}\right)\cdot 26.814922311\\
\text{else} & \Rightarrow .
\end{pmatrix}
\end{aligned}
$$

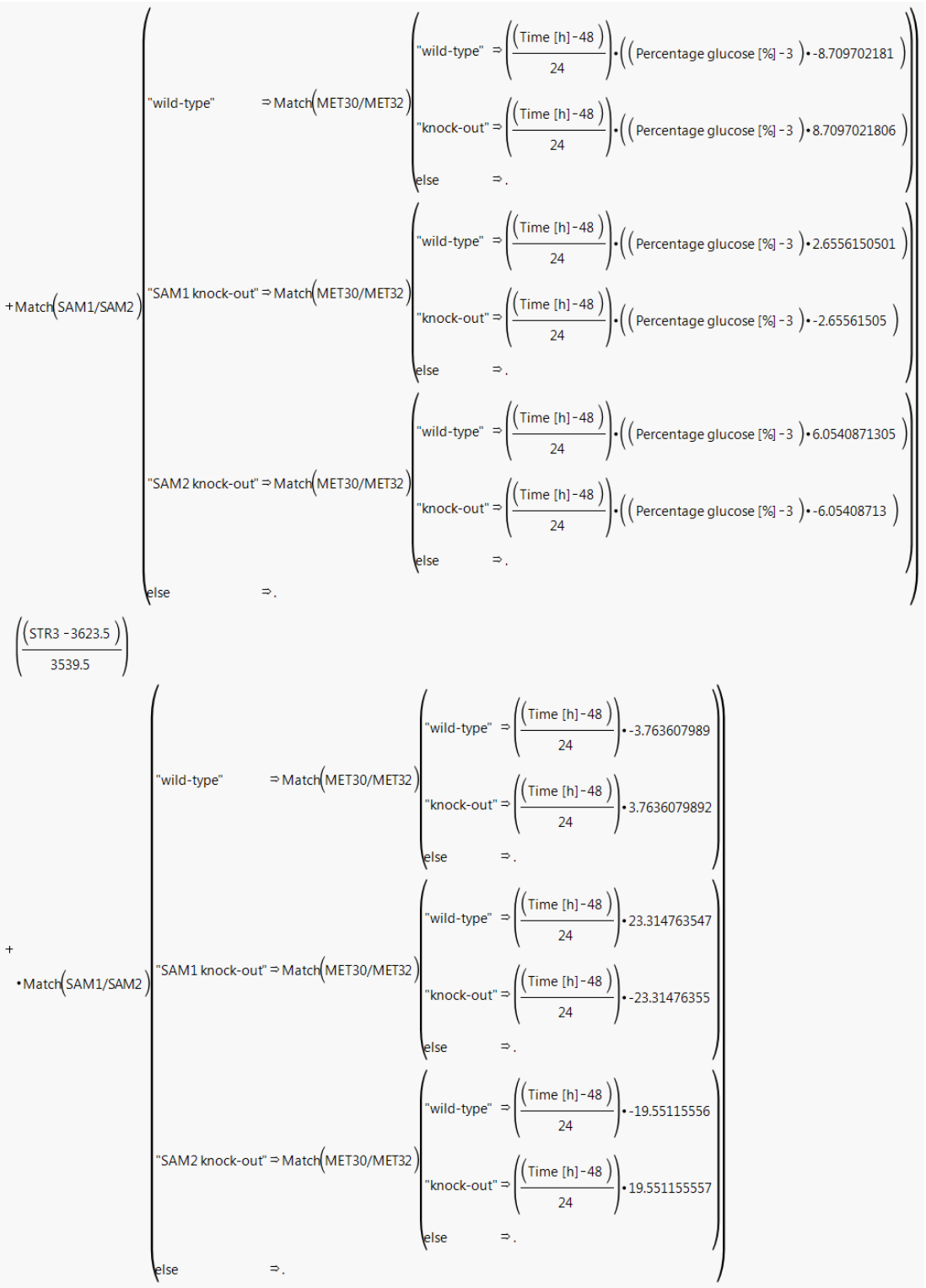
+Match(SAM1/SAM2)
"wild-type" ⇒ Match(MET30/MET32)
"wild-type" ⇒ ((Time [h] - 48)/24) • ((Percentage glucose [%] - 3) • -8.709702181)
"knock-out" ⇒ ((Time [h] - 48)/24) • ((Percentage glucose [%] - 3) • 8.7097021806)
else ⇒ .
"SAM1 knock-out" ⇒ Match(MET30/MET32)
"wild-type" ⇒ ((Time [h] - 48)/24) • ((Percentage glucose [%] - 3) • 2.6556150501)
"knock-out" ⇒ ((Time [h] - 48)/24) • ((Percentage glucose [%] - 3) • -2.65561505)
else ⇒ .
"SAM2 knock-out" ⇒ Match(MET30/MET32)
"wild-type" ⇒ ((Time [h] - 48)/24) • ((Percentage glucose [%] - 3) • 6.0540871305)
"knock-out" ⇒ ((Time [h] - 48)/24) • ((Percentage glucose [%] - 3) • -6.05408713)
else ⇒ .
else ⇒ .
((STR3 - 3623.5)/3539.5)
+
• Match(SAM1/SAM2)
"wild-type" ⇒ Match(MET30/MET32)
"wild-type" ⇒ ((Time [h] - 48)/24) • -3.763607989
"knock-out" ⇒ ((Time [h] - 48)/24) • 3.7636079892
else ⇒ .
"SAM1 knock-out" ⇒ Match(MET30/MET32)
"wild-type" ⇒ ((Time [h] - 48)/24) • 23.314763547
"knock-out" ⇒ ((Time [h] - 48)/24) • -23.31476355
else ⇒ .
"SAM2 knock-out" ⇒ Match(MET30/MET32)
"wild-type" ⇒ ((Time [h] - 48)/24) • -19.55115556
"knock-out" ⇒ ((Time [h] - 48)/24) • 19.551155557
else ⇒ .
else ⇒ .

$$
\begin{aligned}
&+\left(\frac{(\text{SAH1} - 3758)}{3405}\right) \cdot \left(\left(\frac{(\text{Time [h]} - 48)}{24}\right) \cdot 7.3894207007\right) \\
&+\left(\frac{(\text{ADO1} - 3623.5)}{3539.5}\right) \cdot \left((\text{Percentage glucose [\%]} - 3) \cdot -8.456572303\right) \\
&+\left(\frac{(\text{STR3} - 3623.5)}{3539.5}\right) \cdot \left((\text{Percentage glucose [\%]} - 3) \cdot -18.43107219\right) \\
&+\text{Match}(\text{SAM1/SAM2}) \begin{pmatrix} \text{"wild-type"} \Rightarrow \text{Match}(\text{MET30/MET32}) \begin{pmatrix} \text{"wild-type"} \Rightarrow (\text{Percentage glucose [\%]} - 3) \cdot -9.402786253 \\ \text{"knock-out"} \Rightarrow (\text{Percentage glucose [\%]} - 3) \cdot 9.4027862533 \\ \text{else} \Rightarrow . \end{pmatrix} \\ \text{"SAM1 knock-out"} \Rightarrow \text{Match}(\text{MET30/MET32}) \begin{pmatrix} \text{"wild-type"} \Rightarrow (\text{Percentage glucose [\%]} - 3) \cdot 16.500763465 \\ \text{"knock-out"} \Rightarrow (\text{Percentage glucose [\%]} - 3) \cdot -16.50076347 \\ \text{else} \Rightarrow . \end{pmatrix} \\ \text{"SAM2 knock-out"} \Rightarrow \text{Match}(\text{MET30/MET32}) \begin{pmatrix} \text{"wild-type"} \Rightarrow (\text{Percentage glucose [\%]} - 3) \cdot -7.097977212 \\ \text{"knock-out"} \Rightarrow (\text{Percentage glucose [\%]} - 3) \cdot 7.097977212 \\ \text{else} \Rightarrow . \end{pmatrix} \\ \text{else} \Rightarrow . \end{pmatrix} \\
&+\left(\frac{(\text{SAH1} - 3758)}{3405}\right) \cdot \left((\text{Percentage glucose [\%]} - 3) \cdot -4.278727898\right) \\
&+\left(\frac{(\text{MET6} - 3758)}{3405}\right) \cdot \left((\text{Percentage glucose [\%]} - 3) \cdot 6.1719219901\right) \\
&+\text{Match}(\text{SAM1/SAM2}) \begin{pmatrix} \text{"wild-type"} \Rightarrow \left(\frac{(\text{Time [h]} - 48)}{24}\right) \cdot 4.9309300916 \\ \text{"SAM1 knock-out"} \Rightarrow \left(\frac{(\text{Time [h]} - 48)}{24}\right) \cdot -12.93555975 \\ \text{"SAM2 knock-out"} \Rightarrow \left(\frac{(\text{Time [h]} - 48)}{24}\right) \cdot 8.0046296623 \\ \text{else} \Rightarrow . \end{pmatrix}
\end{aligned}
$$

$$\left(\frac{(\text{MET6} - 3758)}{3405}\right)$$
$$+ \bullet \text{Match}(\text{MET30/MET32}) \begin{cases} \text{"wild-type"} \Rightarrow \left(\frac{(\text{Time [h]} - 48)}{24}\right) \bullet \left((\text{Percentage glucose [\%]} - 3) \bullet -4.358734179\right) \\ \text{"knock-out"} \Rightarrow \left(\frac{(\text{Time [h]} - 48)}{24}\right) \bullet \left((\text{Percentage glucose [\%]} - 3) \bullet 4.3587341791\right) \\ \text{else} \Rightarrow . \end{cases}$$
$$+ \left(\frac{(\text{Time [h]} - 48)}{24}\right) \bullet \left((\text{Percentage glucose [\%]} - 3) \bullet -11.15065838\right)$$
$$+ \left(\frac{(\text{MET6} - 3758)}{3405}\right) \bullet \left(\left(\frac{(\text{Time [h]} - 48)}{24}\right) \bullet \left((\text{Percentage glucose [\%]} - 3) \bullet -14.84405519\right)\right)$$

Scaled Estimates

The full list of Scaled Estimates can be found below.

Scaled Estimates

Nominal factors expanded to all levels

Term	Scaled Estimate	Std Error	Prob>|t|
Intercept	199.39989	10.0976	<.0001*
MET6(353,7163)	158.1201	48.35109	0.0114*
MET6*STR3	125.90887	49.08265	0.0334*
MET6*SAM1/SAM2[SAM2 knock-out]	70.878286	13.81251	0.0009*
SAM1/SAM2[wild-type]*MET30/MET32[knock-out]*Time [h]	41.284514	13.2714	0.0144*
SAM1/SAM2[SAM2 knock-out]	41.057882	13.23753	0.0146*
MET30/MET32[knock-out]*Percentage glucose [%]	38.592685	3.837239	<.0001*
SAM1/SAM2[SAM1 knock-out]*MET30/MET32[wild-type]*Time [h]	35.914622	17.75774	0.0778
MET30/MET32[knock-out]	31.175373	6.083785	0.0009*
MET6*MET30/MET32[knock-out]	27.735549	12.15633	0.0519
MET30/MET32[knock-out]*Time [h]	26.814922	12.52378	0.0647
STR3*SAM1/SAM2[SAM1 knock-out]*MET30/MET32[wild-type]*Time [h]	23.314764	16.02219	0.1837
STR3*SAM1/SAM2[SAM2 knock-out]*MET30/MET32[knock-out]*Time [h]	19.551156	37.09366	0.6124
SAM1/SAM2[SAM2 knock-out]*Percentage glucose [%]	18.238797	7.055094	0.0324*
Percentage glucose [%](2,4)	17.232436	4.45263	0.0047*
SAM1/SAM2[SAM1 knock-out]*MET30/MET32[wild-type]*Percentage glucose [%]	16.500763	7.007112	0.0463*
SAM1/SAM2[wild-type]*MET30/MET32[knock-out]*Percentage glucose [%]	9.4027863	6.322133	0.1753
SAM1/SAM2[wild-type]*MET30/MET32[knock-out]*Time [h]*Percentage glucose [%]	8.7097022	4.720567	0.1022
SAM1/SAM2[SAM2 knock-out]*Time [h]	8.0046297	22.02348	0.7257
MET30/MET32[knock-out]*Time [h]*Percentage glucose [%]	7.6907757	3.523861	0.0606
SAH1*Time [h]	7.3894207	6.162532	0.2648
SAM1/SAM2[SAM2 knock-out]*MET30/MET32[knock-out]*Percentage glucose [%]	7.0979772	7.66605	0.3816
MET6*Percentage glucose [%]	6.171922	7.612803	0.4410
SAM1/SAM2[SAM2 knock-out]*MET30/MET32[wild-type]*Time [h]*Percentage glucose [%]	6.0540871	4.159984	0.1837
SAM1/SAM2[SAM2 knock-out]*MET30/MET32[wild-type]*Time [h]	5.3698922	9.128685	0.5726

SAM1/SAM2[wild-type]*Time [h]	4.9309301		10.17906	0.6411
MET6*MET30/MET32[knock-out]*Time [h]*Percentage glucose [%]	4.3587342		6.465788	0.5192
STR3*SAM1/SAM2[wild-type]*MET30/MET32[knock-out]*Time [h]	3.763608		47.62646	0.9390
SAM1/SAM2[SAM1 knock-out]*MET30/MET32[wild-type]*Time [h]*Percentage glucose [%]	2.6556151		3.610868	0.4831
SAH1(353,7163)	1.9791776		6.162532	0.7563
SAM1/SAM2[SAM1 knock-out]*MET30/MET32[knock-out]*Time [h]*Percentage glucose [%]	-2.655615		3.610868	0.4831
SAM1/SAM2[wild-type]*Percentage glucose [%]	-3.229148		6.728851	0.6441
STR3*SAM1/SAM2[wild-type]*MET30/MET32[wild-type]*Time [h]	-3.763608		47.62646	0.9390
SAH1*Percentage glucose [%]	-4.278728		4.93995	0.4116
MET6*MET30/MET32[wild-type]*Time [h]*Percentage glucose [%]	-4.358734		6.465788	0.5192
SAM1/SAM2[SAM2 knock-out]*MET30/MET32[knock-out]*Time [h]	-5.369892		9.128685	0.5726
SAM1/SAM2[SAM2 knock-out]*MET30/MET32[knock-out]*Time [h]*Percentage glucose [%]	-6.054087		4.159984	0.1837
SAM1/SAM2[SAM2 knock-out]*MET30/MET32[wild-type]*Percentage glucose [%]	-7.097977		7.66605	0.3816
MET30/MET32[wild-type]*Time [h]*Percentage glucose [%]	-7.690776		3.523861	0.0606
ADO1*Percentage glucose [%]	-8.456572		4.757936	0.1134
SAM1/SAM2[wild-type]*MET30/MET32[wild-type]*Time [h]*Percentage glucose [%]	-8.709702		4.720567	0.1022
SAM1/SAM2[wild-type]*MET30/MET32[wild-type]*Percentage glucose [%]	-9.402786		6.322133	0.1753
Time [h]*Percentage glucose [%]	-11.15066		3.837886	0.0197*
SAM1/SAM2[SAM1 knock-out]*Time [h]	-12.93556		15.24365	0.4208
MET6*Time [h]*Percentage glucose [%]	-14.84406		5.273673	0.0227*
SAM1/SAM2[SAM1 knock-out]*Percentage glucose [%]	-15.00965		3.97102	0.0054*
SAM1/SAM2[SAM1 knock-out]*MET30/MET32[knock-out]*Percentage glucose [%]	-16.50076		7.007112	0.0463*
SAM1/SAM2[wild-type]	-17.12599		17.73085	0.3624
ADO1(84,7163)	-17.68766		11.21925	0.1536
STR3*Percentage glucose [%]	-18.43107		8.812087	0.0698
STR3*SAM1/SAM2[SAM2 knock-out]*MET30/MET32[wild-type]*Time [h]	-19.55116		37.09366	0.6124
Time [h](24,72)	-19.60815		9.450239	0.0717
STR3*SAM1/SAM2[SAM1 knock-out]*MET30/MET32[knock-out]*Time [h]	-23.31476		16.02219	0.1837
STR3(84,7163)	-23.54118		14.33331	0.1391
ADO1*Time [h]	-23.77184		5.562249	0.0027*
SAM1/SAM2[SAM1 knock-out]	-23.93189		6.538751	0.0064*
MET30/MET32[wild-type]*Time [h]	-26.81492		12.52378	0.0647
MET6*MET30/MET32[wild-type]	-27.73555		12.15633	0.0519
MET6*SAM1/SAM2[SAM1 knock-out]	-29.9796		14.51535	0.0728
MET30/MET32[wild-type]	-31.17537		6.083785	0.0009*
MET6*Time [h]	-34.16968		10.71029	0.0128*
SAM1/SAM2[SAM1 knock-out]*MET30/MET32[knock-out]*Time [h]	-35.91462		17.75774	0.0778
MET30/MET32[wild-type]*Percentage glucose [%]	-38.59268		3.837239	<.0001*
MET6*SAM1/SAM2[wild-type]	-40.89868		23.24584	0.1166
SAM1/SAM2[wild-type]*MET30/MET32[wild-type]*Time [h]	-41.28451		13.2714	0.0144*
STR3*Time [h]	-57.16247		12.62401	0.0019*